Production of smoke and carbon monoxide in underventilated enclosure fires

Sebastian Ukleja, MSc Eng

Faculty of Art, Design and Built Environment of the University of Ulster

Thesis submitted for the degree of Doctor of Philosophy

June 2012

Table of contents

LIST OF FIGURES

LIST OF TABLES

ACKNOWLEDGEMENTS

I am very grateful that I got the opportunity to conduct my research with assistance of so many great people and in the lab so adequately equipped. Such an opportunity can be called a good fortune, but for me it was a gift given to me by God.

I would like to acknowledge assistance of all people who helped and guided me during course of my study however it is not possible to list them all, so I will focus only on those who significantly helped me during this work.

Firstly, I am grateful to professor Michael Delichatsios, my first supervisor, who accepted my as his PhD student and kept me on track during this research program. I learnt a lot under his supervision and I really enjoyed this time. I am also grateful to him that he trusted in me and offered me employment in the FireSERT lab as a Project Engineer at a later stage of my research.

I believe that I would not have completed my work without support and love of my wife, Ludwika, and without the assistance of my friends in the office: Maurice McKee, Billy Veighey and Krzysztof Kowalski. They not only offered practical help but also supported me during tough times and lifted my spirit when I was loosing my motivation. Trying to be more specific, I gratefully acknowledge that Maurice introduced me into the laboratory work, guided and mentored me during the whole duration of my project, and assisted with overcoming many organizational and technical difficulties. I acknowledge technical assistance of Billy who constructed the whole experimental rig for me and was very helpful on all technical problems related to my experimental setup. I acknowledge assistance from Krzysztof who introduced me into LabView software and helped to create whole data logging setup for my work. Finally, all three of them assisted in performing my experiments.

I would like to express my gratitude to my second supervisor, Dr. Jianping Zhang, for his suggestions and careful proof-reading of my manuscript. I would like also to thank professors Vladimir Molkov and Ali Nadjai for serving as my second supervisor in the past.

I am indebted to my supervisor's wife, Mary Delichatsios for her contributions to two of my papers and continuous encouragement during course of my research.

I would like to acknowledge also assistance of Professor Bogdan Długogorski. He gave me many valuable ideas regarding design of my experimental rig during his visit in Ulster. I also benefited a lot from sharing ideas and valuable discussions with Dr Tarek Beji who started his Phd study at the same time with me.

I would like to acknowledge the support form University of Ulster as I was awarded the Vice-Chancellor Research Scholarship which allowed me to come to Northern Ireland and conduct my research. Also a student travel grant from The International Forum of Fire Research Directors is acknowledged – this grant allowed me to attend the IAFSS conference in Germany and to meet and have valuable discussions with many fire scientists.

Finally, I am grateful to my friend, Dr. Mathieu Suzanne, for careful reading of my manuscript and all his comments and suggestions.

SUMMARY

This work is an experimental and theoretical analysis of factors and conditions affecting smoke and carbon monoxide (CO) production in corridor-like enclosure fires. Thirty eight experiments were performed in a three metre long corridor-like enclosure having a cross section 0.5 m x 0.5 m, door-like openings in the front panel and a propane gas burner located near the closed end. Measurements of smoke and carbon monoxide concentrations were performed at locations inside the enclosure and also in the exhaust duct of a hood collecting the combustion products.

The main conclusion of this work is that smoke production depends not only on the fuel and Global Equivalence Ratio (GER) - as is reported in the literature - but also on the temperatures and residence time inside the enclosure, at least for the experimental conditions examined in this study.

Additionaly, it was found that smoke concentration inside the enclosure was increasing during the ventilation controlled regime even after external burning started. Such increase was verified by temperature, smoke and velocity measurements inside the enclosure. The increase was due to reverse flow behind the flames travelling along the corridor. Namely, the gases reversed direction behind the flames with hot gases travelling in the upper layer backwards towards the closed end of the corridor in contrast to hot gas movements towards the opening in front of the flames. This recirculation was confirmed by velocity and oxygen concentration measurements in the upper and lower layers inside the enclosure.

In addition, the present results show that the relationship reported in the literature between smoke and carbon monoxide production during overventilated conditions $y_{co}/y_s \approx$ constant, is no longer valid during an underventilated enclosure fire. The ratio y_{co}/y_s increases for the Global Equivalence Ratios of the enclosure greater than one.

The obtained results are useful for CFD validation and specifically applicable for assessing smoke hazards in corridor fires in buildings where smoke concentrations can be much larger than anticipated owing to leakage to adjacent rooms behind travelling flames.

NOMENCLATURE

A	m^2	Area of the opening
A_T	m^2	Total area of the enclosure
B_{EO}	cd/m^2	Brightness of signs
C	g/m^3 of gas	Mass concentration of smoke
C_a	kg/s	Proportionality factor used for determination of mass inflow into the enclosure
ΔH_c	kJ/kg	Heat of combustion
E	MJ/kg	Heat Released per kilogram of O_2 consumed (taken as 12.68 for propane)
E_{co}	MJ/kg	Net Heat Release per unit mass of O_2 consumed for combustion of CO to CO_2 (approximately 17.6 MJ/kg of O_2)
f_v	ppm	Smoke volume fraction
$\dot{G}''_j$	g/m^2s	Mass generation rate of product j, for instance smoke
H	m	Height of the opening
$H_{p\text{-}c}$	m	Distance from top of the pan (burner) to ceiling
h_c	W/m^2K	Effective convective heat transfer coefficient
HRR	kW	Heat Release Rate
$HRR_{theoretical}$	kW	Theoretical Heat Release Rate determined from gas supply rate
HRR_{Vmax}	kW	Ventilation controlled Heat Release Rate
I/I_0	-	Ratio of transmitted to incident light
k	1/m	Light extinction coefficient
L	m	Path length through the smoke
L_{ill}	$1m/m^2$	$1/\pi$ of mean illuminance of illuminating light from all directions in smoke
L_f	m	Length of the flames below the ceiling
L_{sp}	m	Laminar smoke point height
$L_{sp(mm)}$	mm	Laminar smoke point height
M_a	kg/kmol	Molecular weight of incoming air taking into account relative humidity
M_{CO_2}	kg/kmol	Molecular weight of carbon dioxide
M_{dry}	kg/kmol	Molecular weight of dry air (≈ 29 kg/kmol)
M_{H_2O}	kg/kmol	Molecular weight of H_20 (≈ 18 kg/kmol)
M_{O_2}	kg/kmol	Molecular weight of oxygen (32 kg/kmol)
$\dot{m}''$	g/m^2s	Mass loss rate of material normalised by area
$\dot{m}_a$	kg/s	Mass inflow into the enclosure
$\dot{m}_{CO}$	kg/s	Mass flow rate of CO at the sampling point
$\dot{m}_{CO_2}$	kg/s	Mass flow rate of CO_2 at the sampling point
$\dot{m}_{CO_2}$	kg/s	Initial mass flow rate of CO_2 at the sampling

		point
$\dot{m}_e$	kg/s	Mass flow rate in the duct
$\dot{m}_f$	g/s	Mass loss rate of fuel
$\dot{m}_{f_{stochiometric}} / \dot{m}_{a_{stochiometric}}$	-	Stochiometric fuel to air mass ratio
$\dot{m}_{f_{stochiometric}} / \dot{m}_{oxygen_{stochiometric}}$	-	Stochiometric fuel to oxygen mass ratio
m_s	g	Mass of smoke collected on a filter
p_a	Pa	Air pressure
p_s	Pa	Saturation pressure of water vapour
Oxy_{dep}	-	Oxygen depletion factor (fraction of the incoming air which is fully depleted of its oxygen)
$\dot{q}$	MW	Heat Release Rate from O_2, CO_2, and CO measurements in the exhaust duct (Eq. 34 yields units of MW)
$\tilde{Q}$	-	Non dimensional heat release rate according to Wieczorek definition (2003)
$\dot{Q}_{ideal}$	kW	Amount of heat release obtained from fuel supply rate
$\dot{Q}_{Flame\_extensions}$	kW	Minimum theoretical Heat Release Rate for flame tip to reach the compartment opening
RH	%	Relative Humidity of the incoming air
S	-	Air to fuel mass stoichiometric ratio
SEA_f	m^2/g	Specific extinction area on fuel mass loss basis (σ_f)
SPR	m^2/s	Smoke Production Rate
T	°C	Gas temperature
T_a	K	Air temperature used in Eq. 30
T_{1mm}	°C	Uncorrected readings of thermocouple with 1 mm bare bead
$T_{0.25mm}$	°C	Uncorrected readings of thermocouple with 0.25 mm bare bead
$T_{corrected}$	°C	Gas temperature corrected for re-radiation error
T_p	°C	Temperature at the probe or sampling line entrance
T_∞	°C	Ambient temperature
V	m^3	Volume of the enclosure
$\dot{V}$	m^3/s	Volumetric flow of gases
V_g	m^3	Total volume of sampled gas based on ambient temperature
$Visibility$	m	Visibility of signs at the obscuration threshold
X	°	Function of Φ used by Gottuk and Lattimer (2008)
$X_{CO_2}^A$	-	Measured mole fraction of CO_2 in the exhaust gases

$X_{CO_2}^{A^0}$	-	Initial mole fraction of CO_2 in incoming air
X_{CO}^{A}	-	Measured mole fraction of CO in the exhaust gases
$X_{O_2}^{A}$	-	Measured mole fraction of O_2 in the exhaust gases
$X_{O_2}^{A^0}$	-	Initial mole fraction of O_2 in incoming air
$X_{H_2O}^{0}$	-	Mole fraction of H_2O in the incoming air
Y_{oxygen}	-	Mass fraction of oxygen in air (0.23)
y_{co}	g/g	Carbon monoxide yield
$(y_{co})_{vc}$	g/g	Carbon monoxide yield for ventilation controlled conditions
$(y_{co})_{wv}$	g/g	Carbon monoxide yield for well ventilated conditions
y_{CO_2}	g/g	Carbon dioxide yield
$(y_{CO_2})_{vc}$	g/g	Carbon dioxide yield for ventilation controlled conditions
$(y_{CO_2})_{wv}$	g/g	Carbon dioxide yield for well ventilated conditions
y_j	g/g	Yield of product defined as grams of product per grams of material burnt
y_s	g/g	Smoke yield
$(y_s)_{vc}$	g/g	Yield of smoke for ventilation controlled conditions
$(y_s)_{wv}$	g/g	Yield of smoke for well ventilated conditions
Y_{oxygen}	-	Mass fraction of oxygen in air (0.23)

Greek symbols

α	-	Fuel dependent factor used by Tewarson (2008)
α_{exp}	-	Combustion expansion factor, taken as 1.105
α_s	-	Reflectance of a sign
β	°	Factor used by Wieczorek (2003)
δ	-	Standard uncertainty of the indicated quantities
δ_c	-	Contrast threshold of signs in smoke at the obscuration threshold (0.01 ~ 0.05)
η_s	-	Generation efficiency of smoke
ξ	-	Fuel dependent factor used by Tewarson (2008)
ρ_a	g/m^3	Density of ambient air
ρ_g	g/m^3	Density of surrounding gases
ρ_s	g/m^3	Density of soot particulates
σ_f	m^2/g	Specific extinction area on fuel mass loss basis (SEA_f)
σ_s	m^2/g	Specific extinction coefficient of combustion generated particles
τ_{res}	s	Residence time
Φ	-	Equivalence Ratio
Ψ_s	g/g	Maximum theoretical yield of smoke (g/g)

Ω	-	Constant value, depended on the wavelength; for red light Ω =7.0

NOTE ON ACCESS TO CONTENTS

CHAPTER ONE

Introduction

"General public is unaware of how fast a fire can grow and of how much smoke can be produced by a fire, and this unawareness extends to many designers and other related professionals."

(Klote and Milke, 1992)

General public is also unaware that the main killer is not a fire itself but fire effluents, namely toxic gases and smoke evolved as a result of a fire (Department for Communities and Local Government, 2007). Many fire victims die in locations far away from fire origin. For instance the second greatest hotel fire in the USA resulted in 85 deaths, out of which 65 occurred many floors above the fire location (Figure 1) because of smoke and toxic gases travelling far away from the fire origin (Best and Demers, 1982).

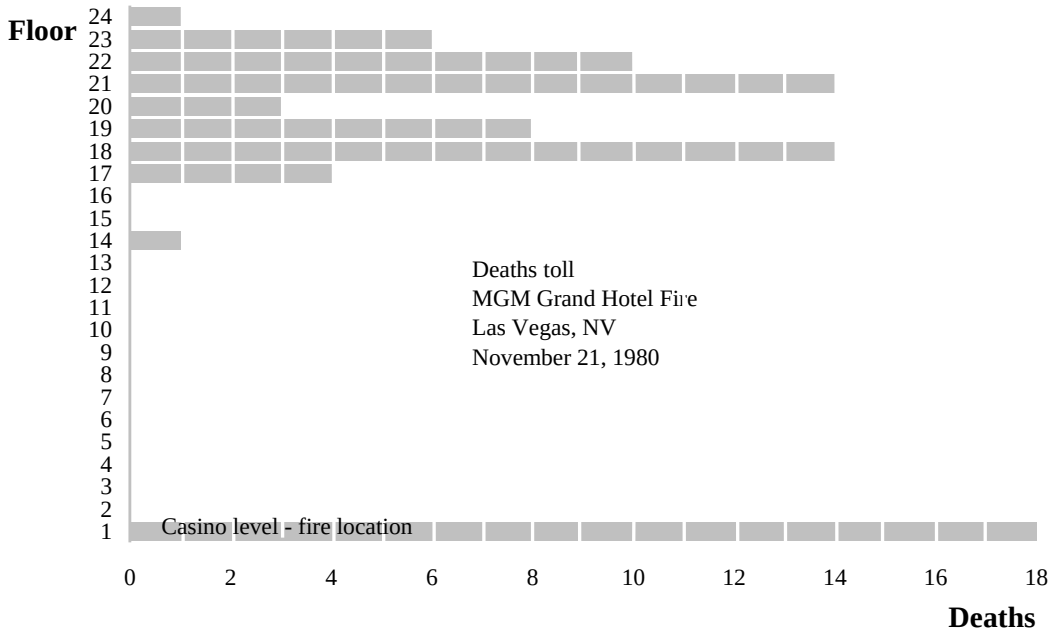

Figure 1. Deaths by floor, fire located on the first floor. Data from Best and Demers (1982), graph adapted from Klote (1992).

Moreover, smoke can be even more lethal in transportation systems, because of the space and evacuation constraints. To illustrate this issue, the fire on the ferry "Scandinavian Star" in 1990 is cited. In that disaster 158 people died, and it was suggested that - for at least 125 of them - the cause of death was inhalation of carbon monoxide in locations remote from fire origin (Robinson, 1999). Consequently, it is very often not the thermal hazard associated with fire which kills but lethality coming from smoke and toxic gases.

Lethality of fire effluent is mainly related to the presence of soot particulates and gases evolved from a fire. Soot particulates are responsible for the obscuration of visible light whereas toxicity comes mainly from inhaling the evolving gases and to some extend particulates in smoke. The spectrum of produced gases varies, but the main killer is still carbon monoxide. One could argue that other gases are more lethal, but carbon monoxide is often produced in large concentrations and independently of materials being burnt (Purser, 2002; Babrauskas et al., 1998).

Even though fire effluents are a by-product of every fire, it is important to examine which types of fires are associated with most of the fatalities. Statistics show that about two third of fire victims die each year not in catastrophic fires in hotels or means of public transport but in dwelling fires (Department for Communities and Local Government, 2011). Dwelling fires can develop to a stage where there is not enough air for complete combustion (underventilated fires) so that production of smoke and carbon monoxide may be completely different compared to an open, well ventilated fire. Moreover, it has been claimed recently that fires in dwellings are neglected and that area needs more focused research (Babrauskas, 2011). Therefore, this study was aimed at studying the production of smoke and carbon monoxide during underventilated enclosure fires in order to better understand the phenomena associated with most of fire related deaths and improve fire safety design for these situations.

The thesis is organised in the following way. Chapter two presents a review of the literature relevant to the production of smoke and carbon monoxide in enclosure fires. This review is concluded with a hypothesis on factors governing smoke and carbon monoxide production in underventilated fires. That hypothesis led to design of an experimental enclosure and methodology described in chapter three. Chapter four presents present data and analysis confirming that hypothesis and thus enabling

an improvement of a fire safety design by a deeper understanding of smoke and carbon monoxide production during underventilated fires. Conclusions are presented in chapter five followed by recommendations for future work on this topic. Finally, additional information is given in appendices.

CHAPTER TWO

Literature review

This work is focused on two hazards related to fire effluent: smoke and carbon monoxide. Initially, these phenomena are discussed separately and subsequently, their interaction is presented. Therefore, this literature review is divided into three subsections: the first one is dealing with smoke, the second one with carbon monoxide as the main gas contributing to fire related toxicity, and the third one will link these two together. Finally, a working hypothesis is presented.

2.1. Generation of smoke in fires

This subsection introduces basics concepts related to smoke, explains the difference between many definitions of smoke, clarifies the term soot, and discus various factors governing smoke production.

2.1.1. Definition of smoke

Mulholland (2008) defined smoke as: "the smoke aerosol or condensed phase component of the products of combustion". A similar definition is given by International Organization for Standardization (ISO) stating that smoke is a "visible part of fire effluent" (2010). While the second definition is shorter, scope is similar: both include neither gases/vapours emitted from fire nor air entrained into the fire.

Other sources state that evolved gases shall be included in the term "smoke", for instance Quintiere (1998), and even air mixed with combustion products shall be seen as a smoke component as well (NFPA, 2005) cited in Milke (2008).

To conclude, this research is based on the definition proposed by Mulholland (2008) and this work distinguishes between smoke (the visible part of the fire effluent) and carbon monoxide (evolved gas from the fire). Both smoke and carbon

monoxide are part of a “fire effluent” defined by ISO as “totality of gases and aerosols, including suspended particles, created by combustion” (2010).

Smoke causes light obscuration because it contains tiny particles which scatter and absorb light. There are two types of these particles: agglomerations of soot particles joined together as chain and clusters (Drysdale, 1998) (defined in the next subsection) and liquid droplets (aerosol mist) (Friedman, 1998). These droplets are created as result of cooling and condensation. In addition, smoke may contain also some tiny particles of combustible material which were not completely burnt.

Different distinction between smoke and soot was suggested by Ostman (1996). She was using terminology based on the measurement technique being used. If the optical means were used, the term smoke should apply; and if the gravimetric sampling, then the term soot is more appropriate.

For this work however, the term soot is defined as minute particulate matter created in the flaming zone and released to smoke. Precise description of soot particulates is given in the next subsection.

2.1.2. Definition of soot

The term “soot” is used in a combustion research to describe all types of carbon particulates generated in flames and later present also in smoke (Watson and Valberg, 2001; Bond and Bergstrom, 2006). Soot presence in flames causes radiation, and thus brightness and yellow glow of flames. However, when soot particles cool down, they are black and their presence in the post flame smoke causes obscuration of the visible light. The first person who has drawn scientific attention to soot was Michael Faraday, his work was made public by series of lectures given by him in 1860-61 (Shaddix and Williams, 2007). It was him who stated that “it is to this presence of solid particles in the candle-flame that it owes its brilliancy” (Faraday, 2002).

Soot is a ‘by-product’ of incomplete combustion of materials containing carbon. Very precise characterisation of soot formation during combustion it beyond the scope of this work and can be found elsewhere (Hayes, 1991; Richter and Howard, 2000; Watson and Valberg, 2001; Siegmann et al., 2002).

Soot is formed in flames, therefore this process strongly depends on combustion conditions (pressure, stoichiometry, amount of air available, mode of burning) and

consequently the properties of soot differ between different conditions (Watson and Valberg, 2001).

Soot has a form of primary spherules bonded together as agglomerates (Bond and Bergstrom, 2006), as presented below in Figure 2 adapted from Widmann (2003).

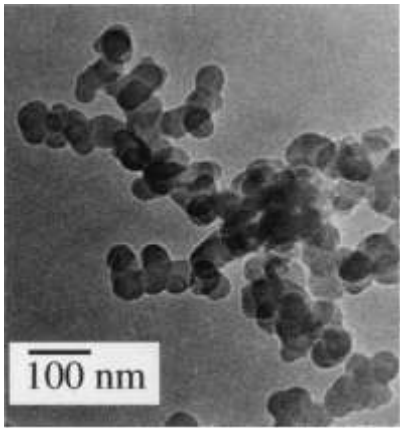

Figure 2. Structure of soot agglomerate. Smoke generated by stochiometric diffusion propane. Adapted from Widmann (2003) with permission.

Formation and oxidation of soot is of great importance for post flame smoke production because smoke consist mainly of soot particulates produced within flame envelope which have not been oxidized inside (Kent and Wagner, 1984; Delichatsios, 1993). In other words, what is seen as particulate smoke, it has been generated in flaming zone - as soot - and conditions within the flame (size of flame and thus residence time, temperature, shape, size of soot and its trajectory within the flame) will determine how much soot can escape.

2.1.3. Post-flame smoke as a result of soot formation and oxidation in flames

Formation and oxidation of soot in flames has been studied for many years, Kennedy (1997) published a very comprehensive review of work prior to 1997 and some newer models were mentioned recently for instance by Beji (2009; 2011b)

It is generally assumed that polycyclic aromatic hydrocarbons (PAHs) are formed as results of fuel molecule breakdown and these PAHs serve as a base for soot formation within flames.

There are different modelling approaches to describe soot formation and oxidation, starting with detailed chemistry models then models with simplified chemistry and finally global soot models.

The model in hand was developed recently by formed PhD student at FireSERT and published elsewhere (Beji, 2009; Beji et al., 2011b). The model is related to a former work of Delichatsios (Delichatsios, 1994) and has some similarities to the model proposed by Lautenberger et al. (Lautenberger et al., 2005). This model is semi-empirical and based on the mixture fraction approach (Bilger, 1977). In this model different fuels can be used by employing the laminar smoke point concept (Delichatsios, 1994). Only basic chemistry information is required – i.e. stochiometry of the fuel and the laminar smoke point height. Consequently soot formation is dependent only on the mixture fraction and temperature. Soot oxidation is assumed constant, other models take into account various factors including partial pressure of oxygen.

The model described is applicable for laminar diffusion flames, and has not been fully validated in turbulent flames within enclosure (Beji, 2009; Beji et al., 2011b). Consequently soot formation can be seen as a ground for the post flame smoke production but it is currently impossible to predict smoke production entirely from soot models for turbulent combustion, especially within an enclosure. Current models cannot fully resolve problems like: enclosure geometry, mixing of gases and size of the fire. All these factors will affect the escaping of soot from flames and thus post flame smoke production (Rasbash and Drysdale, 1982; Mulholland, 2008; Tewarson, 2008). These factors will be discussed in subsections to follow.

2.1.4. Factors affecting smoke production

"Predictions of smoke production are far less developed than predictions of heat release"

(Ostman, 1996)

That opening quote was written about 15 years ago and a question arises what is the state-of-the-art now? It seems that despite progress made in the recent years, there are still many gaps in understanding of smoke generation.

There is a tremendous progress in CFD applications, and design of smoke control systems, however our basic understanding of the factors governing smoke production remains similar to knowledge reported by Rashbash and Drysdale three decades ago (1982). We have much better measuring techniques, more is understood on chemical and physical properties of soot, and the amount of publications is

growing rapidly (Figure 3), but “it is not possible at the present time to predict smoke emission as a function of fuel chemistry and combustion conditions” (Mulholland, 2008). One may argue that current CFD models are doing that very well, but that will be examined in the section devoted to visibility in smoke. At this point, discussion will focus on what is known about various factors influencing smoke production.

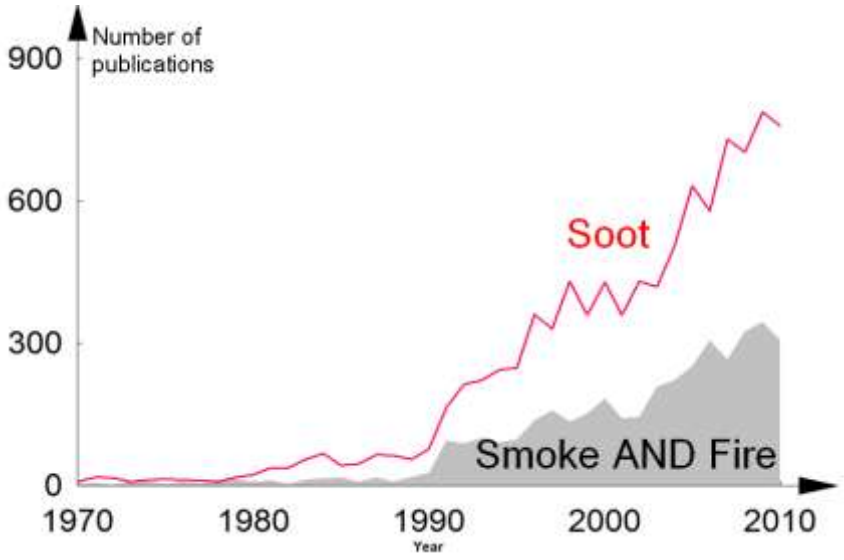

Figure 3. Number of publications for keywords “smoke” AND “fire” and separately for keyword “soot”. Compilation produced by author based on the Thomas Reuters Web of Knowledge.

Basically, smoke is a fraction of soot produced within flame envelope which has not been oxidized inside (Delichatsios, 1993). In other words, what is seen as particulate smoke, it has been generated in the flaming zone - as soot - and conditions within the flame (size of flame and thus residence time, temperature, shape, size of soot and its trajectory within the flame) will determine how much soot can escape. Therefore, factors like: enclosure geometry, mixing of gases and size of the fire will affect the escaping of soot from flames (Rasbash and Drysdale, 1982; Mulholland, 2008; Tewarson, 2008).

The factors governing smoke production, listed above, will be discussed in the following subsections. The following aspects will be discussed: ventilation conditions, chemistry of the fuel, residence time both in flames and also in hot upper zone, effect of scale and temperature. Modes of combustion, namely smouldering versus flaming flames, will not be covered in this review, because this work is only focused on flaming fires. Detailed discussion on the differences between smoke

from smouldering versus flaming fires can be found for instance in the following publications (Rasbash and Drysdale, 1982; Drysdale, 1998; Mulholland, 2008).

2.1.4.1. Effect of ventilation conditions on smoke production

"Smoke is a product of incomplete combustion" (Rasbash and Drysdale, 1982) Incomplete combustion may be caused by not enough air available therefore changes in ventilation conditions will affect smoke production. Yet, it can not be simply assumed that the less the available air the more smoke will be produced (Ouf et al., 2008). That relationship between ventilation and smoke generation will be explained in next section.

Ventilation conditions can be defined either by equivalence ratio, i.e. ratio of available fuel to available air normalised by stochiometric fuel to air ratio; or by vitiation, i.e. reduction of oxygen level in surrounding air but with the adequate amount of air being available.

2.1.4.1.1. Equivalence ratio

As mentioned above, the equivalence ratio (Φ) is defined as ratio of mass of fuel to mass of air normalised by stochiometric fuel to air mass. By definition, $\Phi > 1$ means that there is not enough air for complete combustion (fuel rich or underventilated); $\Phi < 1$ means there is more than required air for complete combustion (fuel lean or overventilated); $\Phi = 1$ indicates stochiometric conditions.

Equivalence ratio was probably firstly introduced to describe enclosure fires by Beyler (1983; 1986a; 1986b), however fuel to air ratio normalised by stochiometric fuel to air ratio was earlier used for example by Cetegen (1982). Moreover Tewarson (1983; 1984) was using a reciprocal value called a stochiometric fraction. All these research efforts were published in early eighties, yet it is attributed to Beyler that he was the first one to develop correlation between species yields and the equivalence ratio.

It is important to note that commonly used definition involves the amount of air, yet Tewarson used for example the amount of oxygen. That will be further discussed in section devoted to Tewarson's correlations and effect of vitiation.

The calculation of the equivalence ratio depends on the control volume considered, therefore one can calculate a plume, an upper layer, a local or a global

equivalence ratio depending on the control volume chosen. For instance, the term Global Equivalence Ratio was defined by Pitts (1992; 1994a; 1995) as a mass ratio in the upper layer during steady state conditions of Beyler's hood experiments.

Concise summary of different types of Equivalence ratio is given for instance by Wieczorek (2003):

> *"Plume Equivalence Ratio (PER) – the ratio of the gaseous fuel generation rate at the fuel surface to the air entrainment rate into the flame between the fuel surface and the hot layer/cold layer interface normalized by the stoichiometric ratio for the fuel. [Beyler 1983, Pitts 1994]*
>
> *Upper Layer Equivalence Ratio – the ratio of the mass of gas in the upper layer derived from the fuel divided by that introduced from air normalized by the stoichiometric ratio for the fuel. [Morehart et al. 1990, Pitts 1994, Gottuk et al. 2002]*
>
> *Global Equivalence Ratio – The ratio of the fuel mass loss rate within the compartment to the air flow rate into the compartment, normalized by the stoichiometric ratio for the fuel. [Pitts 1994, Gottuk et al. 2002]"*

2.1.4.1.2. Effect of reduced ventilation

The structure of post-flame soot particulates is different for higher equivalence ratios. That was observed by Leonard et al. (1994) in small scale tests. It was reported that smoke generated for higher equivalence ratios is "mainly organic rather than graphitic and it has an agglutinated structure rather than an agglomerate structure" (Leonard et al., 1994). It can be qualitatively observed in Figure 4 reprinted from Widmann (2003).

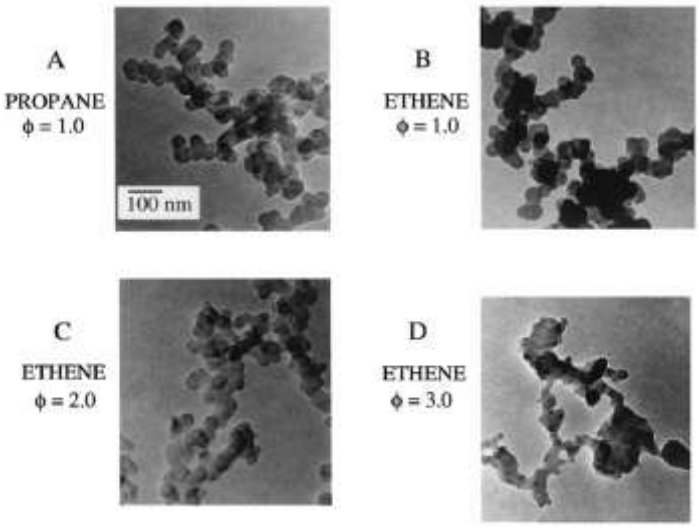

Figure 4. Structure of soot for various equivalence ratios. Reprinted from Widmann (2003) with permission.

Leonard et al. used a small scale apparatus to study behaviour of smoke as a function of Equivalence Ratio (Φ) for methane and ethylene. They expressed smoke production as smoke yield, which is a ratio of mass of smoke produced (in grams) to mass of fuel consumed (in grams). Figure 5 shows results of their work, confirming an increase in smoke yield as equivalence ratio increased towards unity followed by a decrease for higher values of equivalence ratios. They suggested that smaller flames at higher equivalence ratios and thus shorter residence times were responsible for lower yields of smoke during underventilated conditions. Moreover, they speculated that change in structure of agglomerates and higher organic content may also be resulting from smaller flames and thus "quenching of the smoke growth at an early stage" (Leonard et al., 1994).

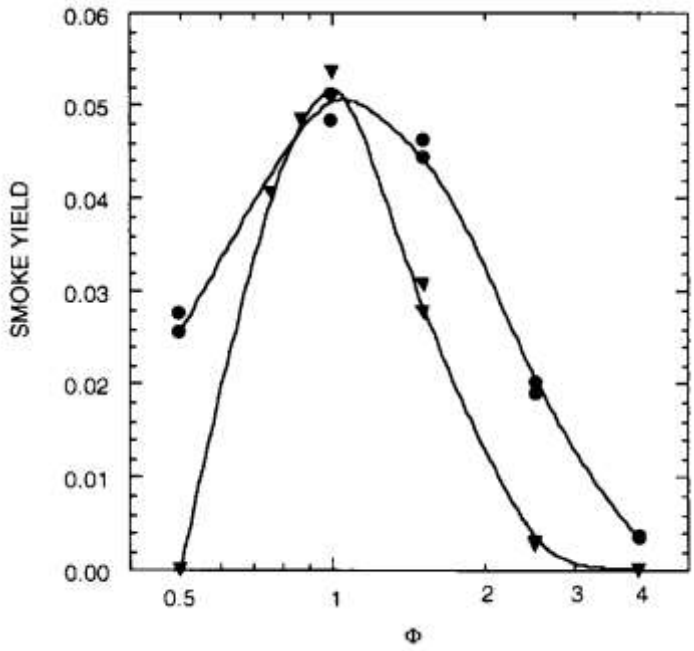

Figure 5. Smoke yield from ethylene flames, (● flow rate of fuel 6.4 cm^3/s, ▼ 3.2 cm^3/s). Data adapted from Leonard (1994) with permission.

Different behaviour was reported by Tewarson (1993; 2002; 2008). His database, probably the most comprehensive one on material properties during fires, was firstly widely available in 1988 based on his work in the Factory Mutual Corporation. However, his database was mainly focused on showing variability in smoke yields between different materials but for overventilated conditions only. Notwithstanding, there is a section devoted to effects of ventilation. He published results on seven polymers (wood and six synthetic ones) for various Equivalence ratios, obtained in his bench scale Fire Propagation Apparatus (ASTM, 2003). He was varying equivalence ratio by lowering oxygen level in the forced co-flow of air. His results re-drawn below (Figure 6) clearly indicate that a strong power relationship between smoke yield and equivalence ratio was observed only for polystyrene (PS) and for polyvinyl chloride (PVC) to some extent. Other materials did not show strong dependence on equivalence ratio. His correlation is shown below, and Figure 6 was drawn based on his data published in SFPE Handbook (Tewarson, 2008).

$$\frac{(y_s)_{vc}}{(y_s)_{wv}} = 1 + \frac{\alpha}{\exp\left(2.5\Phi^{-\xi}\right)} \qquad (1)$$

Where: $(y_s)_{vc}$ – yield of smoke for ventilation controlled conditions, $(y_s)_{wv}$ – yield of smoke for well ventilated conditions, α, ξ – fuel dependent factors listed below.

Table 1. Fuel dependent factors for carbon monoxide yields correlations (Tewarson, 2008)

	Smoke	
Material	α	ξ
PS	2.8	1.3
PP	2.2	1.0
PE	2.2	1.0
Nylon	1.7	0.8
PMMA	1.6	0.6
Wood	2.5	1.2
PVC	0.38	8.0

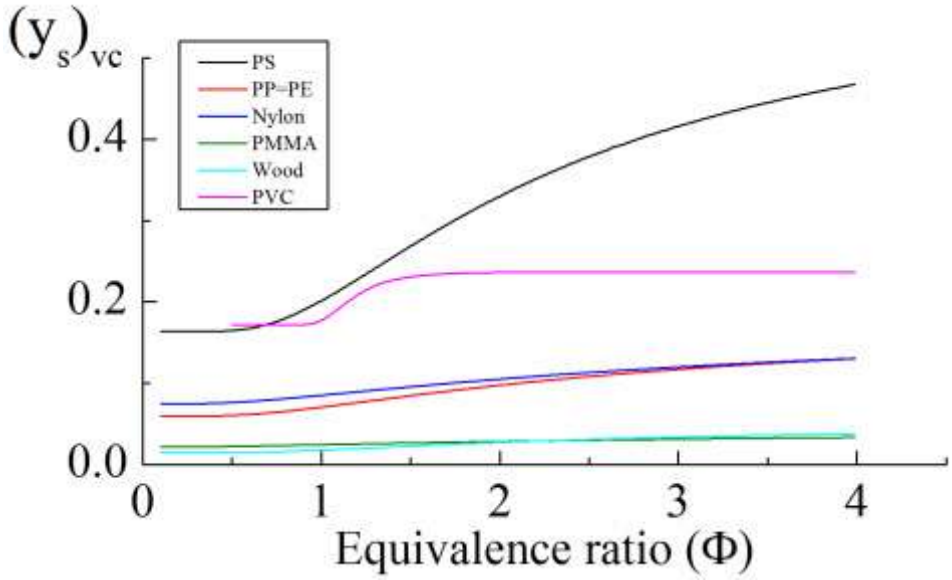

Figure 6. Smoke yields as a function of Equivalence Ratio for seven polymers (Tewarson, 2008).

On the other hand, data published by Dod (1989) indicated radically different trends at least for wood and other cellulosic materials. Production of smoke was "increased dramatically with restricted ventilation."

Another information about sensitivity of smoke yields to ventilation conditions can be found in a paper by Drysdale and Abdul-Rahim cited in (Drysdale, 1998). These authors were investigating sensitivity of smoke yield to conditions like radiant heat flux, oxygen concentration, ventilation conditions and sample orientation (Drysdale, 1998). However that was established based on small scale NBS chamber test without measurement of mass loss, i.e. different rates were lumped into general smoke obscuration. Summing up, limitation of that study was due to the "fact that only the total amounts of smoke were studied; it was not possible to characterise whether the reduced smoke emission for smouldering combustion were due to

reduced mass loss rate or due to less smoke being emitted per unit mass" (Ostman, 1996).

Another conclusion can be derived from experiments on a larger scale. Recently, researches at National Institute of Standard and Technology (USA) conducted systematic research on generation of combustion products in compartment fires, both at reduced scale with moderate HRR <1 MW (Ko et al., 2009) and at full scale inside an ISO 9705 room with large HRR (Lock et al., 2008).

Experiments at reduced scale were performed in an enclosure which was 2/5 scale model of the full scale ISO 9705 room (ISO, 1993) with the dimensions as follows: 0.98 m wide, 0.98 m high, and 1.46 m deep. Smoke measurements were performed gravimetrically from inside the enclosure and reported as soot yields. Time averaged measurements showing soot yields from three different fuels are presented in Figure 7 in a function of Local Equivalence Ratio.

Figure 7 shows that yields of soot in underventialted, moderate scale fires (HRR <1 MW) tends to increase for higher equivalence ratio. Such behaviour differs from the observations reported earlier from small scale experiments, however one has to keep in mind that different fuels are compared.

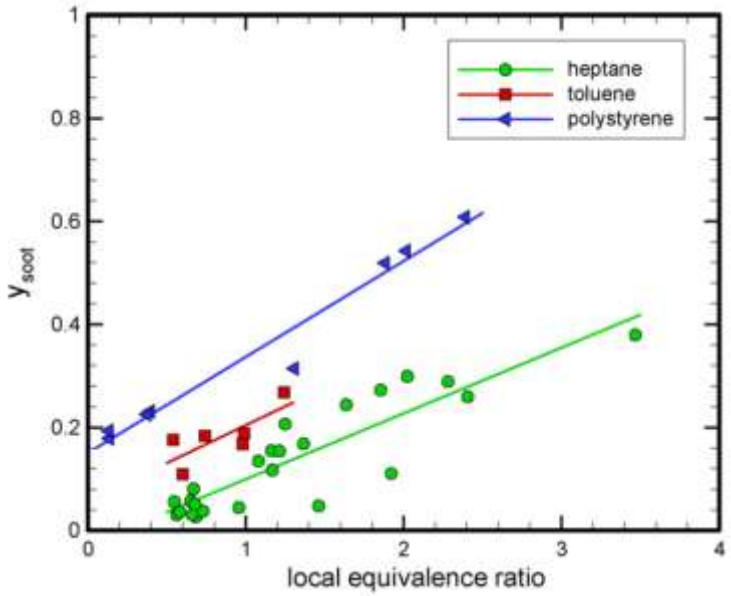

Figure 7. Soot yield as a function of Local Equivalence Ratio in a moderated scale experiments at NIST. Reprinted from Ko et al. (2009) with permission.

A separate section is required to discuss smoke yields derived from so-called Purser tube (British Standards Institution, 2003) used for toxic hazard evaluation of different materials. The design of the apparatus enables creation of various

equivalence ratios for fixed temperature regimes. Standard conditions are listed which should correspond to different stages of a fire and different scenarios (pre or post flashover, ventilation or fuel controlled). This test enables determination of yields of species (and smoke) as a function of equivalence ratio. However, this test has been criticised for example by Babrauskas (1995) for not simulating a real fire situation. In addition, heat flux to a tiny sample is not known, and physics of combustion are not adequately represented. The employed technique of smoke measurement (measurement in a chamber) has similar limitations to NBS chamber discussed earlier, including lack of information on transient mass loss rate and the deposition of soot on the walls of the chamber. On the other hand, there are publications indicating that smoke data obtained from the Purser tube were comparable with large scale data for limited number of cases (Stec et al., 2009). The published data were very sensitive to testing conditions and showed large variations between different fuels therefore no generalised relationship was proposed.

2.1.4.1.3. Effect of vitiation

Effect of vitiation was studied by Santo and Delichatsios (1984), and later by Mulholland (1991a). Santo and Delichatsios found that the supply of the vitiated air, in the range from 17.5% to ambient concentration of oxygen (by volume) did not remarkably influence carbon monoxide production, but reduced significantly the radiation from flames (per unit height). They reported that less luminous flames were observed for lower oxygen concentrations thus indicating lower amount of soot being produced. Santo and Delichatsios concluded that reduction of the amount of soot in flames was “probably due primarily to the decrease in the adiabatic flame temperature”. There was no measurement of post flame smoke however their qualitative statement regarding luminosity of flames may suggest that the amount of smoke may be reduced as a result of vitiation.

On the other hand, Mulholland et al. (1991a) indicated that there was no significant effect of reduced oxygen concentration on smoke production from four different solid materials. It is also important to note that they kept the air flow constant and thus ensured that Equivalence Ratio was low for all oxygen concentrations (GER<0.29) so effect of reduced ventilation was not affecting their data.

Study of Tewarson and Steciak (1983) indicated different behaviour but his results were also based on higher GER, therefore effect of ventilation was not separated.

2.1.4.2. Effect of fuel chemistry

The next factor which determines the smoke production is related to a chemical composition of a fuel. No general relationship applicable for all fuels has been found yet, only some general trends were reported in the available literature (Rasbash and Drysdale, 1982; Mulholland, 2008; Tewarson, 2008).

Fuel chemistry seems to be the mostly known factor affecting smoke production, yet one has to keep in mind limitations of the majority of publications on that topic. These limitations are briefly listed for instance by Mulholland (2008): most of the tests were performed in a small to bench scale, with majority derived either from the Cone Calorimeter or the Flammability Propagation Apparatus with large database published by Tewarson (2008). Recently data were obtained also from so called Purser tube (Stec et al., 2009). Moreover, most of the data (with the exception of the Purser tube) were derived from free burnings tests, i.e. for overventilated conditions.

Current tests methods are based on the assumption that "the smoke yield is principally a function of a material and that the 'fire environment' has only a second order effect. Insufficient attention has been paid to smoke production as part of the overall fire 'system' or 'scenario'" (Rasbash and Drysdale, 1982)

Limitations listed above should be kept in mind when models are proposed based only on yields derived from free burning on a small scale.

2.1.4.3. Effect of scale

> *"Fundamental to the viability of small scale 'smoke testing' is that the chemical and physical nature of the material, rather than the fire environment, or 'scenario', are the dominant factors in determining smoke yield."*
>
> (Rasbash and Drysdale, 1982)

There were many attempts to understand the effect of scale and correlate smoke production between small and large scale 'real' fires.

Christian and Waterman (1971) tried to correlate in the early seventies various small scale tests used at that time with some full scale tests, however without great success.

It was hypothesized later by Rasbash and Drysdale (1982) that larger scale tests with larger flames will result in longer residence time of fuel volatiles in flames. That in turn could lead to more smoke being produced. That was confirmed for instance by Rasbash (1980). This research compared results from NBS smoke chamber (ASTM, 1979) concluding that large scale tests of wood cribs result in smoke production six times larger than reported in accumulated small scale test – NBS chamber. They also examined other data with some agreement for three out of six lining materials, but more data were needed to propose general correlations.

Study of Östman (1991), firstly published in 1988, reported only direct comparison between Cone Calorimeter data and full scale room corner tests of some lining materials. She suggested that smoke production per heat release rate was the most promising candidate parameter for direct comparison. No distinction was made for ventilation conditions during large scale tests. However, she published later a full report (Ostman, 1992), cited in Heskestad and Hovde (1993) where seven different linear correlations were proposed.

More comprehensive approach was adopted by Mulholland et al. (1989). They reported that direct comparison between smoke in small and larger scale tests was possible provided that the mass loss rate per unit area was matched.

For instance, they reported the following smoke yields for small and large scale respectively: “heptane 0.011 vs. 0.013g/g, Prudhoe Bay crude oil 0.088 vs. 0.090g/g, wood 0.004 vs. 0.003g/g, and rigid polyurethane 0.093 vs. 0.080g/g.

The main difficulty was to determine the area of burning specimen for more complex fuel geometries, like for instance wood cribs. Moreover this research was based also only on overventilated conditions.

Another systematic attempt was made by Heskestad and Hovde (1993; 1994), (Heskestad, 1994) yet still related mostly to open burning. At the same time, other study was also published by Hirschler (1993).

On the basis of the scientific evidence mentioned beforehand, the assumption that one can obtain data from small scale tests and use it in model to predict large scale, real fires must be taken with caution. Therefore attempts to predict smoke production in real fires from tests like tube furnace (British Standards Institution,

2003), being a cost effective solution, may be inappropriate without better understanding of physics involved in smoke production.

2.1.4.4. Effect of temperature

Effect of post flame temperature on smoke volume fractions has been investigated by Tolocka et al. (1999). Their research on ethylene air diffusion flames indicated that higher post flame temperature was responsible for reduction of soot volume fractions. That effect was even stronger for higher equivalence ratios (Figure 8).

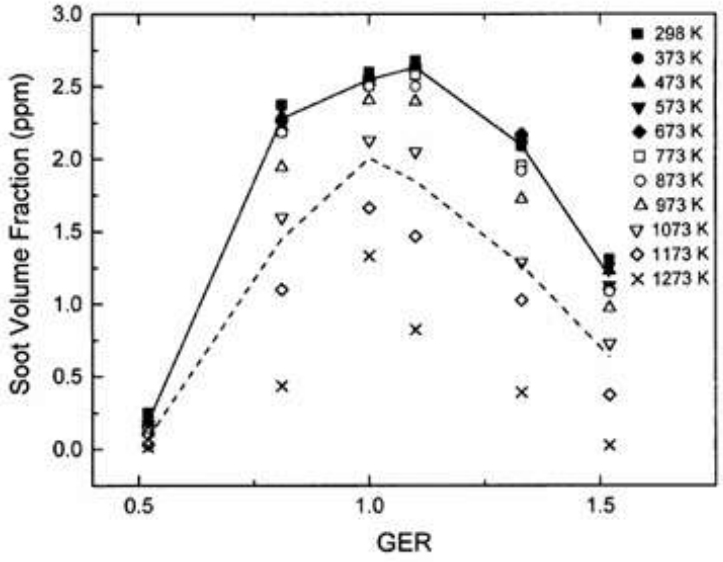

Figure 8. Effect of post flame temperature on soot volume fraction. Reprinted from (Tolocka et al., 1999) with permission.

That dependency was explained by increased oxidation of soot at higher temperatures affecting also levels of carbon monoxide. That cross correlation between smoke and carbon monoxide will be further discussed in section 2.4 devoted to relationships between CO and smoke production.

It is also important to notice that the maximum smoke yield was occurring at Global Equivalence Ratio just above one, irrespective of the temperature. Moreover, the trend that experiments at higher GERs produce lower smoke yield is in good agreement with data from (Leonard et al., 1994) discussed earlier.

2.1.4.5. Effect of opening geometry

The effect of opening geometry was examined by Stark in his study on smoke and toxic gases from plastics (1972). He reported that smoke measured outside of a

large compartment was much smaller when horizontal high level vent was used instead of vertical vent. His comparison involved slightly different opening factors ($AH^{1/2}$) and fuel loads, nevertheless optical densities were larger with vertical opening even by an order of magnitude. He claimed that horizontal opening aided mixing of fresh air with fire gases and smoke and some secondary combustion was possible. On the other hand, vertical opening "allowed air to reach the fuel directly, and fire gases and smoke to escape with far less mixing" (Stark, 1972).

2.1.4.6. Summary of factors affecting smoke production

"If our concern is with smoke production from materials involved in 'real' building fires, then in addition to problems of scale, the effects of the enclosure must also be considered. In the post-flashover, ventilation controlled fire, complex flows are set up within the enclosure and it becomes impossible to identify any flame 'structure' or to refer to 'pyrolisis' and 'combustion' zones."

(Rasbash and Drysdale, 1982)

The amount of smoke produced is very often seen only as a sole material property, frequently determined only from bench scale tests. On the other hand, results from small scale tests may not be applicable in a larger scale, as reported for example by Rasbash and Pratt (1980). Their smoke data obtained in large scale post flashover fire were 6 times higher than data from small scale test of the same material.

Another valuable comment was made by Babrauskas (1995) who pointed out that hazards related to smoke cannot be assessed only based on smoke yield without any relation to mass burning rate – as for conditions with relatively small burning rate even materials with high smoke yield will not produce copious amounts of smoke. Therefore it is not adequate to report only smoke yield as a function of material if one aims at full characterisation of risks from smoke in a given fire scenario.

Consequently, a brief section on quantification of smoke is required before any further discussion. In other words, before one can answer a question of Mulholland (1982) "How well are we measuring smoke?" one has to understand "How are we measuring smoke?" This will be dealt with in the next section.

2.2. Quantification of smoke production in fires

This subsection explains various approaches to smoke quantification and explains numerous quantities used to characterise smoke production.

2.2.1. Introduction

Smoke can be quantified either by gravimetric or optical measurements. The first method is based on the measurement of a mass of soot deposited on a filter after extraction of smoke via a probe. If the volumetric flow through a sampling probe is known, then the mass concentration (mass of smoke in a given volume) can be calculated. The major disadvantage of this method is related to averaging over period of time so transient changes cannot be observed. Moreover deposition of soot inside the sampling probes and necessity of conditioning the filters make it relatively cumbersome. In addition, this method is invasive and not always can be applied. Another approach is based on light extinction measurements. This non-intrusive technique enables monitoring transient changes and can be related to reduction of visibility caused by smoke via some empirical correlations. On the other hand, the information derived from light extinction measurements can be only related to mass of smoke assuming some constant values derived from literature data. All these limitations will be explained in sections to follow.

2.2.2. Light extinction caused by smoke

One of properties associated with smoke is a light extinction coefficient that describes the amount of visible radiation being extinct by a given amount of smoke along a known optical path. Extinction is caused by two major phenomena: scattering and absorption (Figure 9).

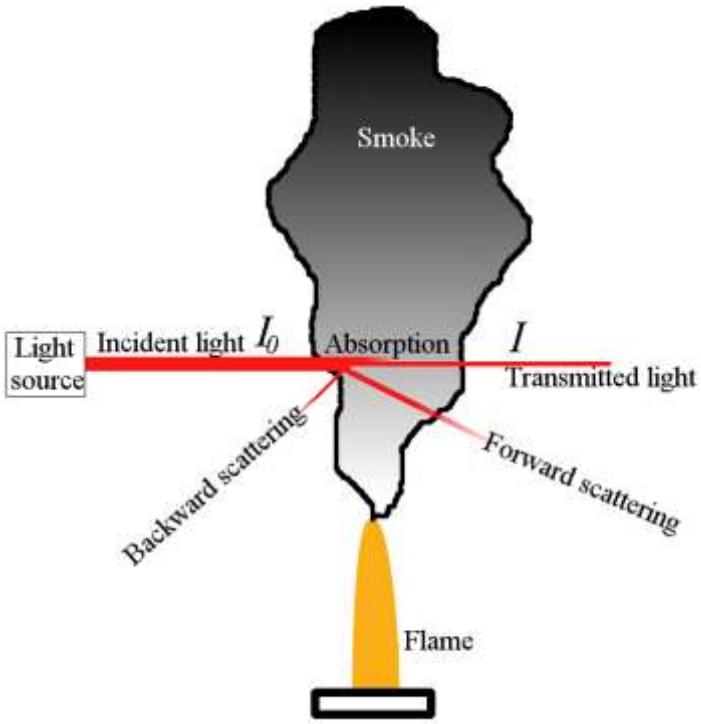

Figure 9. Extinction of light by smoke. Contribution of absorption and scattering.

When a light beam is passed through smoke then the ratio of transmitted to incident light can be obtained from simplified version of Beer–Lambert–Bouguer law (British Standards Institution, 1998; Whiteley, 2008):

$$I/I_0 = e^{-kL} \tag{2}$$

where:
I/I_0 – ratio of transmitted to incident light (-), L – path length through the smoke (m), k – light extinction coefficient (1/m)

Rearranging the above equation gives the formulae for the light extinction coefficient, theoretically valid for monochromatic light:

$$k = \frac{1}{L}\ln\left(\frac{I_0}{I}\right) \tag{3}$$

2.2.3. Smokiness of a fuel

Once light extinction coefficient has been measured, smokiness of a fuel can be determined as outlined below.

2.2.3.1. Specific Extinction Area (SEA - σ_f)

One possible method to describe the amount of smoke released from a given fuel is based on normalisation of the light extinction coefficient by the mass loss rate of a fuel times the volumetric flow rate in the measurement section. As a result, the Specific Extinction Area is obtained (SEA_f or σ_f), sometimes called the Specific Extinction Area on a fuel mass loss basis. This approach is used, for instance, in the Cone Calorimeter test (Babrauskas and Mulholland, 1987; Babrauskas, 2002):

$$\sigma_f = \frac{k}{\dot{m}_f / \dot{V}} \tag{4}$$

where:
σ_f - Specific Extinction Area on a fuel mass loss basis (m^2/g), k – light extinction coefficient (1/m)
$\dot{m}_f$ - mass loss rate of fuel (g/sec) , $\dot{V}$ - Volumetric flow of gases through the duct (m^3/sec)

2.2.3.2. Smoke Production Rate

A different methodology describing smokiness of a fuel is adopted in the Single Burning Item test (European Committee for Standardisation, 2002) used to certificate building products in the European Union according to Euro-Class. In that test, a parameter called Smoke Production Rate is calculated:

$$SPR(t) = k \times \dot{V} \tag{5}$$

where:
SPR – Smoke Production Rate (m^2/s), k – light extinction coefficient (1/m),
$\dot{V}$ - Volumetric flow of smoke (m^3/sec)

SPR can be understand as “total effective cross-sectional area of all the smoke particles” (British Standards Institution, 1998) released per unit time. On its basis, the total smoke production rate and the smoke growth rate index are computed, which combined with Heat Release Rate determines the Euro-Class of a product. However, this is not relevant for this project and will not be further discussed here.

2.2.3.3. Smoke yield

Another parameter describing “smokiness of material” is smoke yield (y_s). It is defined as “mass of smoke aerosol (particulates or droplets) produced per mass of

material burned" (Mulholland and Croarkin, 2000) and it is expressed in units mass per mass, usually (g/g).

Smoke yield can be obtained either by weighting the soot particulates collected on a filter (Ostman, 1996) , or derived from the light extinction measurements. The latter approach is described for instance by Mulholland (2000) or by Tewarson (1995). In brief, smoke yield can be derived from the following formulae:

$$y_s = \frac{\sigma_f}{\sigma_s} \tag{6}$$

The numerator is calculated as shown in Eq. 4. The denominator, σ_s, is called the mass-specific extinction coefficient on a smoke mass basis. It is related to mass concentration of smoke in a given volume and and is wavelength specific. Appendix I presents list of σ_s for different fuels and different ventilation conditions as published in the literature.

Nevertheless, the underlying assumption for Eq. 6 is that the value of σ_s is constant. This assumption allows one to calculate smoke yield only from light extinction measurements. However, there is significant difference between values of σ_s proposed by Mullholand and used by Tewarson. The former author conducted a review of many experimental data (Mulholland and Croarkin, 2000) and suggested a value 8.7 ± 1.1 (m^2/g) for most hydrocarbons in over-ventilated combustion. In contrary, Tewarson is using σ_s close to 10.0 m^2/g, which comes from earlier research by Newman and Steciak (1987).

Discrepancy between values proposed by Mulholland and Tewarson is not the only factor contributing to possible error in smoke yield calculations. Another is that both values were derived from experiments in over-ventilated combustion and should not be used for under-ventilated conditions. For instance, Gottuk (1992) suggested that using data from over-ventilated in under-ventilated conditions may produce 50% error. Widmann (2003; 2005) published data which show that σ_s tends to decrease for higher equivalence ratios for ethane. Widmann (2005) proposed correlation, experimentally validated for ethane:

$$\sigma_s = 9.09 \exp\left(-0.118\Phi\right) \tag{7}$$

where Φ is the equivalence ratio.

For instance, for ethane at Global Equivalence Ratio GER=3, σ_s is 6.4 ± 0.2 m^2/g. In that case using value σ_s about 10.0 m^2/g as proposed by Tewarson (1995) gives smoke yield smaller by 36% than using value computed from Equation 7, as reported by Widmann et al. (2005).

A comprehensive list of smoke yield obtained in over-ventilated conditions can be found for instance in few review publications (Mulholland, 2008; Tewarson, 2008). However, as mentioned earlier, Mulholland (2008) highlighted that most of that data were obtained during free burning and for small-scale samples. There is lack of data on smoke properties for under-ventilated conditions. Some rare experiments were described already in section 2.1.4.1.2.

2.2.3.4. Smoke generation rate

From the smoke yield and burning rate of a material one can estimate smoke generation rate, which describes how much smoke is produced from a given amount of a fuel being burnt.

$$\dot{G}_j'' = y_j \dot{m}'' \tag{8}$$

where:
$\dot{G}_j''$ - the mass generation rate of product j, for instance smoke (g/m^2s), y_j – yield of product (g/g) defined as grams of product per grams of material burnt $\dot{m}''$ - mass loss rate of material (g/m^2s)

2.2.3.5. Smoke point

Another approach used to determine generation rate of smoke is based on the ‘smoke point’ method. Smoke point is defined as “a minimum laminar axisymetric diffusion flame height (…) at which smoke just escapes from the flame tip” (Tewarson 2002).

Based on this value, generation efficiency of smoke can be derived from the following formula:

$$\eta_s = -\left[0.0515 \ln\left(L_{sp}\right) + 0.0700\right] \tag{9}$$

where:
ηs -generation efficiency of smoke (dimensionless), L_{sp} – laminar smoke point height (m)

Smoke yield for over-ventilated conditions can be calculated from generation efficiency of smoke (η_s), when maximum (theoretical) smoke yield is derived from fuel chemistry (Tewarson 2002):

$$y_s = \eta_s \times \Psi_s \tag{10}$$

where:
y_s – smoke yield (g/g), Ψ_s – maximum theoretical yield of smoke (g/g), based on an assumption that smoke is pure carbon (Tewarson 2002)

Another approach was proposed by Delichatsios (1993) who suggested that smoke yield and smoke point are correlated as follows:

$$y_s = 0.084 \frac{S+1}{L_{sp(mm)}} \tag{11}$$

where:
S – air to fuel mass stoichiometric ratio, $L_{sp(mm)}$ – laminar smoke point height (mm)

There are some discrepancies between equations proposed by Tewarson and Delichatsios, however they give at least some estimation of smoke yield from smoke point measurements. There was no relationship found in the available literature which allows calculation of the smoke yield in under-ventilated conditions based on the smoke point concept.

2.2.3.6. Conclusions on smokiness of a fuel

In conclusion, in this section a few parameters which characterise smokiness of a fuel were discussed. These parameters were based on the light extinction coefficient, which was normalised either by mass loss rate of the sample per volume flow rate or only multiplied by volume flow rate. The former approach gives Specific Extinction Area (SEA), the latter Smoke Production Rate. Moreover, smoke yield and mass generation rate of smoke were described. Finally, smoke point approach was also introduced.

In addition to smokiness of fuel, it is also crucial to establish how smoke affects visibility. That problem will be discussed in the section to follow.

2.2.4. Mass concentration of smoke

It is a common knowledge that smoke reduces visibility but to quantify this phenomenon one needs to describe the amount of smoke being present in a given volume. Parameters presented in previous sections are insufficient for that task and another measure is required: the mass concentration of smoke *(C)*. It describes how many grams of smoke are present in a given volume and it is expressed in grams per cubic metre of gas. Knowing it, one can calculate approximately time to smoke detector activation, visibility, heat flux from smoke, provided that one knows the upper layer temperature and the amount of smoke deposited on internal surfaces (Mulholland and Croarkin, 2000). Mass concentration of smoke can be obtained from gravimetric sampling, although this technique is costly and labour consuming and does not allow continuous readings. Briefly, gravimetric technique requires sampling smoke and collecting it on a filter. If the filter is weighted before and after the experiment, the mass concentration of the smoke in a specific time period may be obtained from the following relationship (Choi et al., 1995):

$$C = \frac{m_s}{V_g} \times \frac{T_\infty}{T_p} \tag{12}$$

where:
C – mass concentration of smoke (g/m^3 of gas); m_s – mass of smoke collected on a filter (g);
T_∞ - ambient temperature (°C); T_p – temperature at the probe or sampling line entrance (°C);
V_g – total volume of sampled gas based on ambient temperature; (m^3)

Continuous measurements of mass concentration of smoke can be performed by employing a tapered element oscillating microbalance (TEOM). It was verified that obtained results are in good agreement with data from filter sampling (Ouf et al., 2008). The main limitation however is the cost of the equipment.

Instead of using that approach, Mulholland (2000) proposed a novel methodology to derive mass concentration from the light extinction measurement without the constraints related to gravimetric sampling. This method complies with the report of Putorti (1999), which gives recommendations on smoke measurements. The formula to obtain the mass concentration using that methodology is:

$$C = k / \sigma_s \quad (13)$$

where: C – mass concentration of smoke (g/m^3 of gas), k – light extinction coefficient (1/m), σ_s – mass-specific extinction coefficient of combustion generated particles (m^2/g)

The underlying assumption is that σ_s is nearly constant for smoke from hydrocarbons in over-ventilated combustion (Mulholland and Croarkin, 2000). This point was discussed in previous section related to smoke yield (cf. section 2.2.3.3). It was highlighted already that it is not valid for under-ventilated fires, as σ_s decreases when there is insufficient air for complete combustion.

Summing up all the previous points, mass concentration of smoke describes how many grams of smoke are present in a given volume of gas and, from it, visibility through given smoke can be estimated, as is shown in the next section.

2.2.5. Visibility in smoke

It is obvious that visibility in smoke is crucial for fire safety. During a risk assessment it is vitally important to predict the visibility range for which the conditions are still tenable. Design of smoke control systems also requires information on visibility requirements.

Nowadays, visibility in a given fire scenario is often predicted from computer models such as Fire Dynamics Simulator (FDS) (McGrattan et al., 2007) These models need reliable input data to compute visibility but next paragraphs present some shortcomings related to visibility determination found in the methodology employed by these models.

Extensive experimental study on visibility in smoke was carried out by Jin (Jin, 1978; Jin and Yamada, 1989; Jin and Yamada, 1990; Jin, 2002). Results of these studies are widely accepted and implemented for instance in FDS (McGrattan et al., 2007) and in the British Standard related to smoke measurements (British Standards Institution, 1998). A simple exit signs visibility model proposed by Jin (2002) is described by the following equations, the first one for self-illuminated signs and the second one for light reflecting signs:

$$Visibility = \frac{1}{k}\ln\left(\frac{B_{EO}C}{\delta_c L_{ill}}\right) \tag{14}$$

where:
Visibility – visibility of signs at the obscuration threshold (m); k – light extinction coefficient (1/m); B_{EO}- brightness of signs (cd/m^2); δc – contrast threshold of signs in smoke at the obscuration threshold (0.01 ~ 0.05); C – mass concentration of smoke (g/m^3 of gas); C= k/σ_s; σ_s – mass specific extinction coefficient (m^2/g); L_{ill} – 1/π of mean illuminance of illuminating light from all directions in smoke (m/m^2)

For reflecting signs the modified equation is valid:

$$Visibility = \frac{1}{k}\ln\left(\frac{\alpha_s C}{\delta_C}\right) \tag{15}$$

where:
α_s – reflectance of a sign

Summing up, visibility in smoke depends linearly on light extinction coefficient and also on mass concentration of smoke (Eq. 15). The latter is related to mass specific extinction coefficient (σ_s). Thus the uncertainty in that parameter is important for visibility assessment.

Nevertheless, a product of visibility and the light extinction coefficient is almost constant, therefore the following equations can be used:

$$Visibility = (5\sim10)/k \text{ (m) for a light emitting sign} \tag{16}$$

and

$$Visibility = (2\sim4)/k \text{ (m) for a reflecting sign} \tag{17}$$

where k – is light extinction coefficient

The constant depends on the reflectance of the sign and brightness of the illuminating light.

Jin (2002) concluded that the second relationship (Eq. 17) may be used not only for visibility of exit signs, but for overall visibility in buildings filled with smoke, but "the minimum value for reflecting signs may be applicable." Unfortunately, British Standard (1998) does not mention that, and states that for overall visibility

the constant equal to 3 shall be used. Moreover, FDS manual (McGrattan et al. 2007) cites only values 3 and 8 for reflecting and self-illuminated signs respectively. There is no mention that these values shall be used with caution since there is not enough validation done so far (Mulholland 2002). Furthermore, FDS is often used to assess the visibility in spaces filled with smoke and using constant value 3 instead of 2 may result in significant over-prediction of visibility. In conclusion, visibility in smoke may be significantly over predicted if incorrect recommendation from British Standard or FDS manual is followed.

Another even more important problem, related to visibility, is hidden in a procedure that is used for instance in FDS to obtain the light extinction coefficient. In FDS, the light extinction coefficient is derived from the mass concentration of smoke (Eq. 13). Subsequently, an inappropriate value of σ_s has a significant impact on the light extinction coefficient and thus on visibility estimation. For instance, FDS uses value 8.7 as proposed by Mulholland and Croarkin (2000). It has been already explained (cf. section 2.2.3.3) what are the implications of that value for underventilated conditions. It was shown that it may result in over prediction of light extinction coefficient and subsequently visibility. According to an estimation presented in section 2.2.3.3, the error for ethane can be about 36%. There is lack of data for another fuels.

The error in the incorrect usage of factor in Eq.17 and possible error in σ_s for underventilated conditions may fortunately cancel itself out but more research is needed to qualitatively compute visibility. To conclude, results from present methods need to be taken with caution.

2.2.6. Conclusions on smoke in fires

In previous sections a few shortcomings related to smoke prediction were presented and the following knowledge gaps were identified:

- Most of previous efforts were related to over-ventilated conditions. However, a majority of fires in enclosures develops to reach the under-ventilated state, when not enough air is available for complete combustion. Consequently, data from previous research may be not accurate when applied for under-ventilated conditions, because smoke particulates differ significantly under various combustion conditions.

- Only two authors gave correlations which enable calculation of smoke yield under fuel rich regime. However, correlation proposed by Widmann et al. (2005) was experimentally validated only for ethane, therefore it cannot be related to other fuels. On the other hand, correlations proposed by Tewarson (2002), should be questioned as well, because they were based on incorrect assumptions, as it was critically reviewed here (for instance constant value of σ_s).
- There is no relationship based on smoke point which enables to calculate smoke yield in under-ventilated conditions.
- Some problems related to mass-specific extinction coefficient were also presented. The implication is that visibility calculated for under-ventilated fires may be incorrect. In addition, determination of visibility in smoke in some CFD software, for instance in FDS, is inconsistent with research efforts, because some assumptions are not valid. As a result, calculated visibility may be higher than in reality, which is crucial for fire protection design of buildings and transportation means, because a significant hazard for occupants may occur.

Taking into account these shortcomings, it is obvious that further research on smoke under fuel-rich conditions is crucial. Consequently, the contribution of this work will be presented both in the chapter devoted to methodology and to results from this research.

Having discussed factors governing smoke production and quantification of smoke the second part of the literature review will be presented. It is focused on production of carbon monoxide in fires.

2.3. Generation of carbon monoxide in fires

This subsection is focused on production of carbon monoxide in fires and discusses various models and engineering correlations used to predict carbon monoxide generation during enclosure fires.

2.3.1. Introduction

The toxicity of carbon monoxide is associated with its affinity to haemoglobin in the blood. Since haemoglobin has a stronger affinity to carbon monoxide (CO) than to oxygen, the amount of oxygen (in the form of oxyhaemoglobin) transported to all tissues decreases when people are exposed to carbon monoxide. Inhalation of this gas may cause incapacitation within a few minutes, and for fully developed fires faster than in 1 minute in a close vicinity of the fire origin (Purser, 2002). Carbon monoxide is tasteless so a victim usually does not know that there is a high concentration of carbon monoxide in the atmosphere; the only signals given by the body are headache or nausea. These symptoms can be rapidly followed by unconsciousness. Time to incapacitation depends also on the volume of air breathed, because the amount of carbonhaemoglobin depends linearly on it. For instance, the time to incapacitation for children is shorter than for adults (Purser, 2002) because the ratio of volume of air breathed to kilogram of body mass is greater. Finally, even after successful recovery of a victim, carbon monoxide is responsible for delayed neuropsychiatric sequels, described in various references (Christian and Shields, 1998; Kondo et al., 2007). These symptoms can occur within a few days, or several weeks after an incident, and are related to changes in the brain structure. As a result many severe disorders can develop, such as “lethargia, behaviour changes, forgetfulness, memory loss and Parkinsonian features” (Mannaioni et al., 2006).

Having briefly introduced risks associated with toxicity of CO during fires, relevant research on that subject will be discussed in the sections to follow.

2.3.2. Predicting carbon monoxide yields/concentrations

Numerous attempts have been made to predict carbon monoxide formation within enclosure fires over last fifty years. The earliest correlations were proposed in a Fire Research Note prepared in 1966 (Rasbash and Stark, 1966). These early “crude correlations” were based on a ventilation criteria and a fuel load, however

this study was consequently criticised as “fire behaviours in these studies have not been adequately assessed, and the utility of these correlations for actual fires is limited” (Pitts, 1990).

Newer studies which started to emerge in early nineties resulted in a better understanding of CO formation and improved methods to predict that process. These methods will be discussed in the following subsections.

2.3.2.1. Zeroth order approximation

The simplest, “zeroth order approximation” was proposed by Mulholland, referred by him as “Two level CO model” (Mulholland, 1990a; Mulholland, 1990b). He suggested that CO yield should be taken as one constant value for over ventilated conditions and as another constant for under ventilated conditions after flashover. The proposed values for wood burning are given below in Table 2 (Mulholland, 1990b).

Table 2. Two level carbon monoxide model proposed by Mulholland (1990b)

Stage of a fire	Molar CO/CO_2 (-)	CO yield (g/g)
Pre-flashover	0.002	0.002
Post-flashover	0.5	0.3

He suggested that for fires of plastics one should use 0.2 g/g for post flashover conditions with the exception of PMMA and other oxygen containing plastics. For oxygen containing plastics he suggested 0.3 g/g.

2.3.2.2. Models based on Global Equivalence Ratio

More advanced approaches taking into account different ventilation conditions will be introduced in sections to follow. These are based on the relationships between the Equivalence Ratio and yield of carbon monoxide. Studies that will be mentioned in the next subsection have been reviewed in various publications recently (Gottuk, 1992; Pitts, 1995; Forell, 2007) and therefore will be only briefly described without a detailed analysis.

2.3.2.2.1. Correlations derived from hood experiments

The first attempt to correlate carbon monoxide (and other species) with the equivalence ratio was done by Beyler (1983; 1986a; 1986b). His experiments were designed to imitate two layer combustion conditions in a compartment fire by trapping fire products in a hood above the fire. Fire size and distance between fire and hood were systematically varied thus enabling controlling entrainment rate of air before it reached the hood. In addition, fuel vaporization was known from mass loss measurements thus plume equivalence ratio could be calculated defined as mass of fuel volatilised to mass of air entrained into the fire plume normalised by stochiometric fuel of air ratio. Another equivalence ratio was defined as upper layer equivalence ratio, i.e. ratio of fuel to air in the upper layer. For steady state conditions both these equivalence ratios were equal, and that was called later on by Pitts as a Global Equivalence Ratio (Pitts, 1995).

The major conclusions from Beyler's research are listed below, cited after Pitts (1994b):

1) 'major chemical species (including CO) trapped in a hood located above a fire burning in an open laboratory can be correlated in terms of the global equivalence ratio';

2) CO concentrations are constant below $\Phi < 0.5$ and above $\Phi > 1.3$;

3) Much more CO is generated in underventilated conditions compared to fuel lean combustion;

4) He observed fuel dependency of CO formation for underventilated conditions, which could be explained based on fuel structure, for example oxygen containing fuels created larger amounts levels of CO

5) He was also trying to investigate effect of the residence time on carbon monoxide yield (Beyler, 1986a) .

These relationships were further investigated at California Institute of Technology by Zukoski et al. with a slightly modified setup (Zukoski et al., 1985; Zukoski et al., 1989; Morehart et al., 1991). The modification enabled addition of extra air to the upper layer thus enabling creation of conditions where $\Phi_{upper\ layer} < \Phi_{plume}$. Moreover, the different designs resulted in lower temperatures of the upper layer which was attributed to some differences in results. That enabled to

hypothesise that upper layer temperature has also significant contribution to carbon monoxide formation.

2.3.2.2.2. Correlations proposed by Tewarson

Some explanation of the terminology used by Tewarson is required prior to description of his correlations. It is worth noting that he initially used a reciprocal value of equivalence ratio, i.e. air-to-fuel or oxygen-to-fuel normalised mass ratio called by him as 'ventilation parameter' (Tewarson and Steciak, 1983) and then 'stochiometric fraction' (Tewarson, 1984) yet still denoted with Greek letter Phi, *Φ*. He changed it in more recent publications (Tewarson et al., 1993; Tewarson, 2008) to the term 'local equivalence ratio' expressed as fuel to air normalised mass ratios, again labelled Phi. Therefore some confusion may arise when his older publications are compared with his more recent ones.

Tewarson (1993; 2008) proposed fuel dependent correlations for normalised carbon monoxide yields for some selected polymers. Six common, synthetics polymers and one natural (wood) were investigated by him in Fire Propagation Apparatus (ASTM, 2003). Unique design of that apparatus allowed him to vary air supply thus to modify Equivalence Ratio (Tewarson and Steciak, 1983). He concluded that, the generation of CO_2 decreases and generation of CO and smoke (for his correlations on smoke refer to section 2.2.3.3) increases for higher equivalence ratios. Moreover, his correlations for CO_2 are not dependent on chemical structure of fuels, whereas they are dependent for CO and smoke. An adaptation of Tewarson's data is presented below (Figures 10-12). Values of well ventilated yields were taken from his tabulated database (Tewarson, 2008) and his correlations presented below were used:

$$\frac{(y_{CO})_{vc}}{(y_{CO})_{wv}} = 1 + \frac{\alpha}{\exp\left(2.5\Phi^{-\xi}\right)} \tag{18}$$

$$\frac{(y_{CO_2})_{vc}}{(y_{CO_2})_{wv}} = 1 - \frac{1}{\exp(\Phi/2.15)^{-1.2}} \tag{19}$$

Table 3. Fuel dependent factors for carbon monoxide yields correlations (Tewarson, 2008)

	CO	
Material	α	ξ
PS	2	2.5
PP	10	2.8
PE	10	2.8
Nylon	36	3.0
PMMA	43	3.2
Wood	44	3.5
PVC	7	8.0

In addition, he recently suggested (Tewarson, 2008) a constant factor between y_{co}/y_s for overventilated burning of hydrocarbons, equal to 0.34 ± 0.05 (g/g). Author's earlier research (Ukleja et al., 2009) suggested however that this value is not applicable for underventilated combustion, at least for propane.

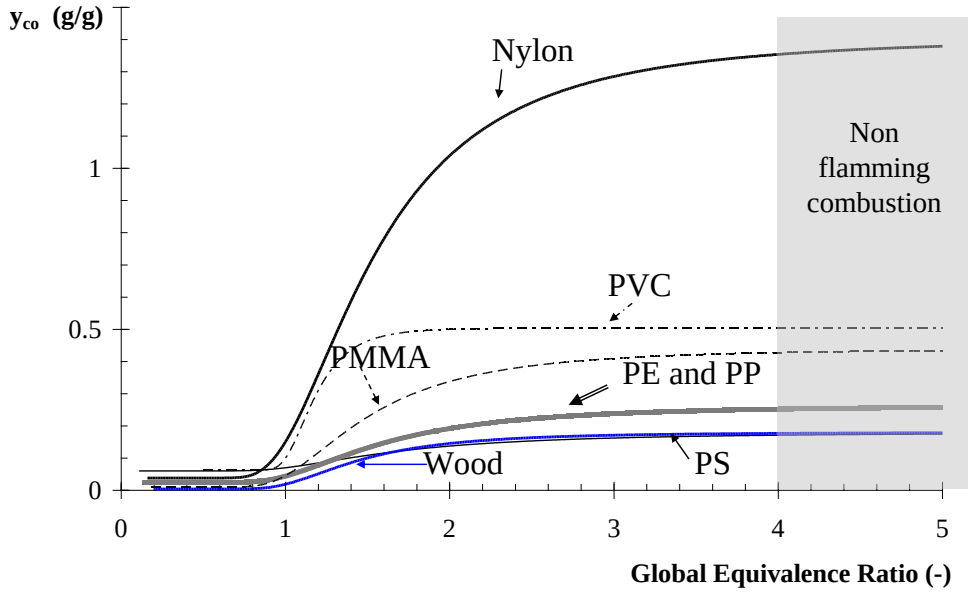

Figure 10. Correlations for non normalised yields of carbon monoxide for 7 polymers. (Tewarson, 2008)

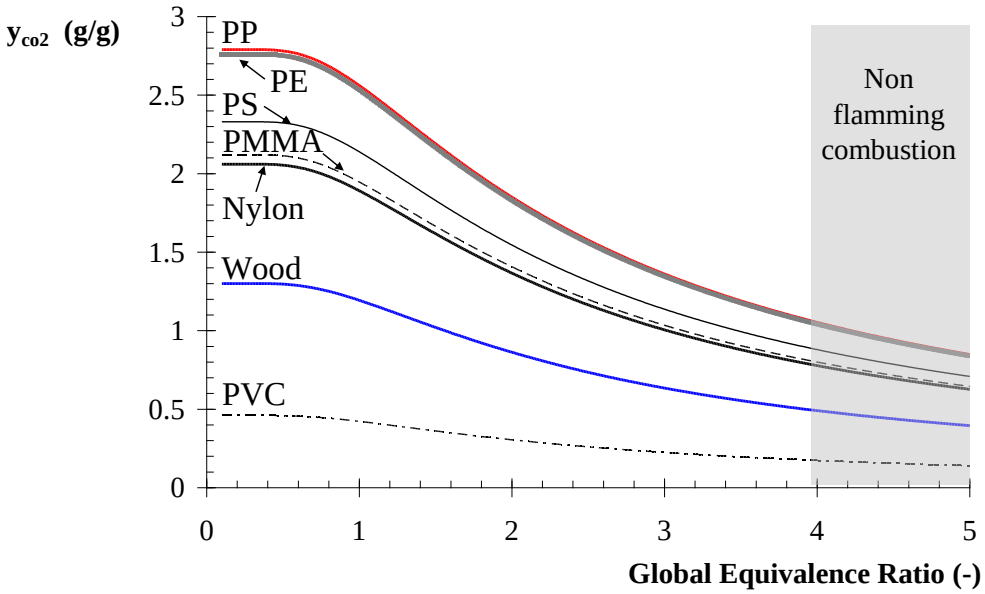

Figure 11. Correlations for non normalised yields of carbon dioxide for 7 polymers (Tewarson, 2008).

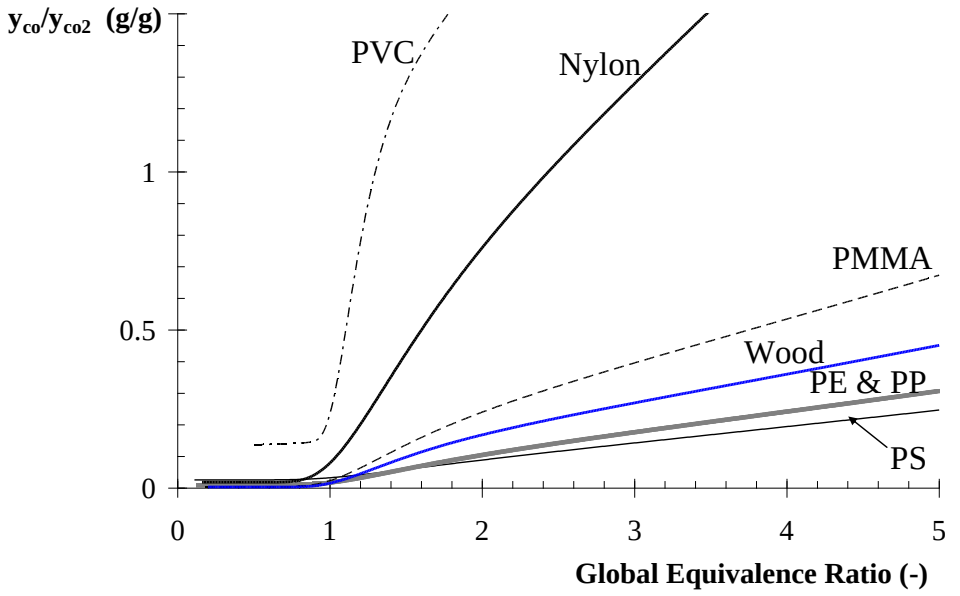

Figure 12. Correlations for non normalised ratios of carbon monoxide to carbon dioxide yields for 7 polymers (Tewarson, 2008).

2.3.2.2.3. Gottuk's engineering methodology

Gottuk and Roby proposed an engineering methodology, published for the first time in 2nd edition of SFPE Handbook (Gottuk and Roby, 1995) and then amended by Gottuk and Lattimer in subsequent editions (2002, 2008).

That model takes into account a few phenomena, including upper layer temperature and occurrence of the external burning. The main correlation proposed

by them is GER dependent. For that correlation with GER, they have proposed two equations. The choice of these equations depends on upper layer temperature limit <800K or >900K. The correlation for lower temperature limit (Eq. 20) is based mainly on Beyler's experiments in hood with hexane, whereas Eq. 21 is based on Gottuk's study in a compartment with separated inflow of air. That design allowed him to derive accurate information about mass of air entrained and thus the plume equivalence ratio (Gottuk, 1992; Gottuk and Lattimer, 2002).

Equations correlating yields of carbon monoxide with Global Equivalence Ratio are presented below with two temperature criteria (Gottuk and Lattimer, 2008) and are plotted in Figure 13.

For T < 800K

$$y_{CO} = (0.19/180)\tan^{-1}(X) + 0.095 \qquad (20)$$

Where:

$X = 10(\Phi - 0.8)$

$\tan^{-1}(X)$ is in degrees

For T > 900K

$$y_{CO} = (0.22/180)\tan^{-1}(X) + 0.11 \qquad (21)$$

where :

$X = 10(\Phi - 1.25)$

$\tan^{-1}(X)$ is in degrees

The above methodology presents non-normalised yields of CO as authors argued that these yields are independent of the fuel. According to these authors, their methodology may not give the maximum levels of yields but generally provided good results.

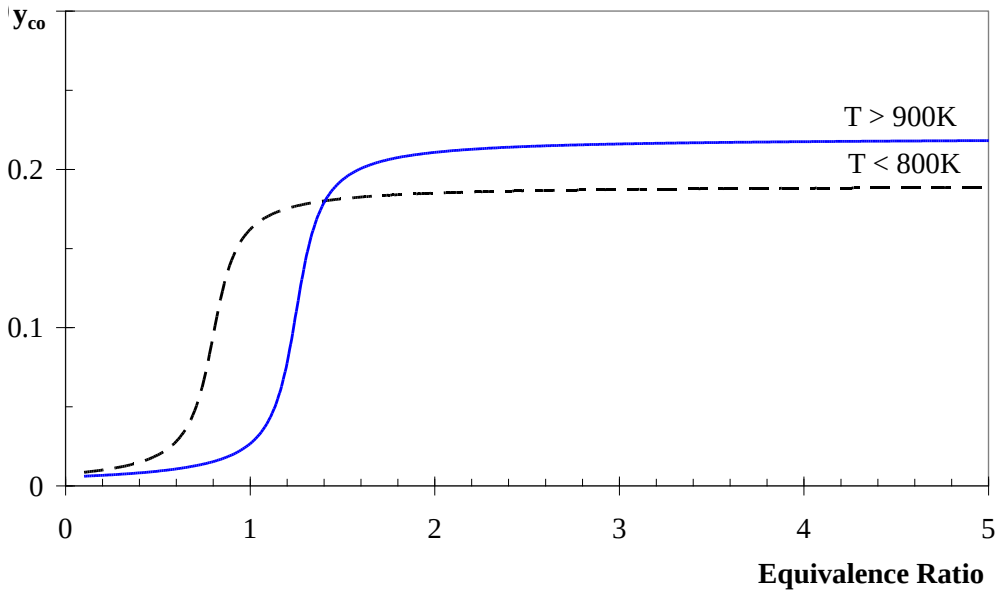

Figure 13. Correlations for carbon monoxide yields (fuel independent) (Gottuk and Lattimer, 2008).

2.3.2.2.4. Algorithm of Pitts

Pitts has studied carbon monoxide production for many years and his review (Pitts, 1995) analysed most of the previous research on that topic. However, he extended the initial concept over following years resulting in publication of an algorithm for CO production in enclosure fires (Pitts, 1997). He did not propose any quantitative correlations but tried to explain governing mechanisms. The main ideas are described below.

The first factor governing CO production was called by him the Global Equivalence Ratio (GER) concept, based on hood experiments described in previous sections. According to Pitts, CO yields can be correlated with GER. That correlation is fuel dependent but can be generalised between different groups of fuels. However, the GER concept can not capture other phenomena which govern CO production. One has to consider additional three different mechanisms explained by Pitts that are listed below:

- direct entrainment of fresh air into hot upper zone
- pyrolizing of wood in hot upper zone
- formation of additional CO in upper zone with very high temperatures close to chemical equilibrium

However, he discovered later (Pitts, 2001) that there was a numerical error in some calculations on which he based his assumptions regarding GER concept in

large scale tests. It did not invalidate his general algorithm however he concluded that GER cannot be globally calculated based on ‘on the fuel mass flow rate and the air flow rate through the doorway’ (Pitts, 2001). According to him some part of the fresh air will not ‘molecularly mix’ with hot vitiated gases therefore new approach to GER is required ‘to include only the mass of air that is directly mixed into the upper-layer combustion gases by entrainment into the fire plume and/or the upper layer’ (Pitts, 2001). In more recent personal communication with Forell he suggested ‘discrete equivalence ratios for the plume, the upper layer and the compartment’ (Pitts, 2007).

2.3.2.2.5. Wieczorek’s correlation

Study performed by Wieczorek et al. (Wieczorek, 2003; Wieczorek et al., 2004a; Wieczorek et al., 2004b) gave a new insight into the carbon monoxide generation in compartment fires. H main conclusions were as follows:

- There is no uniformity of gaseous species concentration in the upper layer even for underventilated fires (Wieczorek et al., 2004b) as opposed to generally assumed well mixed conditions inside upper layer.
- GER concept is not adequate to fully describe formation of carbon monoxide in compartment fires.
- There is dependency of the CO yields on the opening width, not fully captured by GER concept.
- Effect of external burning due to flame extensions can be quantified using new non dimensional HRR, a parameter introduced by Wieczorek. He was able to correlate carbon monoxide yields generated inside the compartment with the new non dimensional HRR.

The above conclusions will be discussed in the following paragraphs.

Lack of uniformity of the gaseous species was concluded from detailed mapping of species concentration in the exit plane done by Wieczorek. He was sampling at different locations in the exit plane and clearly confirmed spatial variations (Wieczorek et al., 2004b) as opposed to generally accepted assumption that gases are well mixed in the upper layer with homogenous concentration. These results were crucial for design of gas sampling system employed for the present study. It will be further explained in the chapter describing the methodology used.

Results obtained by Wieczorek (c.f. Figure 3 in (Wieczorek et al., 2004a)) led him to formulate second claim from the list above, namely that GER concept is not adequate to fully describe formation of carbon monoxide in compartment fires. Moreover, opening width is affecting CO yield, as averaged data did not collapsed into single curve, but separate opening widths created three separate curves as function of the Global Equivalence Ratio.

He claimed that external burning caused by flame extension is playing an important role in CO formation. He observed flames outside for GER < 1 , i.e. for over-ventilated conditions. To account for that he introduced a non-dimensional Heat Release Rate, as defined below:

$$\tilde{Q} = \frac{\dot{Q}_{ideal}}{\dot{Q}_{Flame\_extensions}} \tag{22}$$

where $\dot{Q}_{ideal}$ (kW) is a product of mass loss rate of a fuel (g/s) and Heat of combustion of a fuel (kJ/g) and $\dot{Q}_{Flame\_extensions}$ is the minimum theoretical Heat Release Rate (kW) for flame tip to reach the compartment opening.

In his thesis and subsequent papers he established this value from visual observation during the tests, interpolating between tests without flames outside and with flames outside. However he has proposed a correlation to derive $\dot{Q}_{Flame\_extensions}$ based on earlier work of Hasemi (1995) and Pchelintsev (1997). Wieczorek has adapted the correlation to suit confined plumes, taking into account that "air entrainment into the base of the flame does not occur via the full 360° circumference of the fire plume". He proposed a β factor equal to 90, 120 or 180° for different sizes of doorway width. The final equation is presented below:

$$\dot{Q}_{Flame\_extensions} = \left(\frac{\beta}{360°}\right) 1090 H_{p-c}^{2.5} \left(0.3266 \sqrt{\frac{1}{2.866}\left(\frac{L_f}{H_{p-c}}\right)} \right) \tag{23}$$

where: $H_{p\text{-}c}$ is the distance from top of the pan (burner) to ceiling and L_f is the length of the flames below the ceiling

However, he has not validated the equation experimentally and used visual observation to determine $\dot{Q}_{Flame\_extensions}$. Based on that he was able to correlate yields

of carbon monoxide with the new non dimensional Heat Release Rate ($\tilde{Q}$). However it must be stressed that he calculated yields of carbon monoxide generated only inside the compartment without effect of reactions outside. Therefore it can be considered as only "boundary conditions" at the exit of the compartment and therefore offers limited value for engineering calculations (Forell, 2007).

The other limitation of Wieczorek's methodology was pointed out by Forell (2007). He stressed that gas sampling during Wieczorek's research was done from inside the flame zone during some tests and the sampling probes were not water cooled. It had been shown earlier by Beyler (1986b) that sampling without water-cooling from inside the reaction zone gives higher CO levels, because not cooled probes may result in conversion of unburnt hydrocarbons into carbon monoxide. Beyler gave some examples from earlier work of Gross and Robertson during which both cooled and uncooled probes were used. "The uncooled probe measured 4.1% CO, 7.4% CO_2 and 12.8% O_2, while the cooled probe measured 1.2% CO, 1.5% CO_2, and 20.4% O_2 (all measured on a dry basis)" (Beyler, 1986b). Taking that into account, one has to take with caution the Wieczorek's correlation of CO mole fractions to $\tilde{Q}$ presented in Figure 14. There was not found any further evaluation of Wieczorek's methodology in the available literature.

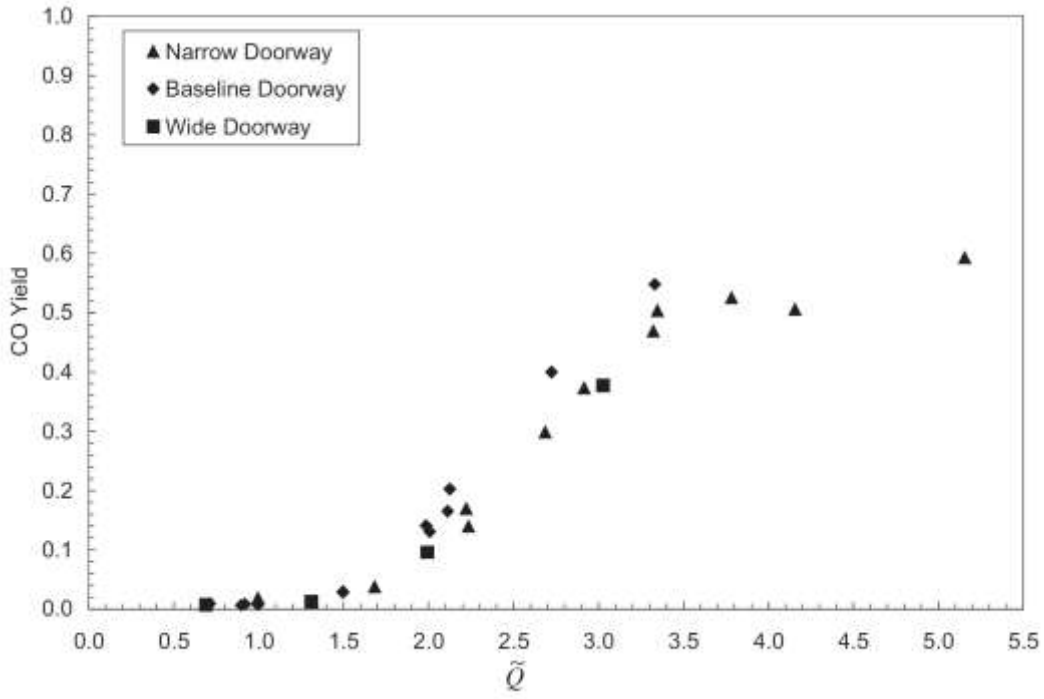

Figure 14. Carbon monoxide yields (based only on fuel consumed within the compartment) as a function of $\tilde{Q}$. Reprinted from Wieczorek et al. (2004a) with permission.

2.3.2.2.6. Forell's research

Further evaluation of Global Equivalence Ratio concept was done by Forell (2007; Forell and Hosser, 2007). He summarised previous efforts of using GER to predict CO production in compartment fires and critically evaluated models up to date. His extensive literature review led him to extend Beyler's ignition index (Beyler, 1984) to predict the occurrence of external burning – as a strong reducer of the amount of CO measured outside of the fire compartment. He was analysing different methodologies to predict external burring and flame extensions and concluded that expanded Ignition index introduced by Beyler in 1984 gives the best results. He used that approach with FDS simulation (ver 4) to assess the viability of ignition index to predict external burning.

2.3.2.2.7. NIST research on medium and large scale, underventilated compartment fires

Another important contribution was done by researchers at NIST. They examined generation of combustion products in compartment fires, both at reduced scale with moderate HRR <1 MW (Ko et al., 2009) and at full scale inside an ISO 9705 room with large HRR (Lock et al., 2008).

These studies attempted to correlate mixture fraction (Bilger, 1977) with generation of different combustion products taking into account carbon monoxide and soot. Mixture fraction is directly related to equivalence ratio (Ko et al., 2009) therefore comparison can be easily made with correlations based on GER.

Figure 15 shows data from experiments in a reduced scale enclosure (0.98 m wide, 0.98 m high and 1.46 m deep) for three different fuels. Presented data show large scatter, at least for heptane, and consequently proposed linear relationships have to be taken with caution.

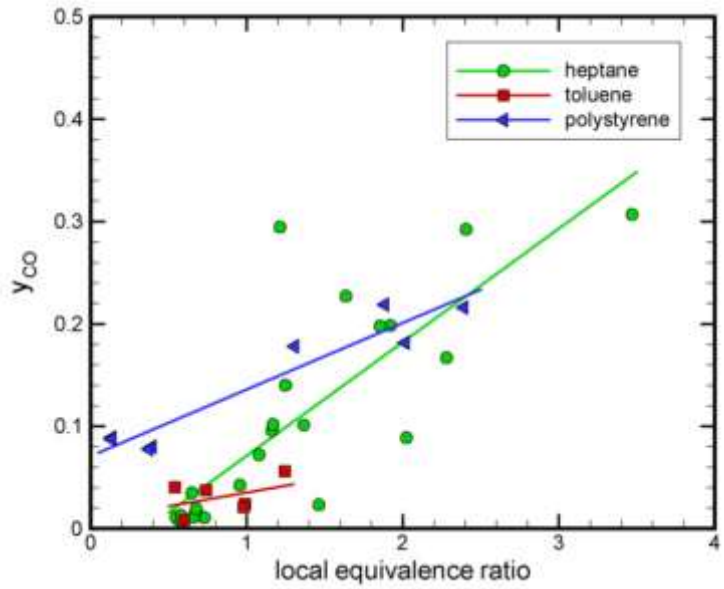

Figure 15. Carbon monoxide yield as a function of Local Equivalence Ratio in a moderated scale experiments at NIST. Reprinted from Ko et al. (2009) with permission.

2.3.2.3. CO yields derived from small scale tests

Another approach is to establish correlations, usually fuel dependent, based on small scale bench tests, for example from the Purser tube (British Standards Institution, 2003). This approach, which is being favoured by toxicology models was criticised for example by Babrauskas (1995). He argued that carbon monoxide yields are not fuel dependent in large scale compartment tests and hardly exceeds 0.2 g/g for underventilated conditions. According to him, data from large and intermediate scale tests indicate that "there is only a very small effect of fuel chemistry on CO yield […] Thus conducting bench-scale tests on different products or materials to quantify a variable which hardly varies is not necessary" (Babrauskas, 1995).

On the other hand, Stec et al. (2009) published recently a comparison of the results from the tube furnace with larger scale tests and found a good agreement, at least for polypropylene and polyamide 66. Yet, no quantitative correlations have been proposed.

Another comparison between small and large scale test of polypropylene and polyamide 66 was published by Andersson et al. (2005). Their data are presented in Figure 16, however agreement between small and large scale data was found only for simple "pool" fire configuration in the large scale. No correlations were found when samples were installed (in the large scale) on the ceiling or on the walls.

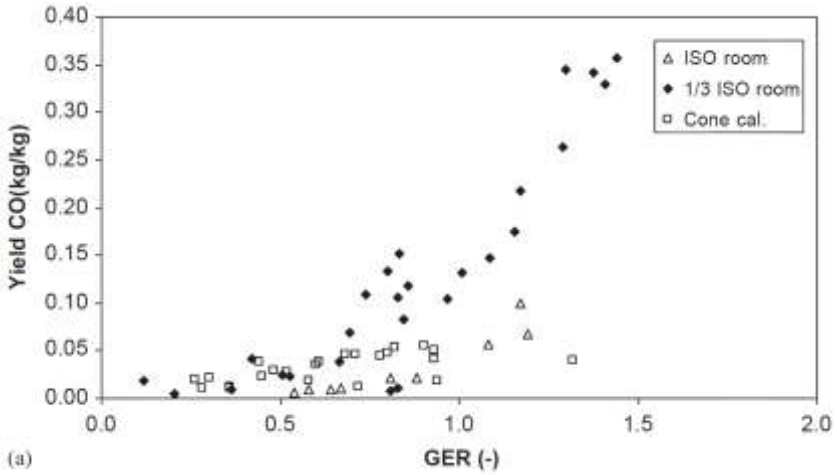

Figure 16. Comparison of CO yields from tests at different scales. Reprinted from Andresson et al. (2005) with permission.

2.3.3. Conclusions on carbon monoxide generation in fires

Having reviewed literature on carbon monoxide production in enclosure fires, it can be concluded that one cannot rely on data obtained from small scale tests only. Fuel dependent models derived from small scale tests cannot address many factors governing CO production listed for instance by Pitts (1997) and in newer publications. Factors that cannot be addressed by small scale test include: effect of external burning or flame extensions, upper layer temperature, incomplete molecular mixing of the available air with fuel, residence time and the effect of adjacent space. In conclusion, bench scale tests may be useful for evaluation toxic potency of a material but not to provide input parameters for carbon monoxide yields for large scale models.

At the end of this literature review on smoke and carbon monoxide production in enclosure fires, one can easily conclude that many factors governing smoke and carbon monoxide production are interdependent. That will be discussed in the next subsection.

2.4. Generation of carbon monoxide in relation to smoke production

Production of smoke and carbon monoxide depends on many factors, as disused in the preceding sections, yet there are still lots of gaps in the current knowledge. However, many of these governing factors are similar for both smoke and carbon monoxide. Question may arise if there is any cross correlation between carbon monoxide and smoke production?

There are a few sources giving correlation in relation to **overventilated** conditions, these are listed in Table 4. However, no publication has been found that reports successful relationship between smoke and carbon monoxide for underventilated conditions. In fact the contrary has been shown by some researches. For instance, Leonard et al. (1994) reported that for underventilated fires CO yield was insensitive to fuel structure (for ethylene and methane) whereas smoke yield was affected, thus there was no proportionality at all between y_s and y_{co}. Similarly, Ouf et al. (2008) studied three different fuels for GER range from 0.009 to 0.547. They reported CO/soot ratio rising from 0.1 to 3 for the investigated range of GERs.

On the other hand, different behaviours were reported by Tolocka et al. (1999). They showed an increase in CO for higher temperatures as a result of oxidation of soot (thus a decrease in concentration of smoke) for richer equivalence ratios (Figure 17). It may suggest that the increase in CO may result in the decrease in smoke concentrations for higher temperatures.

Table 4. Correlations between yield of smoke and yield of carbon monoxide for overventilated conditions

Publication	Details of correlation between smoke and CO
(Friedman, 1986)	"the ratio of optical density to CO concentration is not absolutely constant from material to material, but varies by about a factor of three in the most extreme cases".
(Köylü and Faeth, 1991)	$y_s=(2.7\pm0.7) * y_{co}$
(Mulholland et al., 1991b)	$y_s=(2.3\pm0.4) * y_{co}$
(Tewarson, 2007)	$y_s=(2.94\pm0.43) * y_{co}$

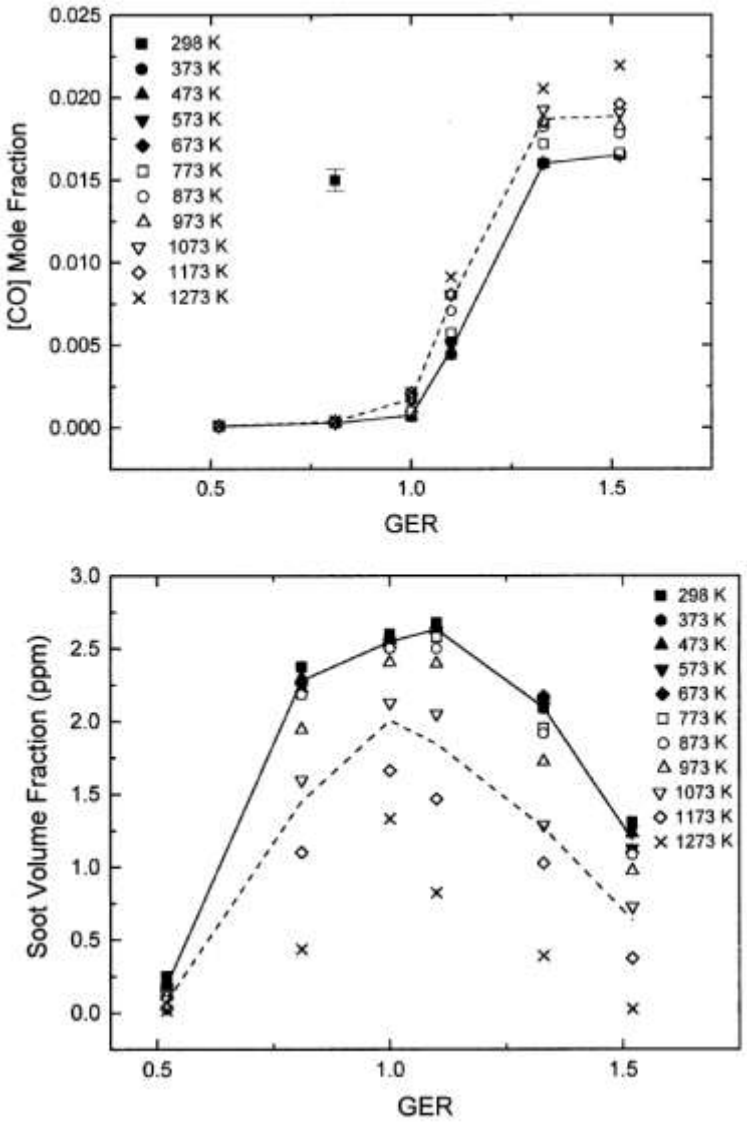

Figure 17. Generation of CO (top) and smoke (bottom) in underventilated conditions for different temperatures. Figure reprinted from Tolocka et al. (1999) with permission.

Finally, a short comment is required on data from large scale experiments performed recently at National Institute of Standard and Technology (USA). Ko et al. (2009) claimed that their results were showing steady ratio between y_{co} and $y_{s.}$ Their compared these data with correlation of Köylü and Faeth (1991). However closer examination of data published by Ko et al. (Figure 18) reveals that their claim should be taken with caution especially for heptane. On the other hand, their data confirm that claim reasonably well for polystyrene and toluene at least for range of conditions tested. Therefore further research is needed to examine relation between y_{co} and y_s during underventialted fires.

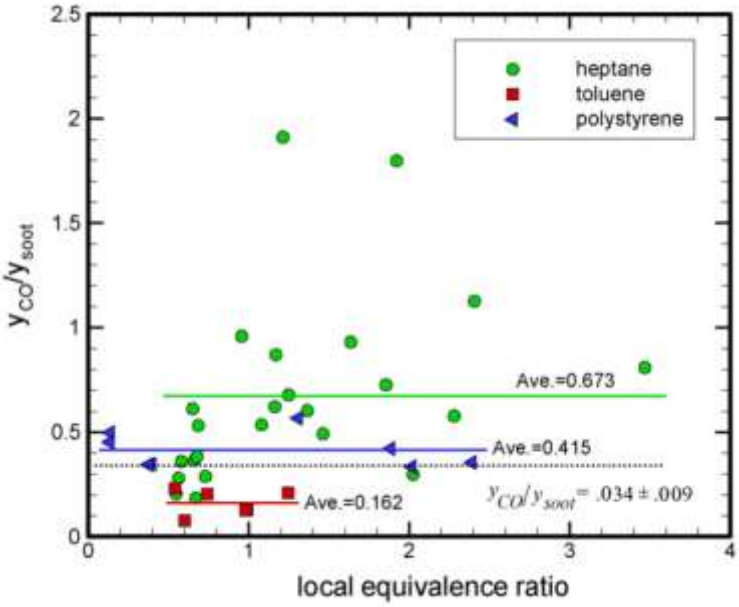

Figure 18. Ratio of carbon monoxide yield to soot yield as a function of Local Equivalence Ratio in moderated scale experiments at NIST. Reprinted from Ko et al. (2009) with permission.

2.5. Working hypothesis on factors affecting smoke and carbon monoxide production

Having reviewed the literature on smoke and carbon monoxide production, a working hypothesis has been formulated that smoke production depends not only on the fuel and Equivalence Ratio but also on the temperatures and residence time inside the enclosure. In addition, it seems that CO and smoke production may be interdependent during underventilated fire, as CO production depends on similar factors.

The examination of both hypotheses was accomplished by set of experiments following the methodology described in the next chapter.

CHAPTER THREE

Experimental methodology

3.1. Introduction

This chapter describes the methodology used during this project. It starts with general information about the experimental rig which was used, then discusses in more details all components including novel parts designed during this work, namely laser smoke meters. Thereafter details of gas sampling techniques are given together with limitations. Next sections focus on calibration procedures and repeatability along with assessment of uncertainty. Finally, recommendations for future improvements are given.

3.2. General layout of experimental rig

This section describes the experimental rig used during the experiments. It also explains why certain experimental procedures were used and shows links between the present approach and other methods found in the literature.

Experiments were performed in a corridor-like enclosure, 3 m long x 0.5 m high x 0.5 m wide. The enclosure was constructed from six cubic sections (A to F) connected together, as illustrated in Figures 19-22.

Dimensions of the enclosure were chosen to resemble a typical corridor however without any reference to any real scale design. Therefore no scaling was performed and only a width to length ratio was selected to match ratio from a typical corridor.

The inner walls were insulated with Unifrax board, having thickness of 0.04 m thus allowing high temperature resistance. The inflow of air was varied by using five different door-like (without sill) openings sizes in the front panel having dimensions (widths and heights, respectively): 0.075 m x 0.2 m, 0.075 m x 0.3 m, 0.1 m x

0.25 m, 0.2 m x 0.2 m and 0.25 m x 0.10 m. These openings sizes were chosen to systematically vary amount of available air.

The fire was produced by a propane sandbox burner (0.1 m x 0.2 m having the longer side parallel to the opening) flush with the floor of the corridor, located in the centre of the last box at the closed end (Box F). The fuel flow rate and hence the theoretical heat release rate was set by a mass flow controller. The theoretical HRR were chosen to systematically vary the amount of fuel in relation to amount of available air.

In the following subsections the experimental measurements will be discussed.

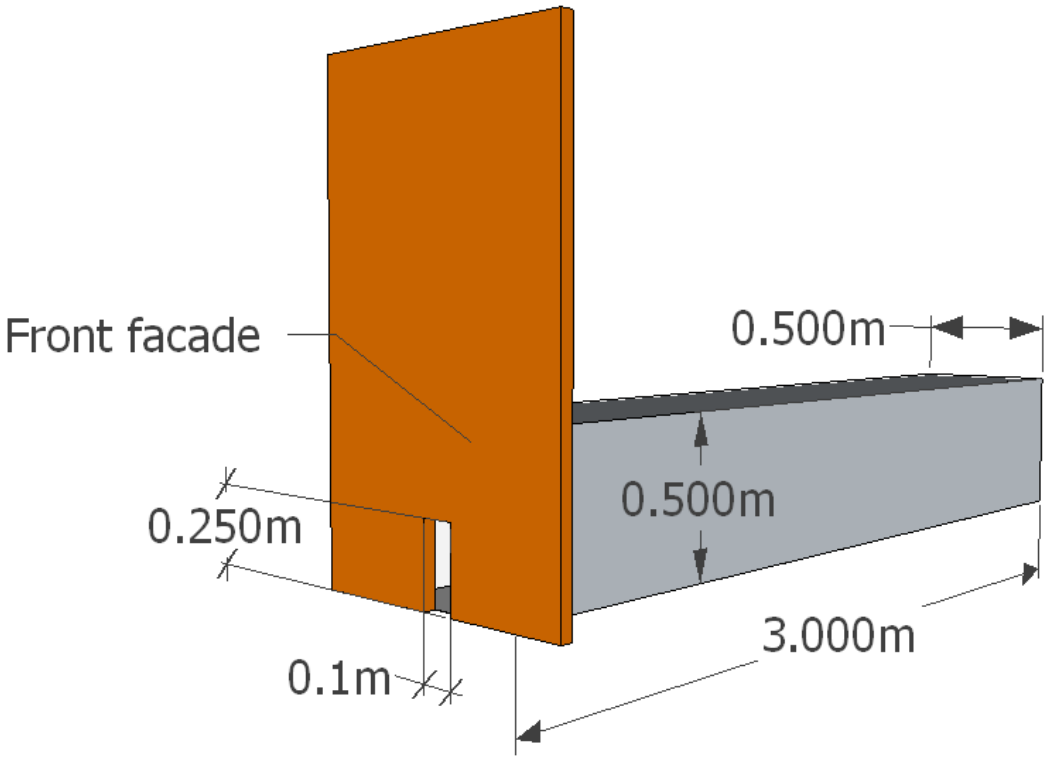

Figure 19. General view of the experimental rig. One sample size of the opening is shown

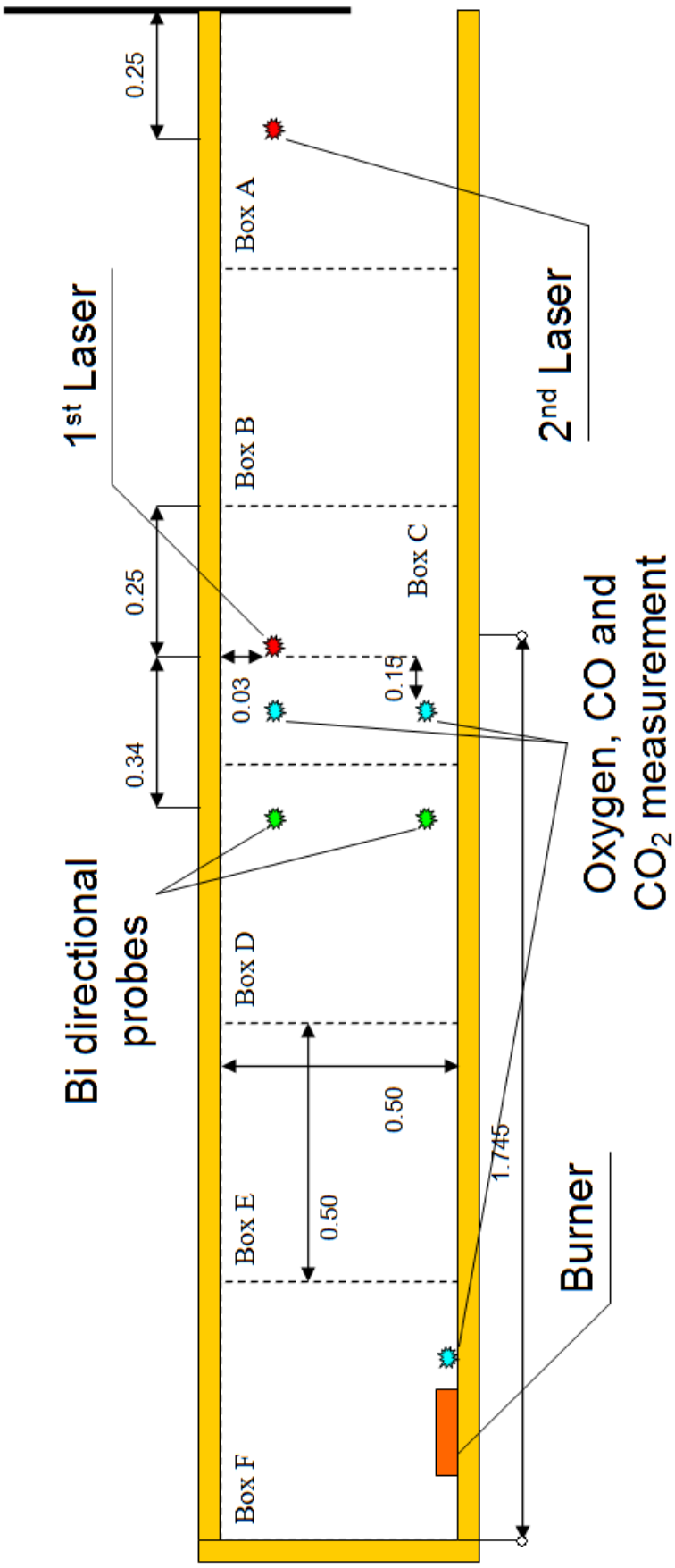

Figure 20. Side view of the experimental compartment (all dimensions in metres)

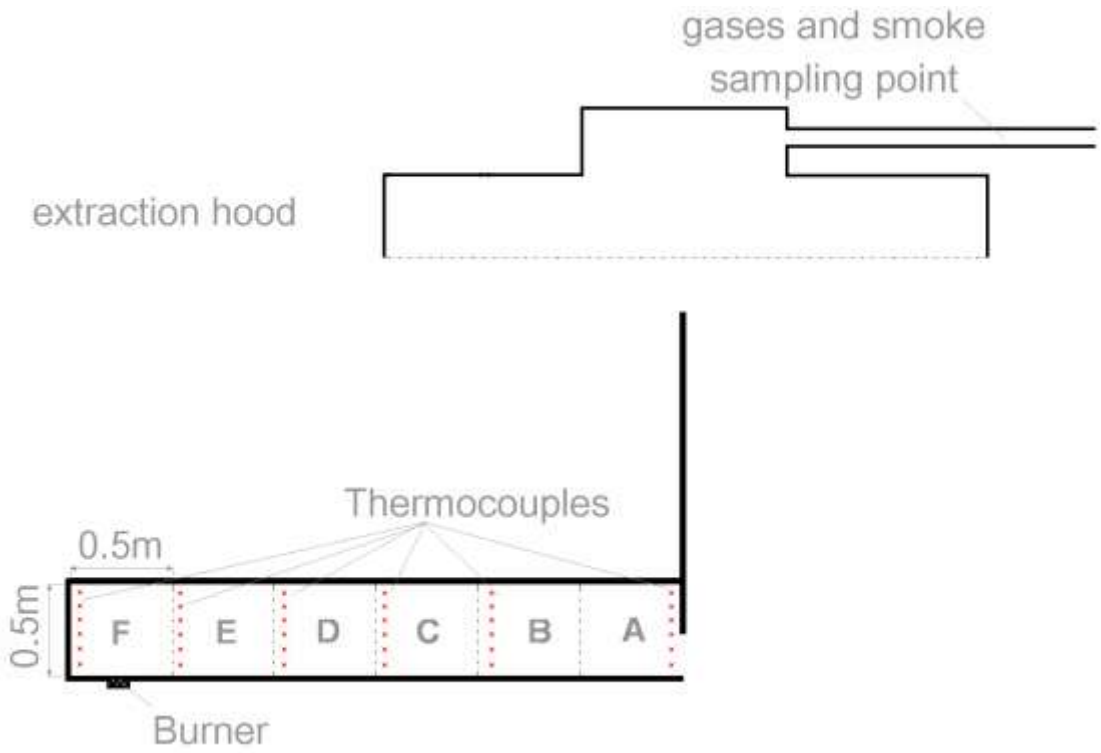

Figure 21. Location of the experimental rig under the 3 metre extraction hood. Figure shows also thermocouples arrangements and location of gases/smoke measurement in the exhaust duct

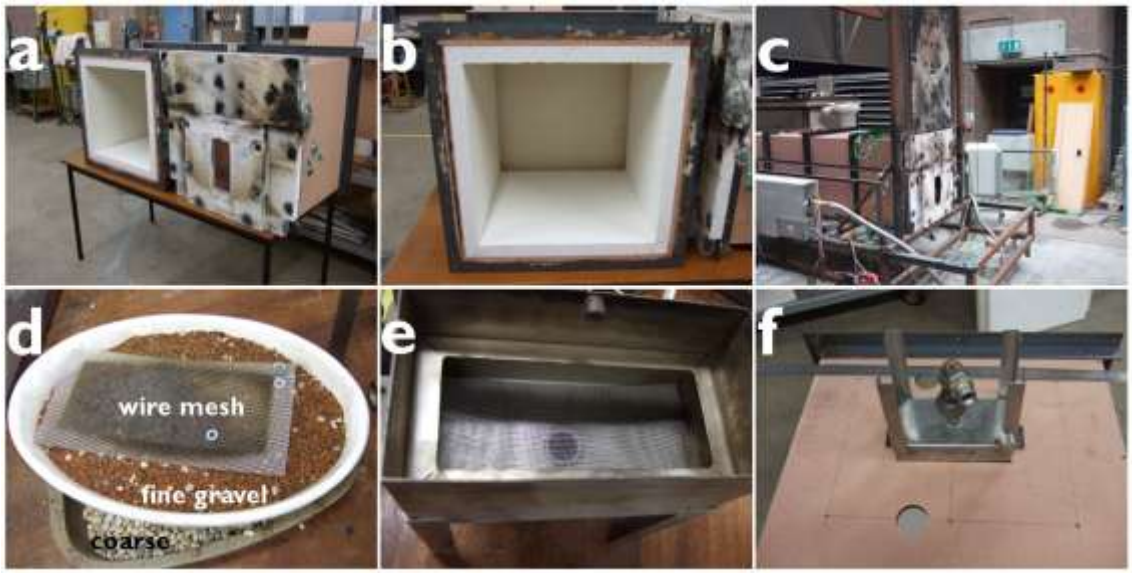

Figure 22. Photos from the construction of the experimental rig. a) separate boxes during construction, b) thermal insulation of a single box c) corridor assembled on the rig with front façade d) two types of gravel used in the burner e) empty gas burner with wire mesh f) installation of the burner below the box (box upside down for installation only)

3.3. Performed measurements

This section describes various measurement techniques employed in this research. Explanation with links to similar methods in literature as well as novel approaches will be covered in the following subsections.

3.3.1. Laser smoke meters for measurements inside the enclosure

Quantification of smoke can be done by two different techniques: either gravimetrically or by measurement of light extinction by smoke (Ostman, 1996; Whiteley, 2008; Levchik et al., 2011). Gravimetric sampling can provide information on mass concentration of smoke, namely on the mass of soot particulates in a given volume of fire effluents. On the other hand, light extinction measurements allow quantification of smoke based on obscuration of visible light by smoke particulates. This non-intrusive technique is much easier to implement and more importantly can provide information instantaneously. Therefore, during this research, measurements based only on light extinction were performed in order to obtain smoke information as a function of time.

Light extinction measurements are commonly performed downstream of a compartment, usually in the exhaust duct, after the effluents are well mixed with fresh air and collected by a collection hood (Mulholland, 1982; Mulholland et al., 2000). This approach is also prescribed by some internationals standards (ISO, 1993; Babrauskas, 2002; European Committee for Standardisation, 2002; British Standards Institution, 2007).

Only a few publications in the literature described measurements of smoke directly inside a compartment or an enclosure (Bundy et al., 2007; Abecassis Empis et al., 2007; Lock et al., 2008). Smoke measurements inside enclosure can provide additional information yet previous publications left space for improvement in the experimental methodology. Therefore, this study was aimed to expand the knowledge about smoke production inside the enclosure by improving measurement techniques.

3.3.1.1. Design of corridor smoke meters

Two laser smoke meters designed for this study were constructed and employed during this research. The present design was based on the Putori's recommendation

(Mulholland, 1982; Mulholland et al., 2000; 1999). The initial design of the smoke meter incorporated a beam splitter and two detectors to check for any intensity fluctuations in the laser beam (Figures 23-24).

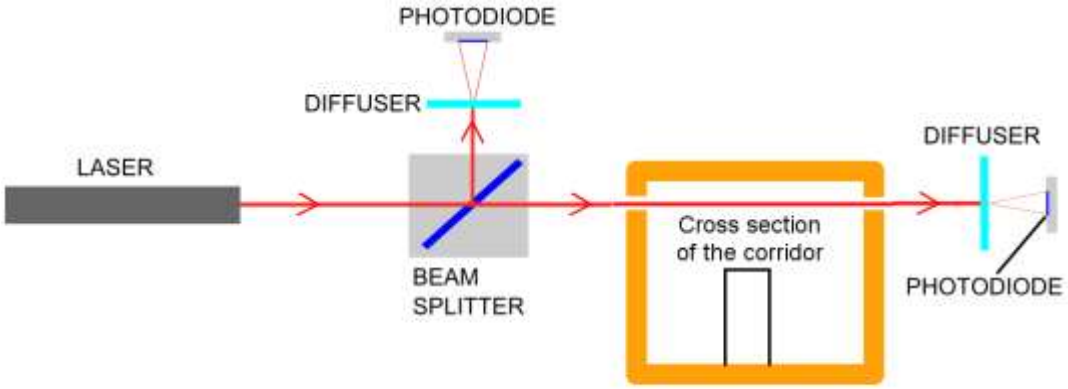

Figure 23. Initial design of smoke meter for measurement inside the enclosure. Cross section view (not to scale)

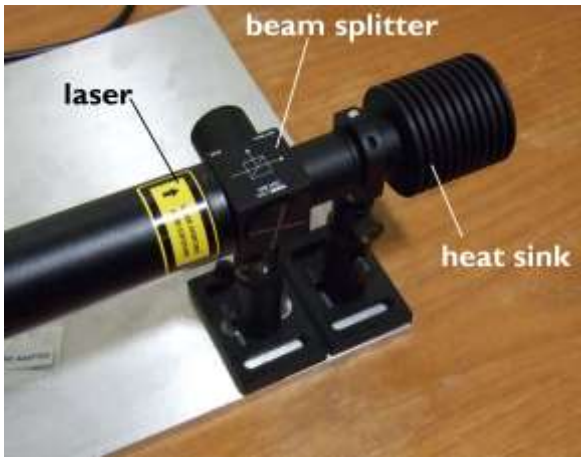

Figure 24. Photo of the initial design of the smoke meter (laser side)

During initial trails, the author constructed a noise cancelling circuit based on the design of Hobbs (1997). However deposition of soot on the beam splitter was causing problems, even with a purging flow of industrial grade nitrogen. Purge flow helped to reduce the deposition but still water condensation on beam splitter was observed. Heating of this element was not feasible therefore an attempt was made to use only one detector. It was found that the *He-Ne* laser, which was used, had very small intensity drift after initial period of warming up (about 60 min). After that period any noise and drift was within recommendation of Putori (1999). Therefore, a simplified design was made and the beam splitter and the noise cancelling unit were eliminated (Figure 25). Consequently, a reverse biased silicon photodiode was used with no amplification in order to reduce any noise. To simplify the design

a commercially available photo detector was obtained from Thorlabs. An appropriate load resistor was chosen to obtain full response from the circuit at about 200mV. Much higher voltages were also possible but resulted in nonlinear response of the detector. Obtained signal was passed through a very short (<1m) coaxial cable to minimize any EMF interference. Data logging unit consisted of 16 bitts analogue – digital converters (ICPDAS) and was sampled with integration time of 60ms and logged in 1 sec intervals. Whole data logging was based on Labview 8.6.

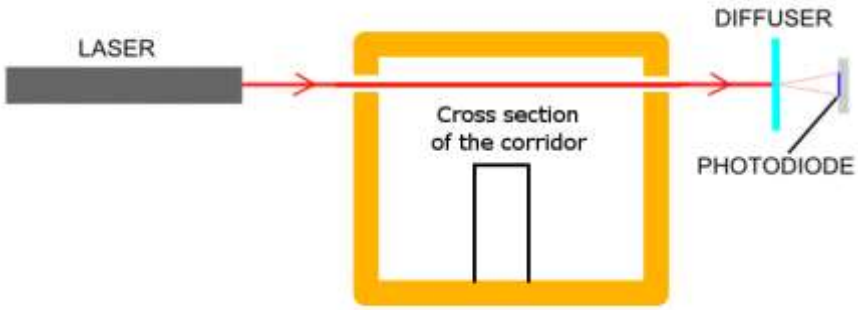

Figure 25. The final design of smoke meter for measurements inside the enclosure. Cross section view (not to scale)

Additional explanation is required to describe problems with soot deposition on detector lenses. Purging was only attempted at the interface between the enclosure and a tube in front of the detector and it was found that it resulted in a faster clogging of a small hole (diameter of 1 cm) drilled in the enclosure wall to allow the measurement. Moreover the usage of nitrogen for purging was not feasible as the experimental rig was placed under the calorimeter hood so additional nitrogen was affecting the oxygen balance in the system. Therefore, instead of purging, an assisted extraction of smoke above the lateral holes in the walls was designed. A small wooden box constructed to cover the whole smoke detector assisted in the smoke extraction because it was equipped with a small extraction fan with capacity of 87 m^3/hr. The extracted smoke was passed to the calorimeter extraction hood thus ensuring that all effluents are collected. The wooden box served also an additional function, namely shielding bystanders from possible laser reflections. This design enabled the rig to comply with the relevant Health and Safety Regulations. Schematic design of the wooden box is presented in Figures 26-27.

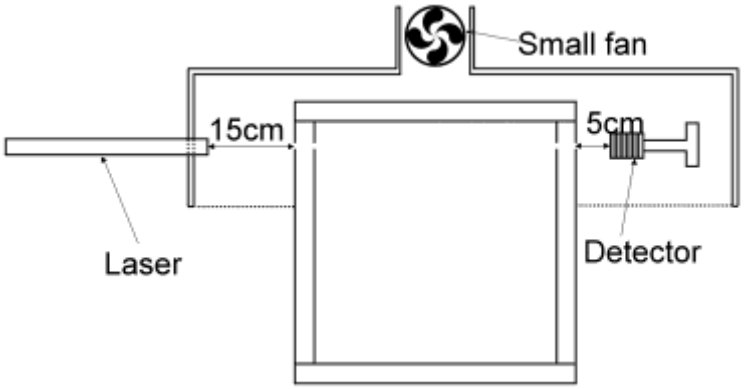

Figure 26. Diagram of small extraction system above the laser smoke meters.

Finally, it was decided to use two similar laser smoke meters located in two boxes A and C (Figures 20, 27). The first was based on laser supplied by Thorlabs, whereas the second by DarkStar Ltd. Both lasers were of the same type (red *He-Ne*) but with different powers (the former has 12mW whereas the latter 3mW). In order to balance the differences in power, two different load resistors were used to bring the readings to similar level.

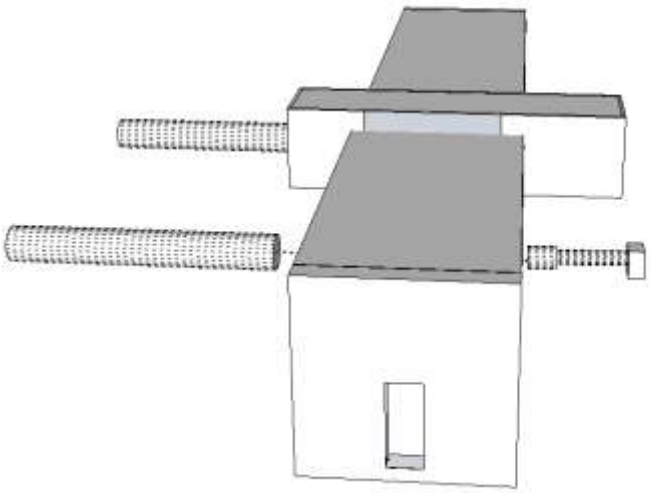

Figure 27. Schematic diagram of wooden hoods installed above the laser smoke meters. Front hood not shown for clarity.

3.3.1.2. Calibration and performance of the constructed smoke meters

The constructed smoke meters were checked against various neutral density filters to confirm the linearity of their response and the range of valid readings. Linearity checks were performed by Neutral Density filters supplied by Thorlabs.

Filters were used having the following optical densities *(OD)*: 0.1, 0.2, 0.3, 0.5, 1.0, 2.0 and combination of 0.5 and 2.0.

The 12mW laser (located in box A) was linear till *OD=3* (Figure 28), whereas the second laser was giving acceptable results till *OD=2.5* (Figure 29).

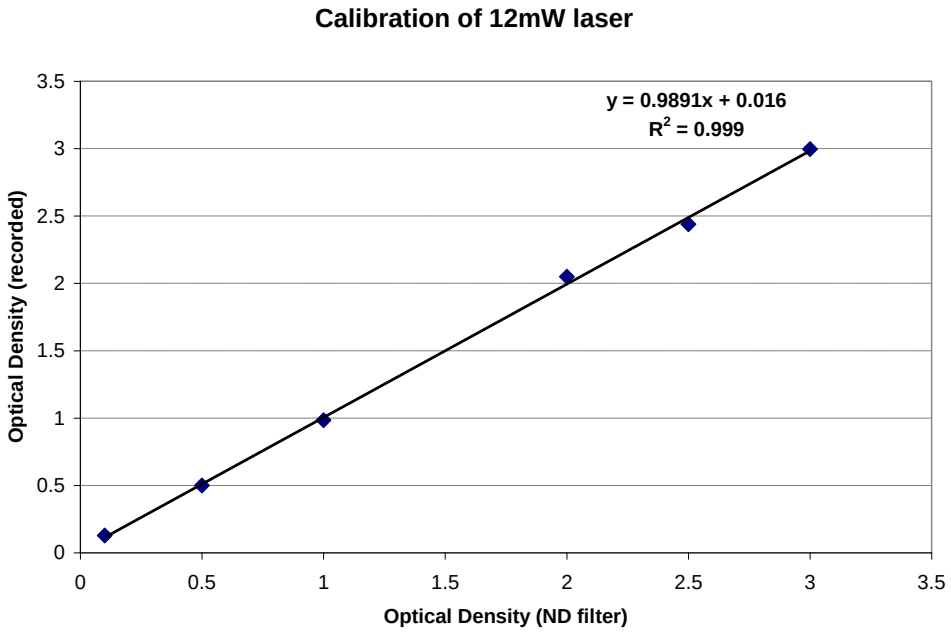

Figure 28. Calibration of 12mW laser performed on 9 December 2009.

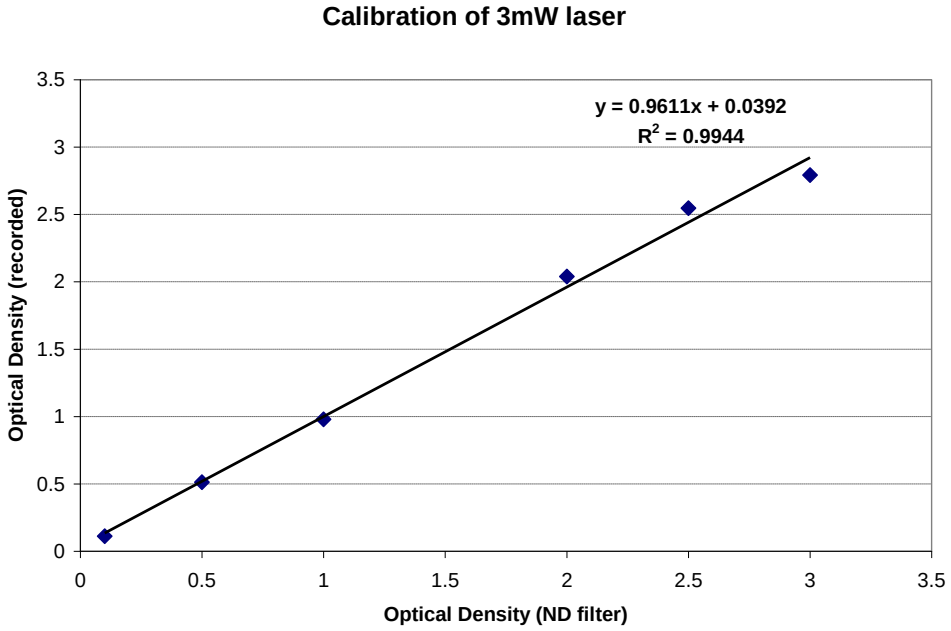

Figure 29. Calibration of 3mW laser performed on 9 December 2009.

Noise and drift were determined according to a methodology described in European Standard (European Committee for Standardisation, 2002). These tests were performed after at least a 30 minutes warming up period (Table 5).

Table 5. Noise and drift of both smoke meters for measurements inside the enclosure. Data from tests performed on 18 June 2010. Warm – up period 1 hour. Duration of test: 30 minutes.

	Drift as % of initial value	Noise as % of initial value
12mW detector - box A	0.00%	0.15%
3mW detector - box C	0.00%	0.16%

In addition, constructed smoke meters were checked against the criteria set by Putori (1999), which were as follows:

- with no smoke present, the value of I/I_o should be between 0.9976 and 1.0024 (which is the other way of checking noise and drift). Obtained values are presented in Table 6, with numbers in red showing measurements exceeding the criteria. Please note the average values for both lasers are within limits.
- for simulation of dense smoke a Neutral density filter with transmittance of 2.5% (Optical Density=1.6) should be used yielding values of I/I_o between 0.0224 and 0. 0279. This test was not possible as it wasn't feasible to obtain such neutral density filter.

Table 6. Both laser smoke meters checked against 1st Putori criterion. Measurement duration - 30 minutes. Values in red exceed limits by Putori, yet the average values for both lasers are within limits

	12mW detector - box A	3mW detector - box C
Maximum ratio	**1.0044**	1.0004
Minimum ratio	0.9976	**0.9964**
Range	0.0068	0.0040
Average value	1.0010+/- 0.0013	0.9984+/-0.0010

3.3.1.3. Discussion on problems reported in the literature

Abecassis Empis et al. (2007) suggested that thermal radiation from flames may significantly affect the reading from smoke meters used for measurements inside the enclosure due to interferences from both visible and infrared radiation. However, in this study, a photodiode was selected that was responsive only at visible wavelengths so no interference was possible from thermal radiation from flames. Regarding interferences at visible wavelengths, it was confirmed experimentally during this study that flame radiation at **visible** wavelengths was not detectable

mainly due to a diffuser before the detector. In addition, the long tube in front of the detector helped also to reduce any forward scattering following the design proposed by Mulholland (2000). Therefore no band pass filter was employed in front of the detector. Consequently, the only problem due to thermal radiation may arise if diode itself is exposed to an elevated temperature and thus start to drift due to different responses at higher temperatures. That could be the case for experiments reported by Abecassis Empis et al. (2007). That risk was minimised in the present study by keeping the detectors outside the enclosure and additionally by wafer heat sinks at the interface between detector and the enclosure.

3.3.1.4. Data reduction to quantify smoke inside the enclosure

Smoke measurements were based on light extinction calculated as explained in section 2.2.2.

From the light extinction coefficient, smoke volume fraction was calculated as follows (Choi et al., 1995):

$$f_v = \frac{k}{\sigma_s \cdot \rho_s} \tag{24}$$

where f_v is the smoke volume fraction (used units yielded f_v in parts per million, ppm), σ_s the mass specific extinction coefficient, which was taken for propane as 8 m^2/g (Mulholland and Croarkin, 2000) and ρ_s the density of soot particulates generated from propane taken as 1.9 g/cm^3 (Wu et al., 1997).

3.3.1.5. Validity of Beer-Lambert law for large values of the light extinction coefficients

According to Bohren and Huffman (1983) cited in Ouf (2008), the product of the light extinction coefficient and a path length trough smoke has to be lower than one for the Beer-Lambert law to be valid. This was often not satisfied for experiments performed in this study due to measurements through not diluted dense smoke. All data are reported in Appendix 4. Smoke levels are reported as smoke volume fractions but one can easily check that the light extinction coefficient was approaching 8 m^{-1} for some of the experiments. Consequently, for the optical path length used being equal to 0.6 m, one obtains the optical depth of 4.8. This is much higher than requirement of being less than one, however this requirement can be relaxed if contribution of scattering is relatively low compared to absorption.

Moreover, an additional discussion on this criterion was published by Seader and Chien (1974) in relation to measurements in the NBS smoke chamber. They cited older literature (Rozenberg, 1966; Zuev et al., 1969; Zuev, 1974) which confirmed that for a small beam of light the optical depth can be much higher reaching even 18 (for small laser beam).

For the present study, an additional information can be obtained from comparison of the smoke volume fractions measured inside and outside before external burning and compare that with the dilution ratio in the exhaust duct. For instance data from test performed on 18 December is presented here. The ratio of light extinction coefficients measured inside the corridor and in the duct was ranging from 90-120 whereas the dilution ratio from entrainment of air into the duct was about 225. These figures differ about two fold but one has to keep in mind the large uncertainty of measurements in the duct and remember that these measurements are done on logarithmic scale. Therefore values obtained, being of the same order of magnitude, confirm that before external burning Beer-Lambert law is obeyed for measurements inside the corridor. On the other hand, there is no means in the present study to examine that for conditions during external burning. Consequently, the validity of obtained results is based on validation found in the literature (Rozenberg, 1966; Zuev et al., 1969; Zuev, 1974) cited in (Seader and Chien, 1974).

Subsequently, a further study is required to verify if the Beer-Lambert law is still valid during external burning for the experimental conditions reported here. For instance one can use smoke meters with laser at lower frequency (contribution from scattering is lower in the infrared) and compare if the ratio of obtained extinction coefficients corresponds to the ratio of used frequencies (Ouf et al., 2008).

3.3.1.6. Measurements of smoke by gravimetric techniques

An attempt was also made to measure the mass concentration of smoke inside the corridor-like enclosure based on the extraction of smoke through a glass filter of prior known mass.

However, a high content of vapours in the effluent badly affected the results and different mass of deposited soot were obtained when filter was kept in a conditioned room for 24 hours after the test and different results when filter was baked in an oven at 105°C after another, but similar test. Moreover clogging of sampling pipe

was another problem. Therefore further attempts were abandoned and no data are reported.

3.3.2. Smoke meter for measurement in the exhaust duct

3.3.2.1. Design of the duct smoke meter

Smoke measurements in the exhaust duct were performed according to ISO standard (ISO, 1993), namely the experimental rig was located under the hood connected to an exhaust duct with instrumentation as per ISO 9705. The whole set-up was constructed by Dark Star Research and no modification was possible. This system consisted of 3mW *He-Ne* red laser with two detectors and beam splitter, and in essence was similar to smoke meter described by Mulholland (Mulholland et al., 2000), with the exception that Dark Star system did not offer detector installed at small angle to reduce backscattering.

3.3.2.2. Calibration and performance of the duct smoke meter

This system was checked by means of two neutral density filters with optical density equal to 0.3 and 0.8. Other filters could not be used as these two came in a special housing provided by Dark Star Research. Unfortunately, no certificates were provided for these filters so it was difficult to assess the accuracy and only qualitative comparison was possible (Figure 30).

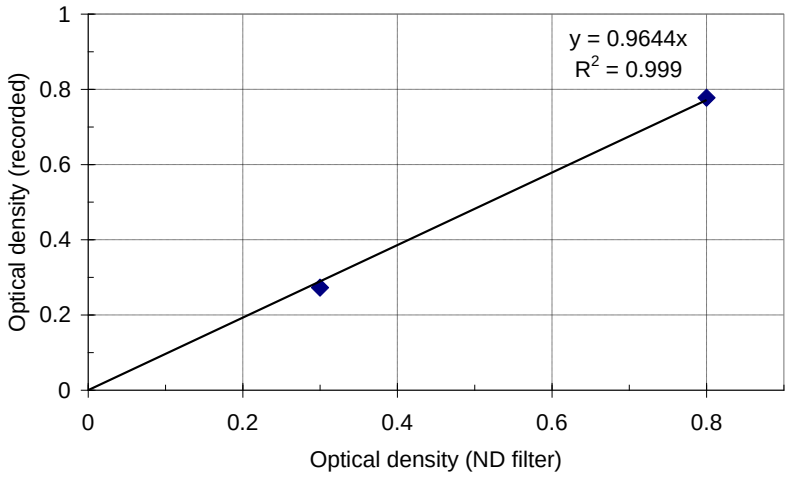

Figure 30. Calibration of the smoke meter in the exhaust duct by means of two neutral density filters.

3.3.2.3. Problems with smoke measurements in the duct

Calibration with the neutral density filters gave good results; however, noise and drift were sometimes too high, as shown in the table below. Both noise and drift were calculated over a 30 min period based on the method described in an European standard (European Committee for Standardisation, 2002). This standard prescribes that both noise and drift should be below 0.5% of the initial value, and the data in Table 7 confirm that only the main detector was performing within specification. This was related to different levels of amplification of the signal from the main and from the reference detector. Figure 31 confirms that problem by showing the response of both detectors as a raw signal in milivolts. It is clearly seen that the signal from the reference detector was over amplified. Therefore, for some of the tests, the reference signal was not taken into account and the first maximum reading from the main detector was taken as initial intensity I_o.

To confirm that, Table 8 compares intensity ratios calculated by two methods, namely main/reference detector and main/maximum reading of the main detector. It is clear that the range of error is smaller for the second case.

Table 7. Noise and drift of the laser smoke meter installed in the extraction duct. Data from check performed on 27 April 2009

	Drift as % of initial value	Noise as % of initial value
Main detector	-0.33%	0.11%
Reference detector	**-1.51%**	0.44%

Table 8. Comparison of different methods to calculate the ratio of incident to transmitted light. Measurement taken for 30 minutes period

	Ratio of signals Main/Reference detector	Ratio of signals Main/Initial Main
Maximum ratio	1.0205	1.0020
Minimum ratio	0.9994	0.9954
Range	**0.0212**	0.0065
Average value	**1.0094**	1.0003

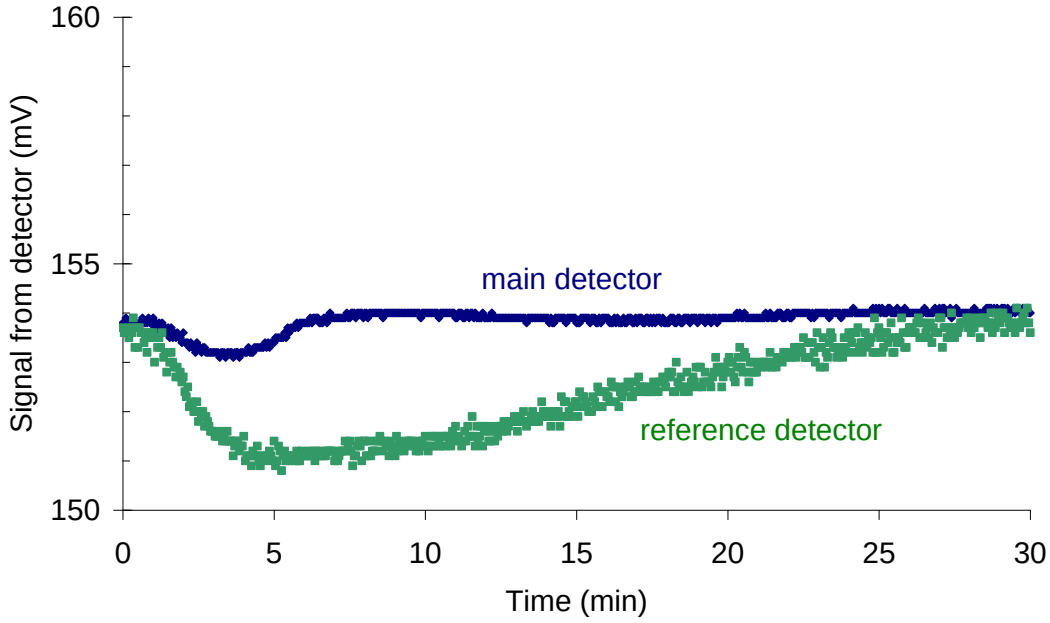

Figure 31. Comparison of different fluctuation of main and reference detectors in the extraction duct.

3.3.2.4. Data reduction to quantify smoke in the exhaust duct

Additional information can be derived from measurements inside the exhaust duct in comparison to measurements inside the enclosure. It is possible to obtain more data because the flow rate through the duct is calculated from bi-directional probes measurement inside. If the flow rate is known, smoke yield can be calculated as explained in section 2.2.3.3.

3.3.3. Sampling of gases from the exhaust duct

3.3.3.1. Technical details of gas analysers

The whole instrumentation for gas sampling from the duct was supplied by Dark Star Research Ltd. and was constructed in accordance with ISO standard (ISO, 1993). The system enabled measurements of: carbon dioxide, carbon monoxide and oxygen. Gas concentration were measured on a dry basis, namely gas samples were passed through a soot filter (Whatman Glass microfibre filter, GF/B, particle retention to 1μm) and through H_2O traps, containing Drierite (active ingredient $CaSO_4$). Moreover all gases were cooled down to temperatures below 2°C to reduce effect of density change with increased temperature and help to reduce amount of water vapours present. Carbon dioxide was measured by a non-dispersive infrared gas analyzer (NDIR), with microprocessor control and linearization analyzer, model

SBA-1 by PP systems. It offered measurement range 0-5% by volume with precision of +/- 1% of full scale. Carbon monoxide was measured with an electrochemical cell, whereas oxygen by paramagnetic analyser. All analysers were calibrated daily with Nitrogen and *CO* and CO_2 mixture of about 1000 ppm CO and 5% CO_2. It was found, however, that these concentrations were never reached during reported experiments; therefore another mixture of 200 ppm of carbon monoxide with 1% of carbon dioxide was used at a later stage. That enabled more accurate measurements of these gases.

3.3.3.2. Data reduction for measurement of gases in the exhaust duct

Most gas analysers require that the mixture of gases is dried before it reaches the apparatus, therefore the reported volume fractions are on dry basis. However in reality the concentrations will be lower, because of the water vapour present in the combustion gases. The actual difference between wet and dry fractions depends on the H_2O concentration and usually is 10 to 20 % by volume. However, the present measurements were not corrected following the methodology described by (Janssens and Parker, 1992) was followed in the present study. Namely, the mole fraction of H_2O in the incoming air was taken into account based on relative humidity measurements. Accordingly, yields were calculated as follows:

$$y_{CO_2} = \frac{\dot{m}_{CO_2} - \dot{m}^0_{CO_2}}{\dot{m}_f} \tag{25}$$

$$\dot{m}_{CO_2} - \dot{m}^0_{CO_2} = \frac{X^A_{CO_2}\left(1 - X^{A^0}_{O_2}\right) - X^{A^0}_{CO_2}\left(1 - X^A_{O_2} - X^A_{CO}\right)}{1 - X^A_{O_2} - X^A_{CO_2} - X^A_{CO}} \frac{M_{CO_2}}{M_a} \frac{\dot{m}_e}{1 + Oxy_{dep} \cdot \left(\alpha_{\exp} - 1\right)} \left(1 - X^0_{H_2O}\right) \tag{26}$$

$$y_{CO} = \frac{\dot{m}_{CO}}{\dot{m}_f} \tag{27}$$

$$\dot{m}_{CO} = \frac{X^A_{CO}\left(1 - X^{A^0}_{O_2} - X^{A^0}_{CO_2}\right)}{1 - X^A_{O_2} - X^A_{CO_2} - X^A_{CO}} \frac{M_{CO}}{M_a} \frac{\dot{m}_e}{1 + Oxy_{dep} \cdot \left(\alpha_{\exp} - 1\right)} \left(1 - X^0_{H_2O}\right) \tag{28}$$

$$X^0_{H_2O} = \frac{RH}{100}\frac{p_s}{p_a} \tag{29}$$

$$p_s = e^{(23.2-3816/(-46-T_a))} \tag{30}$$

$$M_a = M_{dry}\left(1 - X^0_{H_2O}\right) + M_{H_2O}X^0_{H_2O} \tag{31}$$

3.3.4. Sampling of gases from the enclosure

Measurements inside the enclosure can reveal more information about actual phenomena occurring in the compartment in fire. Unfortunately, there is a lack of standard recommendations on that matter. There were some attempts to measure the gas species in the upper part of the opening, and one of the first quantitative comparison between exhaust hood and opening measurements was done by Gottuk (1992; 2002).

This study was designed to give also quantitative information on gas production inside the enclosure and data was obtained simultaneously in three different locations for most of the tests. Three portable gas analysers supplied by Dark Star Research Ltd were used, two of them capable of quantification of oxygen, carbon dioxide and carbon monoxide together with total hydrocarbon levels. Oxygen was measured by an electrochemical cell, whereas other species by an infrared cell. Third gas analyser was only able to measure carbon monoxide and oxygen levels by electrochemical cells.

Method of gas sampling was designed to follow recommendations of Wieczorek et al. (2004b). They reported that assumption of the uniformity of gas inside is incorrect and based that claim on the work of Bryner et al. (1994). Therefore gas sampling should rely on some “averaging technique”. This study followed that recommendation by using stainless steel probes closed at one end and containing a set of holes of different sizes along the whole length of the tube. That allowed averaging of the effluents. Tubes had external diameter of 12 mm, with eleven holes of 4 mm, eleven holes of 3 mm and eleven holes of 2.5 mm. Different holes sizes assisted in uniform sampling from the whole length of the tube. Dimensions are shown in Figure 32.

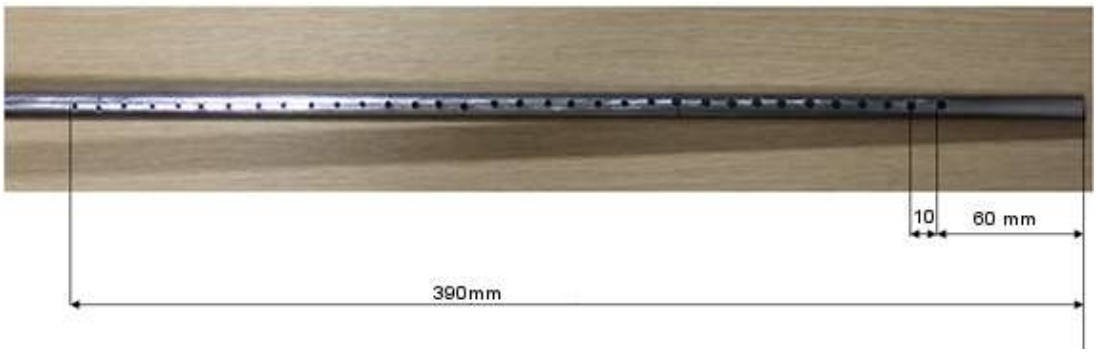

Figure 32. Stainless steel tube for gas sampling inside the enclosure.

3.3.5. Velocity measurements inside the enclosure

At a later stage of the project, it was decided that measurement of the velocities inside the enclosure may reveal some additional important information. Therefore two bi-directional probes (McCaffrey and Heskestad, 1976) were used. As no access to wind tunnel was possible it was decided to use the calibration function proposed by McCaffrey and Heskestad (1976) knowing that some error may be present as the probes used had slightly different ratio of critical dimensions.

The probes were inserted inside the corridor enclosure in the lower and upper part of box C, as shown in Figure 20. The probes were located as close as possible to the smoke meter in the middle of the enclosure as information of the flows in the vicinity of the smoke meter was required for better understanding of obtained data. Moreover probes could not be installed in the vicinity of other smoke meter (box A) due to disturbance of the flows close to the opening.

Due to the wide range of temperatures inside, the viscosity of air was computed following equations proposed by Lemmon and Jacobsen (2004).

3.3.6. Temperature measurements

Gas temperatures inside the compartment were measured by evenly spaced thermocouple trees (Type K, stainless steel sheath thermocouples with bare beads size 1.5 mm) inside each of the cubic boxes. Details of their location are presented in Figures 21 and 33.

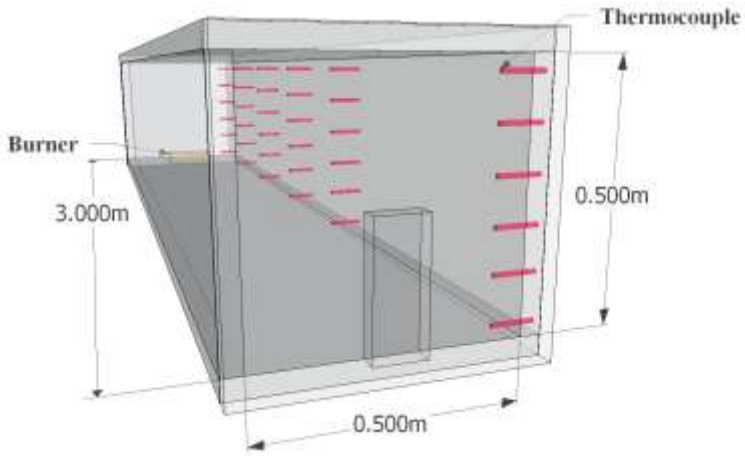

Figure 33. 3D view of thermocouples' location inside experimental corridor.

In order to quantify re-radiation error, two separate experimental methodologies were employed, as described by Ergut and Levendis (2005) and Brohez with co-workers (2004). The first method led to evaluate errors based on measurement with four different thermocouples located very close to each other in the upper layer of box C (bead size 0.25 mm, 0.5 mm, 1 mm and 1.5 mm) and three additional thermocouples in lower layer of box C (bead size 0.5 mm, 1 mm and 1.5 mm). Measurements were made at 1 sec intervals and quantification of error was based on extrapolation to bead size of 0 mm. However, different response times of used thermocouples resulted in erratic results for any period with fast temperature changes. The second methodology (Brohez et al., 2004) was based on readings from two thermocouples (1mm and 0.25mm). Their readings were compared to each other and the following linear relationship was used:

$$T_{corrected} = T_{1mm} + 1.8 \cdot \left(T_{0.25mm} - T_{1mm}\right) \qquad (32)$$

where: $T_{corrected}$ – gas temperature corrected for re-radiation error, T_{1mm} – uncorrected readings of thermocouple with 1 mm bare bead, $T_{0.25mm}$ - uncorrected readings of thermocouple with 0.25 mm bare bead .

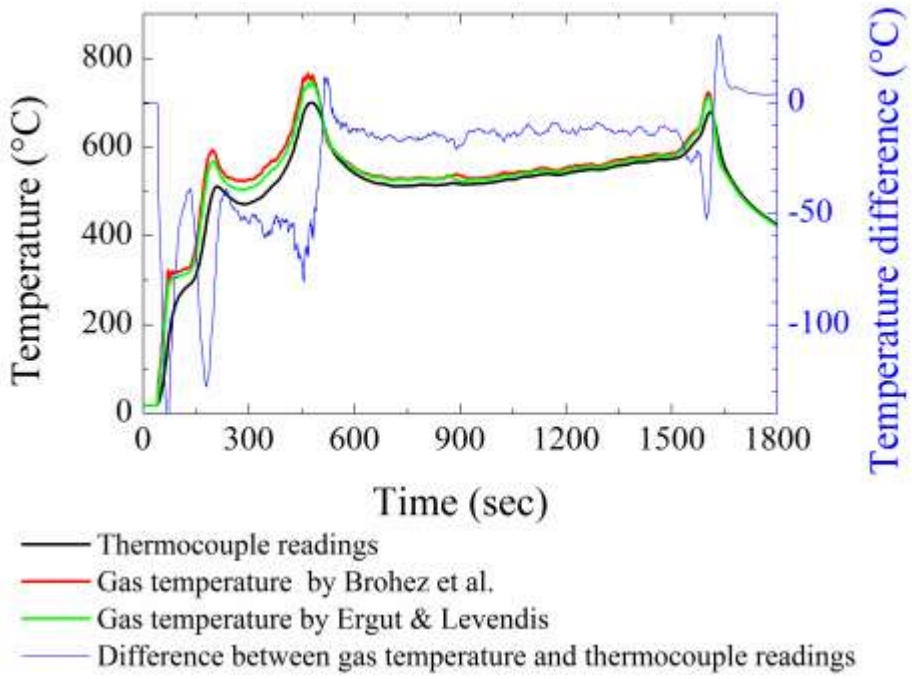

Figure 34. Upper layer temperature measured with a thermocouple and gas temperatures calculated from two different methods.

It was not feasible to apply this methodology for all thermocouple locations due to technical limitations. Moreover, performed analysis confirmed that radiation error was not exceeding 10% of the thermocouple reading during quasi steady state (Figure 34), and that was finally taken into account during uncertainty analysis.

3.3.7. Measurements of Heat Release Rate

Measurements of Heat Release Rate were performed by means of oxygen depletion. All fire effluents were collected by a 3m x 3m hood capable of handling fires up to 1 MW. The calorimeter analyser was supplied by Dark Star Ltd (UK) and was basically designed to meet the criteria of ISO room corner test. (British Standards Institution, 2007).

3.3.7.1. Data reduction to obtain HRR

Data from all analysers were reduced following the methodology described by Janssens and Parker (1992). Basically, readings from O_2, CO_2 and CO analysers were taken into account and additionally the fact that measurements were performed on a dry basis was also incorporated into that methodology. Moreover comparison with other method based only on measurements of CO and CO_2 (Tewarson, 1995;

Tewarson, 2002; Tewarson, 2008) was always performed to indicate in advance any possible problems with *HRR* data.

Oxygen depletion factor was calculated as follows (Janssens and Parker, 1992):

$$Oxy_{dep} = \frac{X_{O_2}^{A^0}\left(1 - X_{CO_2}^{A} - X_{CO}^{A}\right) - X_{O_2}^{A}\left(1 - X_{CO_2}^{A^0}\right)}{\left(1 - X_{O_2}^{A} - X_{CO_2}^{A} - X_{CO}^{A}\right)X_{O_2}^{A^0}} \qquad (33)$$

where: Oxy_{dep} – oxygen depletion factor (fraction of the incoming air which is fully depleted of its oxygen) $X_{CO_2}^{A}$ - measured mole fraction (-) of CO_2 in the exhaust gases, X_{CO}^{A} - measured mole fraction (-) of CO in the exhaust gases, $X_{O_2}^{A}$ - measured mole fraction (-) of O_2 in the exhaust gases, superscript A^o indicates initial measurement before combustion

Heat Release Rate was calculated from (Janssens and Parker, 1992):

$$\dot{q} = \left[E \cdot Oxy_{dep} - \left(E_{CO} - E\right)\frac{1 - Oxy_{dep}}{2}\frac{X_{CO}^{A}}{X_{O_2}^{A}} \right] \frac{\dot{m}_e}{1 + Oxy_{dep}\left(\alpha_{\exp} - 1\right)} \frac{M_{O_2}}{M_a}\left(1 - X_{H_2O}^{0}\right)X_{O_2}^{A^O} \qquad (34)$$

where: $\dot{q}$ - *Heat Release Rate* (MW) from oxygen, CO_2 and CO measurement in the exhaust duct, E – Heat Released per kilogram of O_2 *consumed* (taken as 12.68 MJ/kg of O_2 for propane, E_{co} – Net Heat Release per unit mass of O_2 consumed for combustion of CO to CO_2 (approximately 17.6 MJ/kg of O2), $\dot{m}_e$ - mass flow rate in the duct (kg/s), α – expansion factor taken as 1.105, M_{O_2} - molecular weight of oxygen (32 kg/kmol), M_A - molecular weight of incoming air taking into account relative humidity, $X_{H_2O}^{0}$ - Mole fraction of H_2O in the incoming air

3.3.7.2. Drift of oxygen analyser

The paramagnetic oxygen analyser has a tendency to drift over time. Moreover if not enough time was enabled for equilibration, then the drift was even higher. Therefore the technique described by Bryant et al. (2004) was used to overcome that problem. Additionally, a determination of HRR by means of CO_2 and CO only (Tewarson, 2008) was used to double check the obtained results.

3.3.7.3. Calibrations of HRR

Calibration of the calorimeter was achieved by a separate propane burner located under the hood. Initially calibration was performed at irregular interval, but subsequently it was conducted before each test. Each calibration run consisted of a few steps at different levels of HRR anticipated to occur in the test following the

calibration (Figure 35). However, it must be kept in mind, that the calorimeter hood was designed to much higher (up to 1 MW) fires than those conducted in this project. The same limitation applies to mass flow controllers being used in the rig and in the calibration burner. These were designed to supply the propane gas in the range from 0 – about 7.2 g/s corresponding of about 315 kW of propane fire whereas conducted tests were in the range 10-60 kW resulting in a larger uncertainty. This issue will be further discussed in the next section devoted to uncertainty analysis.

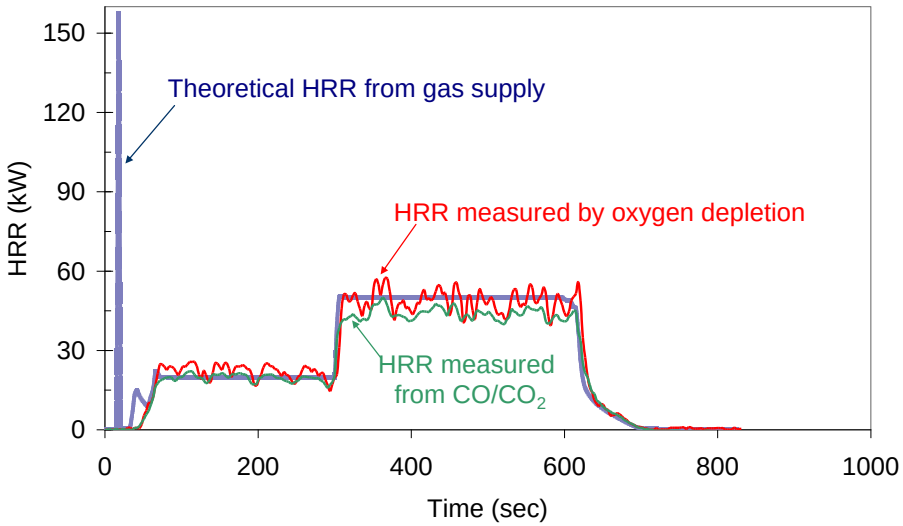

Figure 35. Example of calibration data from 3 metre hood.

3.4. Experimental procedure

In the initial phase of each experiment, a flow rate of propane was set at 10 kW and ignited remotely by an electric spark. Thereafter the fuel flow rate increased linearly to a maximum value prescribed for a given experiment. Upon reaching the maximum desired heat release rate, the fuel supply was kept constant for about 25 minutes for the temperatures inside to reach the quasi-steady state. Longer tests durations were not advised owing to clogging of the sampling lines and the smoke detector ports from within the enclosure.

3.5. Repeatability and uncertainties of measurements

This section presents detailed uncertainty determination for smoke measurements inside the duct and in the corridor together with repeatability of these measurements. Uncertainties of other quantities are only tabulated at the end of the chapter.

3.5.1. Uncertainty of smoke volume fractions

Uncertainty of smoke volume fractions is analysed following the methodology by Mulholland (Mulholland et al., 2000) following NIST guidelines (Taylor and Kuyatt, 1994). Smoke volume fraction being a function of four variables as shown by Eqs. 3 and 24, entails the following error:

$$\delta f_v = \left[\left(\frac{\partial f_v}{\partial L} \delta L \right)^2 + \left(\frac{\partial f_v}{\partial \frac{I_0}{I}} \delta \frac{I_0}{I} \right)^2 + \left(\frac{\partial f_v}{\partial \sigma_s} \delta \sigma_s \right)^2 + \left(\frac{\partial f_v}{\partial \rho_{soot}} \delta \rho_{soot} \right)^2 \right]^{1/2} \quad (35)$$

where δ represents the standard uncertainty of the indicated quantities

Four sensitivity coefficients are calculated as follows:

$$\frac{\partial f_v}{\partial L} = -\frac{1}{L^2} \frac{\ln\left(\frac{I_0}{I}\right)}{\sigma_s \rho_{soot}} \quad (36)$$

$$\frac{\partial f_v}{\partial \frac{I_0}{I}} = \frac{\overline{I}}{L \sigma_s \rho_{soot}} \quad (37)$$

$$\frac{\partial f_v}{\partial \sigma_s} = -\frac{1}{\sigma_s^2} \frac{\ln\left(\frac{I_0}{I}\right)}{L \rho_{soot}} \quad (38)$$

$$\frac{\partial f_v}{\partial \rho_{soot}} = -\frac{1}{\rho_{soot}^2} \frac{\ln\left(\frac{I_0}{I}\right)}{L \sigma_s} \quad (39)$$

Uncertainties of the four identified variables are discussed next.

3.5.1.1. Uncertainty in the path length

The large source of uncertainty in the path length determination is related to smoke escaping through holes in the duct/corridor walls and thus changing the path length trough smoke.

The uncertainty in the path length in the exhaust duct is only 0.1 *cm* because the flow rate in the duct is large enough to prevent any leaks of smoke.

The path length trough smoke inside the corridor was equal to 0.6 metre but the distance between the laser and the detector was larger by about 0.2 metre and that was somehow variable between tests. Therefore the uncertainty in the path length in the corridor was related to the variability of path length between laser and detector optics. Consequently the uncertainty was conservatively assumed to be 0.1 metre which is half of the optical path outside the enclosure.

3.5.1.2. Uncertainty in the intensity ratio

Variation in the intensity ratio is attributed to the noise of the helium-neon laser, the noise of the electronics, and variations in the duct exhaust rate. Variations in extraction rate could affect the amount of air entrained by the extraction hood and thus dilution of the smoke which is not accounted to by Eqs. 3 and 24. Therefore this uncertainty was determined by statistical methods, namely by computing standard deviation/mean of intensity ratios from repeated experiments. This coefficient of variation (calculated as standard deviation over mean value and multiplied by 100) is equal to the relative standard uncertainty for a single measurement (Mulholland et al., 2000). The intensity ratio (I_0/I) is averaged during the quasi steady state period at the end of the test. The obtained values are: 0.7% for duct measurements, 48.8% for laser in box A and 21.9% for laser in box C. Such a large difference between box A and C is due to the fact that box A is the front box having the opening where fluctuations are developed because of flames anchored near the opening.

3.5.1.3. Uncertainty in the mass specific extinction coefficient

The mass specific extinction coefficient for propane was taken from (Mulholland and Croarkin, 2000) and uncertainty reported there was used.

3.5.1.4. Uncertainty in the density of post flame soot

Density of post-flame soot generated by propane fire was taken from (Wu et al., 1997), however no information on uncertainty was reported. Therefore uncertainty was taken from smoke measurements in acetylene/air flames as reported by Choi (1995) where the soot density was similar to the value used in this work.

3.5.1.5. Final statement of uncertainty

In summary, it was established that the total relative standard uncertainty for a) smoke inside box A is 25.8%, b) smoke inside box C is 23.1% and c) smoke in the exhaust duct is 32.2% the latter owing to very small concentrations in the duct. Detailed uncertainty budget for smoke measurements is presented in Tables 9-11.

Table 9. Uncertainty budget for measurement inside the corridor (box A)

Variable	Nominal value	Relative standard uncertainty	Absolute standard uncertainty	Type of uncertainty assessment	Sensitivity coefficients
Path length, L	0.6 (m)	16.7 (%)	0.1 (m)	B	-0.7717
Intensity ratio (I_0/I)	68.2 (-)	48.8 (%)	33.3 (-)	A	0.0016
Mass specific extinction coefficient σ_s	8.0 (m^2/g)	13.8 (%)	1.1 (m^2/g)	B	-0.0579
Density of soot ρ_s	1.9 (g/cm^3)	0.19 (%)	0.1 (g/cm^3)	B	-0.2437

Combined relative standard uncertainty for smoke inside box A is 25.8%
Expanded relative uncertainty is 51.6% with 95% level of confidence

Table 10. Uncertainty budget for measurement inside the corridor (box C)

Variable	Nominal value	Relative standard uncertainty	Absolute standard uncertainty	Type of uncertainty assessment	Sensitivity coefficients
Path length, L	0.6 (m)	16.7 (%)	0.1 (m)	B	-0.8287
Intensity ratio (I_0/I)	93.2	21.9 (%)	20.4 (-)	A	0.0012
Mass specific extinction coefficient σ_s	8.0 (m^2/g)	13.8 (%)	1.1 (m^2/g)	B	-0.0622
Density of soot ρ_s	1.9 (g/cm^3)	0.19 (%)	0.1 (g/cm^3)	B	-0.2617

Combined relative standard uncertainty for smoke inside box C is 23.1%
Expanded relative uncertainty is 46.2% with 95% level of confidence

Table 11. Uncertainty budget for measurement in the exhaust duct

Variable	Nominal value	Relative standard uncertainty	Absolute standard uncertainty	Type of uncertainty assessment	Sensitivity coefficients
Path length, L	0.4 (m)	0.25 (%)	0.001(m)	B	-0.0104
Intensity ratio (I_0/I)	1.0256 $(-)$	0.35 (%)	0.003538 (-)	A	0.1604
Mass specific extinction coefficient σ_s	8.0 (m^2/g)	13.8 (%)	1.1 (m^2/g)	B	-0.0005
Density of soot ρ_{st}	1.9 (g/cm^3)	0.19 (%)	0.1 (g/cm^3)	B	-0.0022

Combined relative standard uncertainty for smoke in the exhaust duct is 32.2%
Expanded relative uncertainty is 64.4% with 95% level of confidence

3.5.1.6. Repeatability of measurements

Repeatability of smoke measurements is established from three tests at the same conditions and graphically depicted in Figure 36. Presented data show smoke volume fractions in the exhaust duct and in the enclosure from the same three repeated tests. The repeatability inside the corridor is good. On the other hand, the repeatability in the duct is good only for the period before the external burning but poor during external burning owing to very low smoke levels being recorded during external burning.

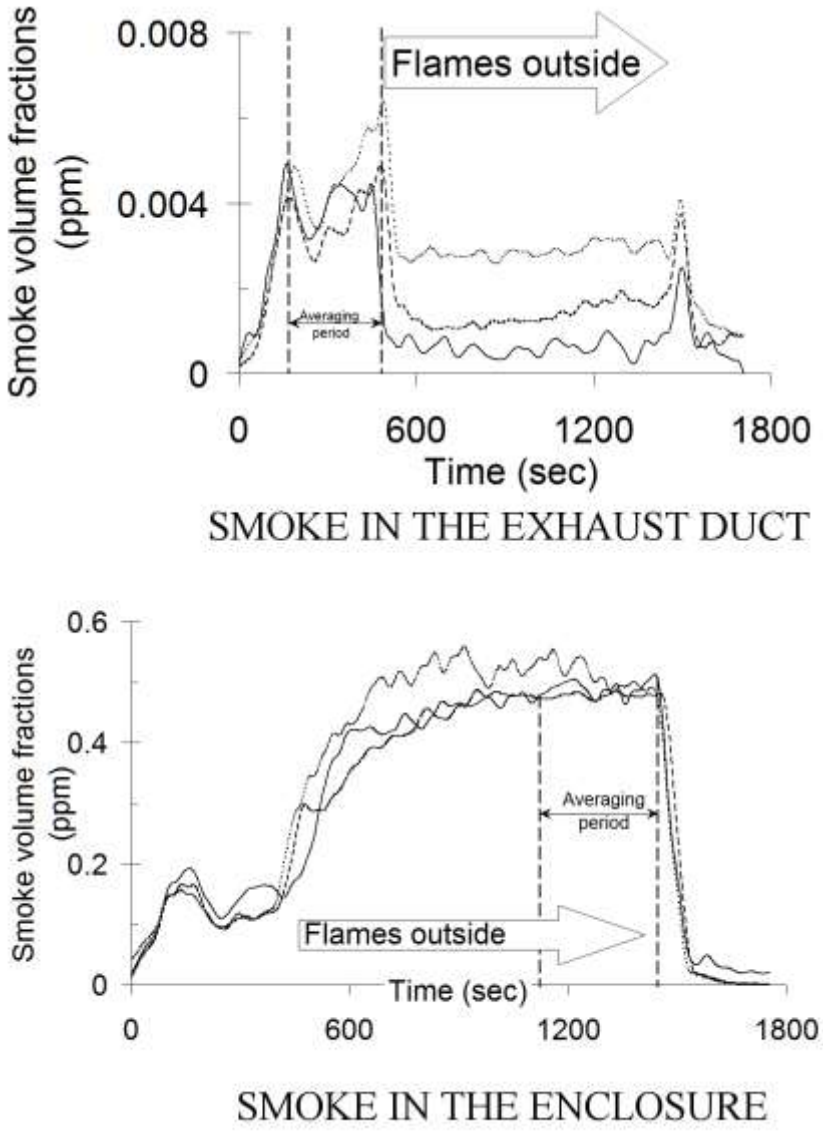

Figure 36. Repeatability of smoke volume fractions in the exhaust duct (top) and inside the corridor (bottom). All data smoothed over a one minute period.

3.5.2. Uncertainty of other measurements

Uncertainties of other measurements were only estimated and their combined uncertainties were calculated as square roots of squared sums of individual components. The table below summarises these estimated uncertainties:

Table 12. Summary of uncertainty analysis for other measurements in this work.

	Type A Uncertainty, u_i	Type B Uncertainty, u_i	Combined Uncertainty u_c
Temperature			-6.5% to 2.5%
Accuracy of K type Thermocouple		+/- 2.5%	
Re-radiation losses		-6% to 0%	
Heat Release Measurements (analyser drift included)			+/- 7.8%
Exhaust Flow Rate		+/-5%	
Accuracy of gas standards for calibration		+/-5%	
		+/-1%	
Instruments Uncertainty		+/-3%	
Global Equivalence Ratio determination			+/-15.8%
Equipment Uncertainty		+/-1%	
Fuel purity		+/-5%	
$\dot{m}_a = AH^{1/2}$ formula	+/- 15%		
Velocity measurements inside			-8.9% to 6.6%
Pressure measurements		+/-1%	
Gas temperature	-6.5% to 2.5%		
Probe factor		+/-6%	
Gas Analyzers			+/-6.6%
Zero and Span Gas		+/-5%	
Equipment Uncertainty		+/-1%	
Mixing and Averaging		+/-3%	
Random error		+/-3%	

3.6. Recommendations for future improvements

Author is well aware that certain procedures could be improved in future and some data obtained in a more precise way. However, some of the recommendations presented below are based on the experience gained during this research program and thus are a contribution to available experimental knowledge. Presented recommendations are only focused on the experimental methodology whereas

recommendation for a further research work as a continuation of this study will be presented in the conclusion of this thesis.

First recommendation is related to a technique of gas sampling from inside of the enclosure. The current method was based on the recommendations of Wieczorek et al. (2004a; 2004b) and thus focused on averaging the concentrations from the whole width of the corridor. Therefore probes with many holes along the whole length were used that could not be cooled easily. Sampling without cooling from the reaction zone may result in unrealistic values as further reactions could take place inside the tube. That could result for instance in further conversion of hydrocarbons into carbon monoxide if enough oxygen was available (Beyler, 1986b). However, the design of water-cooling with multiple holes along the tube length was not feasible during this project.

Secondly, gas analysers used did not offer any hardware ensuring that gas reaching the measurement section was kept at the same temperature, only the flow rate was kept constant. Therefore gases were cooled only by convection and conduction along the stainless steel sampling tubes outside the enclosure. Subsequently, any variation in gas temperature, in comparison to temperature during calibration, was not accounted for.

Thirdly, a further study is required to verify if for the non-diluted smoke present in the experimental conditions reported here, the Beer-Lambert law is still valid. For instance one can use smoke meters with laser at lower frequency (contribution from scattering is lower in the infrared) and compare if the ratio of obtained extinction coefficients corresponds to the ratio of used frequencies (Ouf et al., 2008).

Finally, a quantification of radiation errors in additional locations is recommended, especially outside the enclosure at different elevations. This has not been done due to time constraints and also because it was not seen crucial for reaching the aims of this project.

CHAPTER FOUR

Results and discussion

4.1. Introduction

This section presents experimental results obtained during the course of this research. At the beginning Heat Release Rate (HRR) measurements and calculation of Global Equivalence Ratio (GER) are presented, followed by a qualitative description of fire behaviour during preformed experiments. Then, separate sections are presented on smoke and carbon monoxide production. This chapter is concluded with section on relation between smoke and carbon monoxide production during enclosure fires examined in this research.

4.2. Heat Release Rate (HRR) and Global Equivalence Ratio (GER)

This subsection presents experimental data on the Heat Release Rate followed by an explanation of how the Global Equivalence Ratio was determined in this study. Finally, a comparison is presented of different methods to determine mass inflow of air into a compartment and method used in the present study is validated.

4.2.1. Introduction on Heat Release Rate (HRR)

Figure 37 presents a comparison of theoretical and measured Heat Release Rates for four openings sizes. Measurements were made by oxygen consumption calorimetry (cf. section 3.3.7) whereas theoretical HRR was calculated from the supply of propane gas by multiplying the amount of gas supplied (g/s) by the effective heat of combustion for propane, namely 43.7 kJ/g (Tewarson, 2002). The measured HRR in the exhaust duct (red curve) is plotted together with the theoretical HRR (blue curve). Figure 37 presents also the maximum ventilation controlled HRR (green curve) which is derived from the opening size as will be explained below. In

addition a grey shaded area indicates underventilated conditions before an external burning as discussed below.

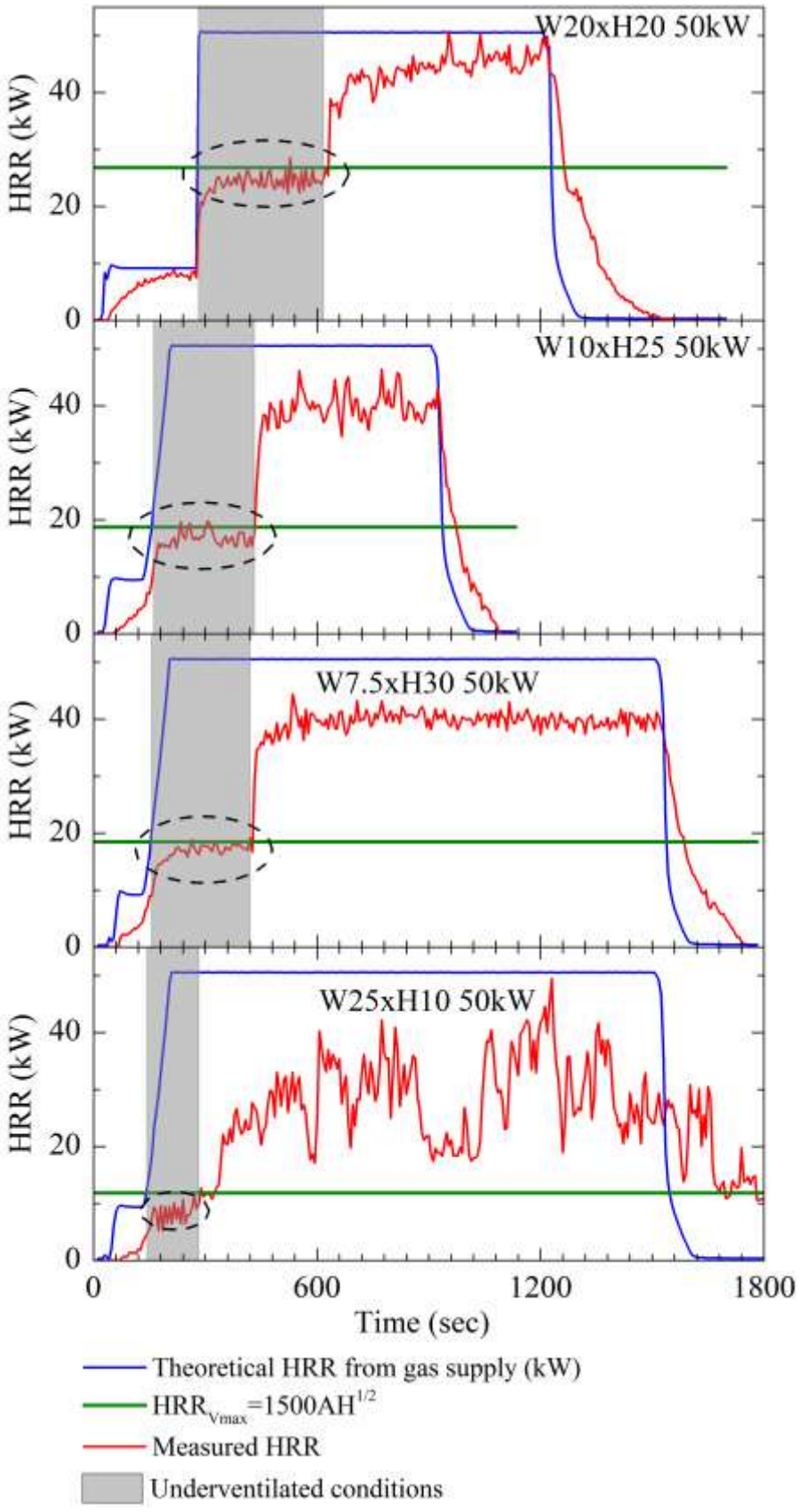

Figure 37. HRR history from tests having four different openings and theoretical HRR = 50kW.

Examination of Figure 37 reveals that after ignition and increase in the fuel supply rate an intermediate plateau is reached in the measured HRR (highlighted by a dashed oval). During this plateau, the theoretical HRR is higher than the HRR measured by oxygen depletion in the duct; it is said that the fire is controlled by the ventilation (opening size) and, consequently, by the amount of air reaching the combustion zone. Indeed, the measured heat release rate in this plateau yields an average value agreeing with the maximum ventilation-controlled HRR (Eq. 41) derived by multiplying the ventilation controlled mass flow of air into the compartment (Eq. 40) (Fujita, n.d.; Kawagoe, 1958; Thomas and Nilsson, 1973) by the energy released per kilogram of air completely consumed inside (about 3000 kJ/kg) (Drysdale, 2011):

$$\dot{m}_a = C_a \times AH^{1/2} \tag{40}$$

$$HRR_{V\max} = 1500AH^{1/2} \tag{41}$$

where C_a is a proportionality factor assumed to be 0.5 (Fujita, n.d.; Kawagoe, 1958; Thomas and Nilsson, 1973) and HRR_{Vmax} is the maximum ventilation controlled Heat Release Rate (kW) and A (m^2) and H (m) are the area and height of the opening, respectively.

Using Eq. 41, the Global Equivalence Ratio (cf. 2.1.4.1.1) can be expressed as (Pitts, 1995; Gottuk and Lattimer, 2002; Lee, 2006; Lee et al., 2007; Ukleja et al., 2009):

$$\Phi = HRR_{theoretical} / HRR_{V\max} \tag{42}$$

Calculation of the Global Equivalence Ratio by Eq. 42 confirms that during this plateau the fire is underventilated both inside and outside the enclosure (grey-shaded area in Figure 37) because the excess fuel does not burn outside due to low gas temperatures.

Subsequently, flames emerge from the opening as confirmed by a sudden increase in the measured HRR to the value corresponding nearly to the theoretical HRR whereas underventilated conditions persist inside the enclosure. The same behaviour was observed for all opening sizes employed in this work.

However, validity of Eq. 40 is questionable when used for estimation of the inflow of air before flashover. Babruaskas et al. (1996) proposed that a more

complex methodology should be used before flashover. In addition, a recent research (Yij et al., 2007) suggested an overestimation of the mass inflow calculated by Eq.40 for openings with large width to height ratios. Contrary to the expectations, the obtained results confirmed the validity of Eqs. 40 and 42 for the experimental conditions employed in this research with the exception of one opening, as presented in the next subsection.

4.2.2. Modified calculation of the Global Equivalence Ratio

Calculation of GER in the present study was based on an equitation proposed by Gottuk and Lattimer (2002; 2008), further modified to adapt to the present research.

Typical definition of Global Equivalence Ratio is presented below (on the left), with version for mass of oxygen instead of mass of air (on the right):

$$\Phi = \frac{\dot{m}_f / \dot{m}_a}{\dot{m}_{f_{stochiometric}} / \dot{m}_{a_{stochiometric}}} = \frac{\dot{m}_f / \dot{m}_a}{\dot{m}_{f_{stochiometric}} Y_{oxygen} / \dot{m}_{oxygen_{stochiometric}}} \quad (43)$$

where Φ is the Global Equivalence Ratio, $\dot{m}_f$ mass loss rate of fuel (g/s), Y_{oxygen} mass fraction of oxygen in air (0.23) and subscript stochiometric indicate values at stochiometric conditions.

Gottuk and Lattimer (2002) proposed some manipulation based on multiplication of the numerator and the denominator by a theoretical heat of combustion. Knowing that the theoretical heat release rate is a product of the theoretical heat of combustion and mass loss rate (or supply of gaseous fuel) one obtains:

$$\Phi = \frac{\Delta H_c \dot{m}_f / \dot{m}_a}{\Delta H_c \dot{m}_{f_{stochiometric}} Y_{oxygen} / \dot{m}_{oxygen_{stochiometric}}} = \frac{HRR_{theoretical} / \dot{m}_a}{\Delta H_c \dot{m}_{f_{stochiometric}} Y_{oxygen} / \dot{m}_{oxygen_{stochiometric}}} \quad (44)$$

The next step is to introduce the amount of energy released per mass of oxygen consumed *E* (Eq. 45) into Eq. 44.

$$E = \frac{HRR}{\dot{m}_{oxygen_{stochiometric}}} = \frac{\Delta H_c \dot{m}_{f_{stochiometric}}}{\dot{m}_{oxygen_{stochiometric}}} \tag{45}$$

That after rearrangements yields the final version of Eq. 46.

$$\Phi = \frac{\frac{HRR_{theoretical}}{\dot{m}_a}}{EY_{oxygen}} \approx \frac{HRR_{theoretical}}{3000 \cdot \dot{m}_a} \tag{46}$$

The simplest approach to derive the mass of available air is to relate it to ventilation factor (Kawagoe, 1958) with the proportionality factor equal to 0.5, as shown in Eq. 40 (Fujita, n.d.; Thomas et al, 1967; Thomas and Nilsson, 1973) :

Therefore a final version of the Global Equivalence Ratio equation will have the following form which was presented in the previous section as Eq. 42:

$$\Phi = HRR_{theoretical} / 1500 A H^{1/2} \tag{47}$$

where $HRR_{theoretical}$ is the theoretical Heat Release Rate derived from the known supply rate of propane

4.2.3. Comparison of different methods to determine mass inflow of air into the enclosure

The accuracy in the calculation of the Global Equivalence Ratio is strongly dependent on the accuracy of measurement or estimation of mass inflow of air into the enclosure. There are many advanced approaches to determine mass flow rates in and out from an enclosure, with an extensive list given by Janssens and Tran (1992). Some of these methods are based on the pioneering work of Kawagoe (1958) and Fujita (n.d.).

Kawagoe (1958) proposed a term called ‘ventilation factor’ cited here after Thomas (2004) as a results of his studies on wooden cribs burning inside an enclosure. He correlated the burning rate with the ventilation factor, however the correlation between mass inflow of air and ventilation factor is related to the work of Fujita (n.d.), cited after Thomas et al. (1973). Nevertheless, it was found later that the correlation is no longer valid for larger openings (Thomas et al., 1967). One of the reasons proposed by Thomas was that air is no longer drawn by pressure difference but by entrainment for large openings. Subsequently it was reported later

that the Kawagoe approach overestimates inflow by as large as 50% for large openings (Babrauskas and Williamson, 1978). Recent study by Yil et al. (2007) analyses that in more details.

Consequently, it was decided to verify if the simple approach based on Eq. 40 can be used in this study to determine the mass inflow of air. Verification of Eq. 40 was done by comparison of GER (from Eq. 42) based on the measured HRR_{Vmax} (dashed ovals in Figure 37) with GER based on the HRR_{Vmax} being a product of Eq. 40 and constant value equal to 3000kJ/kg (energy released per kilogram of air completely consumed). Results of this verification are plotted in Figure 38a. It can be seen that good agreement was reached for all the openings with the exception of one opening having a width of 25 cm and a height of 10 cm. This is related to relatively large ratio of that opening's width to the compartment's width as reported by Yil et al (2007). Consequently for this opening Yil's formulae was used and a value of 0.36 was employed in Eq. 40 instead of 0.5. Corrected results are plotted in Figure 38b confirming validity of that approach.

To conclude, contrary to the expectations, the obtained results confirmed the validity of Eq. 40 for the experimental conditions employed in this research with the exception of one opening having a width of 25 cm and a height of 10 cm. For this opening the methodology proposed by Yil et al. (2007) was used and yielded good results. Subsequently, it was not necessary to use other more advanced methods (Janssens and Tran, 1992).

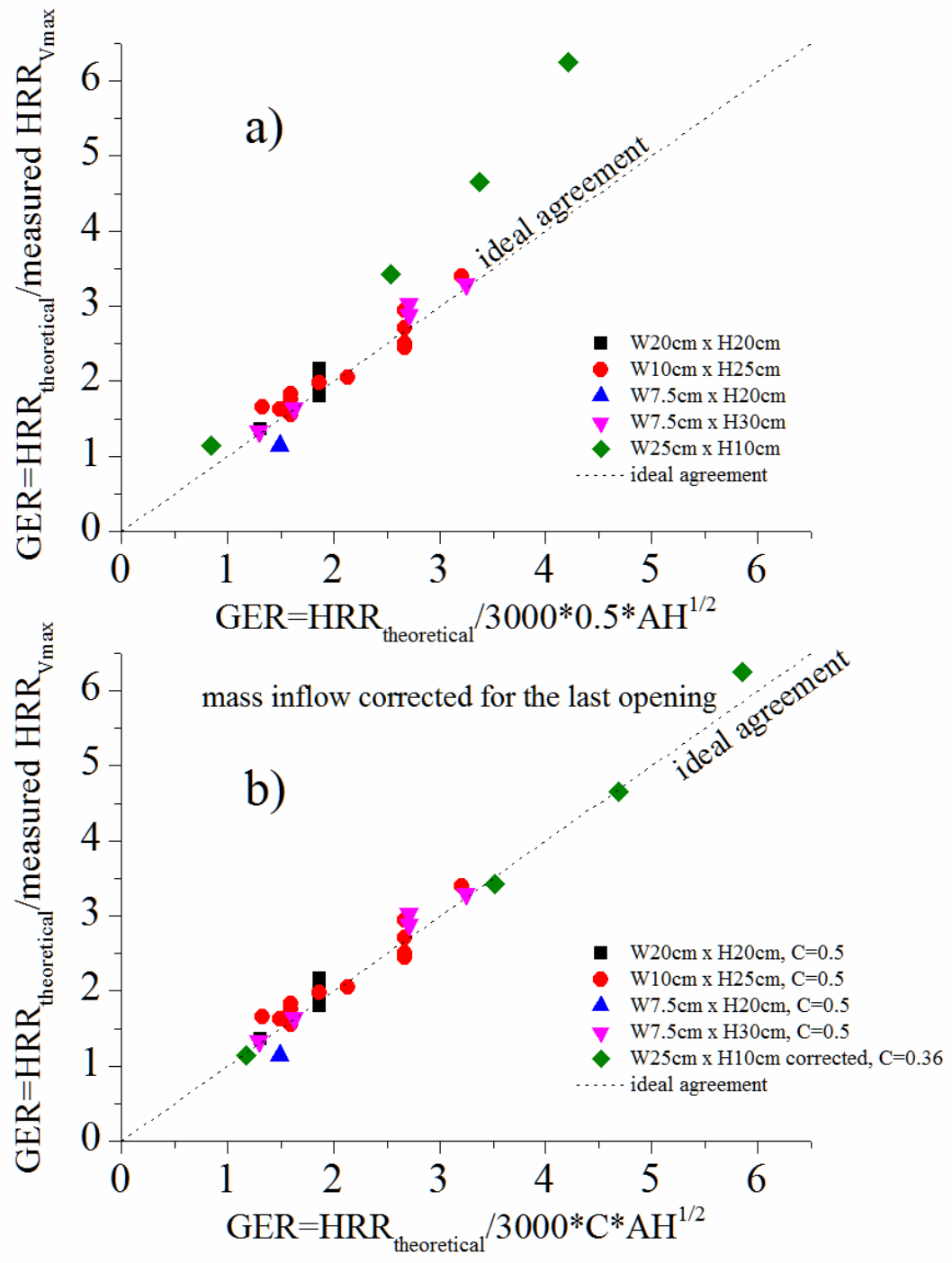

Figure 38. Verification of Eq. 40 with C factor equal to 0.5 for all openings (top figure) and C factor equal to 0.36 for the last opening (bottom figure).

4.2.4. HRR after external burning

Previous subsections (4.2.1-4.2.3) explained how the duration of the underventilated conditions was determined. Moreover, these sections were focused only on the conditions before external burning. There was no discussion on the measured HRR after external burning which will be presented now.

Examination of the Heat Release Rates after flames were visible outside (cf. Figure 37 and Appendix 4) reveals that not always the measured HRR was equal to the theoretical HRR from the fuel supply.

A recent publication by Hu et al. (2012) analyses that problem and reports that amount of excess fuel (in addition to the amount required to provide HRR=1500 $AH^{1/2}$) must be higher than a critical thresholds, namely: critical lower- and upper-fuel supply flow rates. Below the critical upper fuel supply rate only an intermittent burning outside is observed and below the critical lower fuel supply rate no ignition outside takes place. Hu et al. correlated these values with ventilation factor but that is beyond the scope of this work.

4.3. Qualitative behaviour of fires observed in the corridor like enclosure

This section presents a short qualitative description of flame behaviour during the performed experiments.

Three different fire patterns were observed during the performed experiments:

a) some time after the ignition, flames were observed outside – either as only hot glowing soot in smoke or as full bright flames clearly visible outside
b) there were no flames visible outside and no flame propagation was observed inside (via the visual observation through the opening) for the whole duration of a test
c) flames were extinguished due to not enough oxygen being present just few minutes after ignition, which happened just for a few of these experiments.

One needs to keep in mind that this work was focused on production of smoke and carbon monoxide during **underventilated** conditions. Therefore, most of the performed tests were designed to reach these conditions by choosing a theoretical HRR (from known fuel supply rate) which yielded GER>1 (details in section 3.4). This was achieved by choosing theoretical HRR larger than ventilation controlled

HRR which, for largest opening employed in this study, was around 26.85 kW. Consequently, the majority of the tests were performed at HRR>30 kW, but not exceeding 60 kW because it was found earlier that prolonged testing with fires larger than 60 kW was significantly damaging this particular experimental rig. For HRRs in the range 30-60 kW the majority of the performed tests reached a stage where flames were observed outside, in other words, most of the performed experiments were characterised by condition a) above, namely some type of flames was finally observed outside of the enclosure.

Visual observations through the opening revealed that flames were detaching from the burner for tests with GER > 1. After detachment, flames were travelling towards the opening then finally stayed anchored in the vicinity of the opening and protruded outside. This phenomenon, being different from typical external burning or flame extensions (Gottuk and Lattimer, 2008), will be discussed in the next subsection.

4.3.1. Detachment of flames from the burner and propagation towards the opening

Detailed analysis of the available data confirmed that, for tests with GER > 1, flames were detaching from the burner and were travelling towards the opening. After some time, flames were located in the vicinity of the opening. This situation was confirmed by measurements of temperature, concentration of various gases and velocity by bi-directional probes located inside the enclosure. For the majority of the tests with GER>1, the following type of external burning happened: there was no burning deep inside the corridor but most of the flames were at the interface between the corridor and the opening. That required, of course, some time for the flames to travel along the corridor seeking for fresh air. This is schematically shown on Figure 39 which illustrates different stages of a single experiment. Figure 40 shows how internal walls of the enclosure looked like after a single test. That photograph, being taken from outside, shows the walls inside of the corridor close to the opening confirming that no soot deposit was visible on walls because it was oxidized by flames. The interface between flaming and non-flaming regions is indicated by blue dots.

The flame detachment and travel along the enclosure resembles “ghosting flames” reported earlier in the literature (Sugawa et al., 1989; Audouin et al., 1997;

Bertin et al., 2002; Most and Saulnier, 2011). Ghosting flames are characterised by lifting of the flames and complete separation of the flame from the pyrolysis zone. However, lifting of the flames above floor level was not seen in the present study contrary to observations of Sugawa et al. Therefore it would be more appropriate to call these as "travelling flames" which were separating or detaching from the burner.

The rate of flames propagation was earlier investigated by previous PhD student working with a similar enclosure and his findings are briefly summarised below.

Beji (2009; 2011a) revealed and quantified the propagation of flames towards the opening in this enclosure, by means of comparison of temperature history inside. Temperature measurements at the same height but in different cubic boxes along the long axis of the corridor were compared and plotted against time. It was assumed that the peak of the temperature recorded by the highest located thermocouple in a given box indicated the transition of the flame envelope through that point. This temperature cannot be understand as a flame temperature but rather as a gas temperature due to "the unstructured three-dimensional displacement of the flame" (Pearson et al., 2007). Nevertheless Beji overlapped upper layer temperatures in various boxes as a function of time thus peak values of those temperatures were shifted in time and showed the movement of the flames. These data confirmed visual observations that flames were propagating along the corridor towards the opening. Moreover, a sudden decrease in the upper layer temperature in boxes far from the opening confirmed that the flames were no longer attached to the burner. That methodology enabled calculation of the velocity of these travelling flames (Figure 42 and Figure 43). It is worth noting that a similar methodology was used for instance by Bertin (2002) to investigate velocity of the ghosting flame.

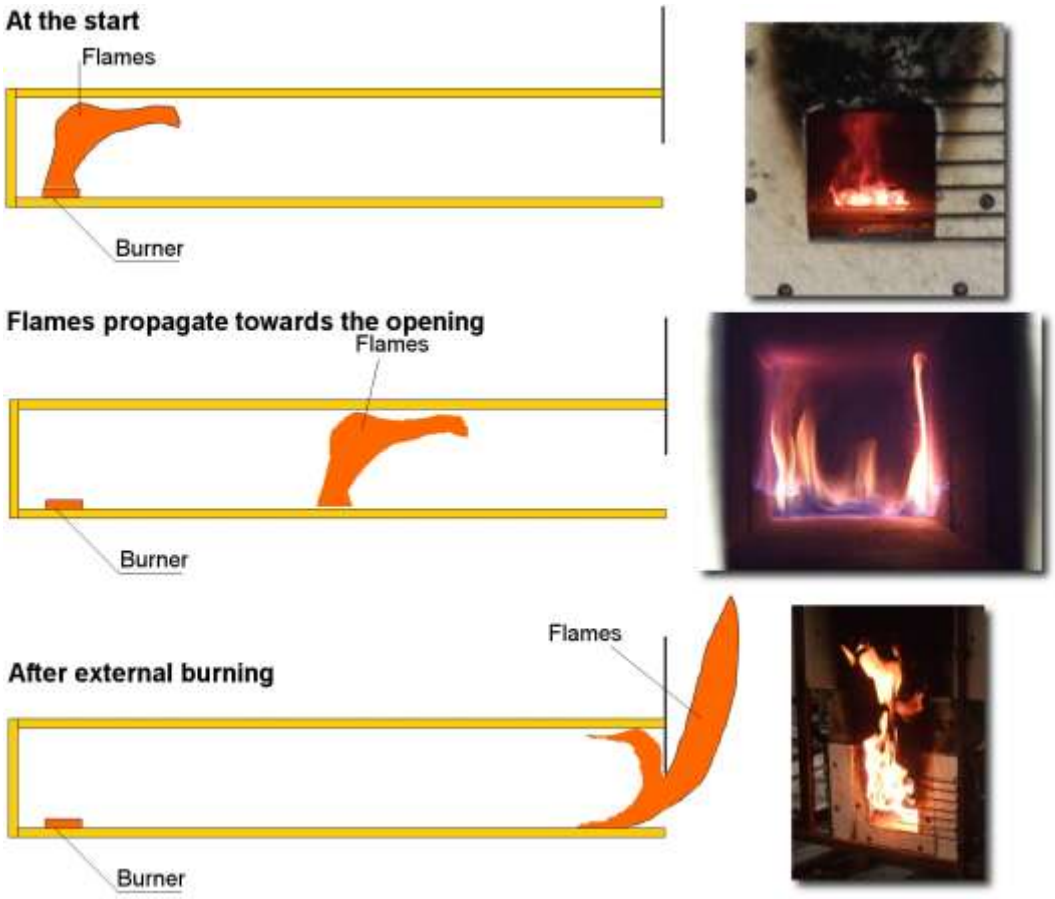

Figure 39. Qualitative illustration of flames behaviour.

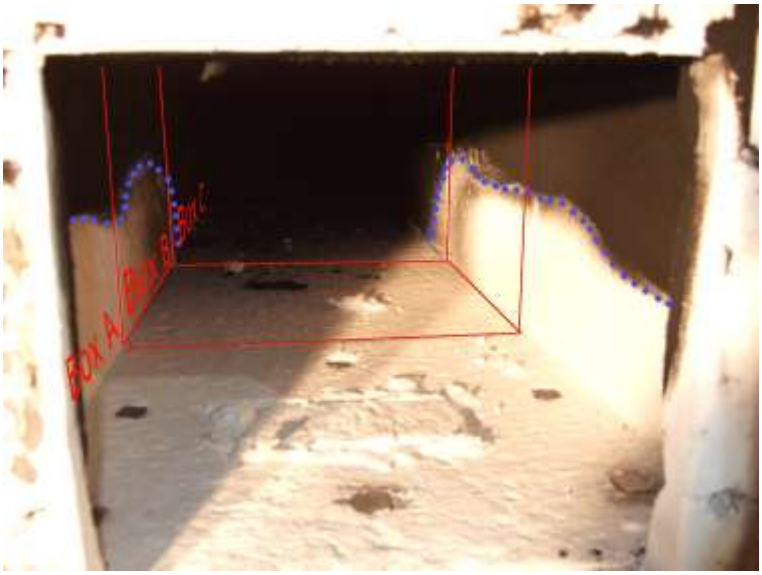

Figure 40. Post fire investigation of soot/flame patterns. Red lines indicate borders of cubic construction elements, blue dotted line indicates flame locations in the last part of the test (no soot patters due to oxidation in flames)

Further investigation was carried out on data obtained not only from thermocouples but also from gas measurements inside. For instance, one test will be analysed below. Details of the test were as follows: opening width 10 cm x height 25 cm, theoretical HRR of 40 kW[*]. Flames were first observed outside 667 seconds after the start of the test (621 seconds after ignition of the burner). Figure 41 shows all temperatures inside the enclosure as a function of time whereas Figure 42 shows only readings from top thermocouples installed in each box. These data clearly confirm advancement of flames over the whole length of the enclosure starting from the box F where the burner was located. Computed location of the peak as a function of time (with linear interpolation in between) is shown in Figure 43, indicating that there were two separate regimes of velocity – flames were propagating on a slower pace between boxes F and E (initial phase) and then at an almost constant velocity of 0.64 *cm/sec* from boxes E till B. However additional data were required for a better understanding of what was happening beyond the flame envelope. A comparison of various gases measured inside (in the lower part of box C) confirmed that behind the flame envelope the oxygen concentration was very low and therefore no flames could exist in boxes F till C at that time (Figure 44). Furthermore, concentration of total unburnt hydrocarbons was exceeding the maximum reading of the analyser, i.e. higher than 3.5%, indicating that the fuel was present feeding flames at the opening.

[*] Data from all experiments performed by author are reported in the Appendix 4. Detailed analysis of temperature data is outside of the scope of this work and was performed for similar tests by Beji (2009; 2011a).

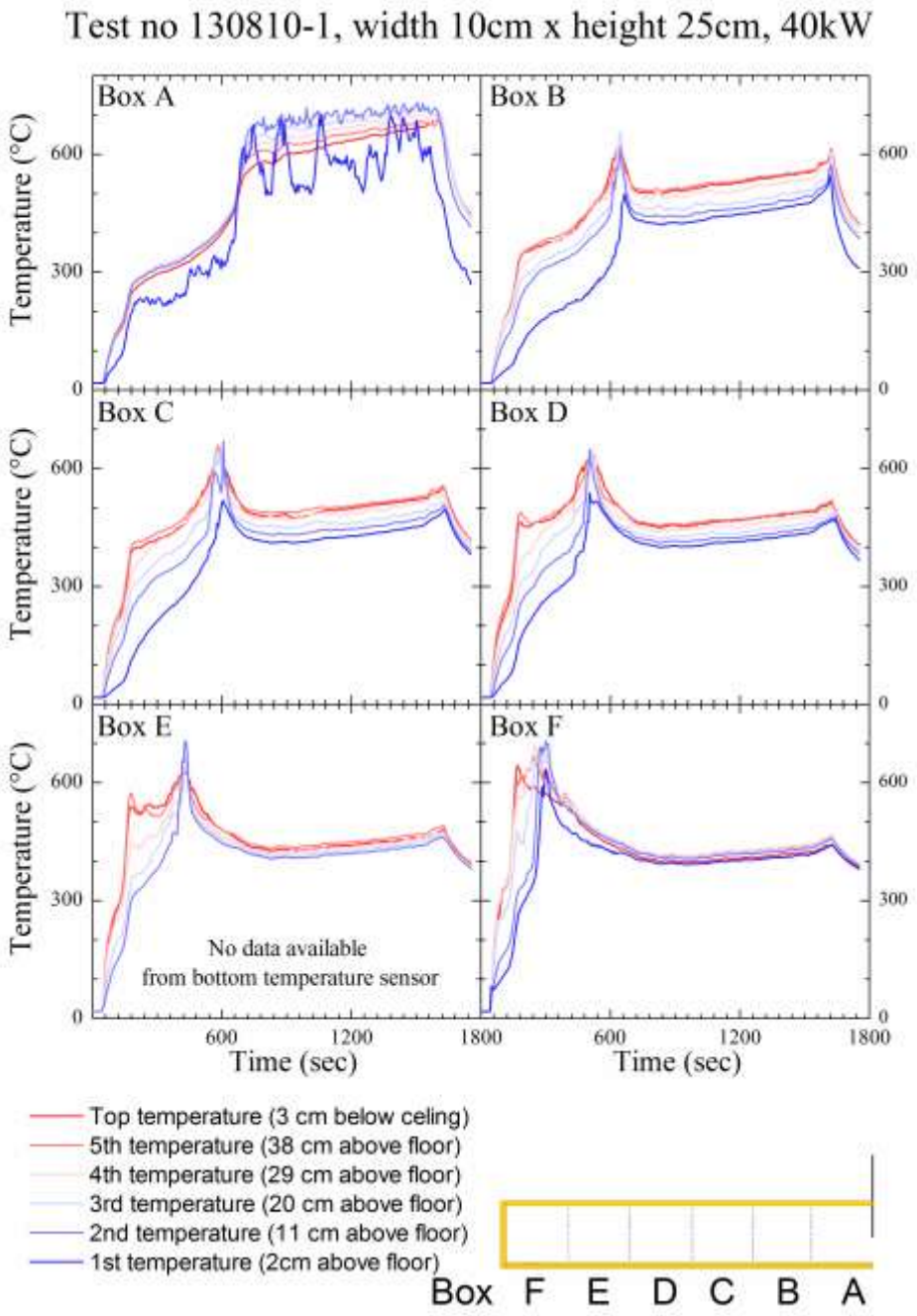

Figure 41. Thermocouple readings from all boxes along the corridor length as a function of time.

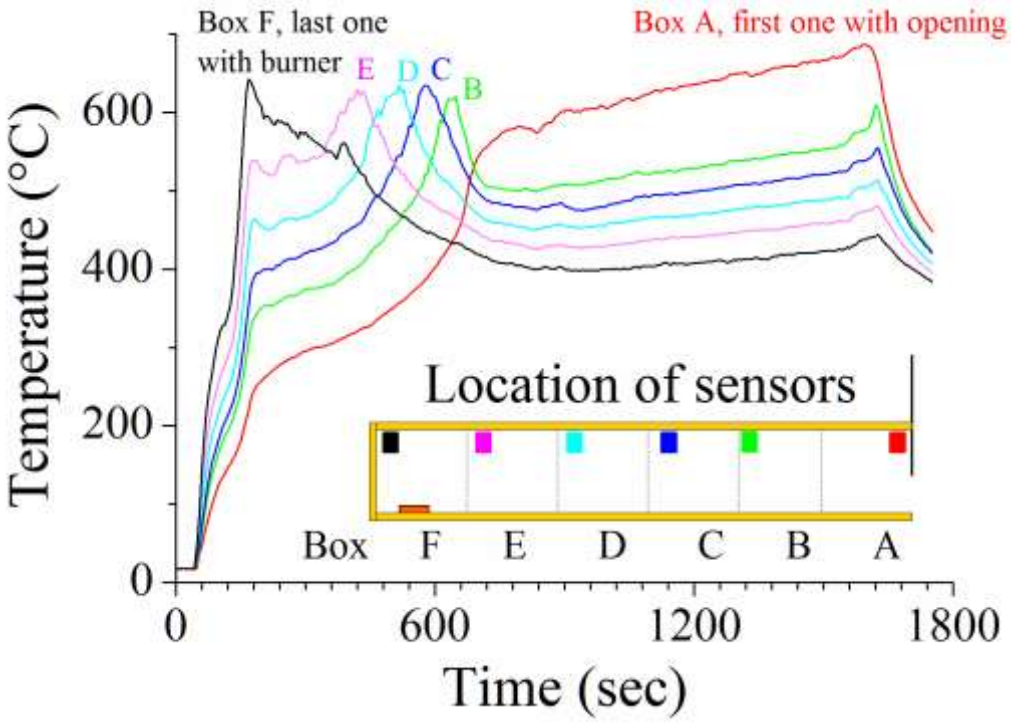

Figure 42. Top thermocouple reading from all boxes along the corridor length as a function of time. Test no 130810-1, W10cm x H25cm, HRR=40kW, GER= 2.13.

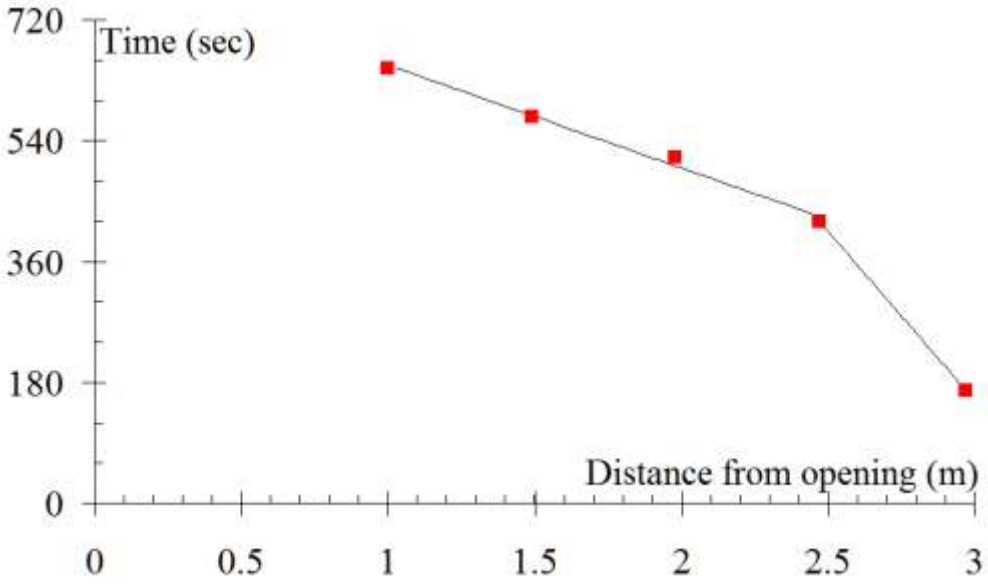

Figure 43. Propagation of the flames through the enclosure as a function of time. Test no 130810-1, W10cm x H25cm, HRR=40kW, GER= 2.13.

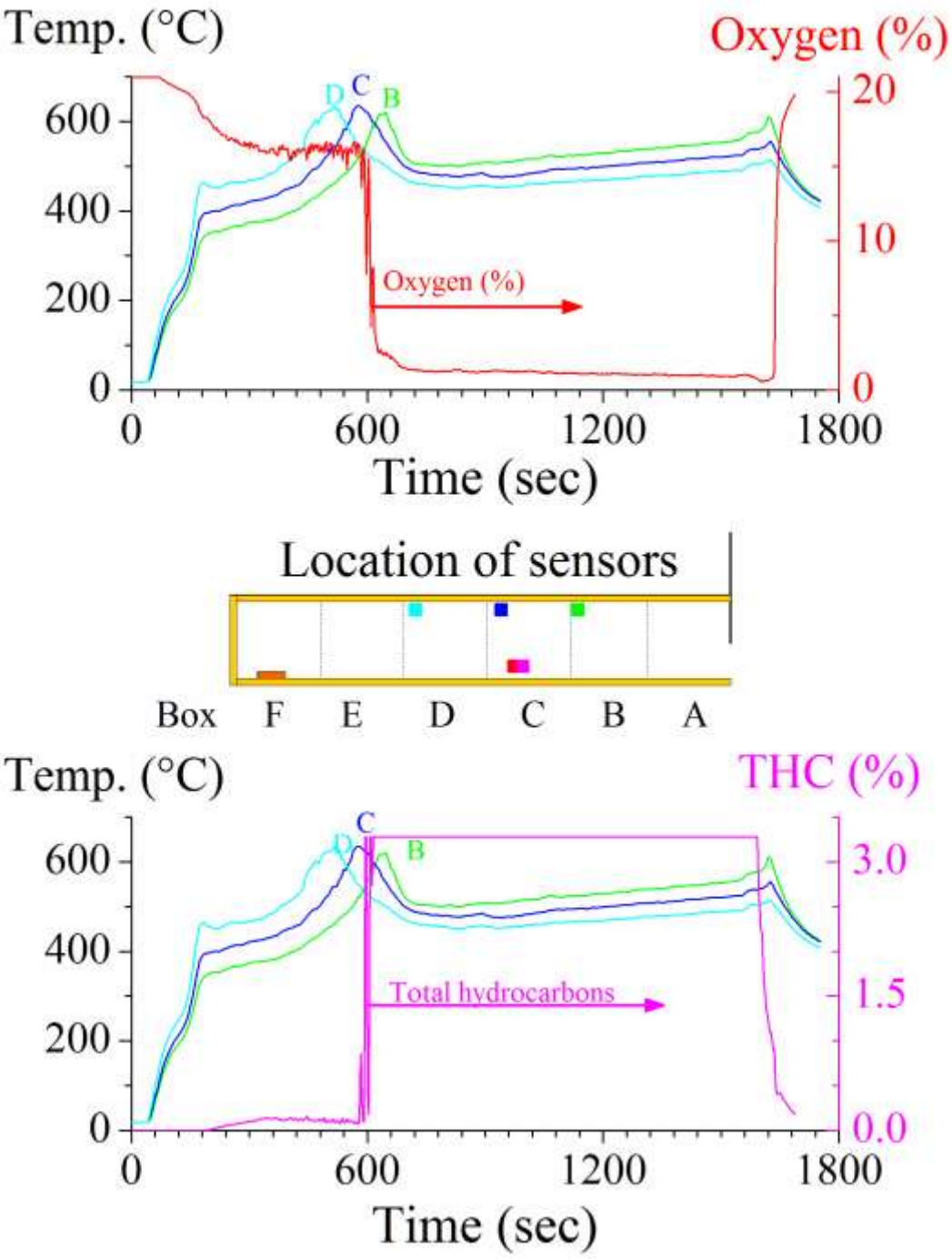

Figure 44. Gases measured in the middle of the enclosure. Top: Oxygen with temperature history, Bottom: Total hydrocarbons with temperature history. Test no 130810-1, W10cm x H25cm, HRR=40kW, GER= 2.13.

Data from the present study was used to obtain velocities of the travelling flames from all tests. It was found that a good correlation exist between velocities of these travelling flames and GER (Figure 45). Remarkably, the obtained velocity range is of the same order of magnitude as the velocities of ghosting flames reported by Audouin (4-8 cm/s) (1997) and Bertin (9 cm/s) (2002). Lower velocities reported here may be related to different range of GER examined and measurement uncertainties.

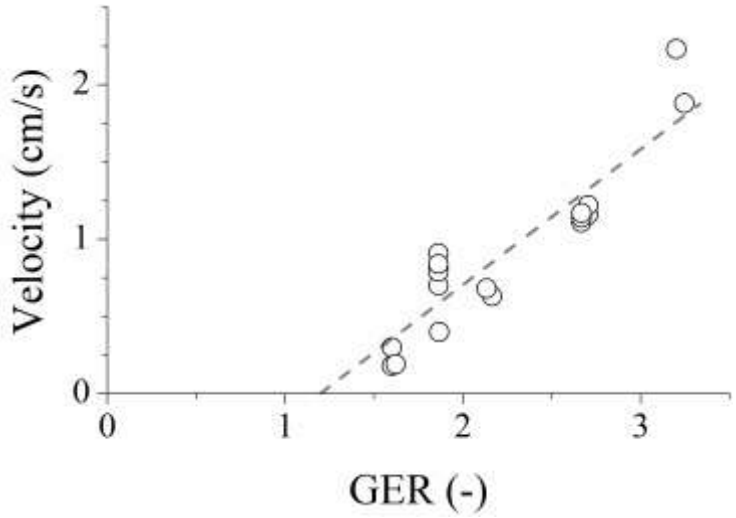

Figure 45. Velocity of the flame travelling along the corridor as a function of Global Equivalence Ratio. Data averaged over boxes B-E.

4.3.2. Detachment of flames from the burner as a result of a drop in oxygen concentration

Additional sensors used in the present study revealed further information on the nature of the detachment of flames reported in the previous section. It was found that the detachment of flames from the burner was directly related to a sharp drop in the oxygen concentration in the vicinity of the burner as shown in Figure 46. That figure shows temperature data from thermocouples installed in last box together with oxygen concentration in the lower layer, in the close vicinity of the burner. As soon as the oxygen concentration significantly dropped, the temperature measured in the upper layer (red curve) dropped also, thus confirming that flames were no longer present. However, extinction was not observed and the flames started to travel towards the opening. This is further confirmed by data in Figure 47 which shows top temperatures along the whole corridor together with oxygen concentration measured in the vicinity of the burner. The transition of the peak temperatures between boxes

F and E coincided with the drop of oxygen level in the vicinity of the burner. After this drop, flames detached the burner and started to travel further towards the opening. This is again confirmed by peaks of temperatures in other boxes (Figure 47).

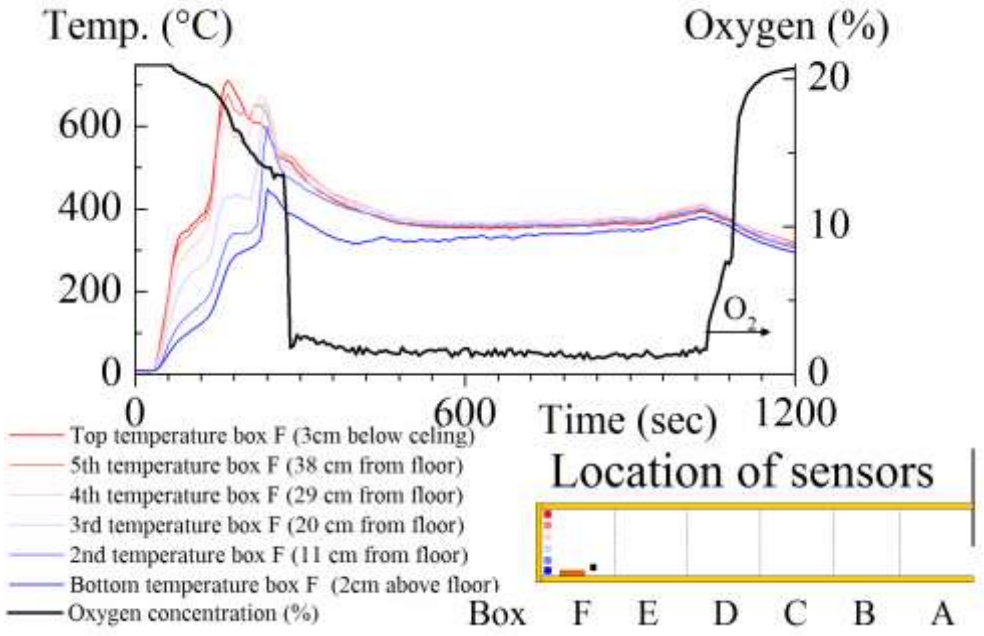

Figure 46. Temperatures in last box together with oxygen concentration showing relation between oxygen concentration in the vicinity of the burner and detachment of flames . Test no 181209-1, Opening size W10cm x H25cm, HRR=50kW, GER= 2.7

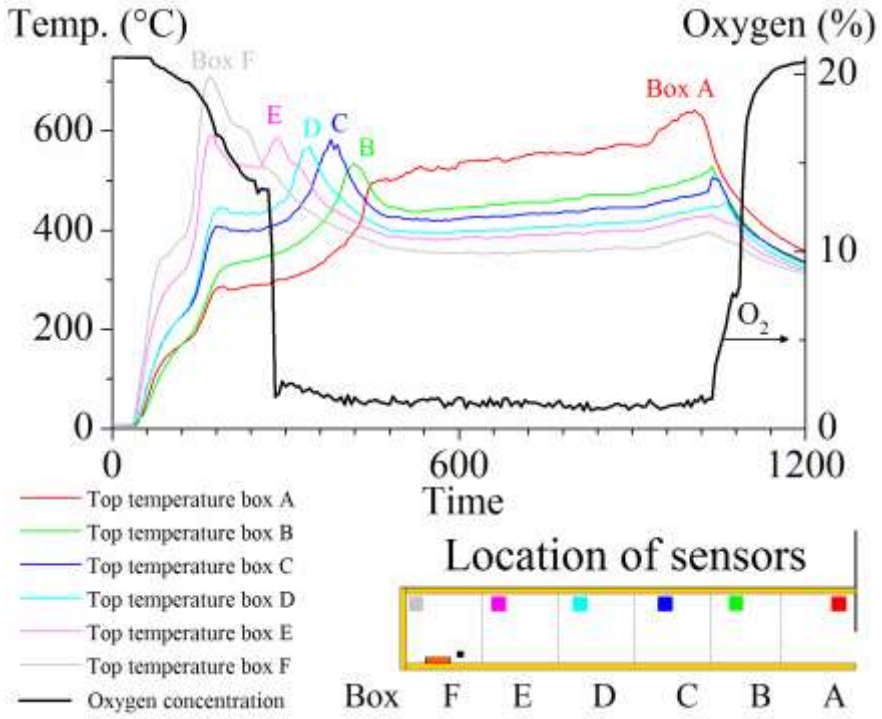

Figure 47. Top layer temperatures along the corridor with oxygen concentration measured close to the burner showing relation between oxygen concentration in the vicinity of the burner and detachment of flames. Test no 181209-1, Opening size W10cm x H25cm, HRR=50kW, GER= 2.7

Further analysis revealed that the detachment of the flames from the burner was correlated with the Global Equivalence Ratio. Figures 45-46 present a correlation between time of detachment and the Global Equivalence Ratio. Time of detachment could be derived from temperature data (Figure 48) or could be based on the drop in oxygen concentration (Figure 49). Results were very similar, just slightly shifted in time. Basically, it confirmed that the detachment of flames was strongly correlated with the Global Equivalence Ratio and all the experiments with GER>1 were characterised by detachment of flames. It is worth noting that these findings show a link between a global parameter (depending on HRR and opening size) with a local phenomenon of time of flame detachment. This could be explained by recirculation of gases inside the enclosure which resulted in depletion of oxygen in the close vicinity of the flame. Model of such recirculation was proposed for instance by (Delichatsios, 1990).

Additionally, it was found that faster detachment of flames can be related to preheating of the enclosure. Preheating is understood as starting a test in an enclosure which did not cool down completely after a previous test. This claim needs however further investigation as it is based only on two tests.

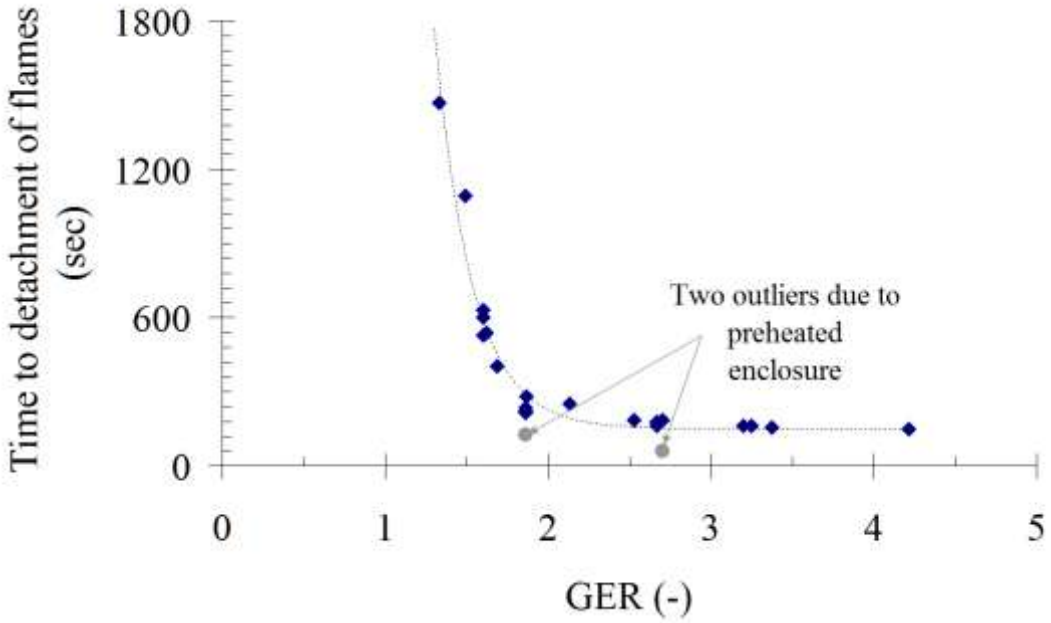

Figure 48. Time of flame detachment (based on temperature drop in the last box) as a function of the Global Equivalence Ratio. Dashed line represents fitted trend.

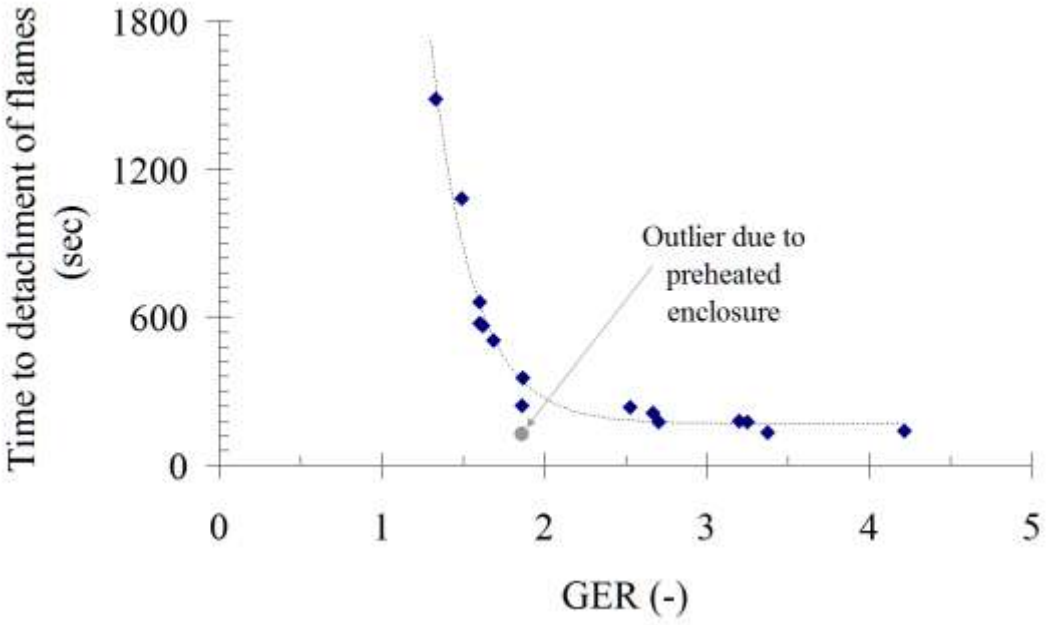

Figure 49. Time of flame detachment (based on drop in oxygen concentration) as a function of the Global Equivalence Ratio. Dashed line represent fitted trend.

4.3.3. Overventilated conditions and no detachment of flames

Previous figures do not present any data for GER ≤ 1, as no detachment of flames was observed for tests in overventilated conditions. An example of such a test is presented in Figure 50 which shows data from tests with the Global Equivalence Ratio equal to 0.8. This graph presents oxygen concentration measured in the vicinity of the burner overlapped with temperature data from the same box. Oxygen level did not drop below 15% and temperature was rising constantly and no flame detachment was visually recorded. This is confirmed by

Figure 51 showing top temperatures from various boxes with no sign of travelling flames.

To conclude, all the experiments with GER>1 were characterised by flame detachment whereas flames stayed anchored to the burner for experiments with GER<1.

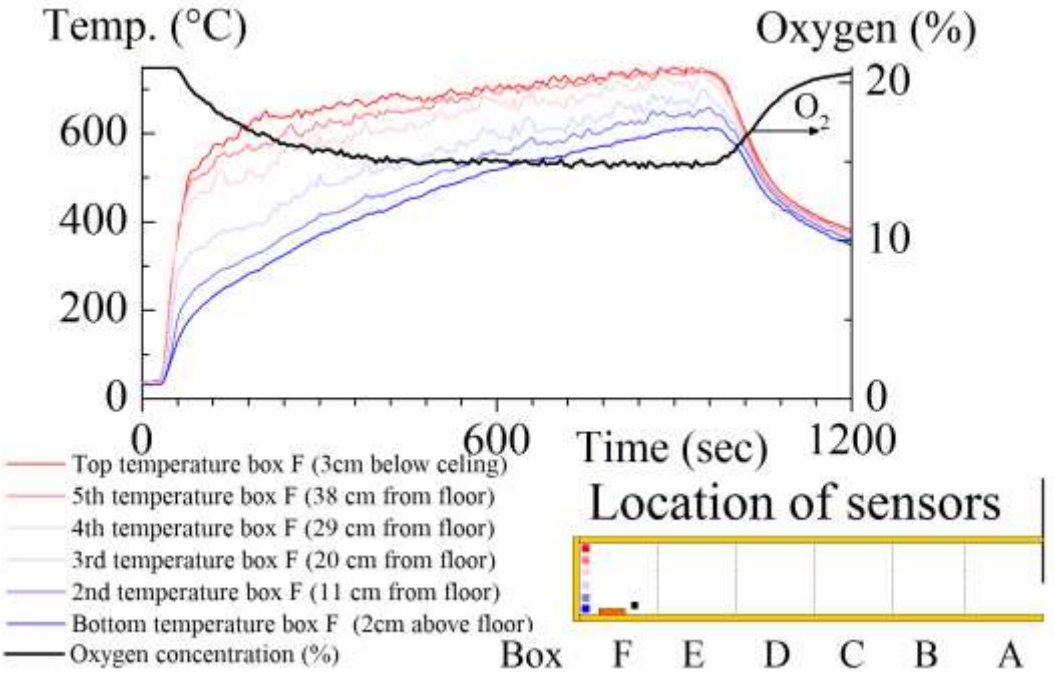

Figure 50. Temperatures in the last box together with oxygen concentration in the vicinity of the burner. Test no 101209-2, Opening size W10cm x H25cm, HRR=15kW, GER= 0.8

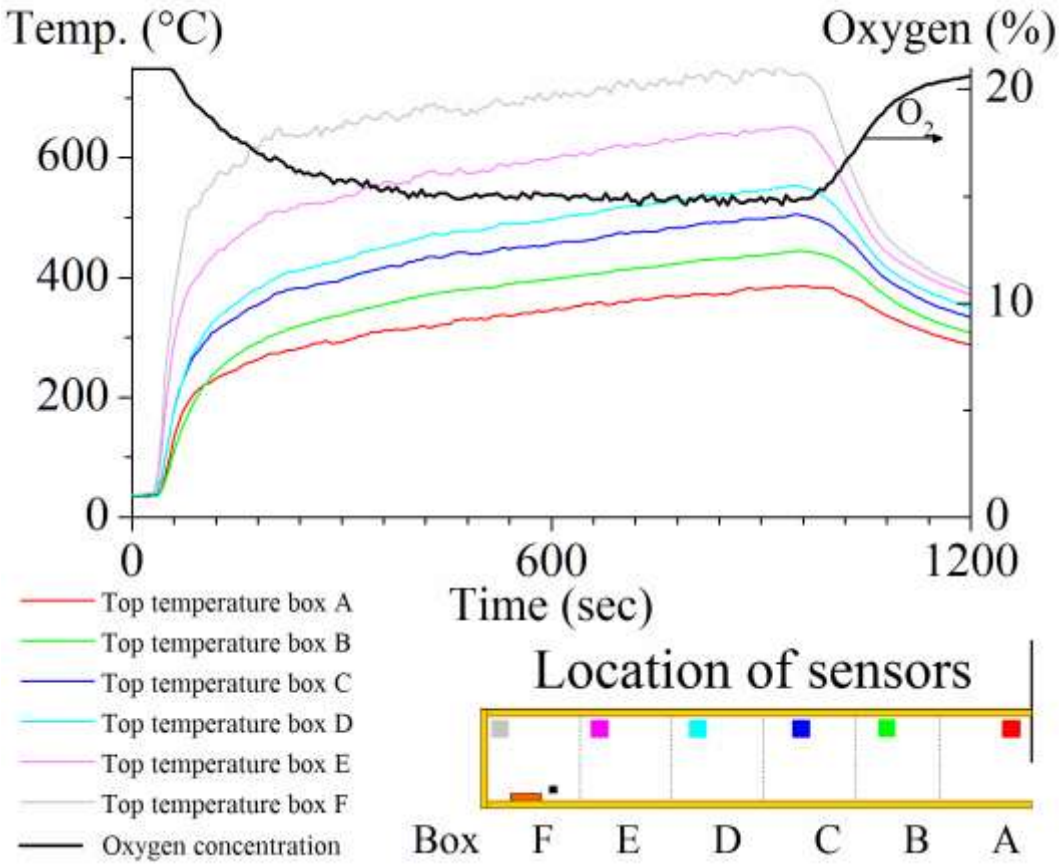

Figure 51. Top layer temperatures in whole corridor with oxygen concentration measured close to the burner. Test no 101209-2, Opening size W10cm x H25cm, HRR=15kW, GER= 0.8

4.4. Production of smoke inside and outside of the enclosure

This section discusses data on smoke concentrations reported as smoke volume fractions. Measurements inside and outside are compared and differences are analysed.

4.4.1. Introduction

One of the aims of this study is to compare data on smoke from measurements performed inside and outside of the corridor (in the exhaust duct). Such a comparison is crucial for better understanding of smoke production in enclosure fires.

For detailed discussion, the smoke behaviour is analysed in relation to three stages of fire development in the experimental rig: 1) globally overventilated conditions at the beginning of each test; 2) globally underventilated conditions before flames emerged outside of the enclosure and finally 3) after flames emerged outside of the enclosure. It is important to note that these stages are not necessary meaning pre- and postflashover. Flashover is related to ignition of all combustible materials inside an enclosure and usually on-set of flashover is associated with the upper layer temperature in the range 500°C to 600°C (Babrauskas and Williamson, 1978). Fire which reaches flashover stage is usually no longer fuel controlled but ventilation controlled and thus become underventilated till flames emerge outside. However it is possible to have underventilated fire which will not reach flashover stage; subsequently fires in enclosure with very large openings can reach flashover and still be overventilated. Therefore this analysis is related to over and under ventilated conditions and not to pre- and postflashover fires.

Behaviour of smoke during three stages mentioned earlier is presented in Figure 52. Data points are presented from six experiments with different opening sizes and theoretical HRRs. Blue curve presents smoke volume fractions inside the exhaust duct (scaled up 100 times), green curve presents smoke volume fractions inside the enclosure and black one presents measured Heat Release Rate. Note that the smoke concentration in the duct was two orders of magnitude lower than that in the

enclosure because of the dilution of the gases in the exhaust duct[*]. Grey shaded area indicate when fire was underventilated globally, such a condition ceased when flames emerged outside the corridor.

Short description of smoke behaviour during these three different stages is presented below; detailed analysis is given in subsections to follow.

Stage I - Shortly after ignition, the fire was well-ventilated as there was still enough air available. During this period, smoke volume fraction increased inside as well as outside of the enclosure.

Stage II – This stage is related to globally underventilated conditions. During that time flames started to move along the corridor towards the opening at the front. Smoke behaviour during these underventilated conditions can be divided into two separate regimes: Initially, immediately after fire became ventilation controlled (grey shaded area in Figure 52) there was a slight decrease in smoke volume fractions (both inside and outside), followed by a second regime during which smoke volume fractions increased.

Stage III – As soon as the flame reached the opening, fire was no longer underventilated, at least globally. Measured HRR reached values close to the maximum designed value (Figure 37) thus confirming that almost all released fuel was consumed, partially inside and partially outside (for additional discussion on HRR during that period consult section 4.2.4). Conditions were globally overventilated and the smoke volume fraction dropped outside the enclosure due to external burning. However, smoke volume fractions inside continued to increase.

Detailed analysis of smoke behaviour during these stages is discussed in sections to follow.

[*] The exhaust flow rate was in the range of 1.3 to 1.5 m^3/s, so for instance for the opening 20cm x 20cm and assuming outflow from the enclosure equal to inflow equal to $0.5AH^{1/2}$ and converting volumetric flow in the duct to the mass flow one can obtain dilution ratio of about 200 which is in a good agreement with two orders of magnitude difference in concentration between duct and inside the enclosure. Detailed analysis is presented in section 3.3.1.5.

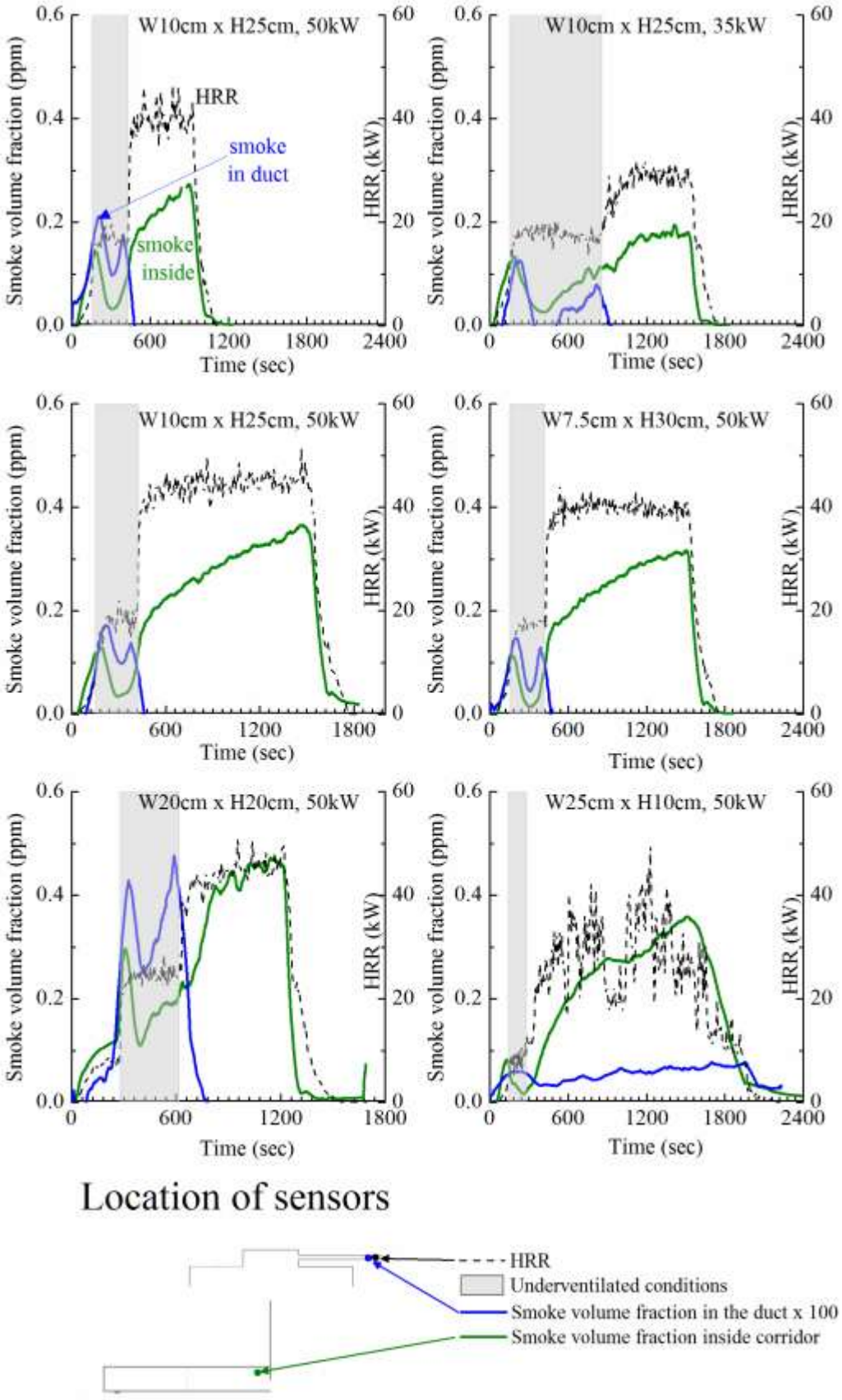

Figure 52. Smoke volume fractions inside the enclosure and outside in the exhaust duct (scaled up 100 times) together with measured HRR during three stages of fire development.

4.4.2. Smoke volume fractions inside the enclosure during Stage I and II

This subsection describes behaviour of smoke during Stages I and II, namely from the ignition till the flames were visible outside.

For most of the tests, the smoke concentration was rising following an increase in the amount of fuel supplied; however an unexpected drop was recorded just as the undervetilated conditions developed (grey shaded area in Figure 52). This was observed for all the tests with GER > 1. It was inferred that the decrease of smoke volume fractions was related to decreasing concentration of oxygen as shown in Figure 53. That decrease of smoke concentration finished as soon as oxygen level dropped significantly and then aerodynamic processes started to dominate as will be explained in sections to follow. Further research is required however in order to fully describe this relationship between oxygen concentration and smoke production.

A similar trend was observed also for carbon monoxide measurements inside, in the location adjacent to smoke measurements. Figure 54 shows data on smoke and carbon monoxide from tests with three different openings but the same HRR (no data is available for the fourth opening). A black curve presents smoke volume fractions inside and a blue curve presents carbon monoxide concentrations measured inside the corridor. A decrease in the carbon monoxide concentration clearly coincides with the decrease in the smoke concentration. At the same time a small increase in carbon dioxide was recorded. This is clearly illustrated in Figure 55. This increase in carbon dioxide indicates conversion of CO and unburnt hydrocarbons to carbon dioxide in the presence of oxygen available in the initial part of the test (Thiry, 2011). Unfortunately there is no confirmation of that phenomenon in temperature data, probably because of short reaction time and the delay in response of the thermocouples. Moreover, data logging of temperature was performed at 6 sec intervals due to the limitations of the hardware (too many channels). It is worth noting that as soon as oxygen level dropped significantly that conversion of CO to CO_2 was stopped.

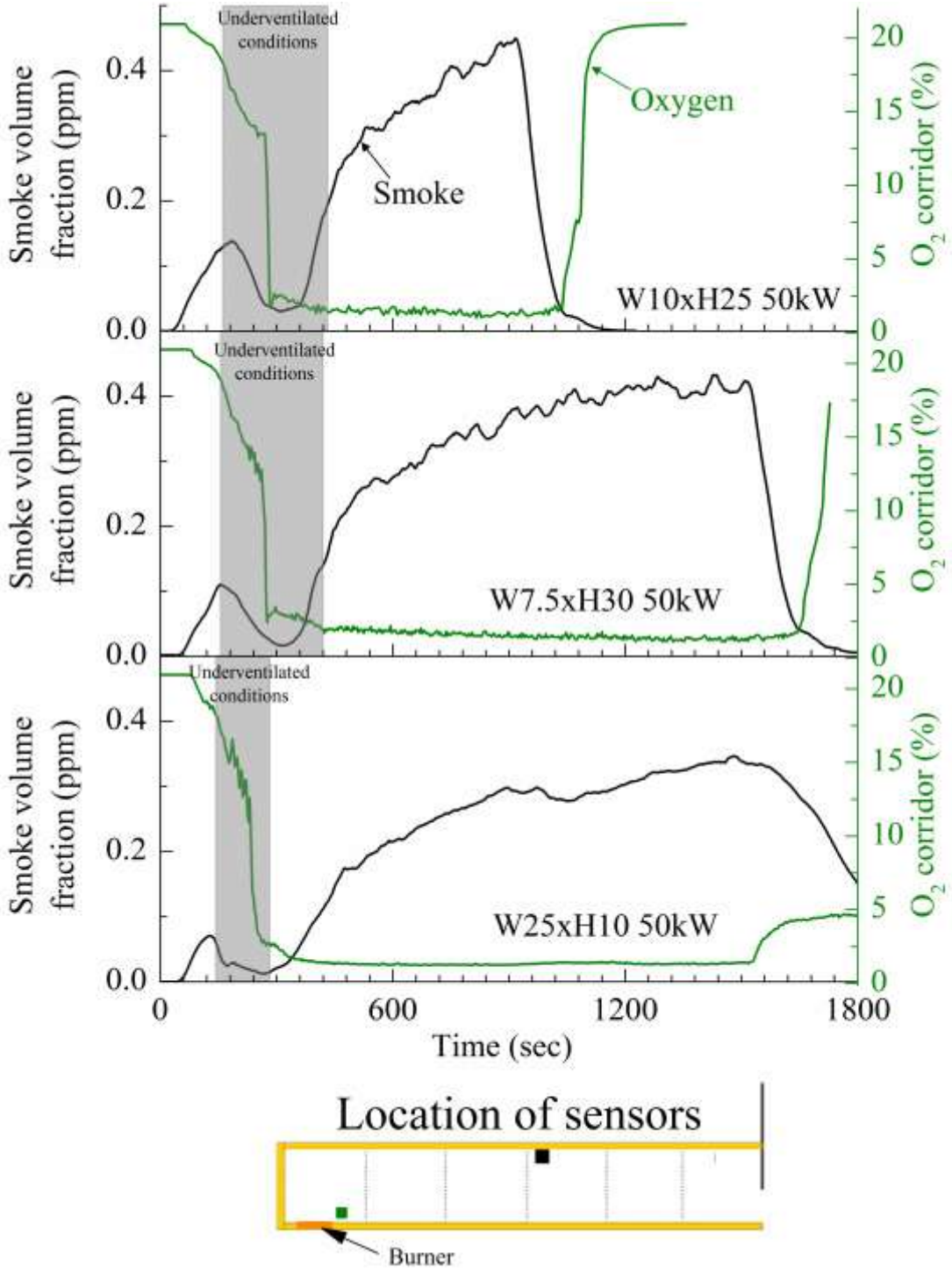

Figure 53. Smoke volume fractions and oxygen concentration (on a dry basis) measured inside the corridor.

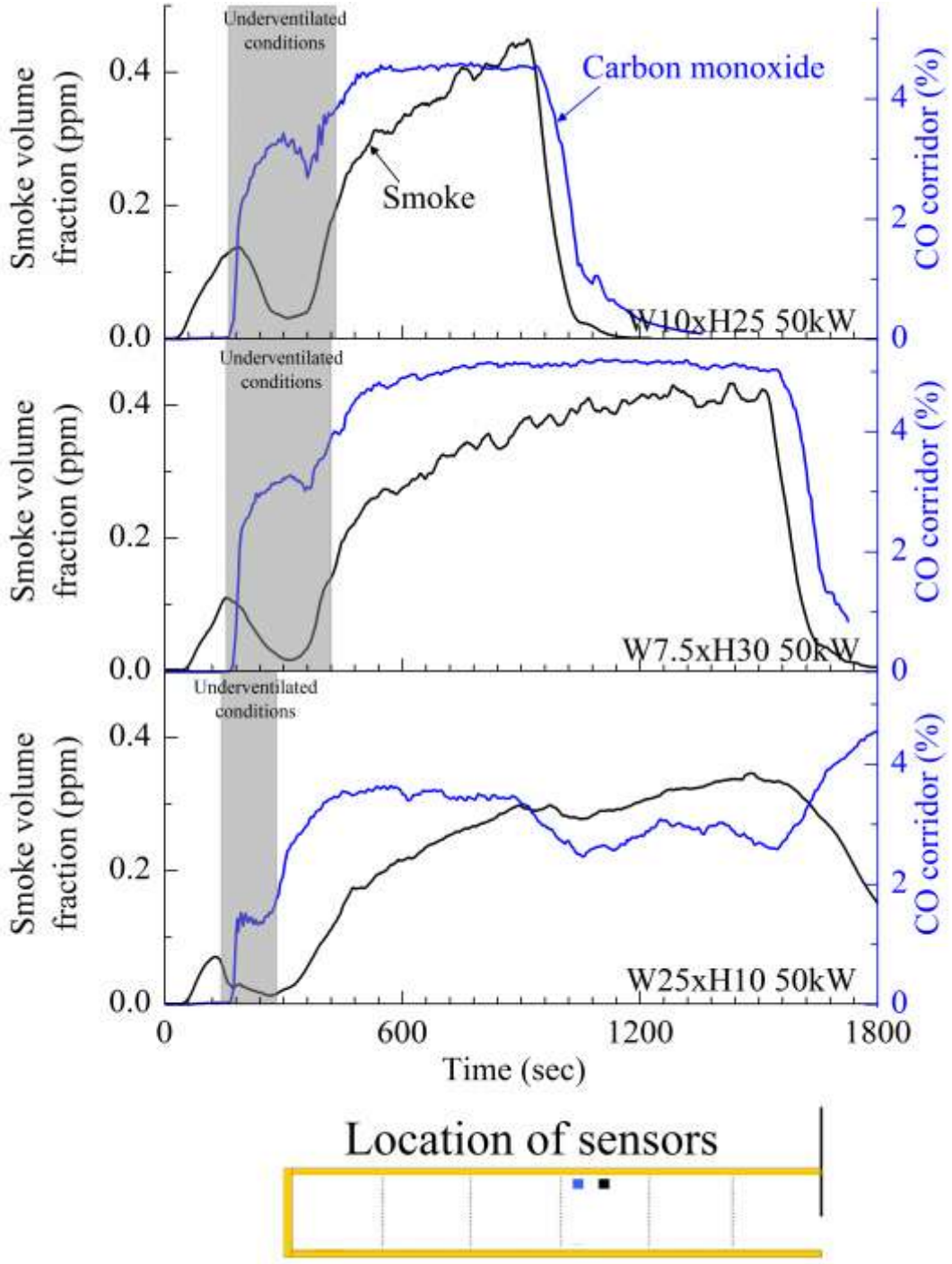

Figure 54. Smoke volume fractions and carbon monoxide concentration (on a dry basis) measured inside the corridor,

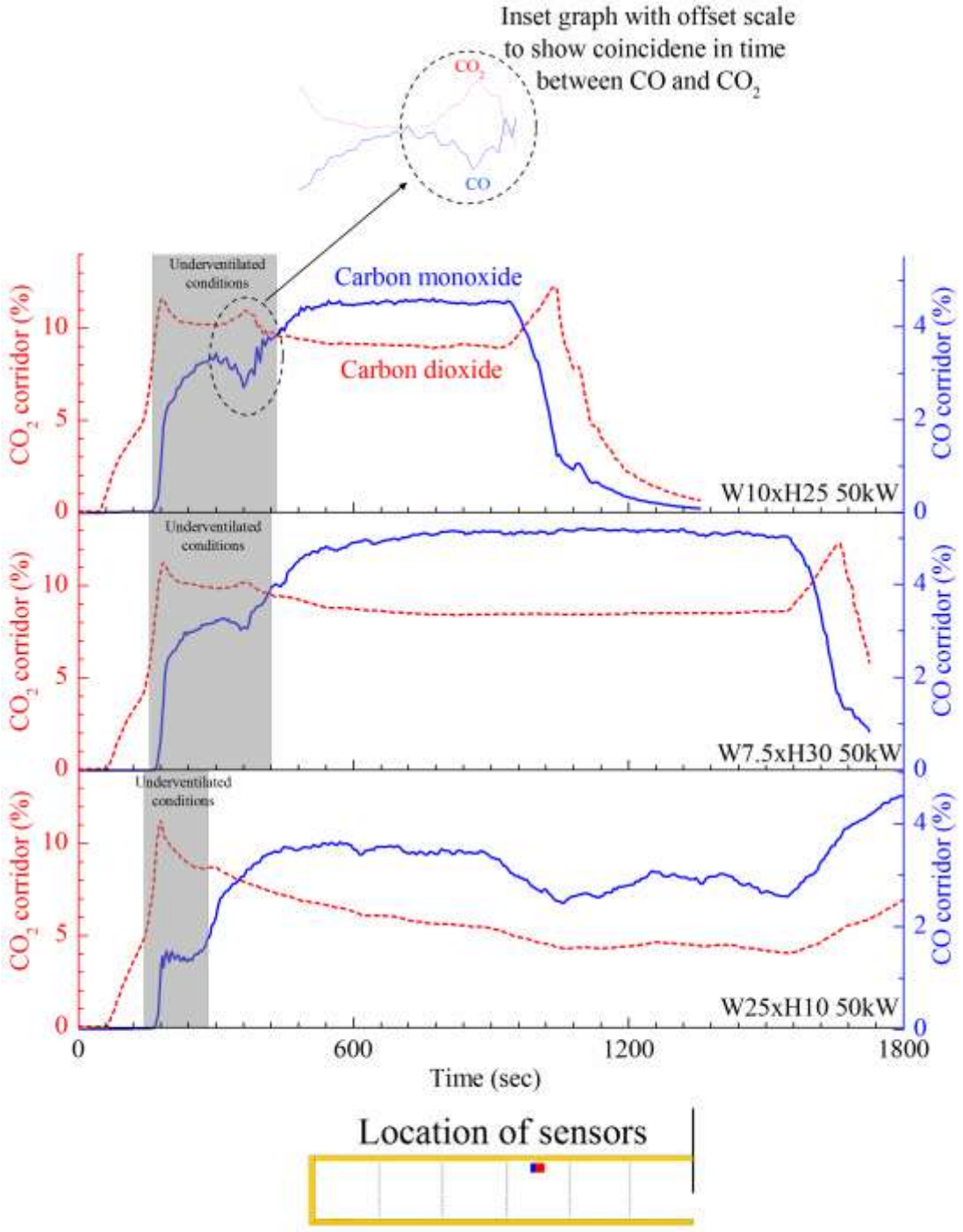

Figure 55. Carbon monoxide and carbon dioxide concentrations (on a dry basis) measured inside the corridor.

4.4.3. An increase in smoke volume fractions inside the enclosure after flames emerge outside (Stage III)

This subsection describes behaviour of smoke during Stage III, namely from the point when the flames were visible outside. As explained before, as soon as the flame reached the opening, conditions were globally overventilated. The smoke volume fraction dropped outside the enclosure whereas an increase in smoke concentration was measured inside the enclosure. The decrease outside is due to the occurrence of external burning which provides environment for further oxidation of soot within flames but the increase inside requires additional explanation.

The author inferred that the increase in smoke volume fractions inside the enclosure is related to the propagation of flames along the corridor (cf. section 4.3.1). It was found unexpectedly that this increase in smoke volume fraction is related to the change of the flow pattern behind the moving flame envelope in the sense that hot gases started to travel near the ceiling backwards towards the closed end of the corridor. This change of flow and recirculation of combustion products is discussed in the next subsection.

4.4.4. Recirculation of gases inside the enclosure

As stated before, the increase in smoke volume fractions inside the corridor is related to recirculation of gases within the enclosure. That recirculation is caused by transition of flames from the burner towards the opening (as explained in the section 4.3.1). Further insight of this process was obtained by two bi-directional probes installed inside the corridor, first one in the lower layer, and second one in the upper layer, close to the middle of the rig (section 3.3.5).

It was found that the change of flow directions inside was taking place behind the flames travelling along the corridor towards the opening. It is schematically depicted in Figure 56. One has to keep in mind however that the presented diagram is based only on 2 dimensional measurement of velocity whereas in reality the flows inside are 3 dimensional.

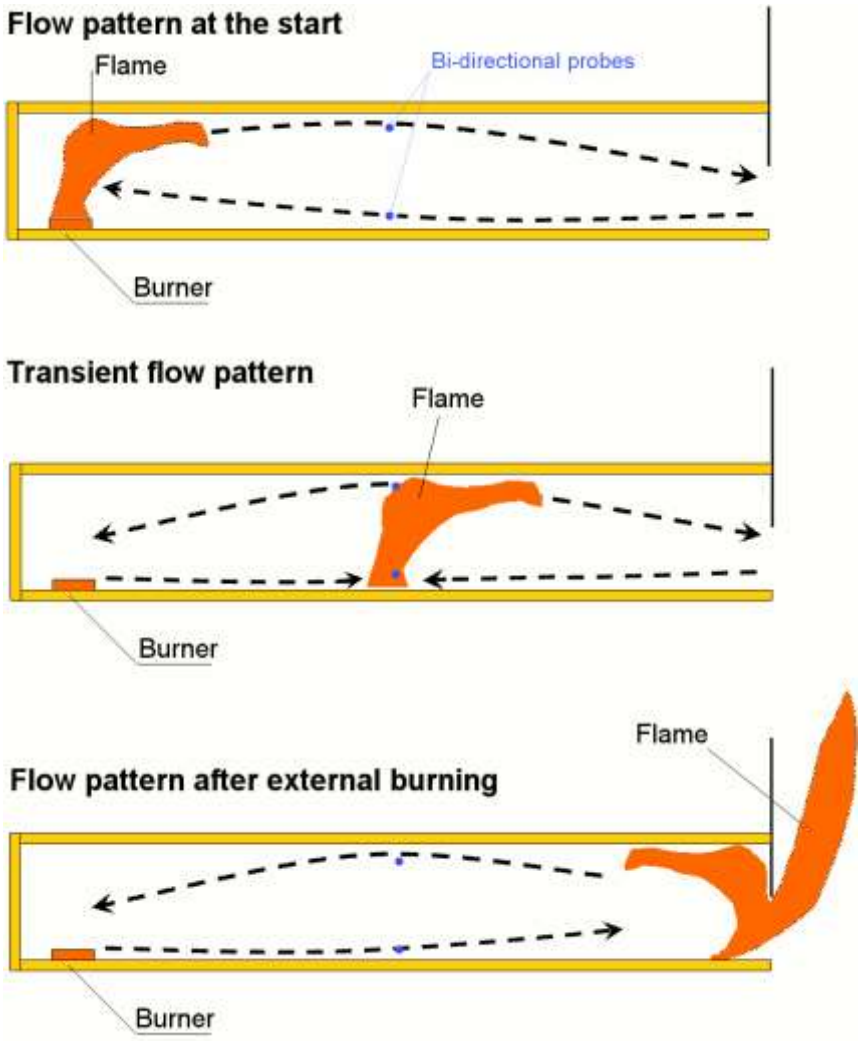

Figure 56. Change of flow pattern inside the enclosure during flame transition towards the opening.

At this point it is important to recall a sketch presented by Audouin et al. (1997) which was published in their study on ghosting flames. A part of this sketch is presented in Figure 57. It can be seen that similar trends were reported regarding reversed flows behind the ghosting flame.

This behaviour was confirmed in the present study by bi-directional probes data, as shown in Figure 58. This figure presents velocities measured in the upper layer (blue shaded contour) and in the lower layer (green shaded contour) overlapped with top layer temperatures measured in boxes D, C, and B. Peaks of upper layer temperatures indicate transition of flames between boxes. Transition through box C (bi-directional probes were located in that box) coincided in time with change of velocity signs. This change of signs was caused by reversion of flow patterns inside, namely gases started to flow towards the opening in the bottom layer and towards the burner in the upper layer. This data confirmed that flows changed as soon as

flames passed the bi-directional probes and proved that that the reversion of flows was occurring behind the travelling flames.

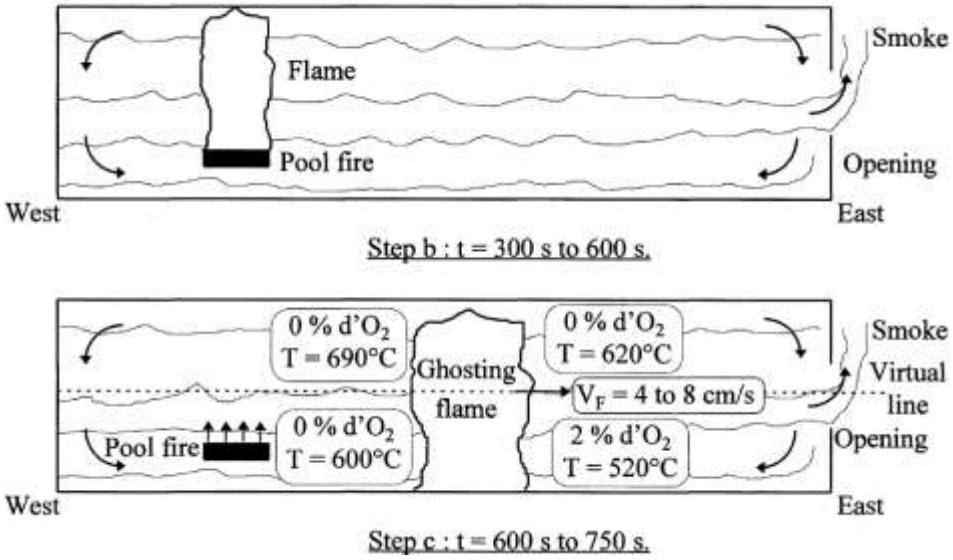

Figure 57. Audouin's diagram showing reversed flow directions behind a ghosting flame. Adapted from Audouin et al. (1997) with permission.

This change of flow directions and recirculation of combustion products was also confirmed by data on the oxygen concentration inside the enclosure as shown in Figure 59. This figure confirms that drop in oxygen concentration coincided in time with reversion of flows at around 600 seconds indicated by change of sign in the measured velocities. Oxygen level dropped because behind the travelling flames there were present only products of combustion and unburnt fuel. This is again in agreement with data on oxygen concentrations presented by Audouin (Figure 57).

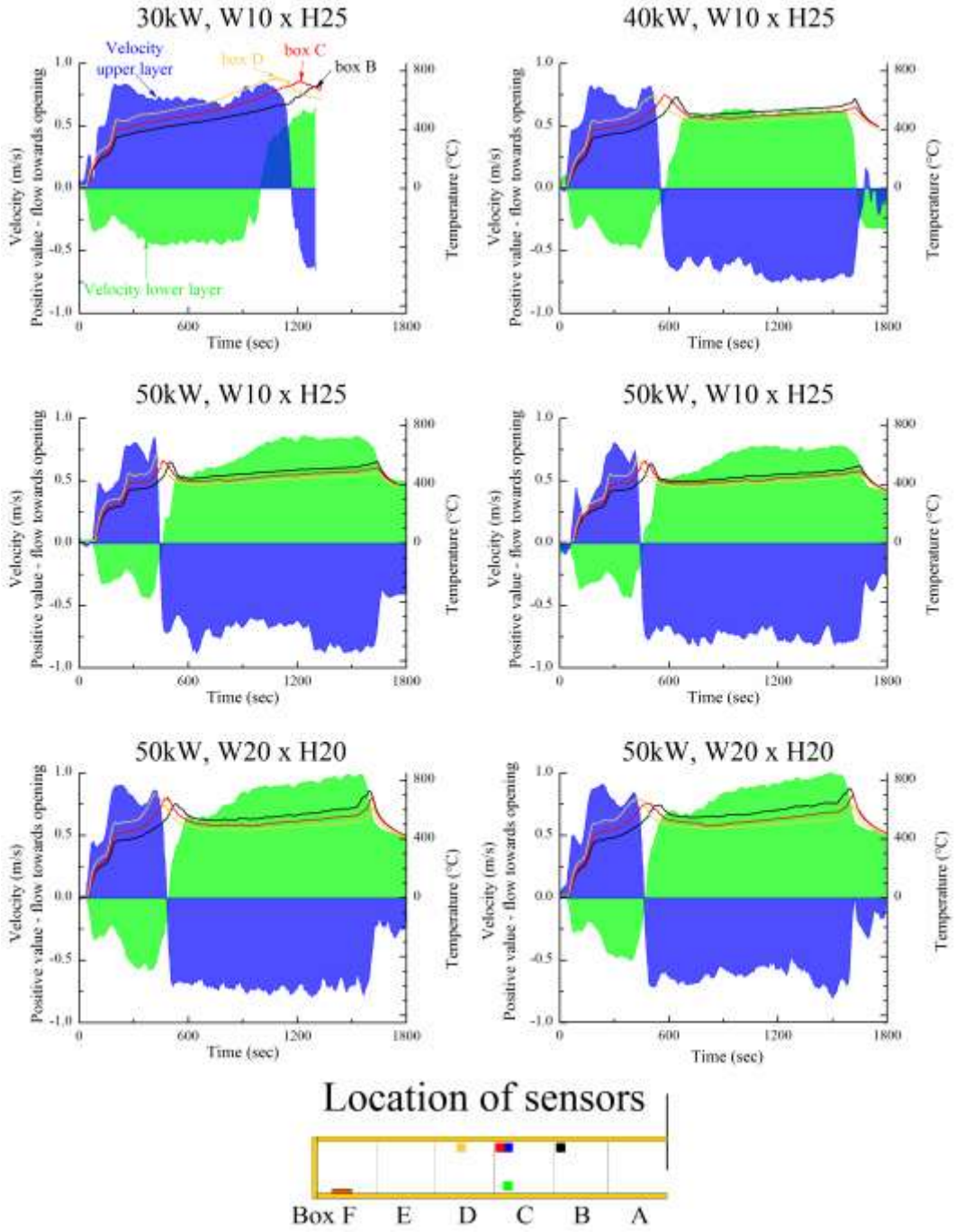

Figure 58. Comparison of 6 tests where bi-directional probes were used showing velocities in the upper and lower layer (measured in box C) together with upper layer temperatures in boxes B, C and D. All data smoothed over 30 sec period.

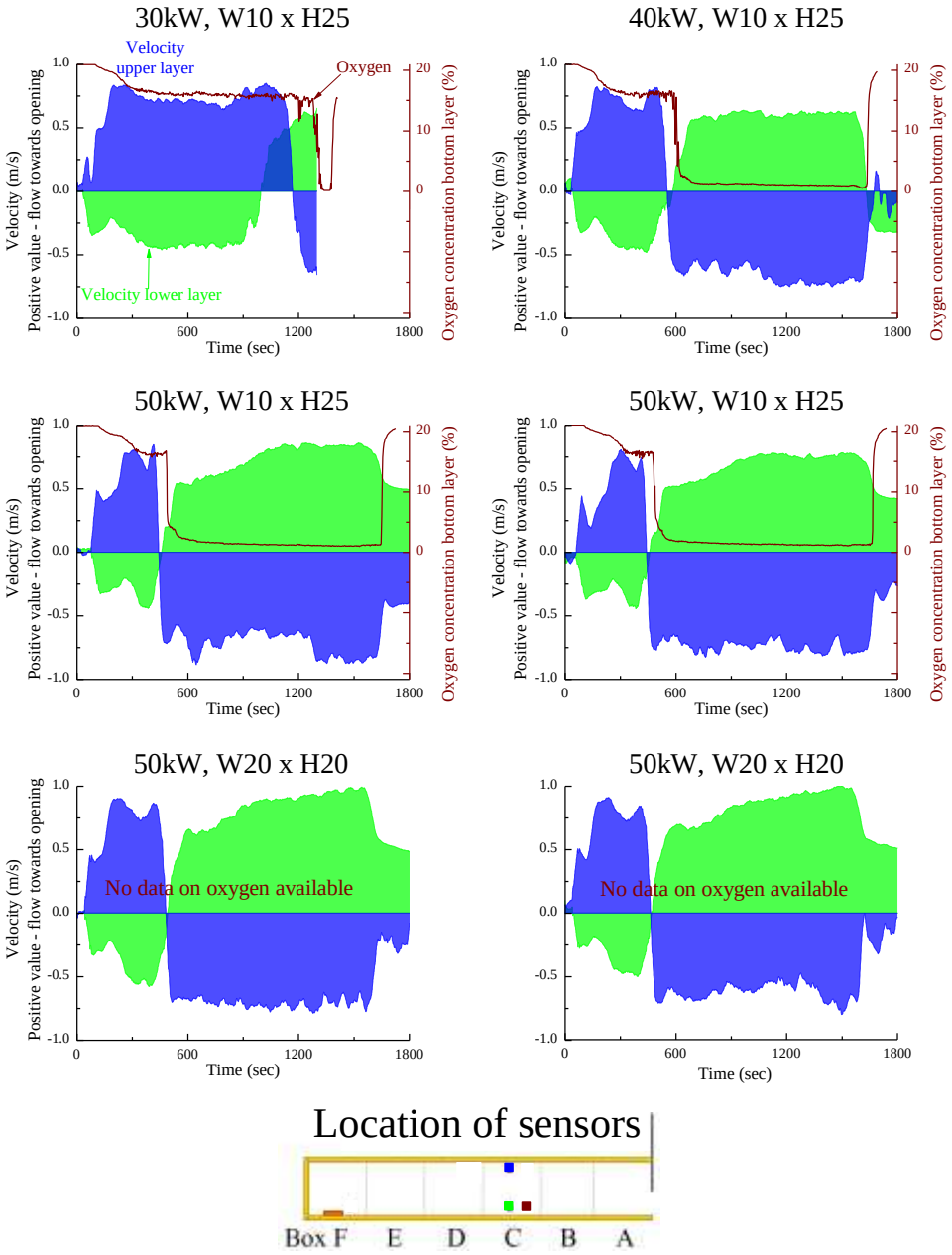

Figure 59*. Comparison of 6 tests where bi-directional probes were used showing velocities in the upper and lower layer (measured in box C) together with oxygen concentration in lower layer of box C. All data smoothed over 30 sec period.

4.4.5. An increase in smoke concentration inside the enclosure as a result of reversed flows

Reversed flows behind the travelling flames were the main reason for the increase in smoke concentration inside. This was confirmed by data presented in

* Please note that Figure 59 depicts the whole tests, showing also data after gas supply was turned off and flame self extinguished thus enabling fresh air to enter the enclosure as confirmed by an increase of oxygen concentration and the return of the flows to the initial directions at the end of the plot.

Figure 60. This figure presents velocities measured in the upper layer (blue shaded contour) and in the lower layer (green shaded contour) overlapped with smoke volume fractions measured in box A (red curve) and C (black curve). Positive sign in velocity measurements indicates flow towards the opening. These data indicated that the increase in smoke levels coincide in time with the reversion of flows. Hot gases started to travel backwards towards the closed end of the corridor and thus contributed to increase in smoke volume fractions inside the enclosure.

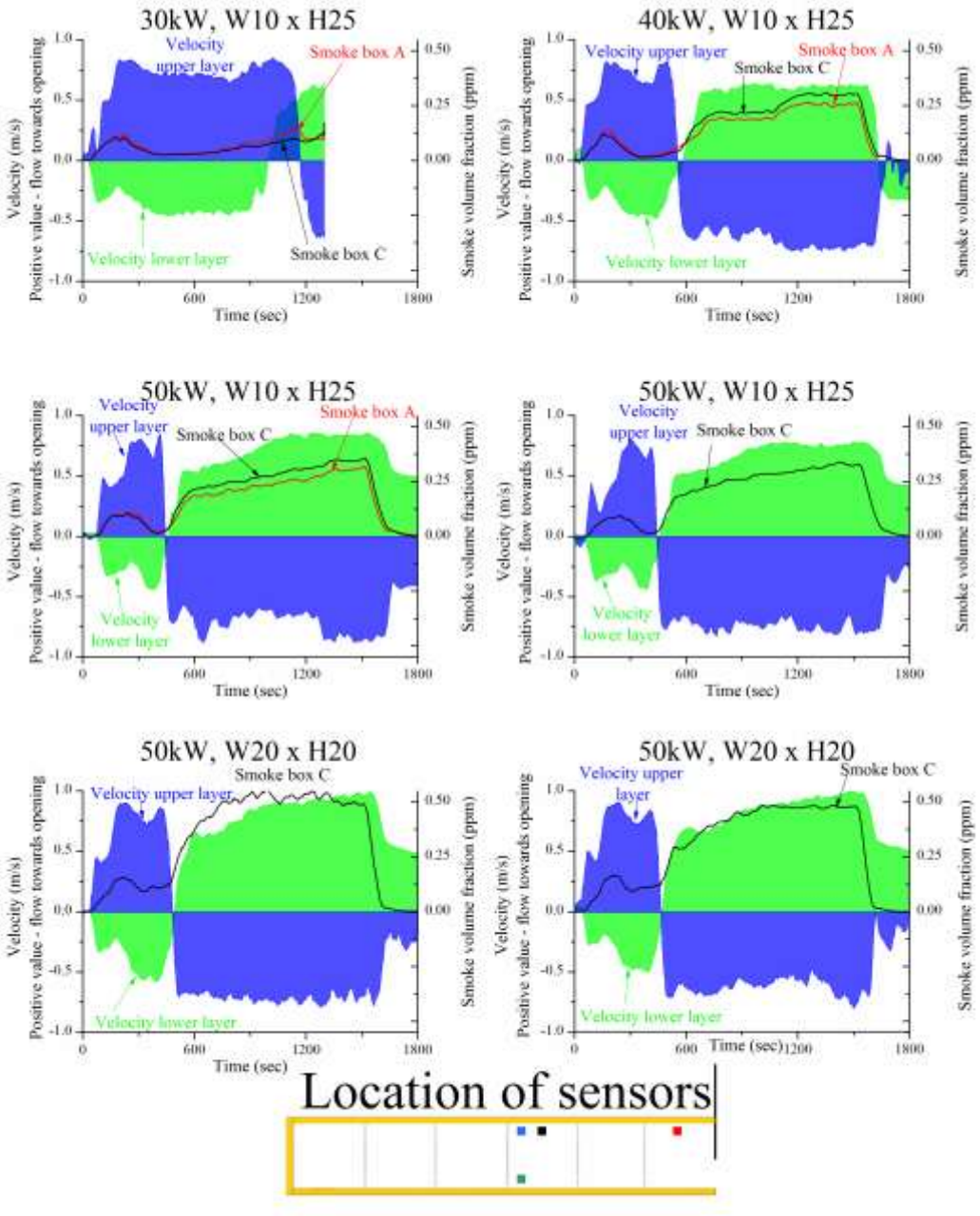

Figure 60. Comparison of 6 tests where bi-directional probes were used showing velocities in the upper and lower layer (measured in box C) together with smoke volume fractions measured inside in box A and C. Data on smoke in box A (red curve) presented only for three experiments due to clogging of holes. All data smoothed over 30 sec period.

4.4.6. Smoke concentration inside the enclosure during overventilated fires

It was found, however, that an increase in smoke volume fractions was also taking place for some tests with GER<1, where no detachment of flames from the burner was occurring. An example of such behaviour is presented in Figure 61. Temperature data only confirmed that there was no detachment of flames yet a continuous rise of temperature was observed in the whole length of the corridor. Unfortunately, no bi-directional probes were installed during these tests, so it is not possible to comment on flow directions. The most likely cause of the increase in smoke volume fractions is related to creation of recirculation zone inside the corridor-like enclosure as discussed by Delichatsios (1990). Moreover one has to keep in mind that these tests were performed at GER equal either 0.5 or even 0.8 so these were not fully overventilated fires as it is known that mass entrainment into plume of open pool fire can be even 12 times the mass stoichiometric requirement of the fuel (Heskestad, 1995). Therefore created experimental conditions were not fully adequate to report these fires as overventilated due to the restriction of the mass inflow of air through the opening. Consequently, it could be hypothesised that not enough air was present. That resulted in a release of some unburnt fuel into to a vitiated upper layer and conditions could develop which were similar to these reported by Pearson et al. (2007). They studied effects of elevated fuel locations within upper layer and reported creation of a “recirculatory motion, driven by buoyancy forces” caused by dilution of gaseous fuel with combustion products. Such a “recirculatory motion” could be responsible for increase in smoke volume fractions in a manner similar phenomena caused by reversed flows during tests with GER>1. Therefore further tests are required to investigate these phenomena in more details.

It may be also hypothesised that the increase in smoke concentration is not only affected by reversed flows but generally by factors like Global Equivalence Ratio, residence time, and temperatures inside. This hypothesis will be discussed in sections to follow.

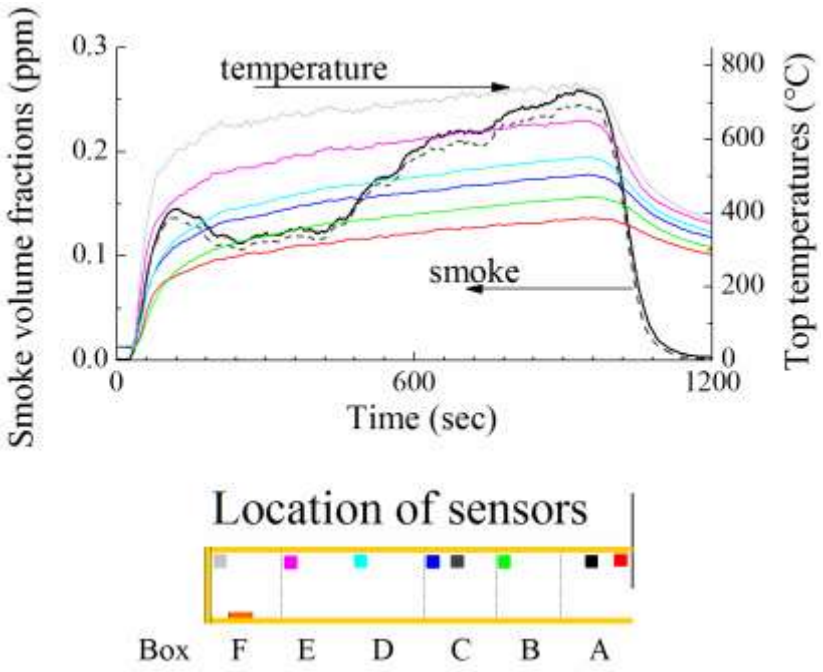

Figure 61. Upper layer temperature together with smoke volume fractions measured in two locations. Test no 101209-2, W10cm x H25cm, HRR=15kW, GER= 0.8

4.4.7. Summary of factors controlling smoke concentration inside the enclosure in the quasi steady state (end of Stage III)

This section discusses factors governing smoke concentrations inside the experimental enclosure during quasi steady state conditions after external burning occurred. Firstly, the dependence on the Global Equivalence Ratio is shown, however correlations with other variables are also required, because GER alone is inadequate to describe the smoke concentration for all performed experiments. Specifically it is found that soot concentration depends on GER, the temperatures and the residence time of the flow inside the enclosure.

Dependence of smoke concentration on GER is shown in Figure 62 that presents the evolution of smoke volume fraction for two experiments with different GERs (1.87 and 2.67) at the same HRR. This comparison, contrary to expectations, shows that smoke concentration inside the enclosure decreases with higher GERs. It is noticeable that use of GER is not sufficient to describe the smoke concentrations, as also confirmed by Figure 63 that shows the smoke volume fraction for experiments with the same GERs but different theoretical HRRs. This behaviour presented in Figure 62 and Figure 63 is explained by the expectation that smoke concentration

should depend also on the temperatures and residence time inside the enclosure as indicated by data plotted in Figure 64.

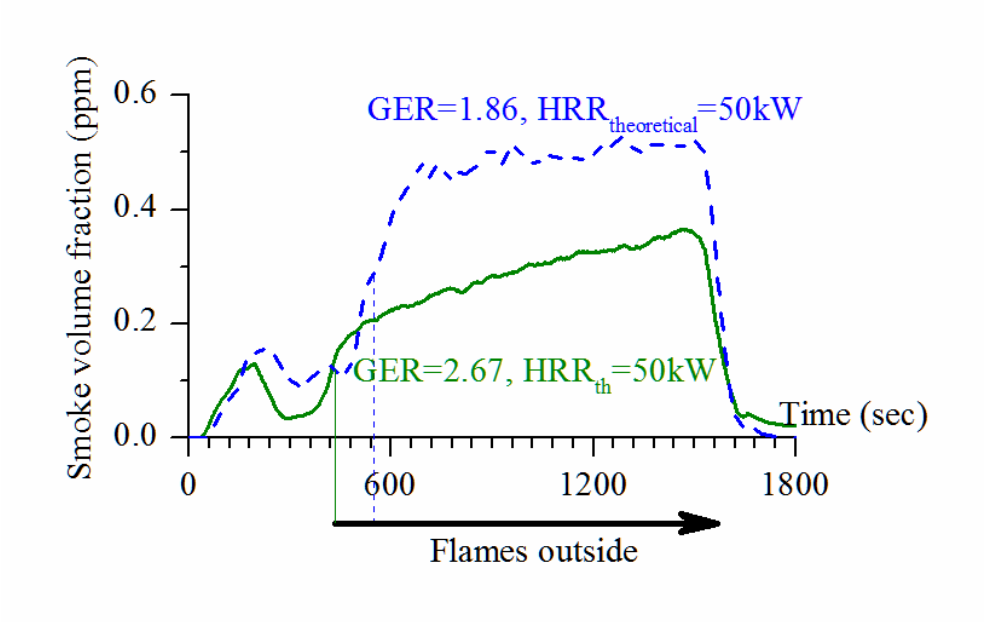

Figure 62. Comparisons of smoke volume fraction for tests with similar HRRs but different GERs. Test 1: GER= 1.86, HRR_{gas}=50kW, HRR_{vmax}=26.8kW, Opening W20cm x H20cm. Test 2: GER= 2.67, HRR_{gas}=50kW, HRR_{vmax}=18.75kW, Opening W10cm x H25cm. All data smoothed over one minute period.

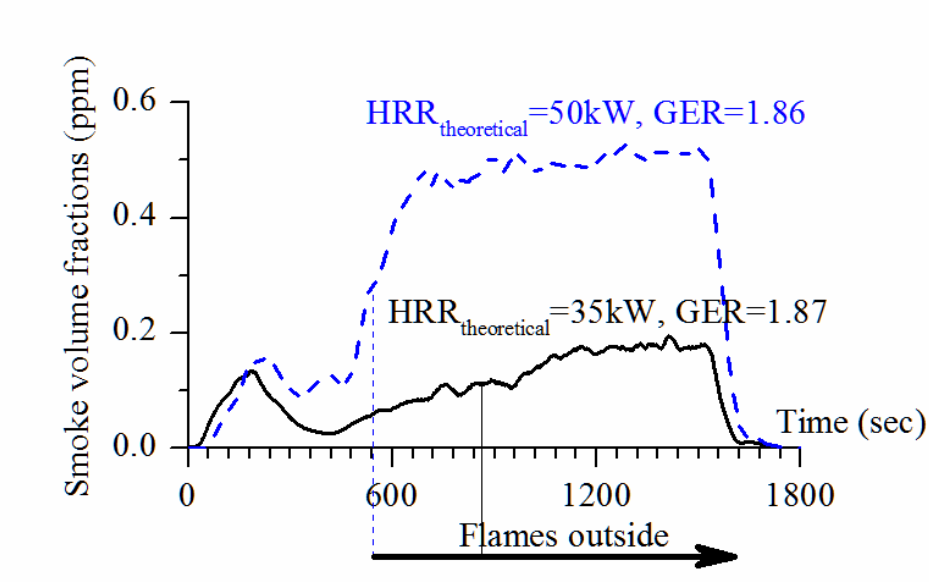

Figure 63. Comparison of smoke volume fraction for tests with similar GERs but different HRRs. Test 1: GER= 1.86, HRR_{gas}=50kW, HRR_{vmax}=26.8kW, Opening W20cm x H20cm. Test 2: GER= 1.87, HRR_{gas}=35kW, HRR_{vmax}=18.75kW, Opening W10cm x H25cm. All data smoothed over one minute period.

Figure 64 shows that smoke concentration depends on GER and also on the ventilation factor $AH^{1/2}$ of the enclosure. The dependence on the ventilation factor $AH^{1/2}$ is explained next by noticing that the smoke volume fraction depends on the

Global Equivalence Ratio, the temperatures and residence time inside the enclosure as expressed by:

$$f_v = \text{fcn}(GER, T, \tau_{res}) \tag{48}$$

where T is the gas enclosure temperature

τ_{res} is the residence time defined by the ratio of volume of the enclosure over the volumetric outflow rate of the gases from the enclosure at ambient conditions, namely:

$$\tau_{res} = V \Big/ \frac{\left(\dot{m}_a + \dot{m}_f\right)}{\rho_a} \tag{49}$$

where ρ_a is the density of ambient air, V is the volume of the enclosure

Using Eq. 40 one obtains:

$$\tau_{res} \sim fcn\left(V, \frac{1}{AH^{1/2}}, \frac{1}{\dot{m}_f}\right) \tag{50}$$

Note that with an increasing opening factor the residence time decreases. Examination of experimental data presented in Table 13 reveals that the effect of fuel supply rate is small compared to contribution from ventilation factor, $AH^{1/2}$.

The temperature rise is determined from heat released inside the enclosure compared to heat losses to the walls as explained by Lee et al. (2007) and Tang et al. (2012):

$$(T - T_o)/T_o = \text{fcn}(1500AH^{1/2}/h_c A_T) \tag{51}$$

where h_c an is effective convective heat transfer coefficient to the walls and A_T is the total area of the enclosure.

Note that with an increasing ventilation factor the enclosure temperature increases.

The temperature and the GER determine the soot reaction rate whereas the residence time together with the reaction time would determine the soot

concentration. Because the volume and the area of the enclosure are constant in these experiments, one cannot assess the effects of temperature (Eq. 51) and residence time (Eq. 50) separately. These effects are manifested in Figure 64 by the opening factor $AH^{1/2}$ implying that for larger openings soot concentrations will be higher owing to higher temperatures inside the enclosure. The present results cannot be directly applied to other corridor geometries because it is not easy to scale soot concentrations that depend on chemical kinetics (via equivalence ratio, temperature). Instead they can be used for the validation of CFD codes. Experimental data supporting the above discussion are presented in Table 13.

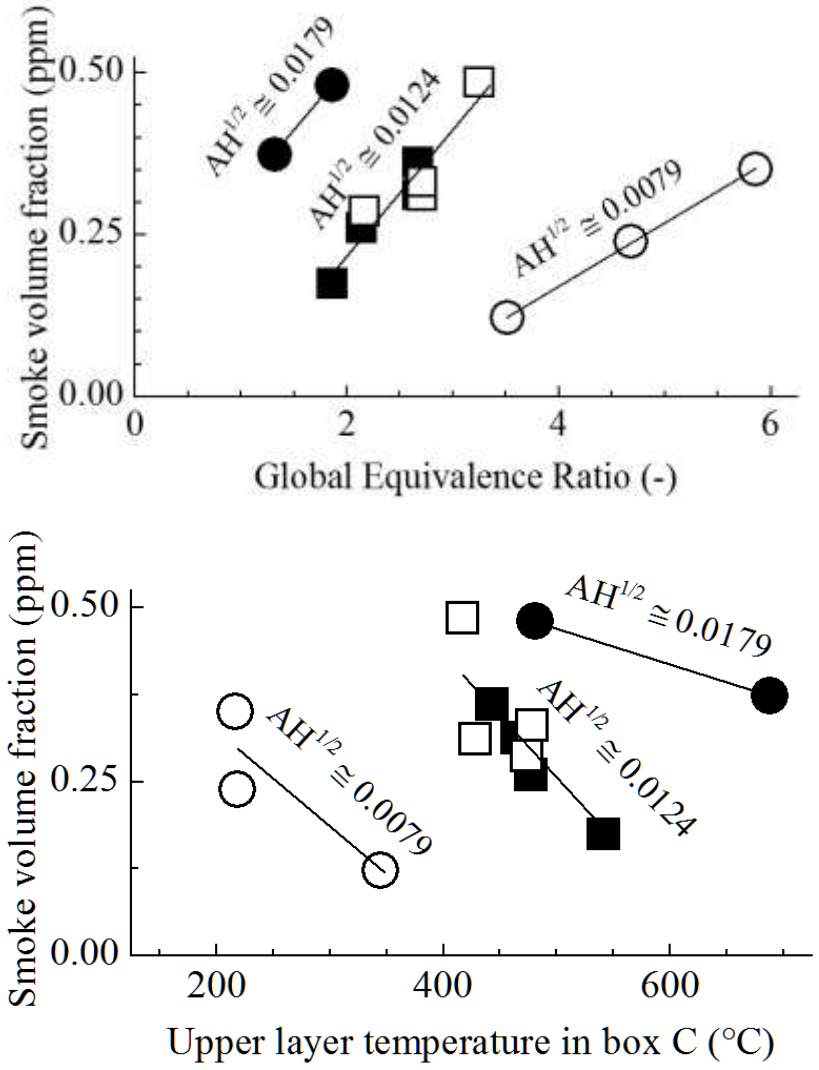

Figure 64. Smoke volume fraction (averaged over one minute) in the quasi steady state period at the end of the test as a function of GER and opening factor $AH^{1/2}$ (top figure) and Upper layer temperature and opening factor $AH^{1/2}$ (bottom figure). Legend for opening sizes: ■Width10cm x Height 25cm; □W7.5cm x H30cm; ●W20cm x H20cm; ○W25cm x H10cm;

Table 13. Data used for Figure 64.

Test date	Opening size W(cm) x H(cm)	HRR_t (kW)	mass of air (g/s)	GER	Residence time (s)*	f_v box A	f_v box C	Temp. box C**
18-Dec-09	W10 x H25	30	6.25	1.6	135		0.20	602
05-Jan-10	W10 x H25	35	6.25	1.9	132	0.17	0.26	542
13-Aug-10	W10 x H25	40	6.25	2.1	127	0.26	0.30	477
07-Jan-10	W10 x H25	50	6.25	2.7	127	0.36	0.40	433
25-Jun-10	W10 x H25	50	6.25	2.7	123	0.31	0.35	465
06-Aug-10	W10 x H25	50	6.25	2.7	123		0.33	440
07-Jan-10	W10 x H25	60	6.25	3.2	119		0.49	443
12-Jan-10	W7.5 x H30	30	6.16	1.6	151		0.17	603
20-Jan-10	W7.5 x H30	40	6.16	2.2	150	0.29	0.30	474
14-Jan-10	W7.5 x H30	50	6.16	2.7	152	0.31	0.41	350
14-Jan-10	W7.5 x H30	50	6.16	2.7	151	0.33		390***
20-Jan-10	W7.5 x H30	60	6.16	3.2	150	0.49	0.48	417
20-Nov-09	W20 x H20	35.36	8.94	1.3	103	0.37		688
04-Nov-09	W20 x H20	50	8.94	1.9	104	0.48	0.49	481
20-Nov-09	W20 x H20	50	8.94	1.9	103		0.57	523
24-May-10	W20 x H20	50	8.94	1.9	101		0.49	493
07-Jun-10	W20 x H20	50	8.94	1.9	102		0.48	510
05-Mar-10	W25 x H10	30	2.85	3.51	328	0.12	0.15	345
08-Mar-10	W25 x H10	40	2.85	4.68	328	0.24	0.26	219
11-Mar-10	W25 x H10	50	2.85	5.86	327	0.35	0.34	217

* Residence time was calculated from Eq. 49 and mass of fuel was not neglected
** Temperature in box C – one minute average of the top thermocouple (3cm below the ceiling) recorded 900 second after an increase in HRR started
*** Test on pre-warmed enclosure

4.4.8. Smoke concentrations and smoke yields measured downstream of the enclosure (in the exhaust duct)

It was shown in the previous subsection that smoke concentration depends on the Global Equivalence Ratio, residence times and temperature. These findings were relevant to measurements inside the corridor-like enclosure. Similarly, one can expect that it would be similar for smoke levels downstream of the corridor. To verify that, the author has analysed yields of smoke measured in the duct, before external burning occurs and plotted these as a function of Global Equivalence Ratio in Figure 65. There was no reason to examine yields downstream of the corridor after external burning because conditions outside were globally overventilated.

Examination of data presented in Figure 65 reveals that smoke yields depends on GER but due to the small number of data points it cannot be verified that different opening sizes affect smoke production. Nevertheless, the general trend observed is in a good agreement with data published by Leonard et al. (1994) shown in Figure 66. Similarly, it was observed in the present study that the peak of smoke yield was at about stochiometric conditions and then was followed by a decrease in yields for higher GERs.

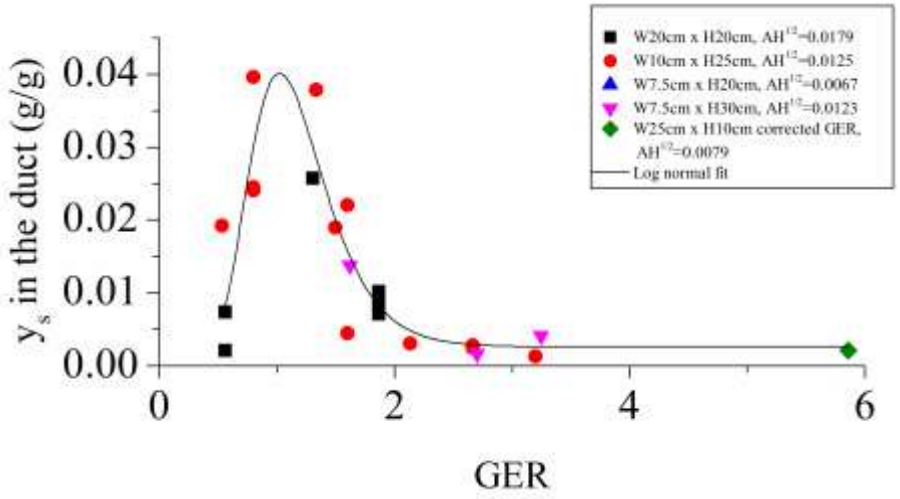

Figure 65. Average smoke yields measured in the duct. For tests with external burning data were averaged before flames were visible outside.

One possible explanation for decreasing yields for GER>1 may be related to the fact that a ghosting or travelling type of flame was observed in the present study (cf. section 4.3.1). Further research is required to explain that behaviour, for instance experiments with other gas as a fuel as it was reported by Most et al. that gas with density smaller than density of air (for instance methane) was not prone to create

ghosting flames (Sugawa et al., 1989; Audouin et al., 1997; Bertin et al., 2002; Most and Saulnier, 2011). Such tests may assist in explaining if ghosting flames are responsible for the decrease in y_{co} at higher GERs or such decrease is related to other phenomena.

Another hypothesis for decreasing smoke yields at higher GERs was given by Leonard et al. (1994). They suggested that smaller flames at higher equivalence ratios and thus shorter residence times were responsible for lower yields of smoke during underventilated conditions (Figure 66). This is in line with present findings on the effect of residence time on smoke production (cf. section 4.4.2). Moreover, they speculated that change in structure of agglomerates and higher organic content may also be resulting from smaller flames and thus "quenching of the smoke growth at an early stage". Consequently both hypotheses require further investigation.

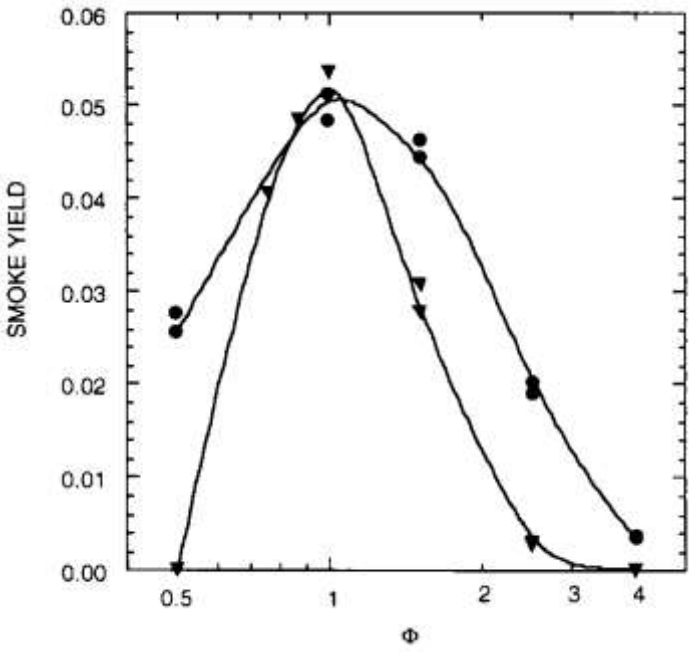

Figure 66. Smoke yield from ethylene flames (● flow rate of fuel 6.4 cm^3/s, ▼ 3.2 cm^3/s). Figure reprinted from Leonard et al. (1994) with permission.

4.4.9. Conclusions on the smoke production

To conclude, it has been shown in the present study that the smoke volume fraction inside the corridor-like enclosure is governed not only by the Global Equivalence Ratio (GER) but also by temperature and residence time, at least for the fuel examined in this study.

In addition, it has been shown that the smoke concentration inside the enclosure was increasing during the ventilation controlled regime even after external burning

started. Such an increase was verified from temperature, smoke and bi-directional probes velocity measurements. The increase was due to reverse flow behind the flames travelling along the corridor. Namely, the gases reversed direction behind the flames with hot gases travelling in the upper layer backwards toward the closed end of the corridor in contrast to hot gas movements towards the opening in the initial regime of an experiment. This recirculation was confirmed by velocity and oxygen concentration measurements in the upper and lower layers inside the enclosure.

Finally, the present experiments show that external burning has a significant effect on reducing the smoke yields measured downstream of the compartment. The measurements confirmed that the smoke yields were a few times higher during overall underventilated conditions before an external burning occurs when compared to overall overventilated conditions after external burning starts.

4.5. Carbon monoxide inside and outside of the enclosure

Having analysed smoke production, attention can be devoted now to data on carbon monoxide. In the following sections, factors controlling carbon monoxide production are analysed in a manner similar to the explanation of smoke production inside this experimental rig as discussed in Section 4.4.7. As explained there, the smoke volume fraction inside the enclosure depends on the Global Equivalence Ratio, the temperatures and residence time inside the enclosure. As smoke and carbon monoxide are products of incomplete combustion it is important to examine if carbon monoxide production is also dependent of the same parameters. The examination is done separately for carbon monoxide inside the enclosure and downstream of it, in the exhaust duct.

4.5.1. Comparison of carbon monoxide concentrations measured inside the corridor and downstream, in the exhaust duct.

Comparison of carbon monoxide concentrations inside versus those outside of the enclosure is presented in Figure 67. A red curve presents concentrations downstream of the corridor (in the exhaust duct) whereas a blue curve presents concentrations inside the enclosure (upper layer of box C). An additional, black curve in Figure 67 presents the measured Heat Release Rate and a grey shaded area indicates the underventilated conditions (cf. section 4.2.1) which become globally overventilated outside the enclosure when flames are visible outside. Yellow shaded area indicates when flames were visible outside. It is important to note, that there is difference in concentration outside and inside the enclosure by two orders of magnitude. That difference was caused by dilution of combustion products with the ambient air being entrained into the exhaust duct. For instance, the first experiment shown in Figure 67 will be examined to check the dilution ratio. Concentration of CO during underventilated conditions was 120 times higher inside the enclosure than in the exhaust duct, the exhaust flow rate was about 1.55 kg/s, and assuming the outflow from the enclosure being a sum of the fuel supply rate and air inflow rate into the enclosure (Eq. 40) one can obtain dilution ratio of about 153 which is in a good agreement with difference in concentrations being equal to 120.

Examination of Figure 67 reveals that the concentration of carbon monoxide outside decreases significantly as soon as external burning starts whereas the concentration inside tends to rise at that point. One can observe that external burning plays a significant role on the reduction of CO concentration downstream as also supported by previous results (Gottuk et al., 1992; Pitts, 1995; Gottuk and Lattimer, 2002; Ukleja et al., 2009). External burning allows additional reactions thus significantly reducing the amount of carbon monoxide and smoke outside the enclosure as shown in Figure 67. An additional observation emerging from Figure 67 is related to a small decrease in CO at the end of underventilated period. This decrease is observed both inside and outside and is related to conversion of CO to CO_2 as explained in section 4.2.2 (cf. Figure 55).

In addition, it is also important to compare carbon monoxide yields, (i.e. mass of carbon monoxide generated per mass of fuel supply rate) inside and outside the enclosure. A methodology proposed by Leonard et al. (1994) is followed in order to obtain yields inside the corridor. As a first approximation this yield can be derived from the mass inflow of air through the opening (cf. Section 4.2.3) and from the fuel supply rate. Total mass flow in the upper layer was converted to a volumetric flow by the ideal gas law. Ambient temperature and pressure were used because measurement of CO concentration and fuel supply was performed also at ambient conditions (cf. section 3.3.4). This correction is in agreement with the methodology described by Leonard et al. (1994). Examination of Figure 67 reveals that yields inside and outside follow similar trend before the external burning and are of the same order of magnitude. Such agreement confirms the validity of the methodology for calculations of yields inside as there are no additional reactions before external burnings so yields inside and outside should be similar.

In conclusion, data presented in Figures 67 and 68 confirm that external burning reduces the amount of carbon monoxide measured downstream of the corridor, reported either as concentration or yield.

The next section presents detailed discussion on factors controlling carbon monoxide levels inside the enclosure followed by separate sections on CO downstream of the corridor.

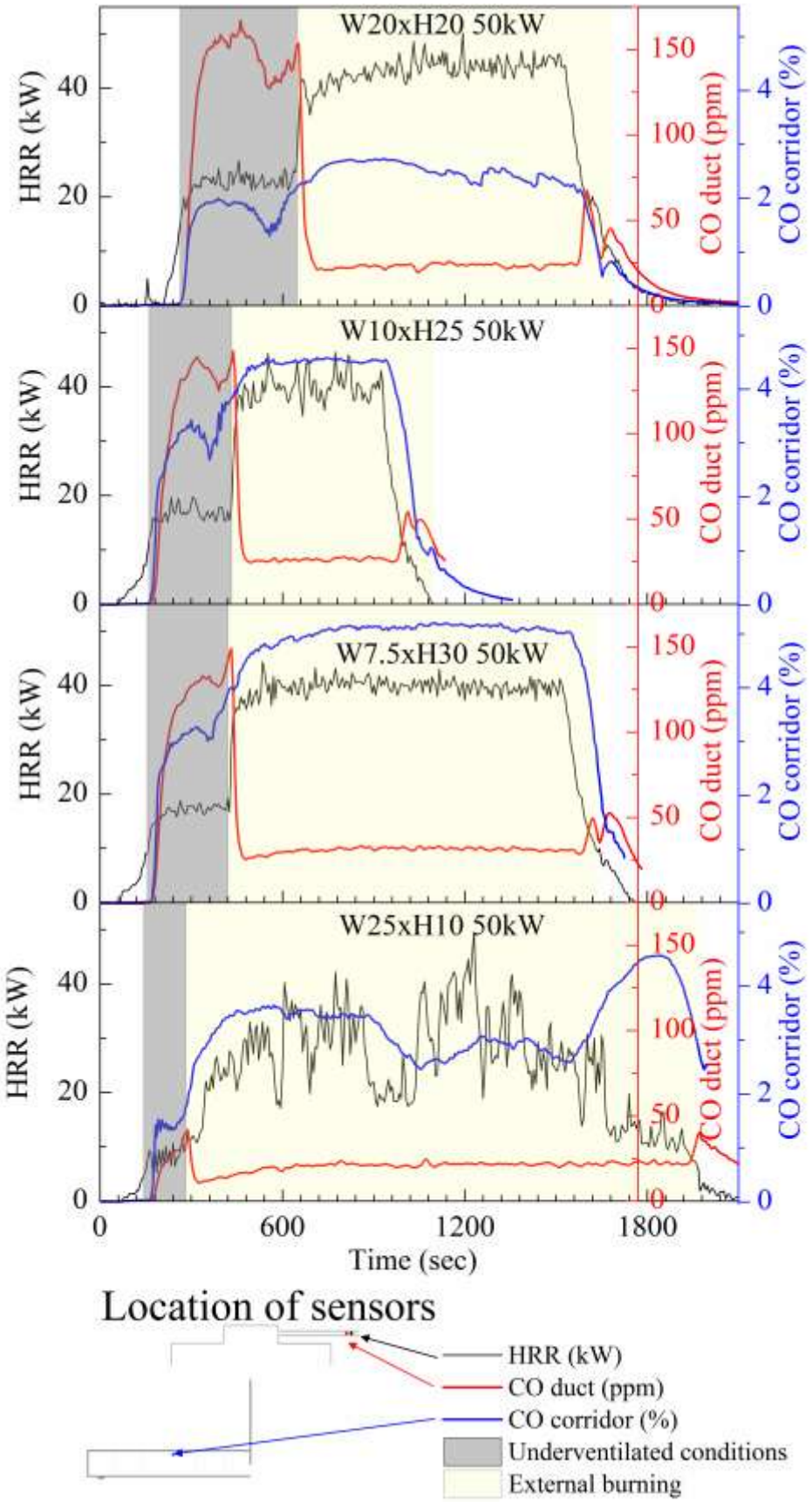

Figure 67. Carbon monoxide inside the corridor in the upper layer of box C and in the exhaust duct together with the measured Heat Release Rate.

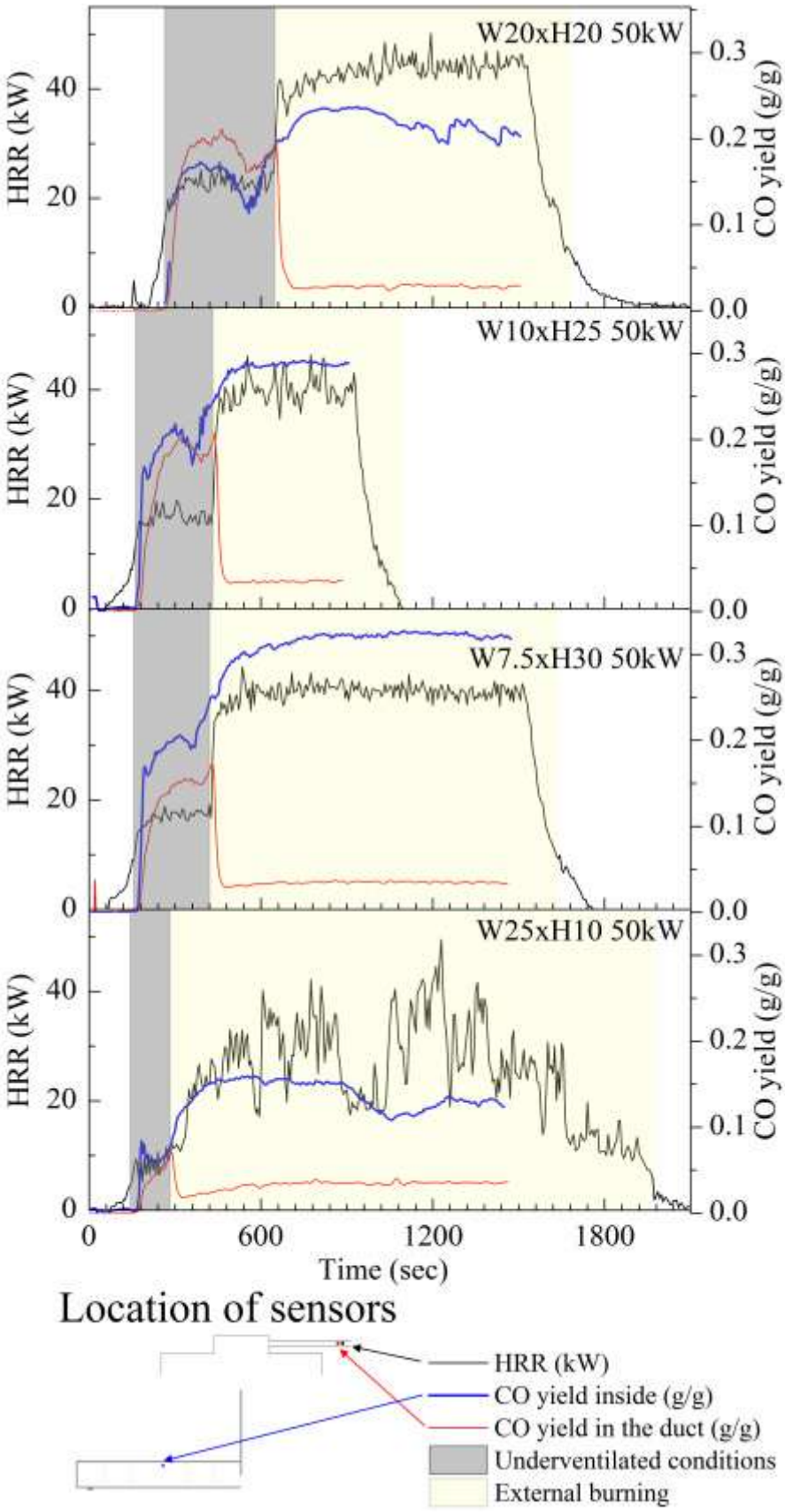

Figure 68. Yields of carbon monoxide inside the corridor measured in the upper layer of box C and in the exhaust duct together with the measured Heat Release Rate.

4.5.2. Factors controlling carbon monoxide yields measured inside the corridor like enclosure

This section analyses carbon monoxide levels inside the corridor; reported as yields and not concentrations because it was verified in the previous section that concentrations measured inside can be successfully converted to yields. Consequently, carbon monoxide yields measured inside the enclosure will be discussed.

Examination of factors affecting carbon monoxide yields inside the corridor was performed for data in the upper layer of box C at which point steady values of CO were measured as shown in Figure 69. This figure shows carbon monoxide concentrations inside the corridor in three different locations. It can be seen that CO in the upper layer in box C (red curve) rises significantly and reaches a steady value after flames are visible outside (end of grey shaded area in Figure 69). Therefore only measurements are compared from sampling in the upper layer in box C as presented in Figure 70.

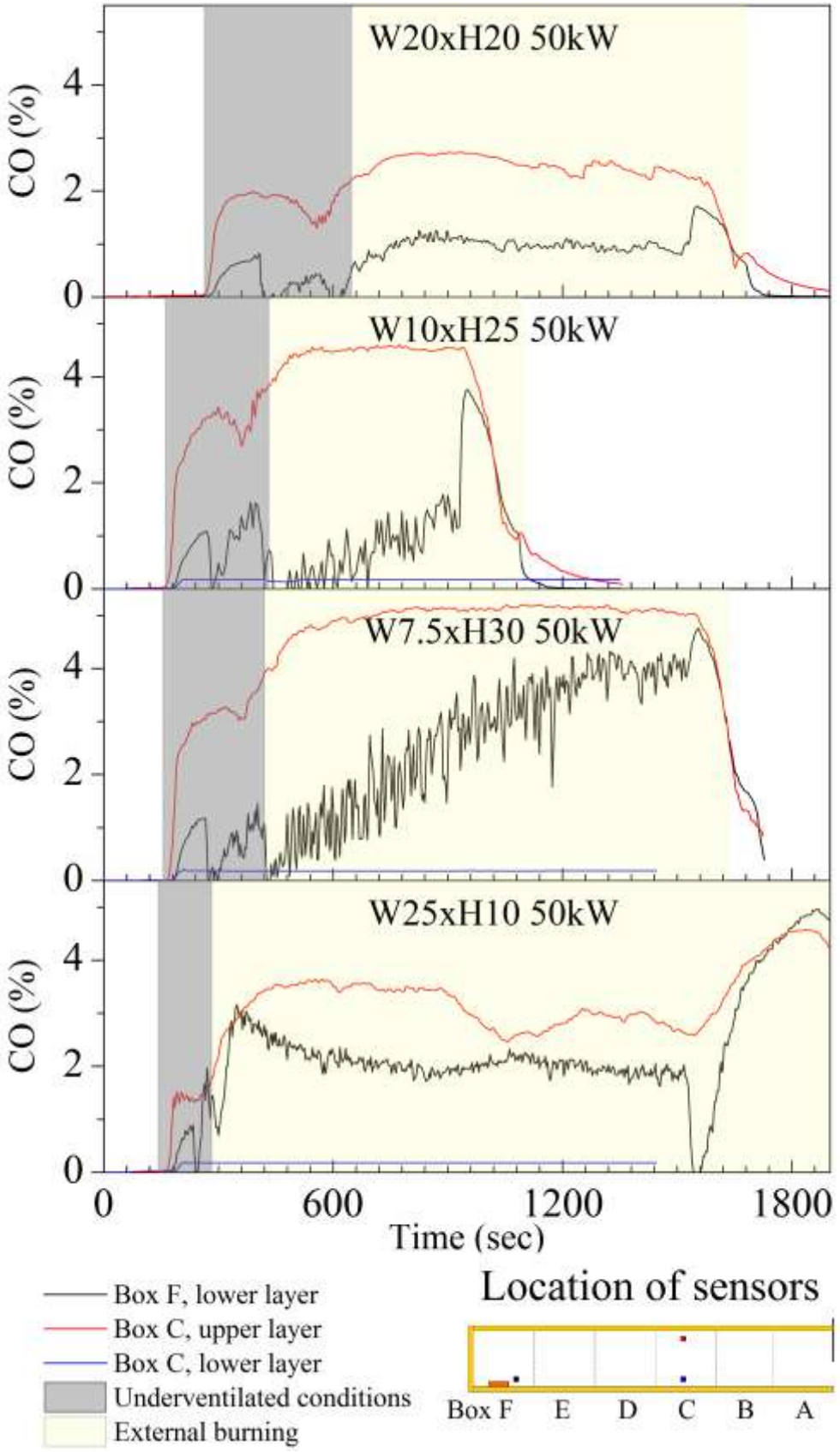

Figure 69. Carbon monoxide concentrations in three locations inside the corridor.

Figure 70 presents data on carbon monoxide yields inside the corridor (in the upper layer of box C) as a function of Global Equivalence Ratio. Figure 70a presents yields measured before external burning whereas Figure 70b presents yields obtained after external burning. Data in the Figure 70b is based on the assumption that conditions **inside** were still underventilated after external burning.

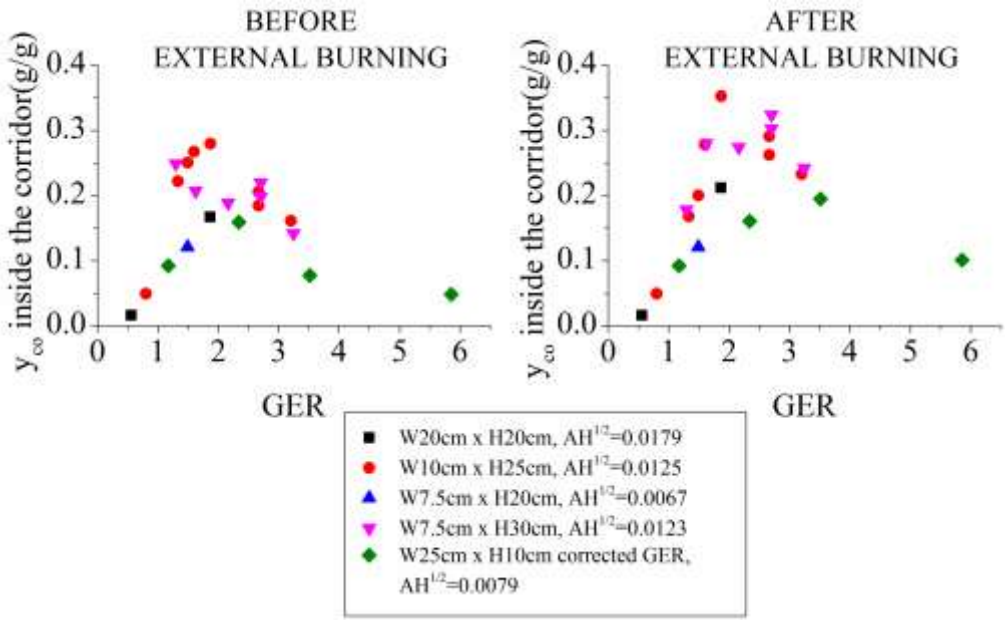

Figure 70. Carbon monoxide yields inside the corridor as a function of Global Equivalence Ratio. Left figure – yields before external burning, right figure – yields after external burning. Data points for last opening were corrected for reduced mass inflow of air (cf. section 4.2.3.)

The purpose of Figure 70 is to verify whether factors other than GER control carbon monoxide production. It was postulated by the author that residence time may be such a factor as it is the case for smoke production (cf. Section 4.4.7). One can recall that the residence time is defined as the ratio of volume of the enclosure over the volumetric outflow rate of the gases from the enclosure, namely

$$\tau_{res} = V \Big/ \frac{\left(\dot{m}_a + \dot{m}_f\right)}{\rho_a} \tag{52}$$

where ρ_a is the density of the ambient air.

Using Eq. 40 one obtains:

$$\tau_{res} \sim fcn\left(V, \frac{1}{AH^{1/2}}, \frac{1}{\dot{m}_f}\right) \tag{53}$$

Consequently, if the residence time is affecting carbon monoxide, separate regimes for different openings should be visible in Figure 70. Examination of presented data confirms that data points from different openings do not collapse to a single curve, which indicates some contribution of residence time. However there is not enough data to clearly distinguish between different openings as it was done before for smoke (cf. Section 4.4.7). One has to also keep in mind limitations of carbon monoxide measurements inside the corridor performed in this study; namely in some cases measured concentrations were outside of the calibrated range of the analyser and no water cooling was used to freeze any conversion of THC to CO (cf. section 3.3.4).

A separate verification was performed to assess effects of temperature on carbon monoxide yields (Figure 71). Yields were plotted against upper layer temperature measured in the same location as the measurement of CO. Moreover, temperature data were averaged over the same time period. As a result, no relationship has been found.

In conclusion, carbon monoxide yields depend primarily on Global Equivalence Ratio with some additional effects caused by residence time of hot gases inside the enclosure.

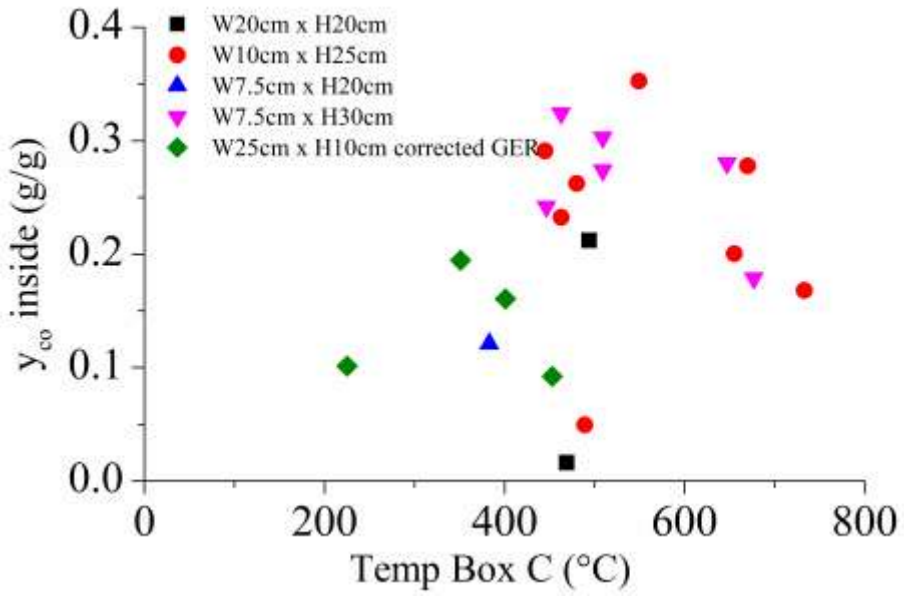

Figure 71. Carbon monoxide yields inside the corridor versus upper layer temperature inside (box C). Data averaged over 300 second during quasi steady state conditions after external burning. Data points for last opening were corrected for reduced mass inflow of air (cf. section 4.2.3.)

4.5.3. Carbon monoxide levels downstream of the corridor, in the exhaust duct.

It was shown in the previous subsection that carbon monoxide yields inside the corridor are correlated primarily with the Global Equivalence Ratio, and also affected to some extend by the residence time, at least for the range of conditions examined in this study. Similarly, one can expect that it would be similar for CO levels downstream of the corridor. To verify that, yields of CO measured before external burning were analysed. There was no reason to examine yields downstream of the corridor after external burning because conditions outside were globally overventilated.

Figure 72 presents yields of carbon monoxide as a function of Global Equivalence Ratio both from inside (top figure) and outside, downstream of the corridor (bottom figure).

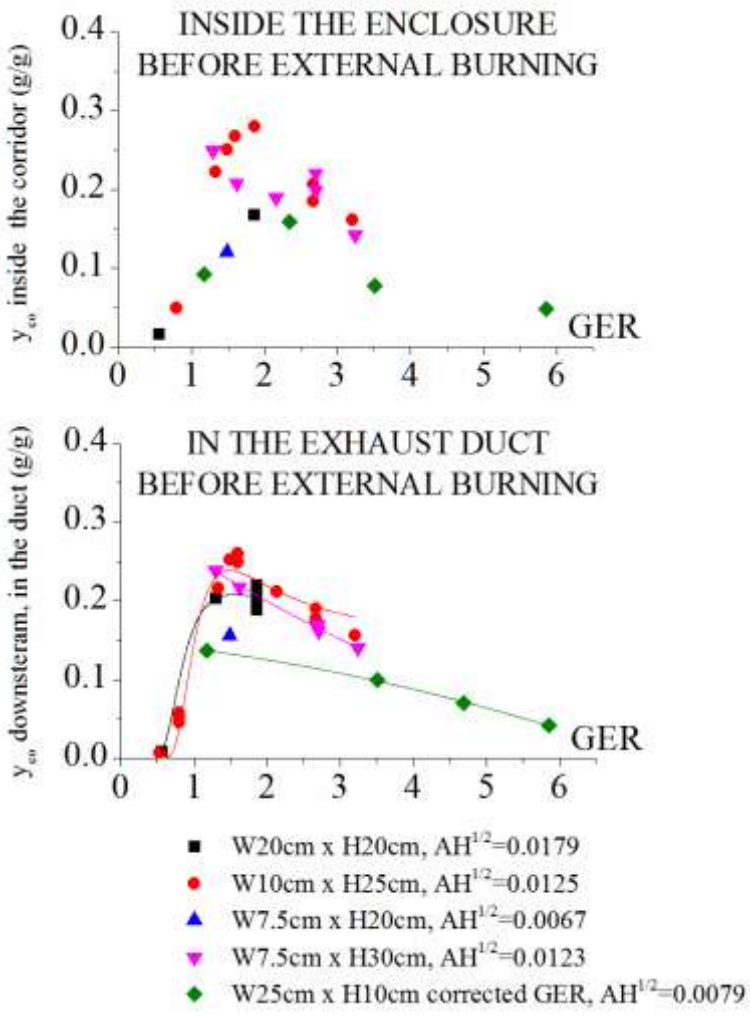

Figure 72. Average carbon monoxide yields versus Global Equivalence Ratio for measurements: inside the corridor (top figure); and in the exhaust duct (bottom figure). Data points for the last opening were corrected for reduced mass inflow of air as explained in section 4.2.3.

It can be seen that carbon monoxide yield correlates with the Global Equivalence Ratio. Similar trends are visible inside and outside, however separation between different openings is somehow better distinguishable for measurements downstream, in the exhaust duct. It is probably due to higher accuracy of reported yields there, as yields inside were calculated with many simplifications (cf. section 4.5.1). Nevertheless, data presented do not collapse to a single curve for all openings and separate regimes are clearly distinguishable for different openings thus confirming that residence time is affecting carbon monoxide yields.

Effect of the opening width on carbon monoxide production was earlier reported by Wieczorek (2003; 2004a; 2004b) (cf. section 2.3.2.2.5), however he did not consider it as the effect of residence time, moreover his experimental methodology was criticised for sampling inside the flaming zone for some tests (Forell, 2007). Nevertheless it was decided to use Wieczorek's concept of presenting the amount of carbon monoxide normalised by the amount of fuel burnt only inside the enclosure. This concept will be discussed in the next section.

4.5.4. The amount of carbon monoxide downstream normalised by fuel burnt only inside the enclosure

Wieczorek reported yields of carbon monoxide as mass of CO per mass of fuel burnt only within his enclosure, the same approach is presented for the author's data in Figure 73. Presented data points were obtained as follows: average production of CO (g/s) was normalised by the fuel burning rate inside (g/s). This rate of mass burnt inside was derived from measured HRR during underventilated conditions (plateau period in Figure 37) divided by heat of combustion of propane (43.7 J/g). Note that CO production was also measured before the external burning.

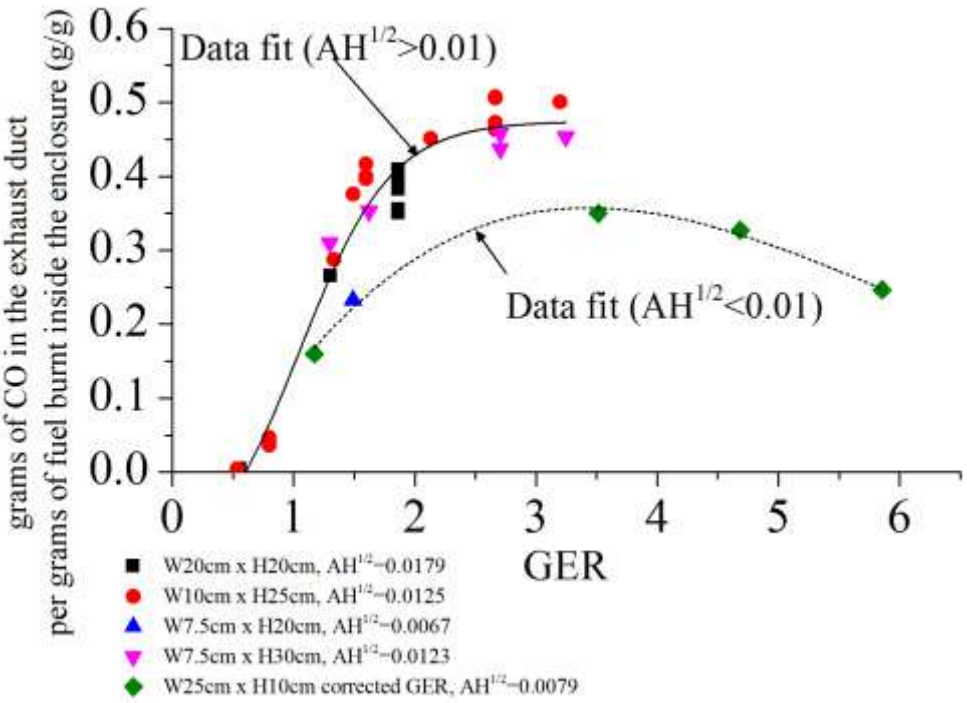

Figure 73. Grams of CO in the exhaust duct per grams of fuel burnt inside the enclosure.

It can be seen that data for three openings ($AH^{1/2} > 0.01$) collapse to one curve and data for two other openings ($AH^{1/2} < 0.01$) to another curve. Existence of two separate regimes confirms again the effect of the residence time (related to the ventilation factor, $AH^{1/2}$, cf. Eq. 53). Further research is required to evaluate these findings in more detail.

4.5.5. Comparison with other literature data on carbon monoxide yields downstream of a compartment

Another important feature of the present results is related to decreasing yields of carbon monoxide for higher Equivalence Ratios. This is in opposition to findings from earlier research reported in the literature review (cf. section 2.3.2.2). For instance, Figure 74 shows the present data compared with the correlations proposed by Gottuk et al. (1995; 2002; 2008). The major difference is that yields reported in this study show almost linear decrease for GER>1 contrary to constant trends proposed by Gottuk et al. One possible explanation may be related to the fact that for GER>1 a ghosting or travelling type of flame was observed in the present study (cf. section 4.3.1). This was not the case for data used by Gottuk so the decrease in y_{co} reported here may result from the travelling flames (similar to ghosting flames) and be fuel specific. Further research is required to explain that behaviour, for instance

experiments with methane as a fuel may assist in explaining if ghosting flames are responsible for decrease in y_{co} at higher GERs. Methane is suggested as a fuel because it was reported that methane being lighter than air (contrary to propane) is not prone to create ghosting flames (Sugawa et al., 1989; Audouin et al., 1997; Bertin et al., 2002; Most and Saulnier, 2011).

Another hypothesis was given by Leonard et al. (1994). It was related to smoke behaviour at higher GERs but qualitatively similar to CO behaviour observed in the present study. Leonard et al. suggested that smaller flames at higher equivalence ratios and thus shorter residence times were responsible for lower yields of smoke during underventilated conditions. Moreover, they speculated that change in structure of agglomerates and higher organic content may also be resulting from smaller flames and thus "quenching of the smoke growth at an early stage". Consequently both hypotheses require further investigation.

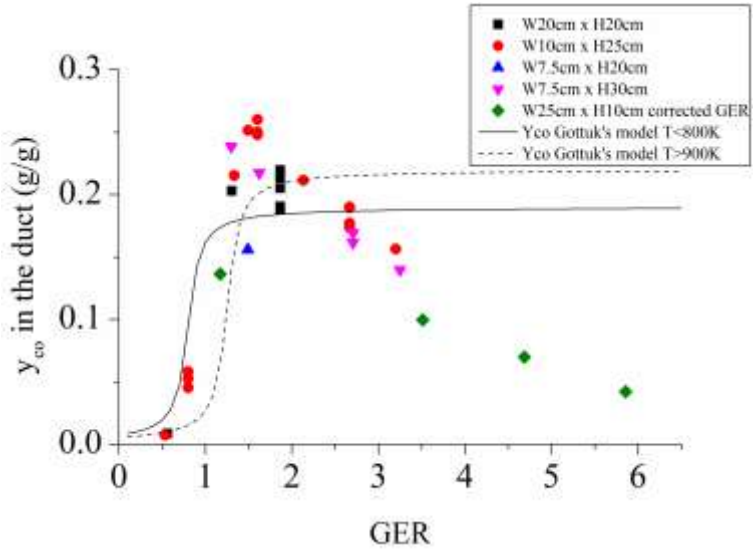

Figure 74. Present experimental data on yields of carbon monoxide downstream of the compartment together with Gottuk's et al. correlations (1995; 2002; 2008).

4.5.6. Carbon monoxide versus smoke yields downstream of a compartment

The second working hypothesis of this study (cf. section 2.5) stated that production of carbon monoxide and smoke in underventilated fires may be interdependent. Earlier publications showed that there is a constant ratio between carbon monoxide and smoke yields for overventilated fires (cf. section 2.4) therefore it was examined if that relationship is still valid during underventilated conditions.

Ratio of y_{co}/y_s is plotted in Figure 75 as a function of Global Equivalence Ratio. It is clearly seen that this ratio is no longer constant and rapidly increases (with one outlier) for higher GERs reaching value of about 110 for GER=3. The amount of data points is not high enough to propose any correlation however the reported trend is in agreement for instance with data published by Ouf et al. (2008). They studied three different fuels for GER range from 0.009 to 0.547 and reported CO/soot ratio staring from 0.1 and rising to 3. On the other hand

Consequently, a constant ratio of CO/soot for higher GERs do not exist anymore but rises as underventilated conditions develop, at least for the conditions examined in this study. This is in opposition to results shown by Ko et al. (2009) (cf. section 2.4), however Ko et al. examined different fuels, moreover some of their data were very scattered. Consequently, further examination is required to verify the effect of fuel on the y_{co}/y_s ratio during underventilated conditions.

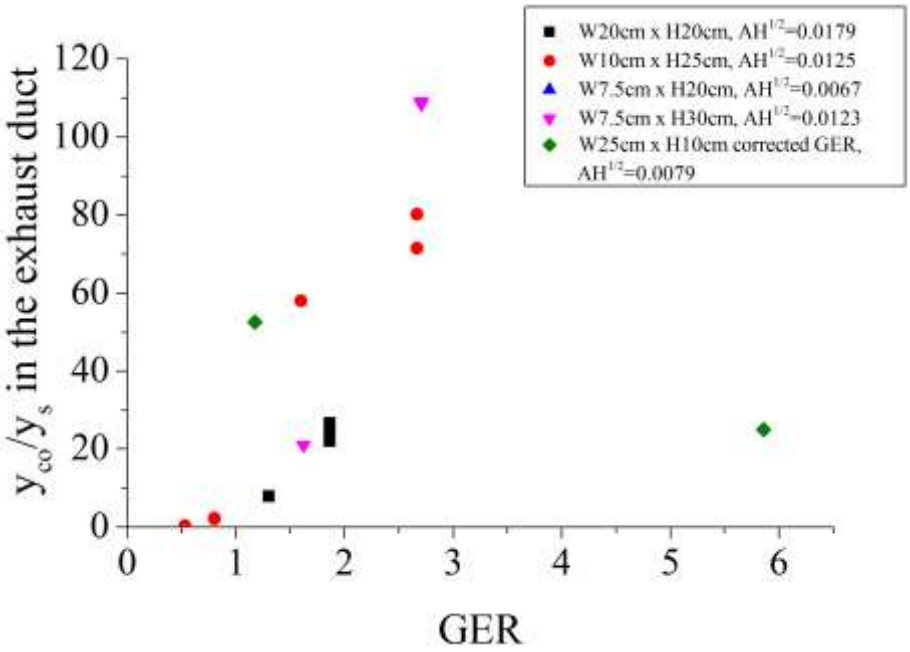

Figure 75. Ratio of carbon monoxide yield to smoke yield as a function of Global Equivalence Ratio.

4.5.7. Conclusions on the carbon monoxide production

To conclude, it has been demonstrated that carbon monoxide yields depend primarily on the Global Equivalence Ratio with some additional effects caused by the residence time of hot gases inside the enclosure. It was shown that there are two separate regimes related to the residence time (being inversely proportional to ventilation factor $AH^{1/2}$) with data collapsing to one curve for $AH^{1/2} > 0.01$ and second curve for $AH^{1/2} < 0.01$.

The present results show that the relationship reported in the literature, between smoke and carbon monoxide production during overventilated conditions, $y_{co}/y_s \approx$constant (cf. section 2.4), is no longer valid during an underventilated enclosure fire, at least for conditions examined in this study. However, no relationship has been found for underventilated conditions. The present results show that the ratio y_{co}/y_s, is not constant but increases for Global Equivalence Ratios of the enclosure greater than one.

In addition, the present experiments show that external burning has a significant effect on reducing the species yields measured downstream of the compartment. The measurements confirmed that the CO yields were a few times higher during overall underventilated conditions before an external burning occurs when compared to overall overventilated conditions after external burning starts. The maximum value of the carbon monoxide yield outside the enclosure occurs just before flames appear outside as it is also true for smoke.

Moreover, it was hypothesized that the disagreement between present data and literature data on decreasing yields of CO for higher GERs may be related to ghosting or wandering type of flames encountered in the present study. Further research with different fuel is required to investigate that claim.

CHAPTER FIVE

Conclusions and recommendations

This work is an experimental and theoretical analysis of factors and conditions affecting smoke and carbon monoxide (CO) production in corridor-like enclosure fires. The main conclusion of this work is that smoke production depends not only on the Global Equivalence Ratio (GER) - as is reported in the literature - but also on the temperatures and residence time inside the enclosure, at least for the fuel examined in this study. In addition, it was shown that carbon monoxide depends also on the Global Equivalence Ratio and the residence time, at least for experimental conditions studied.

Additionally, the results can be used for CFD model validations, especially on the visibility and toxicity inside the enclosure thanks to smoke and CO measurements inside. The author developed a novel design of smoke meter for measurements inside the enclosure with a detailed methodology to reduce problems with smoke deposition on lenses. Furthermore, additional sensors were employed inside the enclosure namely bi-directional probes, gas sampling probes and thermocouples providing a large data set which is very beneficial for future studies on CFD validation and fire safety design.

An extensive and comprehensive set of thirty eight experiments was undertaken. The following sections summarise the main contributions of this study and recommendations for future work.

5.1. Conclusions

The major conclusions are:

1. This work shows that in an underventilated fire inside a corridor-like enclosure the smoke volume fraction inside is governed not only by the Global Equivalence Ratio but also by the temperatures and the residence time inside the

enclosure (cf. section 4.4.7). The GER depends on the opening factor and the fuel burning rate. Temperatures inside the enclosure depend on the HRR, the total area of the enclosure and the opening factor. Finally, the residence time depends on the volume of the enclosure and the inflow of air (related to the opening factor) (cf. Figure 64).

2. The present results show that the relationship reported in the literature between smoke and carbon monoxide production during overventilated conditions $y_{co}/y_s \approx$ constant, (cf. section 2.4), is no longer valid during an underventilated enclosure fire. However, no similar relationship has been found for underventilated conditions. The present results show that the ratio y_{co}/y_s, is not constant but increases when the Global Equivalence Ratio of the enclosure is greater than one (Figure 75).

3. Visual observations through the opening revealed that flames were detaching from the burner and moving towards the opening for experiments with GER > 1 (Figure 39). After some time, the flames were anchored near the opening. This situation was also confirmed by measurements of temperature, gases and velocity by bi-directional probes located inside the enclosure (Figures 42-44). The measurements also revealed that detachment of the flames from the burner was related to a sharp drop in the oxygen concentration in the vicinity of the burner (Figures 46-47). Moreover the time of detachment was correlated with the Global Equivalence Ratio (cf. sections 4.3.1 and 4.3.2).

In addition, the velocities of the travelling flames were measured and correlated with GER (Figure 45). Remarkably, the obtained velocity range is of the same order of magnitude as the velocities of ghosting flames reported by Audouin et al. (1997) and Bertin et al. (2002).

4. The present experiments show that there are three regimes for the fire development in the corridor-like enclosure as is the case for other enclosures: a) an initial fuel controlled regime, b) an intermediate plateau ventilation controlled regime (cf. Figure 37), and c) an external burning regime after the flames move and anchor near the open end (cf. section 4.2.1)

5. The smoke concentration inside the enclosure was increasing during the ventilation controlled regime even after external burning started. Such an increase was verified from temperature, smoke and velocity measurements. The increase was due to the reverse flow behind the flames travelling along the corridor. Namely, the gases reversed direction behind the flames with hot gases travelling in the upper layer backwards toward the closed end of the corridor in contrast to hot gas movements towards the opening in the initial regime of an experiment. This recirculation was confirmed by velocity and oxygen concentration measurements in the upper and lower layers inside the enclosure (Figures 59-60).

6. The present experiments confirm that external burning has a significant effect on reducing the species yields measured downstream of the compartment. The measurements revealed that the CO and smoke yields were a few times higher during overall underventilated conditions before an external burning occurs when compared to overall overventilated conditions after external burning starts. The maximum value of the carbon monoxide yield outside the enclosure occurs just before flames appear outside as it is also true for smoke (Figure 52, Figure 67).

7. This study confirms that in corridor-like enclosure fires carbon monoxide is strongly correlated with GER with an additional effect of residence time. The major difference between the author's data and earlier research was that for higher GER there was a drop in CO yields whereas data in the literature present steady levels of CO for a similar range of GERs.

5.2. Recommendations

1. The present results are specifically applicable for assessing smoke hazards in corridor fires in buildings where smoke concentrations owing to leakage to adjacent rooms behind travelling flames can be much larger than anticipated. They are also a challenging testing ground for CFD validations. Further work is needed to validate popular CFD codes by comparison with the presented results.

2. This study employed only one fuel, namely propane supplied from a sandbox burner. In order to further verify presented findings, a future work should focus on

other gaseous fuels, like methane and propylene, and separately on liquid and solid pool fires.

3. The author found, that the increase in smoke concentrations was also taking place for some experiments with GER<1, where no detachment of flames from the burner was occurring. Unfortunately, no bi-directional probes were installed during these experiments, so it is not possible to determine if reversion of flows was taking place. The most likely cause of the increase in smoke volume fractions is related to creation of a recirculation zone inside as discussed by Delichatsios (1990). Therefore further experiments are required to investigate these phenomena in more details.

APPENDIX 1. TYPICAL VALUES OF THE MASS-SPECIFIC EXTINCTION COEFFICIENT REPORTED IN THE LITERATURE

Table 14. Values of σ_s at wavelength λ=632.8 nm as reported in literature

<table>
<tr><th>Publication</th><th>Results</th><th>Description</th></tr>
<tr><td>(Widmann et al., 2005)</td><td><table><tr><th>Equivalence ratio</th><th>σ_s (m^2/g)</th></tr><tr><td>1</td><td>8.12 ± 0.3</td></tr><tr><td>2</td><td>7.1 ± 0.2</td></tr><tr><td>3</td><td>6.4 ± 0.2</td></tr></table></td><td>fuel - ethane only
high temperature effect within an enclosure is not taken into account</td></tr>
<tr><td>(Widmann et al., 2003)</td><td>Wavelenght 3 μm = 3000 nm
<table><tr><th>Equivalence ratio</th><th>σ_s (m^2/g)</th></tr><tr><td>0.8</td><td>1.56 ± 0.09</td></tr><tr><td>1</td><td>1.64 ± 0.09</td></tr><tr><td>2</td><td>1.24 ± 0.05</td></tr><tr><td>3</td><td>0.8 ± 0.09</td></tr></table>Wavelenght 3.5 μm = 3500 nm
<table><tr><th>Equivalence ratio</th><th>σ_s (m^2/g)</th></tr><tr><td>0.8</td><td>1.32 ± 0.09</td></tr><tr><td>1</td><td>1.37 ± 0.09</td></tr><tr><td>2</td><td>1.02 ± 0.05</td></tr><tr><td>3</td><td>0.63 ± 0.09</td></tr></table>Wavelenght 4 μm = 4000 nm
<table><tr><th>Equivalence ratio</th><th>σ_s (m^2/g)</th></tr><tr><td>0.8</td><td>1.06 ± 0.09</td></tr><tr><td>1</td><td>1.09 ± 0.09</td></tr><tr><td>2</td><td>0.8 ± 0.05</td></tr><tr><td>3</td><td>0.5 ± 0.09</td></tr></table></td><td>Measured only for infra-red

“The soot aerosol was generated in a laminar diffusion burner, diluted with nitrogen, and carried by the combustion gases and N2 to the optical cell.”

“The extinction measurements are obtained by comparing the transmission of radiation through the optical cell with and without soot aerosol present.”</td></tr>
<tr><td>(Widmann, 2003)</td><td>σs (m2/g) = 7.5 ± 0.8</td><td>From literature review. In the original paper, a dimensionless coefficient is given 8.8 ± 0.9. It is</td></tr>
</table>

		converted here to σs based on the assumption that soot density is 1.85 g/cm3.
(Tewarson, 2002)	σ_s (m^2/g) = 10.06	To be used in Cone Calorimeter in order to derive smoke yield from SEA.
(Mulholland and Croarkin, 2000)	σ_s = 8.7 ± 1.1 m^2/g	Over-ventilated conditions From literature review of 29 experimental results for different fuels.
(Krishnan et al., 2000)	σ_s = 7.1 ± 1.3 m^2/g	In the original paper, a dimensionless coefficient is given 8.4 ± 1.5. It is converted here to σ_s based on the assumption that soot density is 1.88 g/cm3 as used in the original paper.
(Mulholland and Choi, 1998)	σ_s (m^2/g) acetylene 7.80 ± 0.08 ethene 8.79 ± 0.28 σ_s (m^2/g) ≈ 7.0 for Equivalence ratio =3.	Fuel: acetylene and ethene Only over-ventilated conditions Turbulent diffusion flame high temperature effect within an enclosure is not taken into account
(Choi et al., 1995)	Equivalence ratio / σ_s (m^2/g) 2.3 / 7.6 2.5 / 8.7 2.5 / 7.6 2.5 / 8.0 2.5 / 7.9 2.5 / 7.9 2.5 / 7.4 **2.5 (average) / 7.92 ± 0.18** 2.7 / 8.6	6cm diameter McKenna Burner Post-flame soot diluted by nitrogen Temperature 500K
(Dobbins et al., 1994)	σ_s (m^2/g) = 7.8 ± 1.2 at 630 nm	Fuel – crude oil Results for aging smoke collected in $1m^3$ chamber
Colbeck I. et al 1989 cited by (Dobbins et al., 1994)	σ_s (m^2/g) = 10-12 at 632 nm	Fuel – from butane flame
(Newman and Steciak, 1987)	σ_s (m^2/g) = 10.2 ± 0.2 average for all fuels	heptane, kerosene, Douglas fir, PMMA, PVC, PC, PS, styrene-butadiene rubber

APPENDIX 2. LIST OF PERFORMED TESTS

Test number	Test date	Opening size WxH	HRR from gas supply (kW)	Ventilation controlled HRR (kW)	GER
1	23-Oct-09	20cm x 20 cm	15.0	26.8	0.6
2	04-Nov-09	20cm x 20 cm	50.0	26.8	1.9
3	20-Nov-09	20cm x 20 cm	35.4	26.8	1.3
4	20-Nov-09	20cm x 20 cm	50.0	26.8	1.9
5	24-Nov-09	20cm x 20 cm	15.0	26.8	0.6
6	26-Nov-09	10cm x 25cm	15.0	18.8	0.8
7	27-Nov-09	10cm x 25cm	10.0	18.8	0.5
8	27-Nov-09	10cm x 25cm	30.0	18.8	1.6
9	10-Dec-09	10cm x 25cm	15.0	18.8	0.8
10	10-Dec-09	10cm x 25cm	15.0	18.8	0.8
11	18-Dec-09	10cm x 25cm	50.0	18.8	2.7
12	18-Dec-09	10cm x 25cm	30.0	18.8	1.6
13	23-Dec-09	10cm x 25cm	25.0	18.8	1.3
14	04-Jan-10	10cm x 25cm	28.0	18.8	1.5
15	05-Jan-10	10cm x 25cm	35.0	18.8	1.9
16	07-Jan-10	10cm x 25cm	50.0	18.8	2.7
17	07-Jan-10	10cm x 25cm	60.0	18.8	3.2
18	11-Jan-10	7.5cm x 20cm	15.0	10.1	1.5
19	12-Jan-10	7.5cm x 30cm	24.4	18.5	1.3
20	12-Jan-10	7.5cm x 30cm	30.0	18.5	1.6
21	14-Jan-10	7.5cm x 30cm	50.0	18.5	2.7
22	14-Jan-10	7.5cm x 30cm	50.0	18.5	2.7
23	20-Jan-10	7.5cm x 30cm	40.0	18.5	2.2
24	20-Jan-10	7.5cm x 30cm	60.0	18.5	3.2
25	11-Feb-10	25cm x 10cm	15.0	11.9	1.3
26	03-Mar-10	25cm x 10cm	10.0	11.9	0.8
27	05-Mar-10	25cm x 10cm	30.0	11.9	2.5
28	08-Mar-10	25cm x 10cm	40.0	11.9	3.4
29	11-Mar-10	25cm x 10cm	50.0	11.9	4.2
30	12-Mar-10	25cm x 10cm	20.0	11.9	1.7
31	30-Apr-10	20cm x 20cm	50.0	26.8	1.9
32	10-May-10	20cm x 20cm	50.0	26.8	1.9
33	24-May-10	20cm x 20cm	50.0	26.8	1.9
34	07-Jun-10	20cm x 20cm	50.0	26.8	1.9
35	25-Jun-10	10cm x 25cm	50.0	18.8	2.7
36	06-Aug-10	10cm x 25cm	50.0	18.8	2.7
37	09-Aug-10	10cm x 25cm	30.0	18.8	1.6
38	13-Aug-10	10cm x 25cm	40.0	18.8	2.1

APPENDIX 3. AUTHOR'S PEER-REVIEWED PUBLICATIONS RELATED TO THIS PHD THESIS

The following papers have been published during course of author's research:

Peer reviewed journals:

Beji, T., Ukleja, S., Zhang, J. and Delichatsios, M. A. (2012), Fire behaviour and external flames in corridor and tunnel-like enclosures. Accepted for publication in Fire Materials, doi: 10.1002/fam.1124

Peer reviewed conferences:

Ukleja, S.**,** Delichatsios, M.A., Delichatsios, M.M. & Lee, Y.P. 2009, "Carbon monoxide and smoke production downstream of a compartment for underventilated fires", *Fire Safety Science. Proceedings of* the *Ninth International Symposium.*The International Association of Fire Safety Science, pp. 849-860.

Beji, T., Ukleja, S., Zhang, J. & Delichatsios, M.A. 2010, "Observations On Flame Behaviour In Corridor And Tunnel Like Enclosure Fires", Proceedings of the sixth International Seminar on Fire and Explosion Hazards University of Leeds, United Kingdom, pp. 219-229.

Ukleja S., Delichatsios M., Zhang, JP., Smoke Concentrations Inside and Outside of Corridor-Like Enclosure Fires, Conference Proceedings of the Seventh Mediterranean Combustion Symposium, Sardinia, Italy, 11-15 September, 2011

Reports:

Author was responsible for supervision of research work of an exchange student M. Bacquet. Author constructed the experimental setup for liquid pool fires with constant level of fuel and implemented it in author's experimental rig, moreover assisted during the experiments of M. Bacquest. His work was summarised in the following report:

M. Bacquet, Pool fire dynamic in a tunnel-like enclosure, 2010, report prepared for University of Ulster and Saint-Cyr Coëtquidan Schools.

APPENDIX 4. PRESENT EXPERIMENTAL DATA

Explanatory notes

Yields of species are plotted only till fuel supply was about to be terminated. Afterwards yields were rising considerably due to minimal fuel supply and delay in decrease in concentrations in the duct.

Test no 1 (231009-1)

Test date 23 October 2009
Theoretical HRR = 15kW
Opening size = 20cm x 20cm
Ventilation controlled HRR = 26.8kW
GER = 0.6

Recorded observations:
1 min 05 sec – ignition
15 min 30 sec – gas turned off
18 min 05 sec – flame self extinguished

Flames were anchored to the burner for the whole test

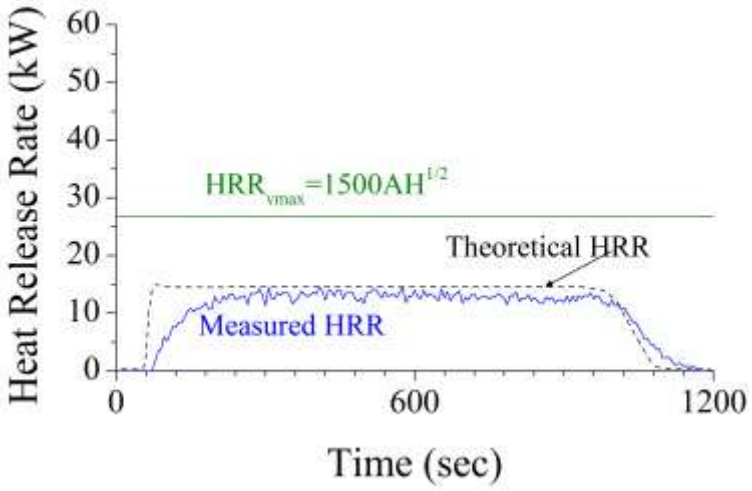

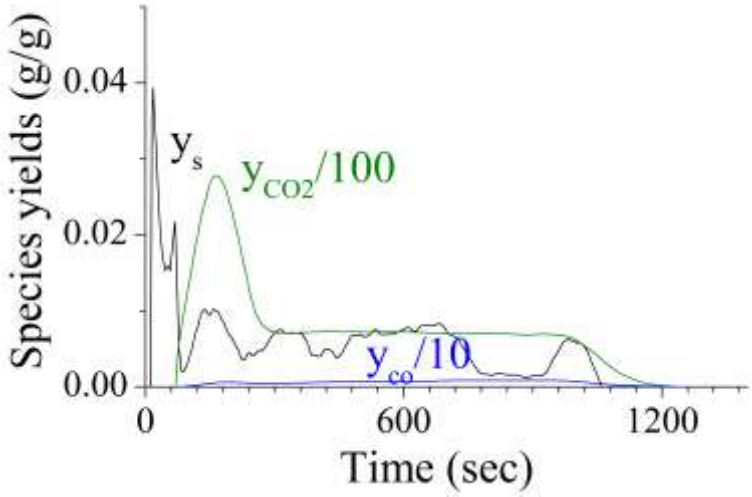

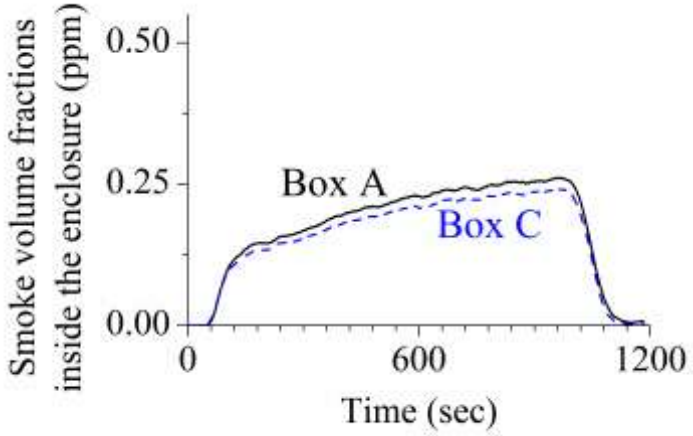
Smoke volume fractions inside the enclosure (ppm)
0.50
0.25
0.00
Box A
Box C
0
600
1200
Time (sec)

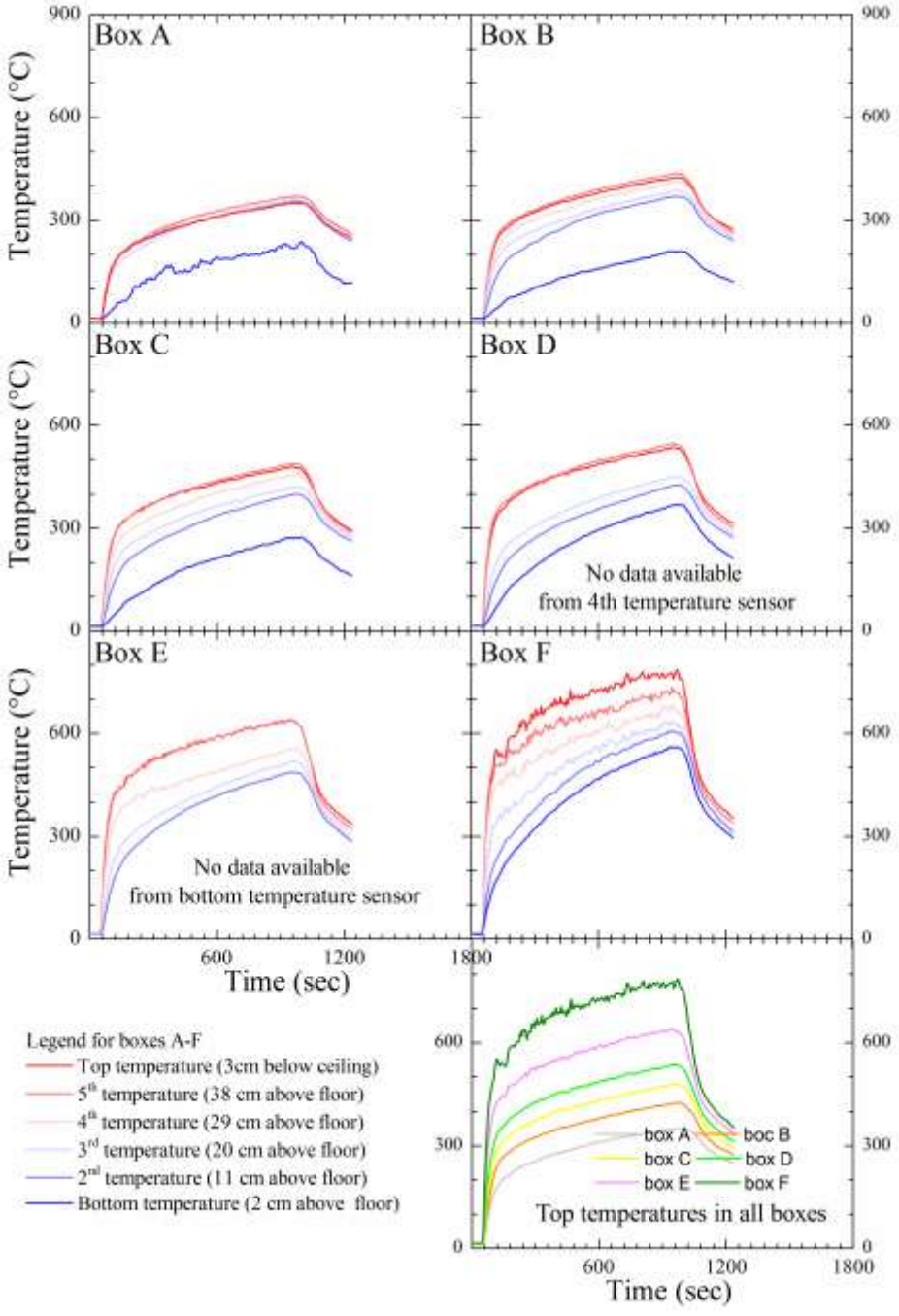
Box A
Box B
Box C
Box D
Box E
Box F
Temperature (°C)
900
600
300
0
No data available
from 4th temperature sensor
No data available
from bottom temperature sensor
600
1200
1800
Time (sec)
Legend for boxes A-F
Top temperature (3cm below ceiling)
5th temperature (38 cm above floor)
4th temperature (29 cm above floor)
3rd temperature (20 cm above floor)
2nd temperature (11 cm above floor)
Bottom temperature (2 cm above floor)
box A
boc B
box C
box D
box E
box F
Top temperatures in all boxes

Test no 2 (041109-1)

Test date 4 November 2009
Theoretical HRR = 50kW
Opening size = 20cm x 20cm
Ventilation controlled HRR = 26.8kW
GER = 1.9

Recorded observations:
2 min – ignition
10 min 51 sec – first flame tip observed outside
25 min 00 sec – gas turned off
28 min 00 sec – flame self extinguished

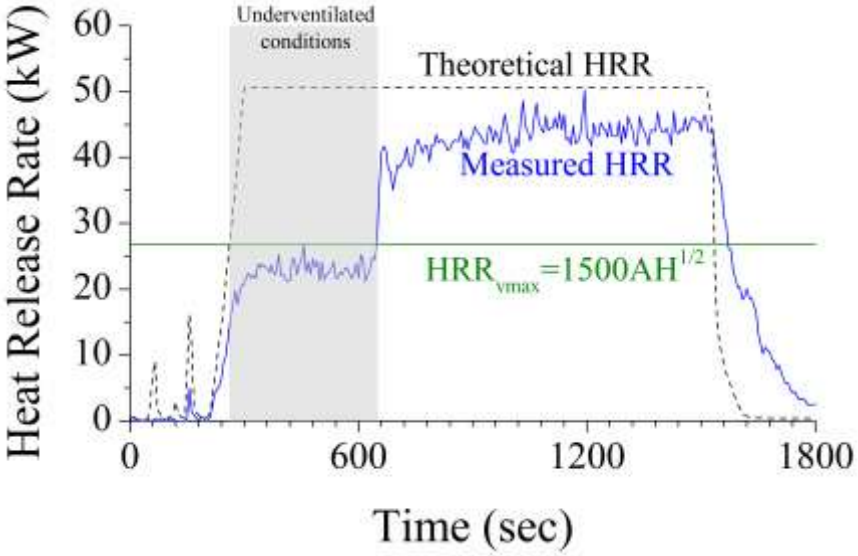

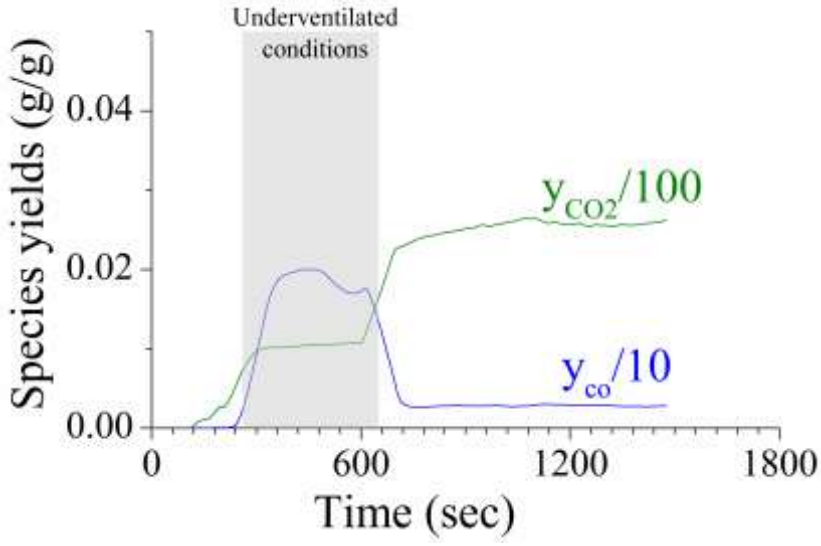

NO SMOKE DATA AVAILABLE for measurements in the duct

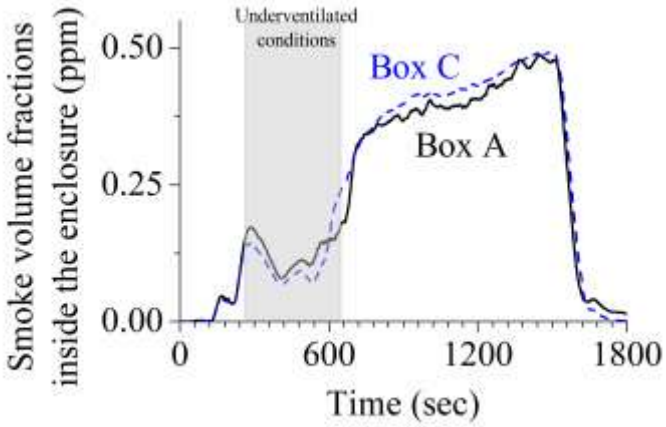
Underventilated conditions
Box C
Box A
Smoke volume fractions inside the enclosure (ppm)
0.50
0.25
0.00
0
600
1200
1800
Time (sec)

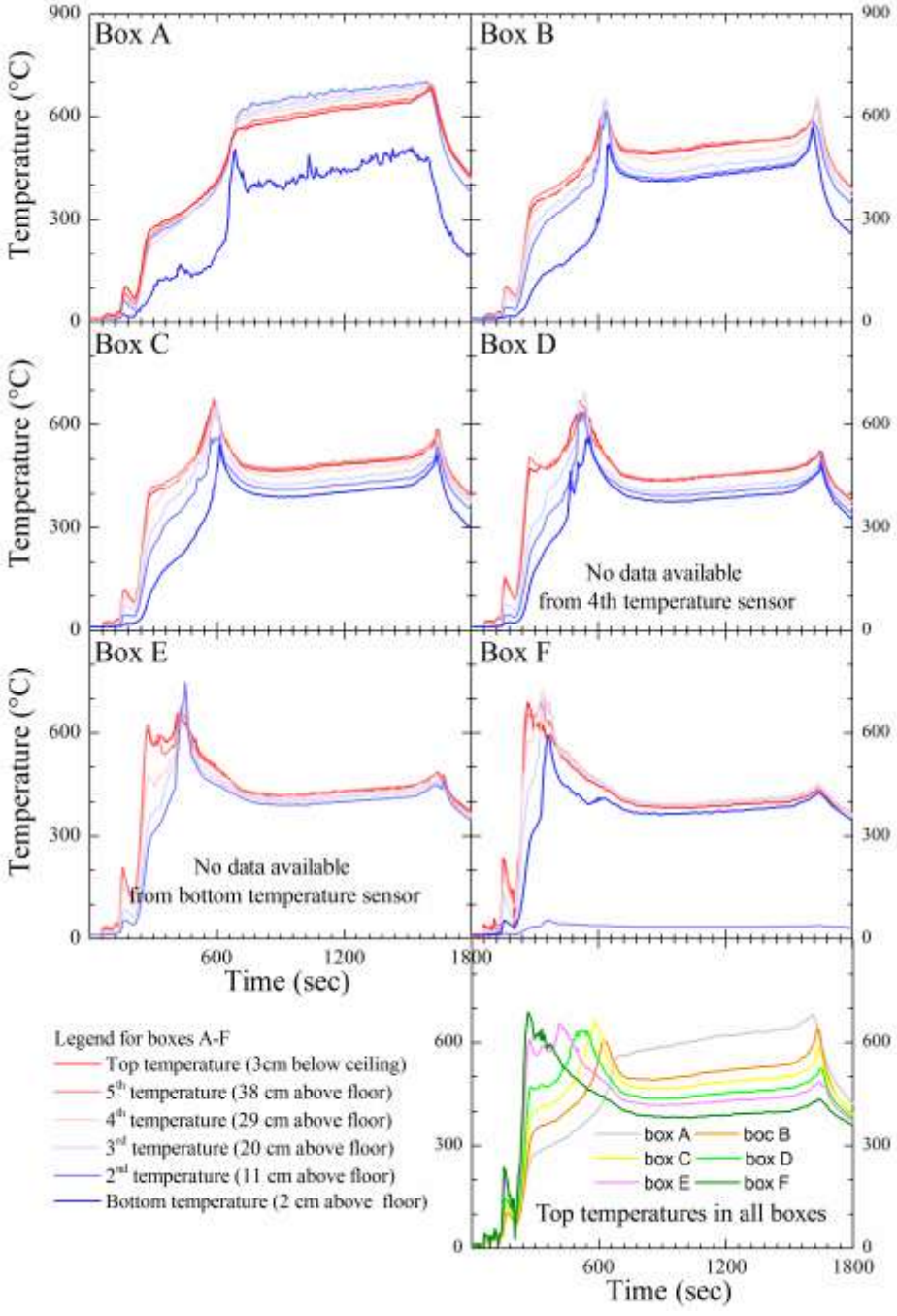
Box A
Box B
Box C
Box D
Box E
Box F
Temperature (°C)
900
600
300
0
No data available from 4th temperature sensor
No data available from bottom temperature sensor
600
1200
1800
Time (sec)
Legend for boxes A-F
Top temperature (3cm below ceiling)
5th temperature (38 cm above floor)
4th temperature (29 cm above floor)
3rd temperature (20 cm above floor)
2nd temperature (11 cm above floor)
Bottom temperature (2 cm above floor)
box A
boc B
box C
box D
box E
box F
Top temperatures in all boxes

Test no 3 (201109-1)

Test date 20 November 2009
Theoretical HRR = 35.4kW
Opening size = 20cm x 20cm
Ventilation controlled HRR = 26.8kW
GER = 1.3

Recorded observations:
45sec – ignition
1 min – automatic control of the burner started
27 min 15 sec – first flame tip visible outside but flames stay inside
29 min 55 sec – gas turned off
31 min 57 sec – flame self extinguished

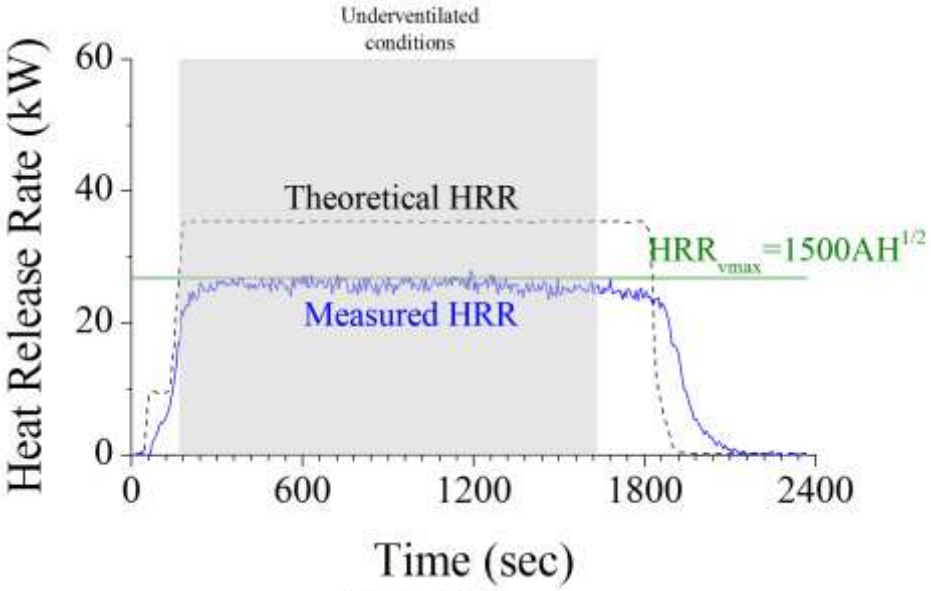

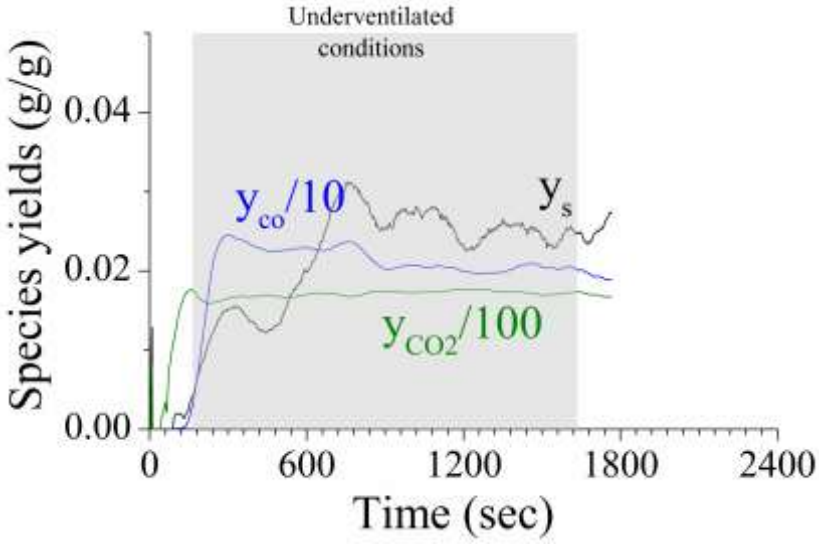

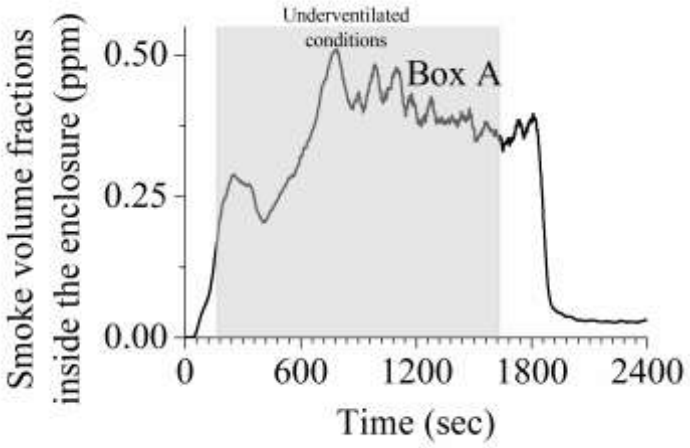
Underventilated conditions
Box A
Smoke volume fractions inside the enclosure (ppm)
0.50
0.25
0.00
0
600
1200
1800
2400
Time (sec)

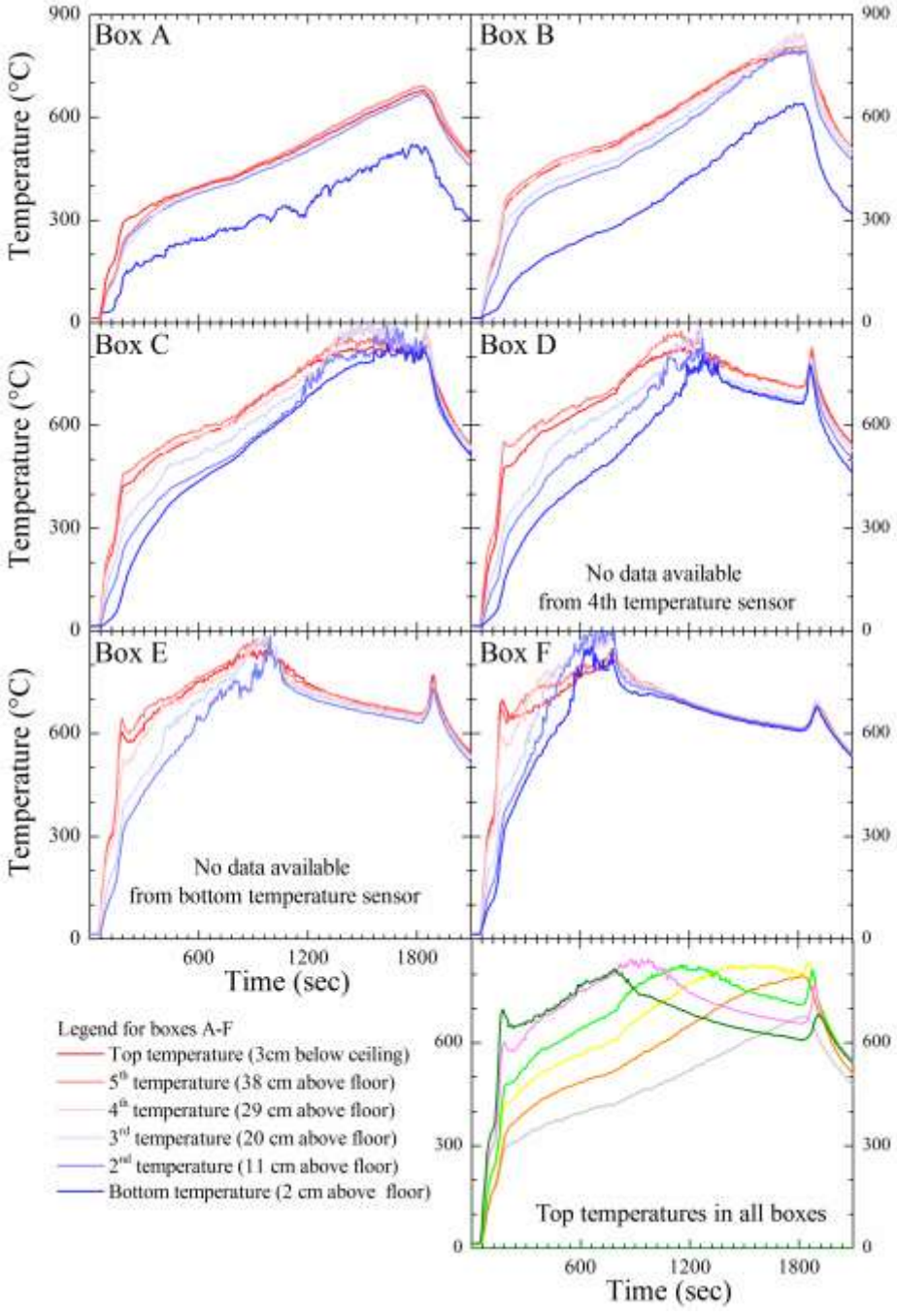
Box A
Box B
Box C
Box D
Box E
Box F
Temperature (°C)
900
600
300
0
No data available from 4th temperature sensor
No data available from bottom temperature sensor
600
1200
1800
Time (sec)
Legend for boxes A-F
Top temperature (3cm below ceiling)
5th temperature (38 cm above floor)
4th temperature (29 cm above floor)
3rd temperature (20 cm above floor)
2nd temperature (11 cm above floor)
Bottom temperature (2 cm above floor)
Top temperatures in all boxes

Test no 4 (201109-2)

Test date 20 November 2009
Theoretical HRR = 50kW
Opening size = 20cm x 20cm
Ventilation controlled HRR = 26.8kW
GER = 1.9

Recorded observations:
<10sec – ignition
3 min 20 sec – logging of gases in sony laptop really started because before there was no line closed up
4 min 30 – automatic control of burner started – (surge in gas supply)
10 min 23 sec – first flame tip visible outside
20 min 00 sec – gas turned off
22 min 44 sec – flame self extinguished

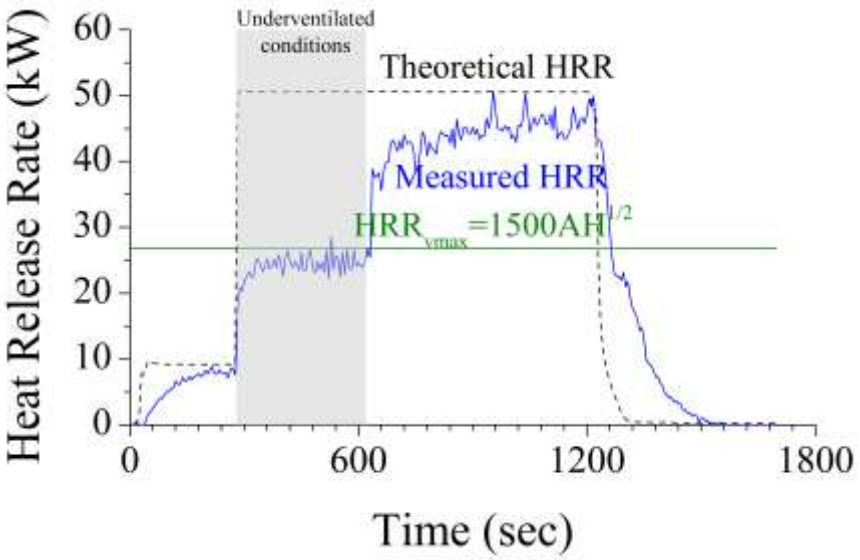

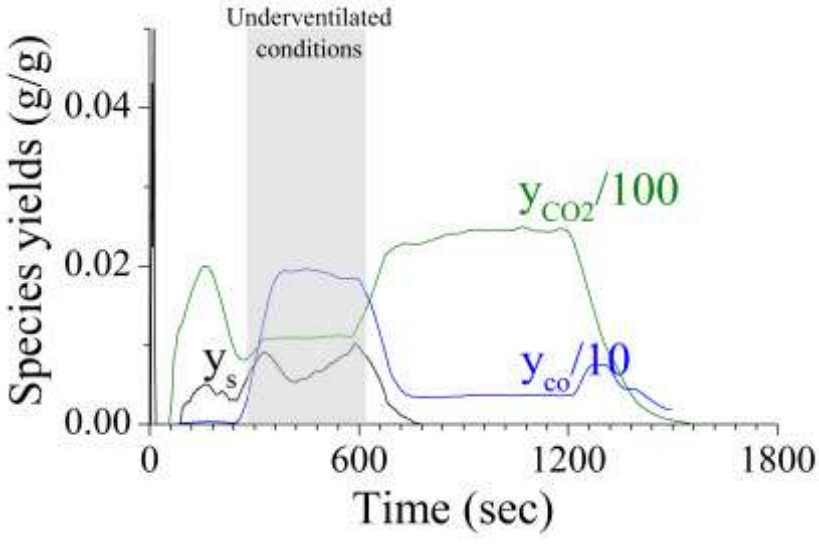

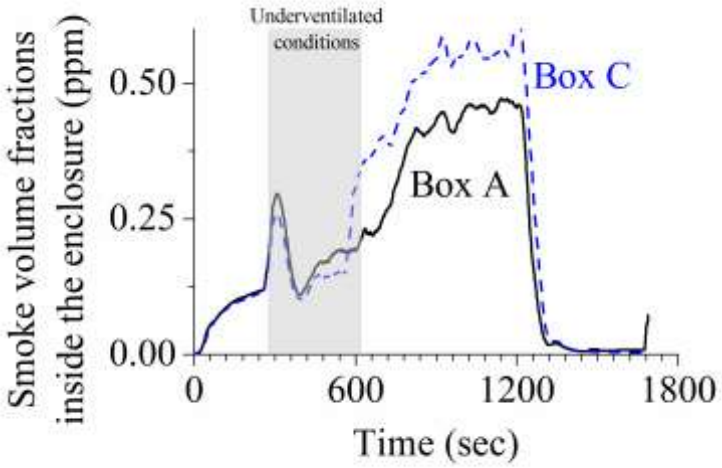
Underventilated
conditions
Box C
Box A
Smoke volume fractions
inside the enclosure (ppm)
0.50
0.25
0.00
0
600
1200
1800
Time (sec)

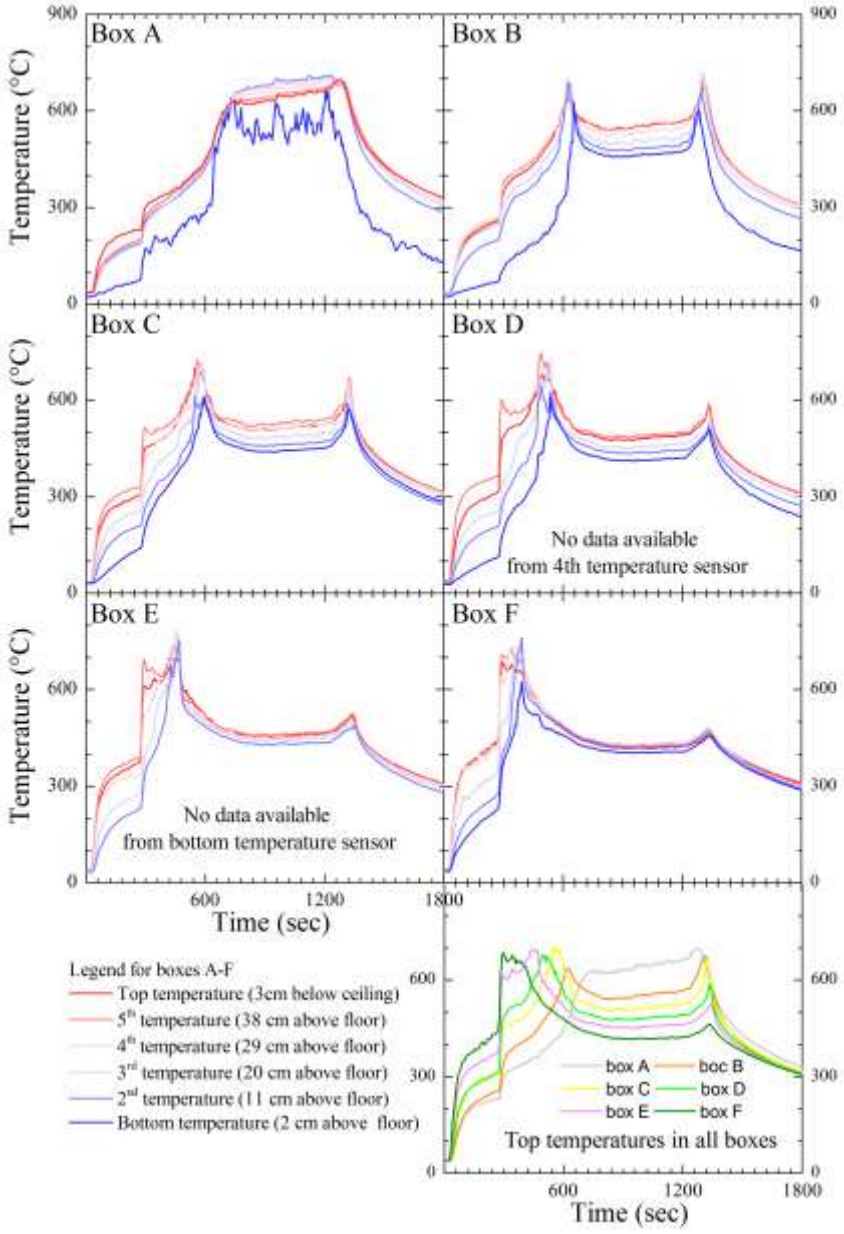
Box A
Box B
Box C
Box D
Box E
Box F
Temperature (°C)
900
600
300
0
No data available
from 4th temperature sensor
No data available
from bottom temperature sensor
600
1200
1800
Time (sec)
Legend for boxes A-F
Top temperature (3cm below ceiling)
5th temperature (38 cm above floor)
4th temperature (29 cm above floor)
3rd temperature (20 cm above floor)
2nd temperature (11 cm above floor)
Bottom temperature (2 cm above floor)
box A
boc B
box C
box D
box E
box F
Top temperatures in all boxes

Test no 5 (241109-1)

Test date 24 November 2009
Theoretical HRR = 15kW
Opening size = 20cm x 20cm
Ventilation controlled HRR = 26.8kW
GER = 0.6

Recorded observations:
31sec – ignition
<4 min 20 sec – problems with gas logging in box F
14 min 58 sec – gas turned off
17 min 26 sec – – flame self extinguished

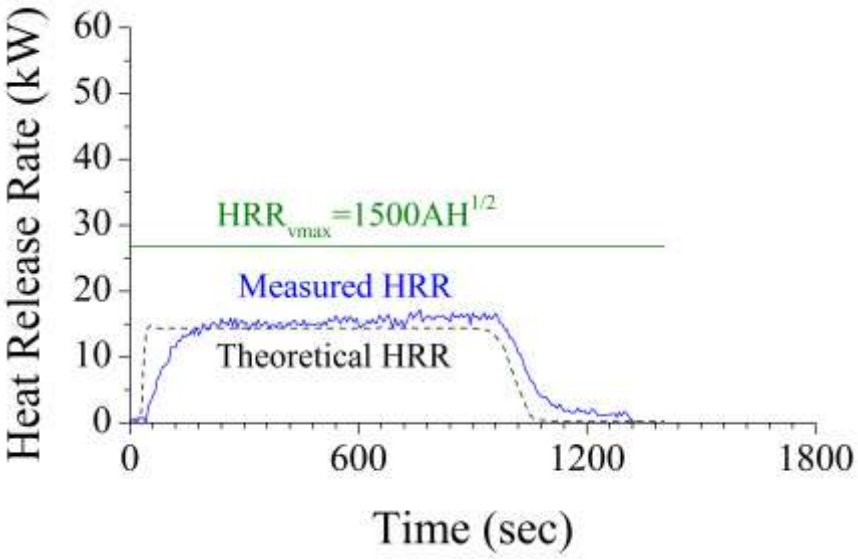

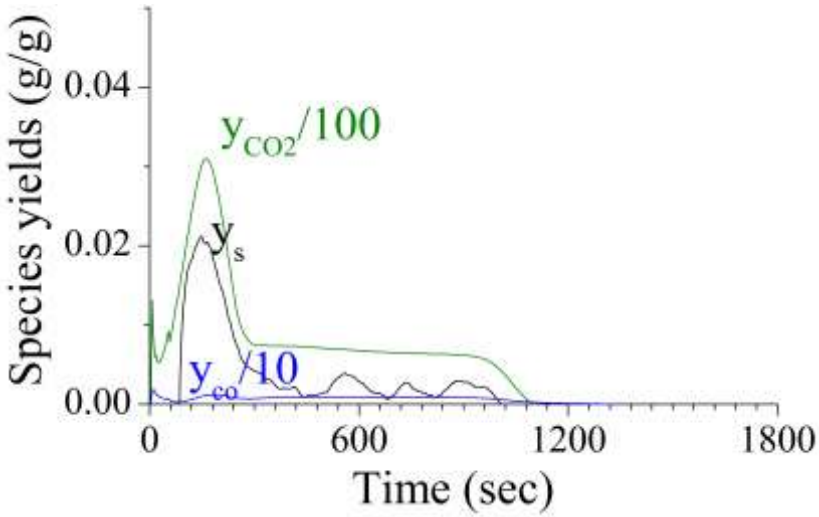

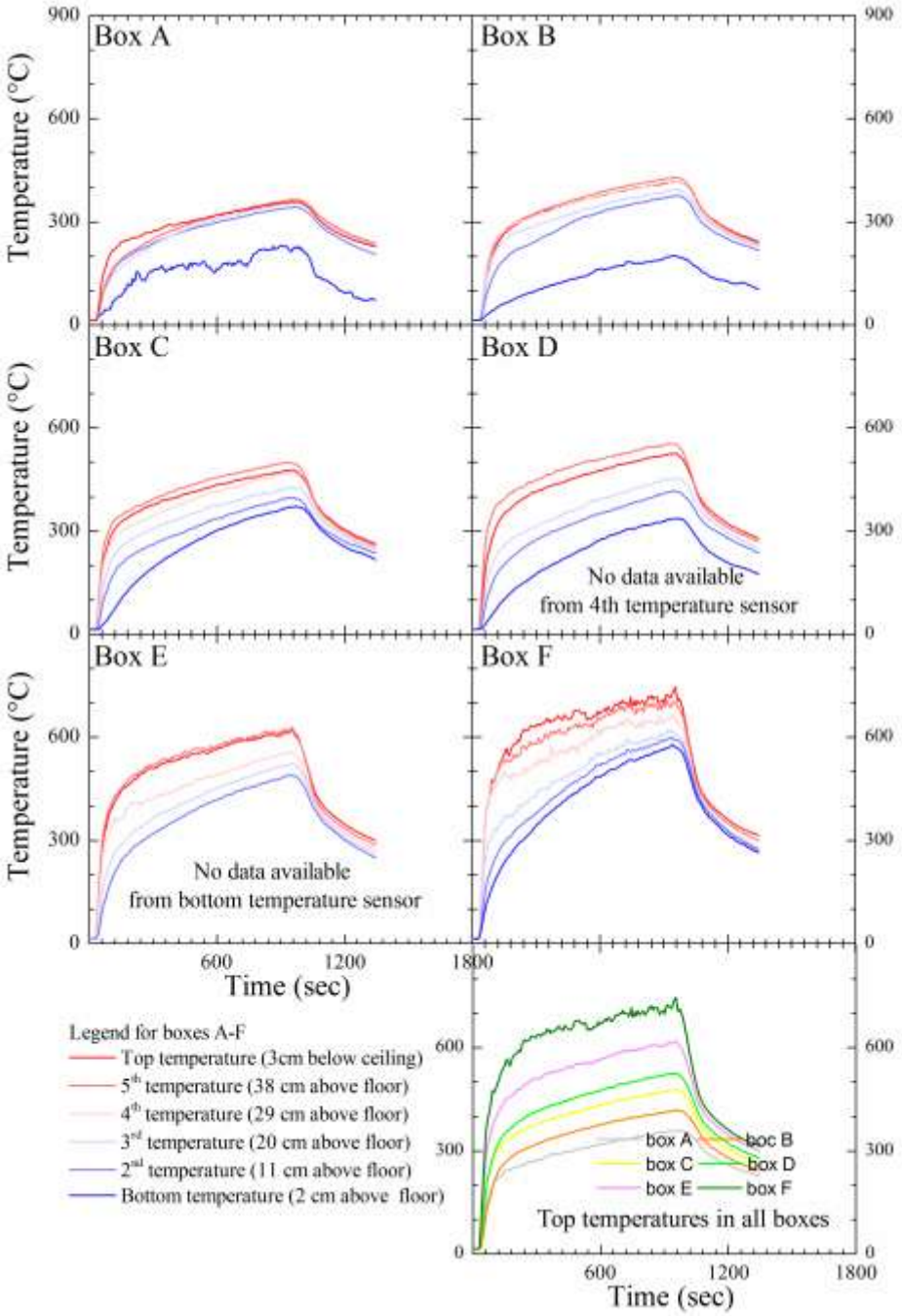
Box A
Box B
Box C
Box D
Box E
Box F
Temperature (°C)
Time (sec)
No data available
from 4th temperature sensor
No data available
from bottom temperature sensor
Legend for boxes A-F
Top temperature (3cm below ceiling)
5th temperature (38 cm above floor)
4th temperature (29 cm above floor)
3rd temperature (20 cm above floor)
2nd temperature (11 cm above floor)
Bottom temperature (2 cm above floor)
box A
box B
box C
box D
box E
box F
Top temperatures in all boxes

Test no 6 (261109-1)

Test date 26 November 2009
Theoretical HRR = 15kW
Opening size = W10cm x H25cm
Ventilation controlled HRR = 18.8kW
GER = 0.8

Recorded observations:
22sec – ignition
15 min – gas turned off
17 min 40 sec – flame self extinguished

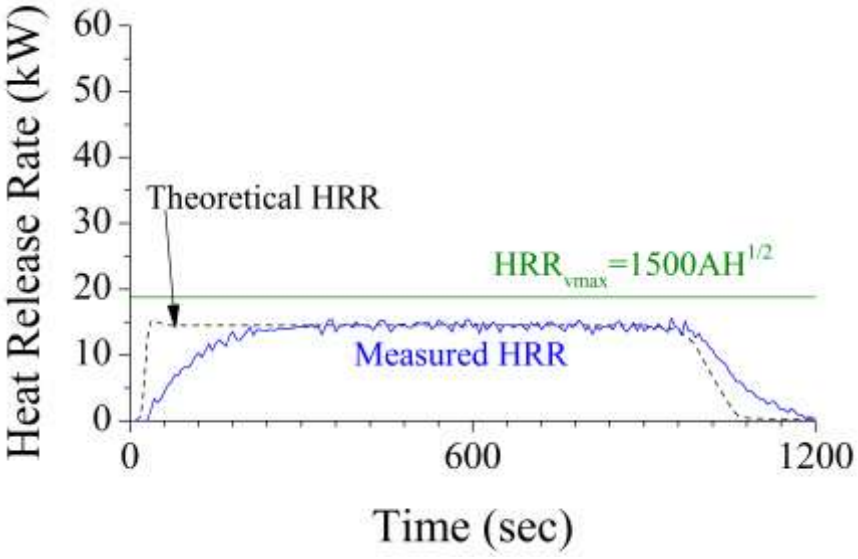

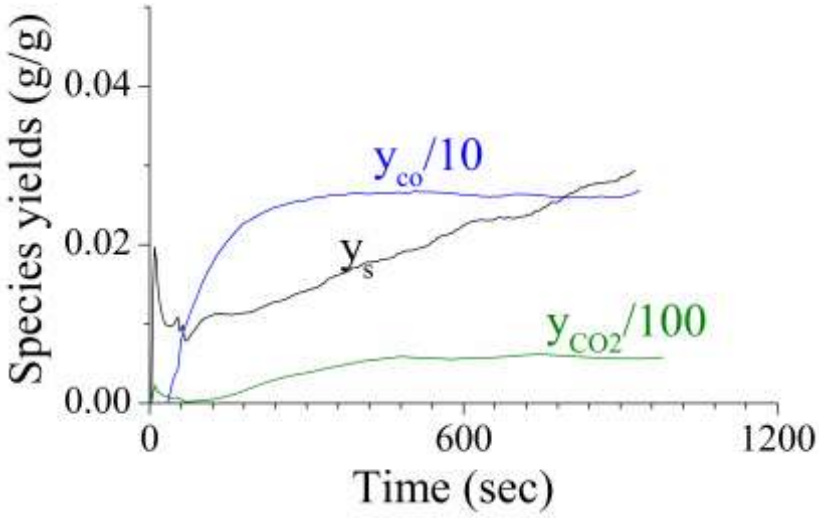

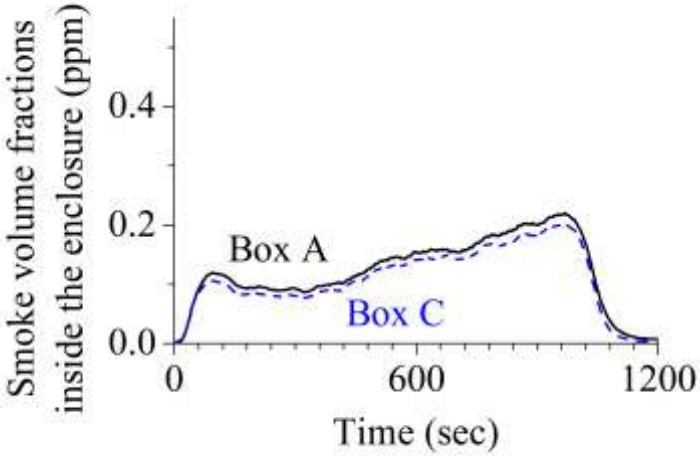
Smoke volume fractions inside the enclosure (ppm)
0.4
0.2
0.0
Box A
Box C
0
600
1200
Time (sec)

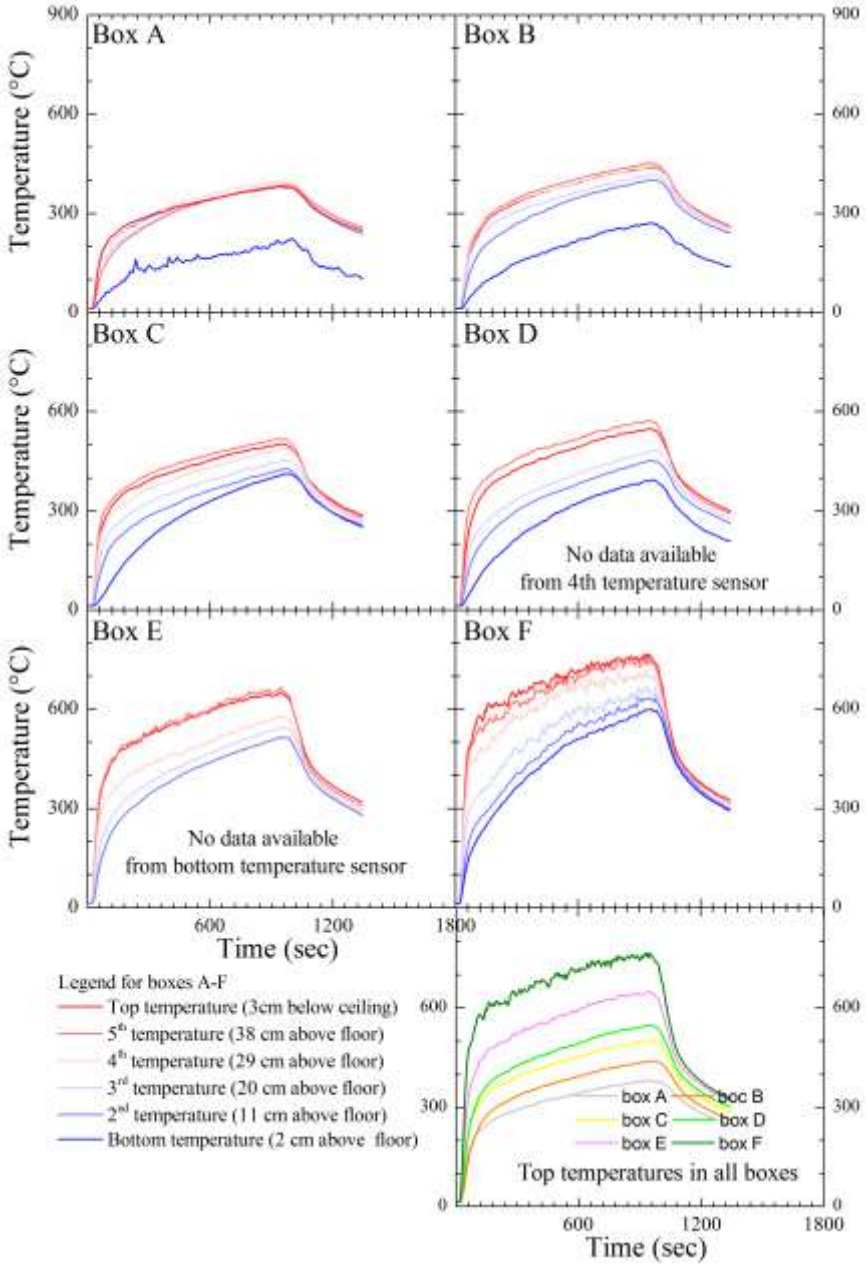
Box A
Box B
Box C
Box D
Box E
Box F
Temperature (°C)
900
600
300
0
No data available
from 4th temperature sensor
No data available
from bottom temperature sensor
600
1200
1800
Time (sec)
Legend for boxes A-F
Top temperature (3cm below ceiling)
5th temperature (38 cm above floor)
4th temperature (29 cm above floor)
3rd temperature (20 cm above floor)
2nd temperature (11 cm above floor)
Bottom temperature (2 cm above floor)
box A
box B
box C
box D
box E
box F
Top temperatures in all boxes

Test no 7 (271109-1)

Test date 27 November 2009
Theoretical HRR = 10kW
Opening size = W10cm x H25cm
Ventilation controlled HRR = 18.8kW
GER = 0.5

Recorded observations:
42sec – ignition
<1 min 36 sec – pump for upper layer gas analyser didn't work
<2 min 20 sec – small extractions fans for lasers in enclosure didn't work
15 min – gas turned off
18 min 10 sec – flame self extinguished

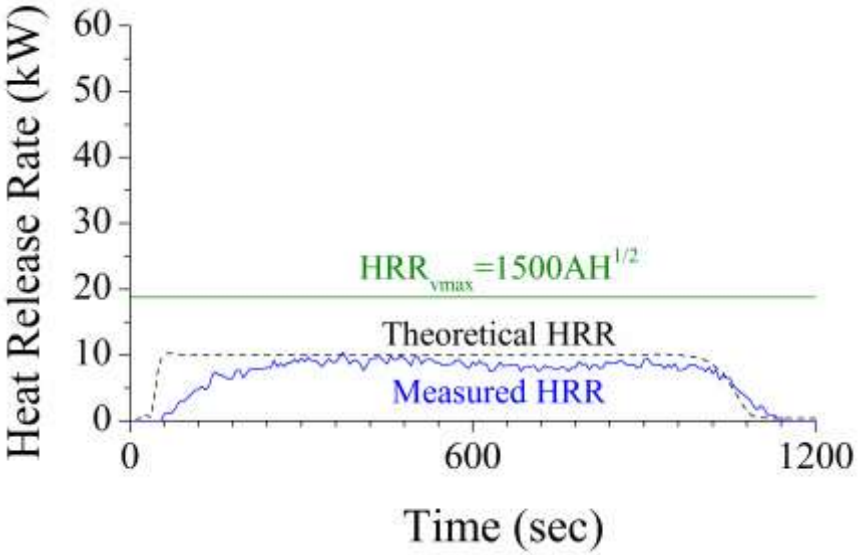

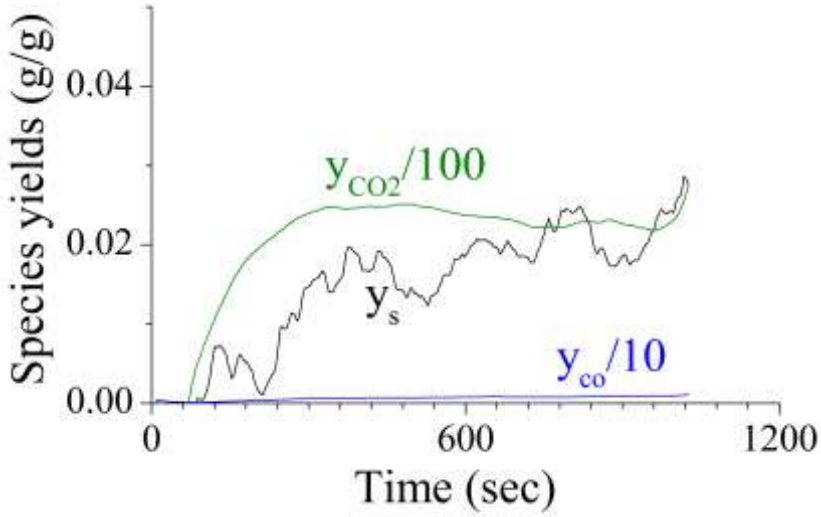

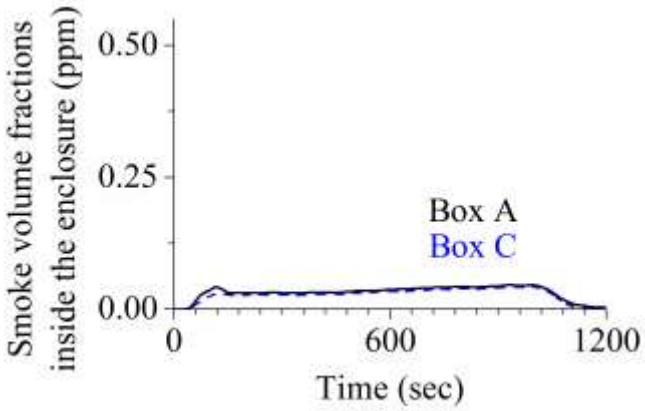
Smoke volume fractions inside the enclosure (ppm)
0.50
0.25
0.00
Box A
Box C
0
600
1200
Time (sec)

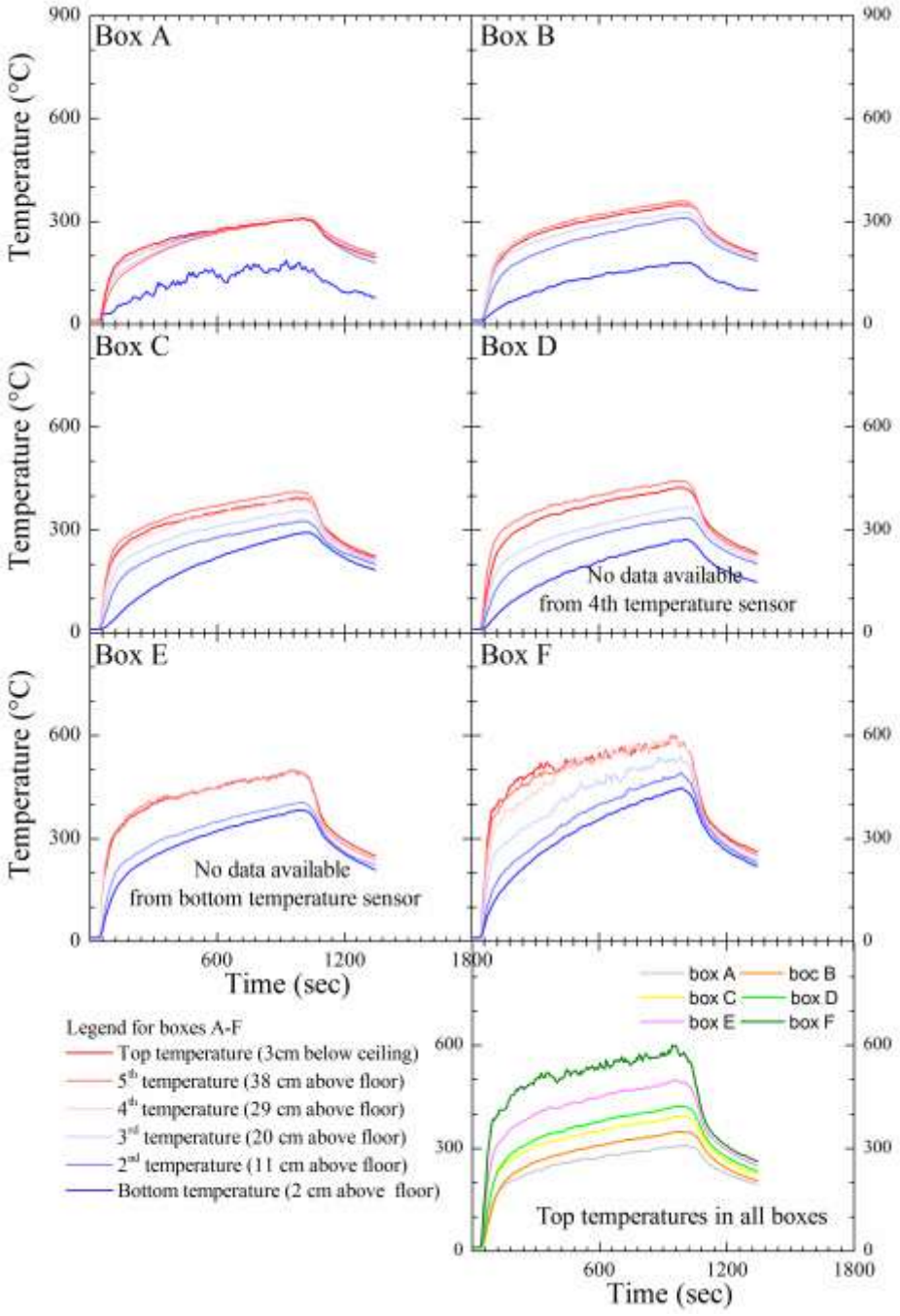
Box A
Box B
Box C
Box D
Box E
Box F
Temperature (°C)
900
600
300
0
No data available
from 4th temperature sensor
No data available
from bottom temperature sensor
600
1200
1800
Time (sec)
Legend for boxes A-F
Top temperature (3cm below ceiling)
5th temperature (38 cm above floor)
4th temperature (29 cm above floor)
3rd temperature (20 cm above floor)
2nd temperature (11 cm above floor)
Bottom temperature (2 cm above floor)
box A
boc B
box C
box D
box E
box F
Top temperatures in all boxes

Test no 8 (271109-2)

Test date 27 November 2009
Theoretical HRR = 30kW
Opening size = W10cm x H25cm
Ventilation controlled HRR = 18.8kW
GER = 1.6

Recorded observations:
41 sec – ignition
1 min 00 sec – automatic control of burner started
22 min 10 sec – flames approaching middle of box C
24 min 17 sec – first small flame tip visible shortly outside
24 min 55 sec – next time when small flame visible outside
27 min 00 sec – flame anchored in box B
28 min 50 sec – flame visible outside for longer periods of time
33 min 20 sec- flames outside all the time
36 min 05 – gas turned off
38 min 17 sec – flame self extinguished

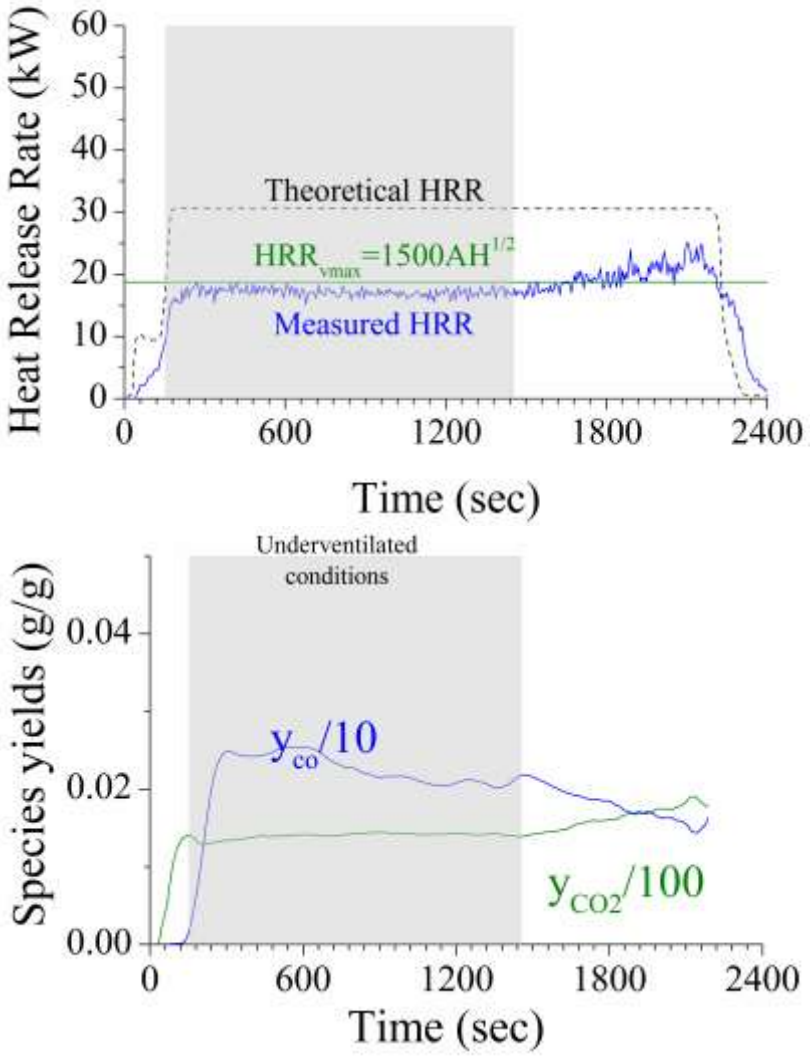

NO SMOKE DATA AVAILABLE for measurements in the duct

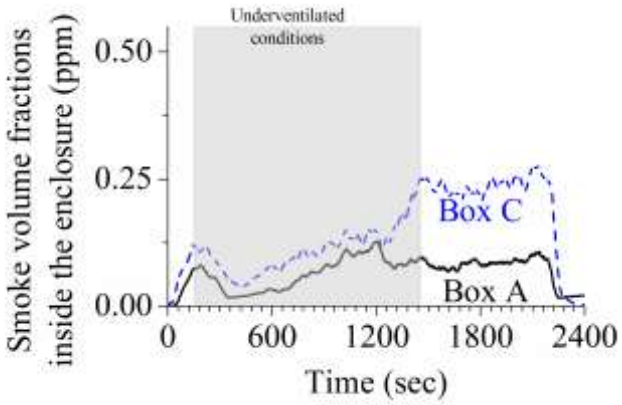
Underventilated conditions
Smoke volume fractions inside the enclosure (ppm)
0.50
0.25
0.00
Box C
Box A
0
600
1200
1800
2400
Time (sec)

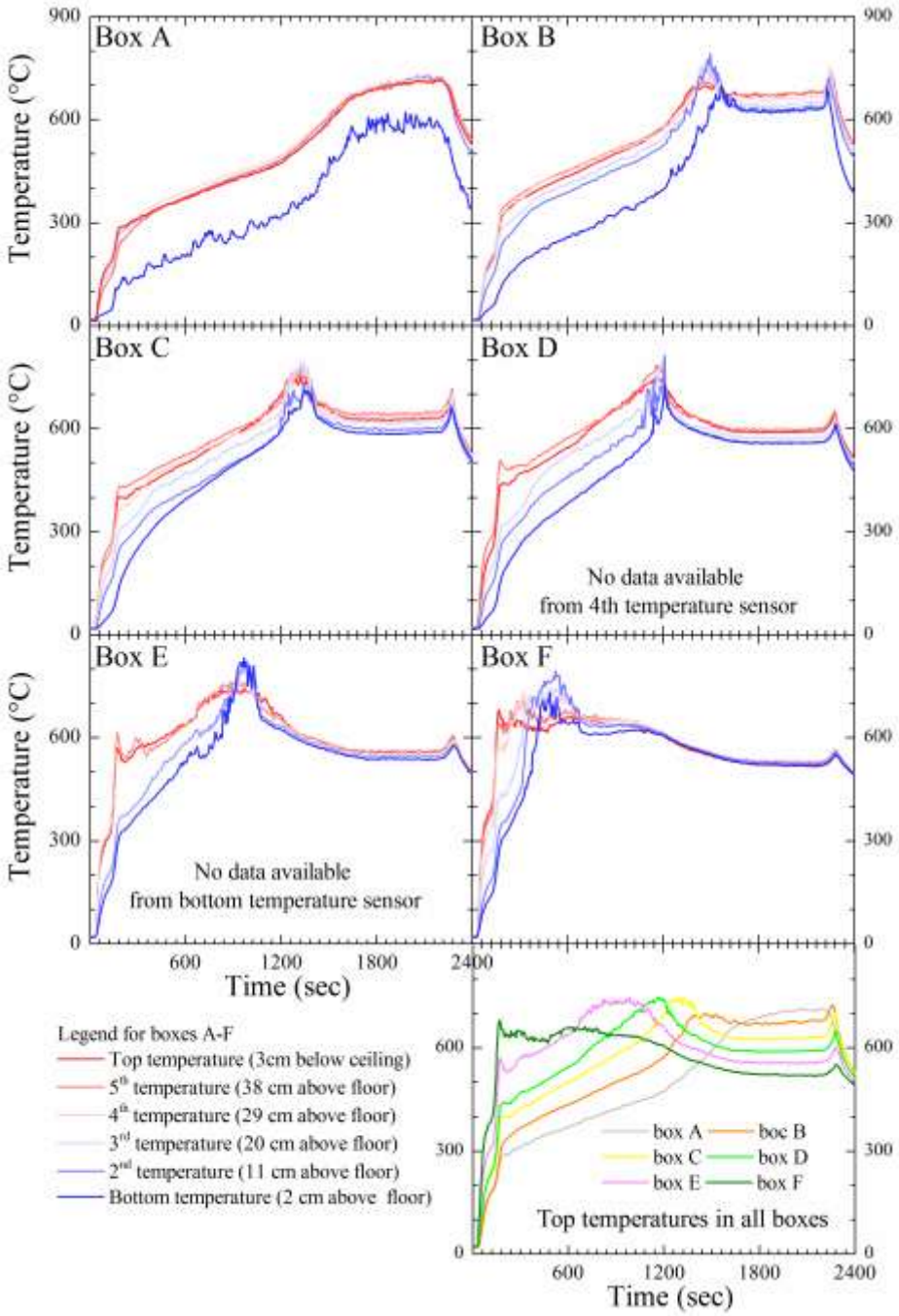
Box A
Box B
Box C
Box D
Box E
Box F
Temperature (°C)
900
600
300
0
No data available from 4th temperature sensor
No data available from bottom temperature sensor
600
1200
1800
2400
Time (sec)
Legend for boxes A-F
Top temperature (3cm below ceiling)
5th temperature (38 cm above floor)
4th temperature (29 cm above floor)
3rd temperature (20 cm above floor)
2nd temperature (11 cm above floor)
Bottom temperature (2 cm above floor)
box A
boc B
box C
box D
box E
box F
Top temperatures in all boxes

Test no 9 (101209-1)

Test date 10 December 2009
Theoretical HRR = 15kW
Opening size = W10cm x H25cm
Ventilation controlled HRR = 18.8kW
GER = 0.8

Recorded observations: (none available)

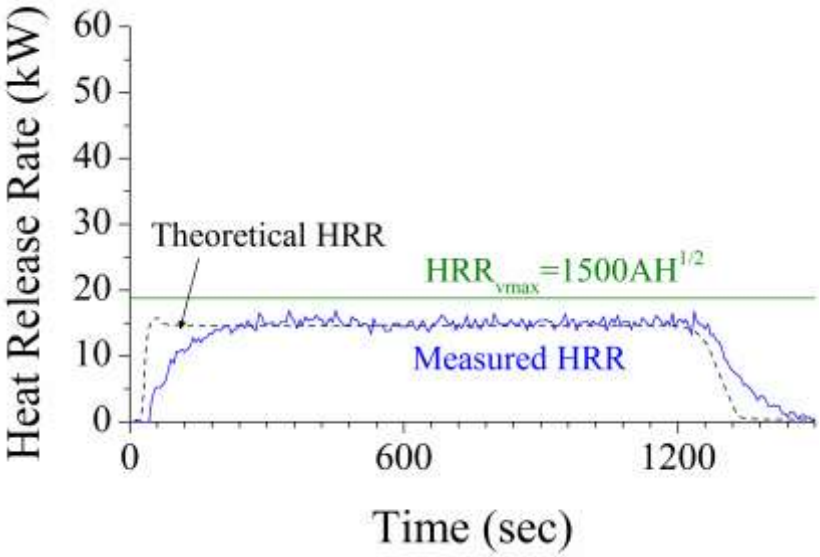

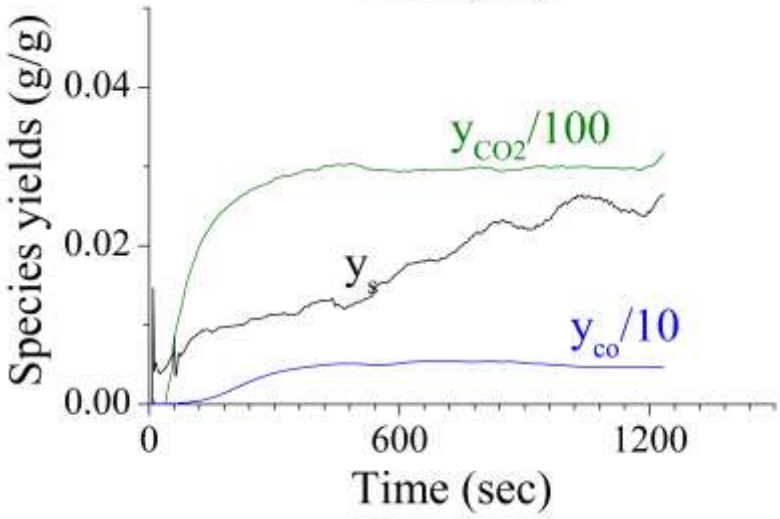

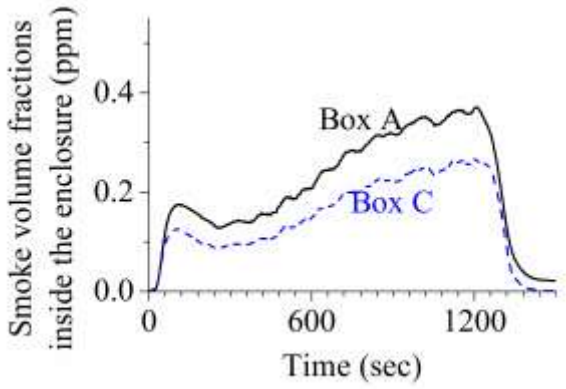
Smoke volume fractions inside the enclosure (ppm)
0.4
0.2
0.0
Box A
Box C
0
600
1200
Time (sec)

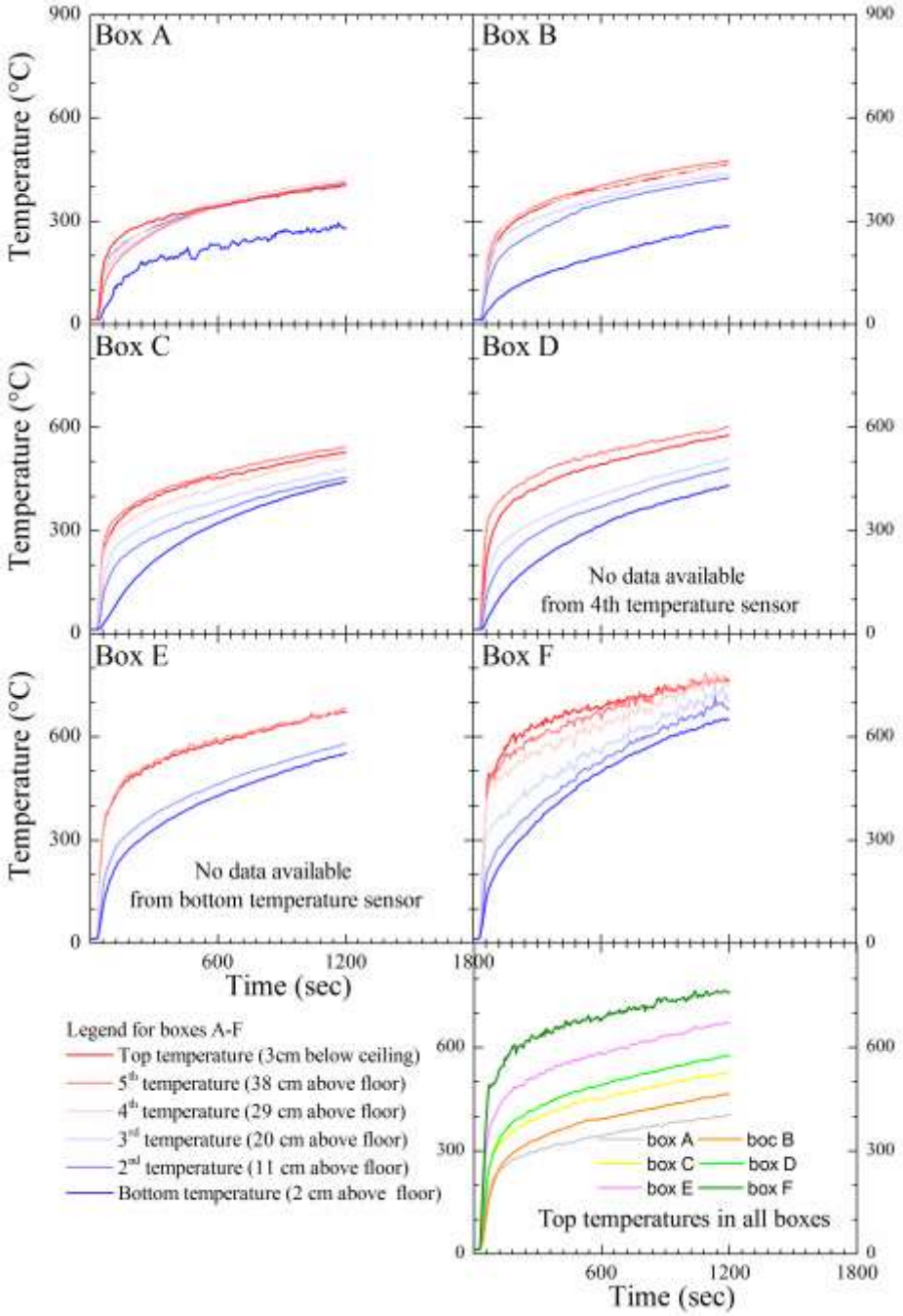
Box A
Box B
Box C
Box D
Box E
Box F
Temperature (°C)
900
600
300
0
No data available
from 4th temperature sensor
No data available
from bottom temperature sensor
600
1200
1800
Time (sec)
Legend for boxes A-F
Top temperature (3cm below ceiling)
5th temperature (38 cm above floor)
4th temperature (29 cm above floor)
3rd temperature (20 cm above floor)
2nd temperature (11 cm above floor)
Bottom temperature (2 cm above floor)
box A
boc B
box C
box D
box E
box F
Top temperatures in all boxes

Test no 10 (101209-2)

Test date 10 December 2009
Theoretical HRR = 15kW
Opening size = W10cm x H25cm
Ventilation controlled HRR = 18.8kW
GER = 0.8
It was repeated test on warmed enclosure

Recorded observations:
<38sec – ignition
15 min – gas turned off
17 min 26 sec – flame self extinguished

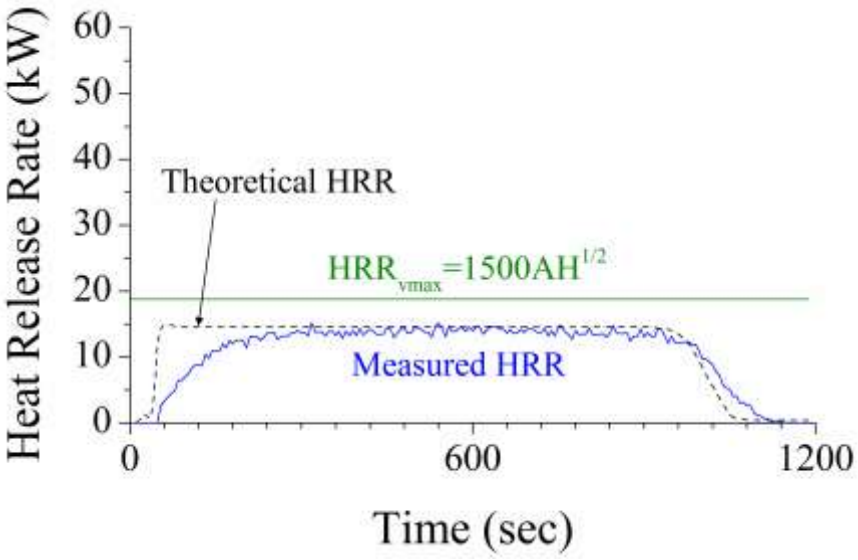

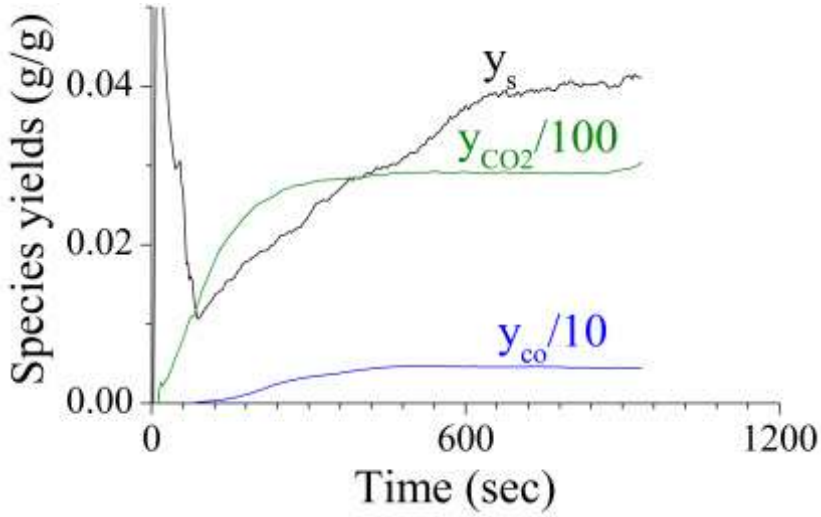

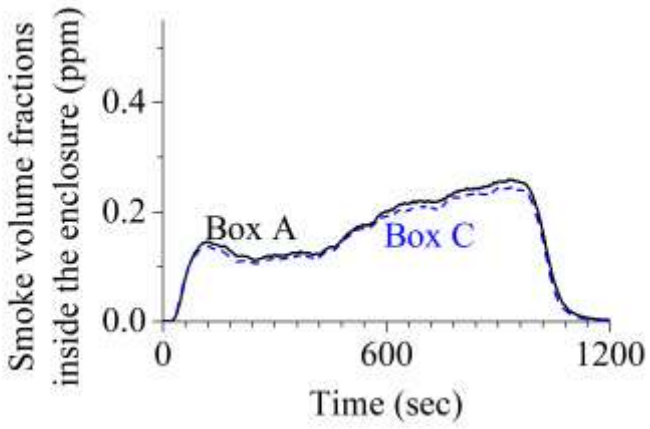
Smoke volume fractions inside the enclosure (ppm)
0.4
0.2
0.0
Box A
Box C
0
600
1200
Time (sec)

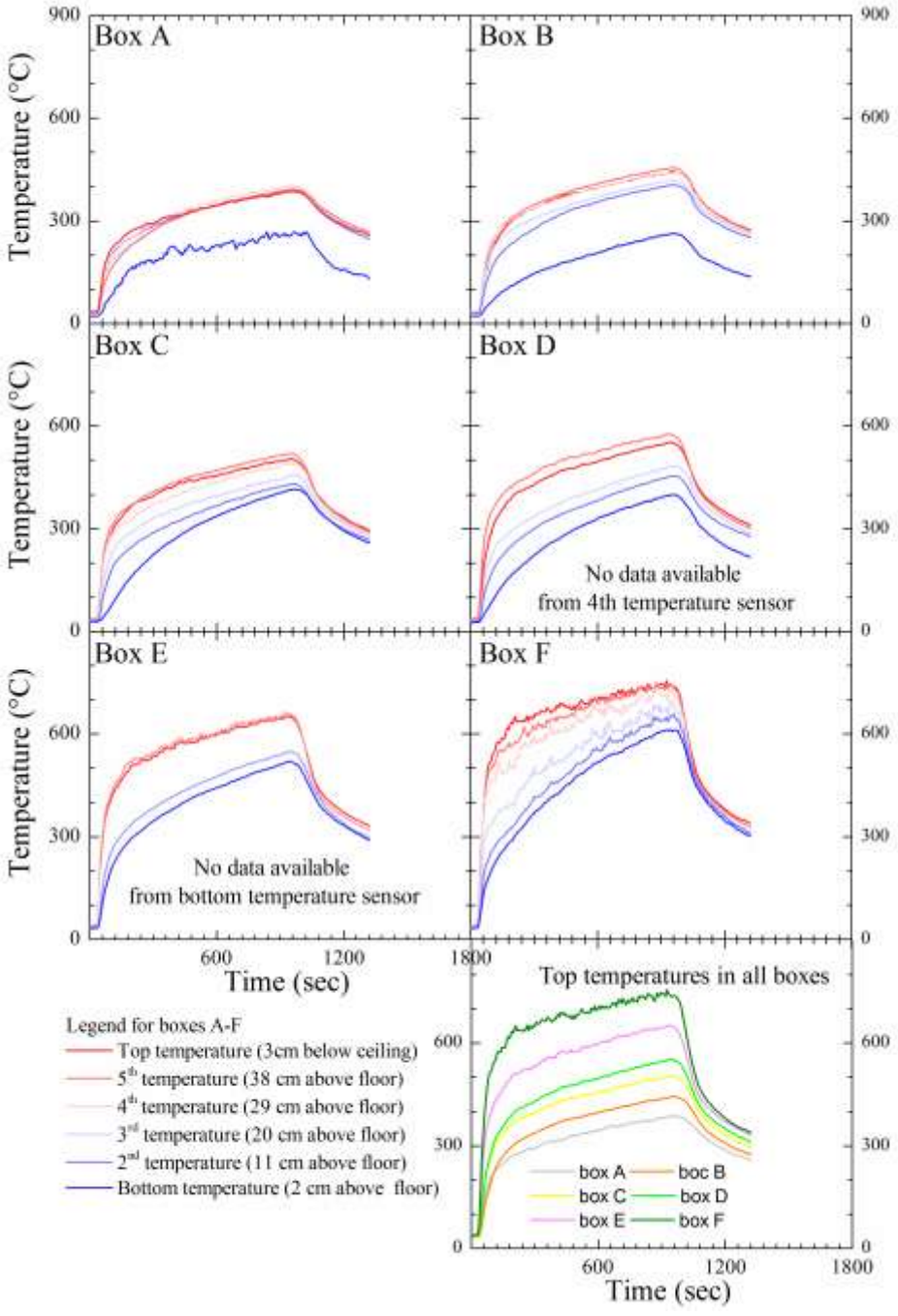
Box A
Box B
Box C
Box D
Box E
Box F
Temperature (°C)
900
600
300
0
No data available
from 4th temperature sensor
No data available
from bottom temperature sensor
600
1200
1800
Time (sec)
Top temperatures in all boxes
box A
boc B
box C
box D
box E
box F
Legend for boxes A-F
Top temperature (3cm below ceiling)
5th temperature (38 cm above floor)
4th temperature (29 cm above floor)
3rd temperature (20 cm above floor)
2nd temperature (11 cm above floor)
Bottom temperature (2 cm above floor)

Test no 11 (181209-1)

Test date 18 December 2009
Theoretical HRR = 50kW
Opening size = W10cm x H25cm
Ventilation controlled HRR = 18.8kW
GER = 2.67

Recorded observations:
38sec – ignition
1 min – automatic control of burner started
5 min 10 sec – flame moving gradually
6 min 20 sec – flames at the sampling line in box C
7 min 15 sec – flame tip outside and stays outside
14 min – smoke meter in box C off for 40 secs
15 min – gas turned off
17 min 05 sec – no flames visible outiside
18 min 14 sec – flame self extinguished

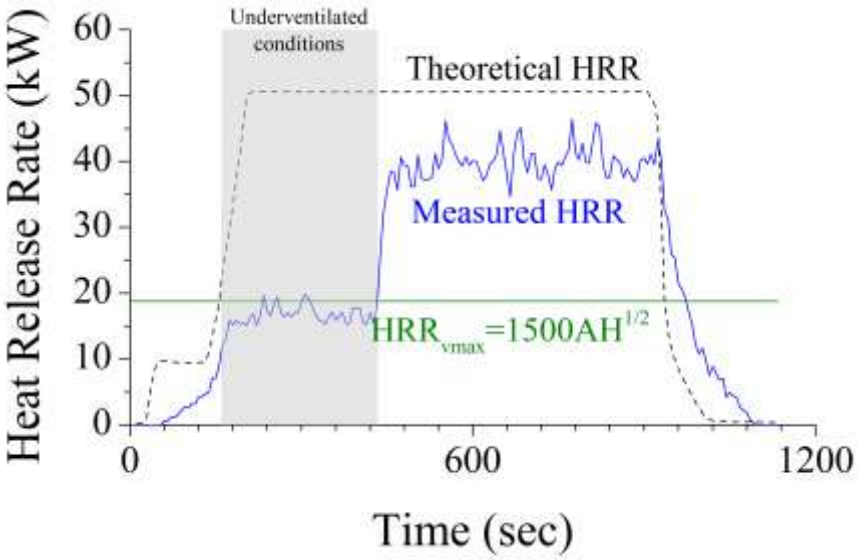

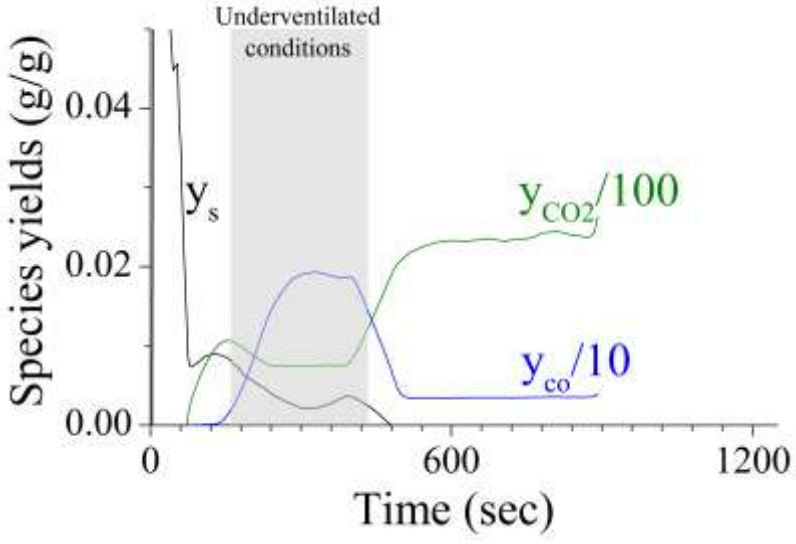

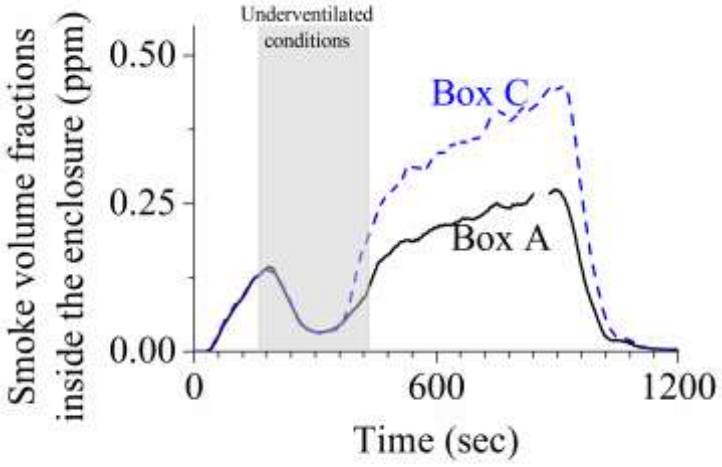
Underventilated conditions
Box C
Box A
Smoke volume fractions inside the enclosure (ppm)
0.50
0.25
0.00
0
600
1200
Time (sec)

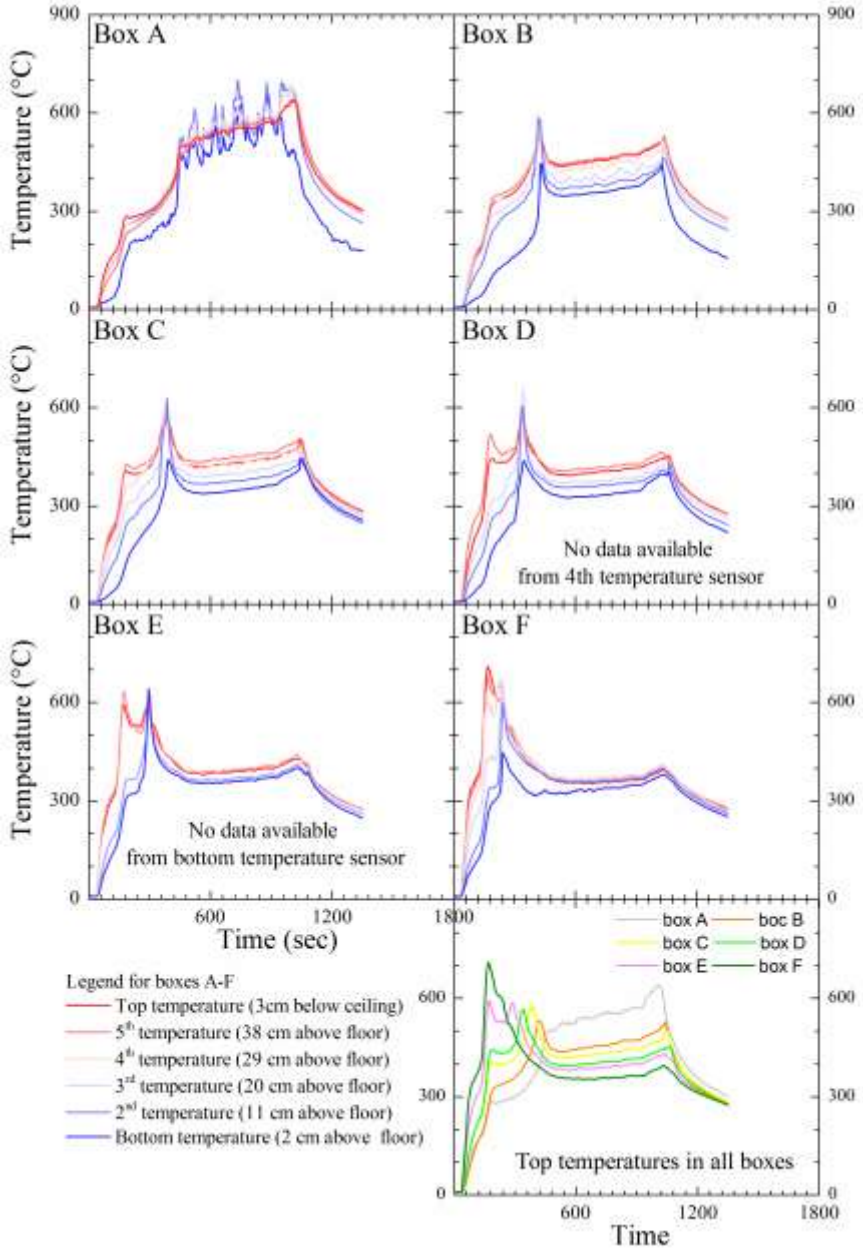
Box A
Box B
Box C
Box D
Box E
Box F
Temperature (°C)
900
600
300
0
No data available from 4th temperature sensor
No data available from bottom temperature sensor
600
1200
1800
Time (sec)
Legend for boxes A-F
Top temperature (3cm below ceiling)
5th temperature (38 cm above floor)
4th temperature (29 cm above floor)
3rd temperature (20 cm above floor)
2nd temperature (11 cm above floor)
Bottom temperature (2 cm above floor)
box A
boc B
box C
box D
box E
box F
Top temperatures in all boxes
Time

Test no 12 (181209-2)

Test date 18 December 2009
Theoretical HRR = 30kW
Opening size = W10cm x H25cm
Ventilation controlled HRR = 18.8kW
GER = 1.6

Recorded observations:
0 min – automatic control of burner started (due to error)
<10sec – ignition
24 min 31 sec – first flame tip visible outside and doesn't stays outside (looks like n extended flame from boxes C-B)
27 min – more flames visible outside
30 min – gas turned off
32 min 30 sec – flame self extinguished

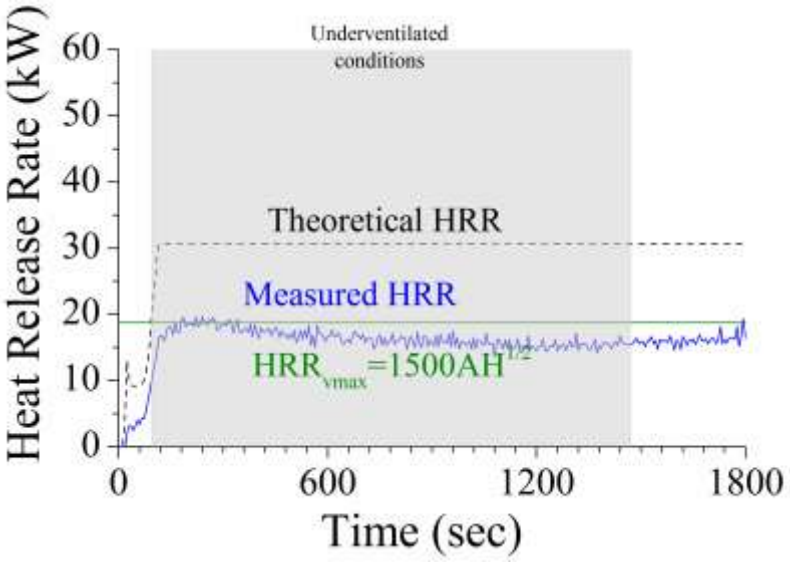

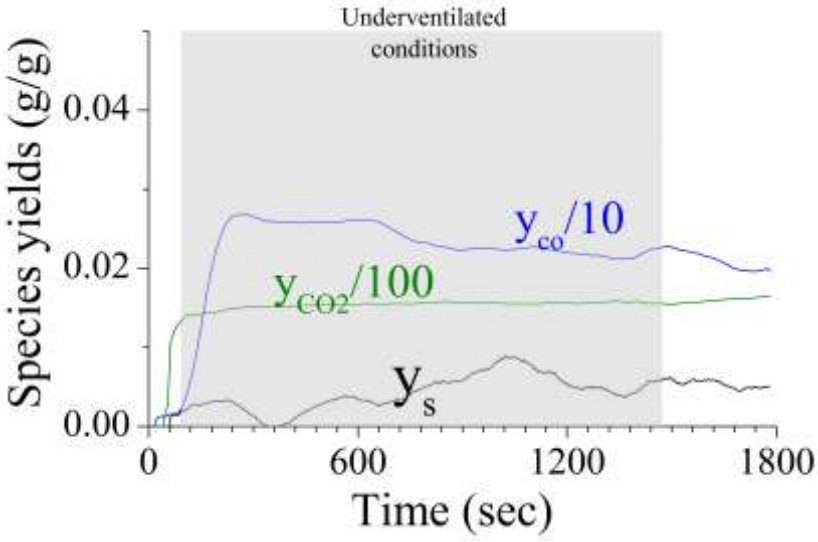

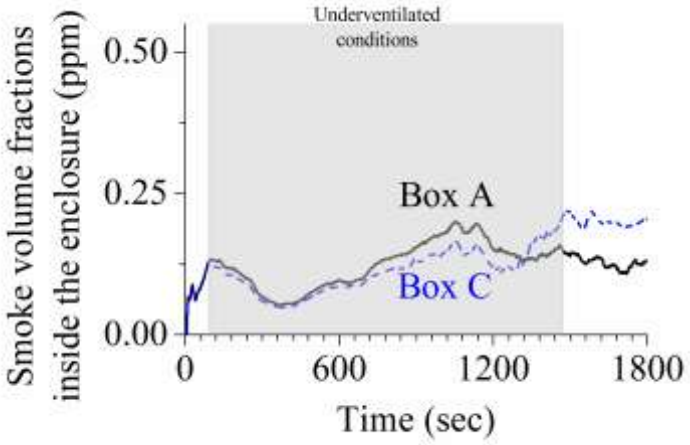
Underventilated
conditions
Smoke volume fractions
inside the enclosure (ppm)
0.50
0.25
0.00
Box A
Box C
0
600
1200
1800
Time (sec)

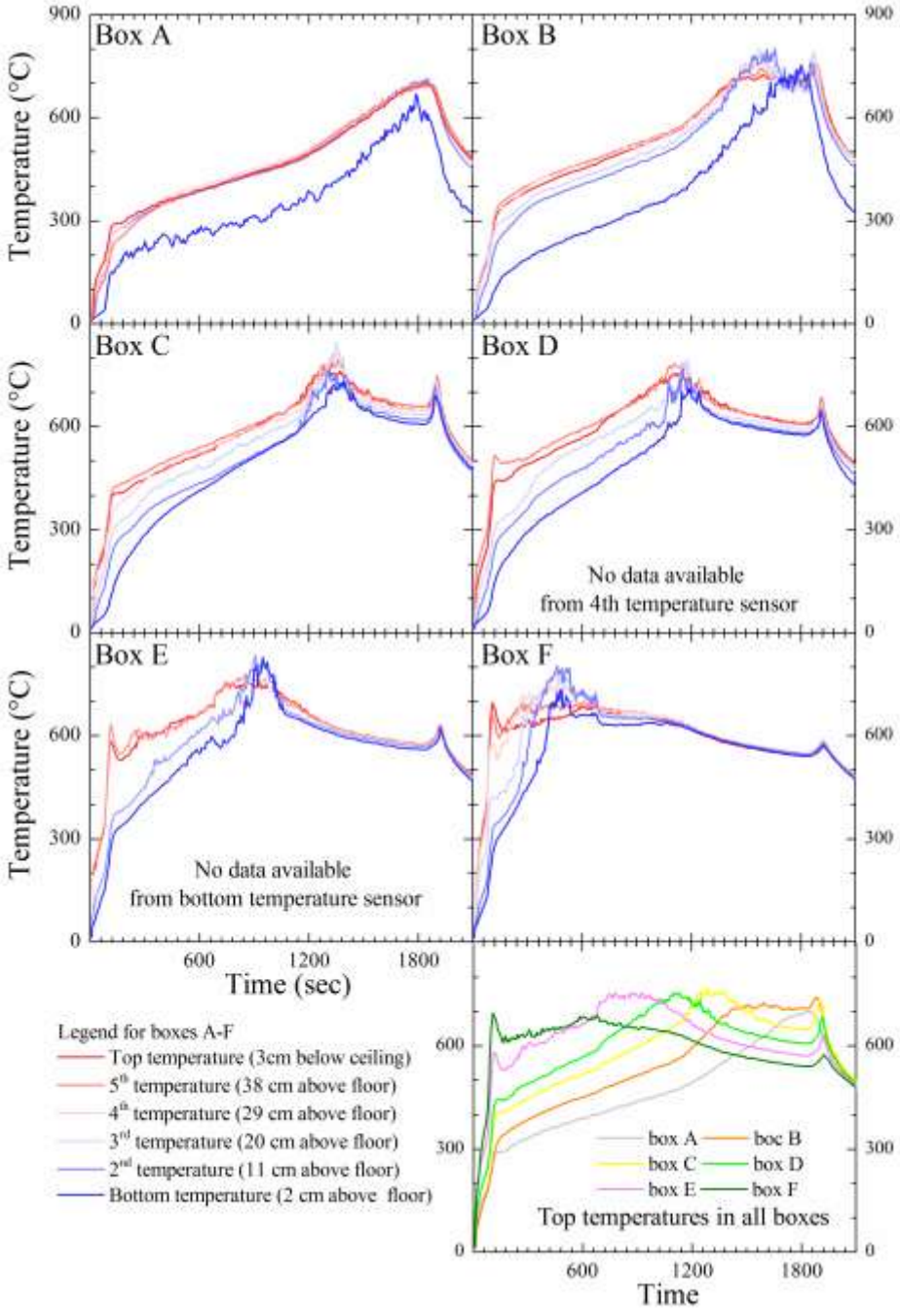
Box A
Box B
Box C
Box D
Box E
Box F
Temperature (°C)
900
600
300
0
No data available
from 4th temperature sensor
No data available
from bottom temperature sensor
600
1200
1800
Time (sec)
Legend for boxes A-F
Top temperature (3cm below ceiling)
5th temperature (38 cm above floor)
4th temperature (29 cm above floor)
3rd temperature (20 cm above floor)
2nd temperature (11 cm above floor)
Bottom temperature (2 cm above floor)
box A
boc B
box C
box D
box E
box F
Top temperatures in all boxes
Time

Test no 13 (231209-1)

Test date 23 December 2009
Theoretical HRR = 25kW
Opening size = W10cm x H25cm
Ventilation controlled HRR = 18.8kW
GER = 1.33

Recorded observations:

38sec – ignition
1 min – automatic control of burner started
1 min 27 sec – smoke fans turned on (delay due to error)
about 21 min – very dense smoke
26 min 44 sec – less smoke visible and flames started to move inside
35 min – gas turned off
37 min - flame self extinguished

At 35 min flames were visually observed around sampling line inside box C

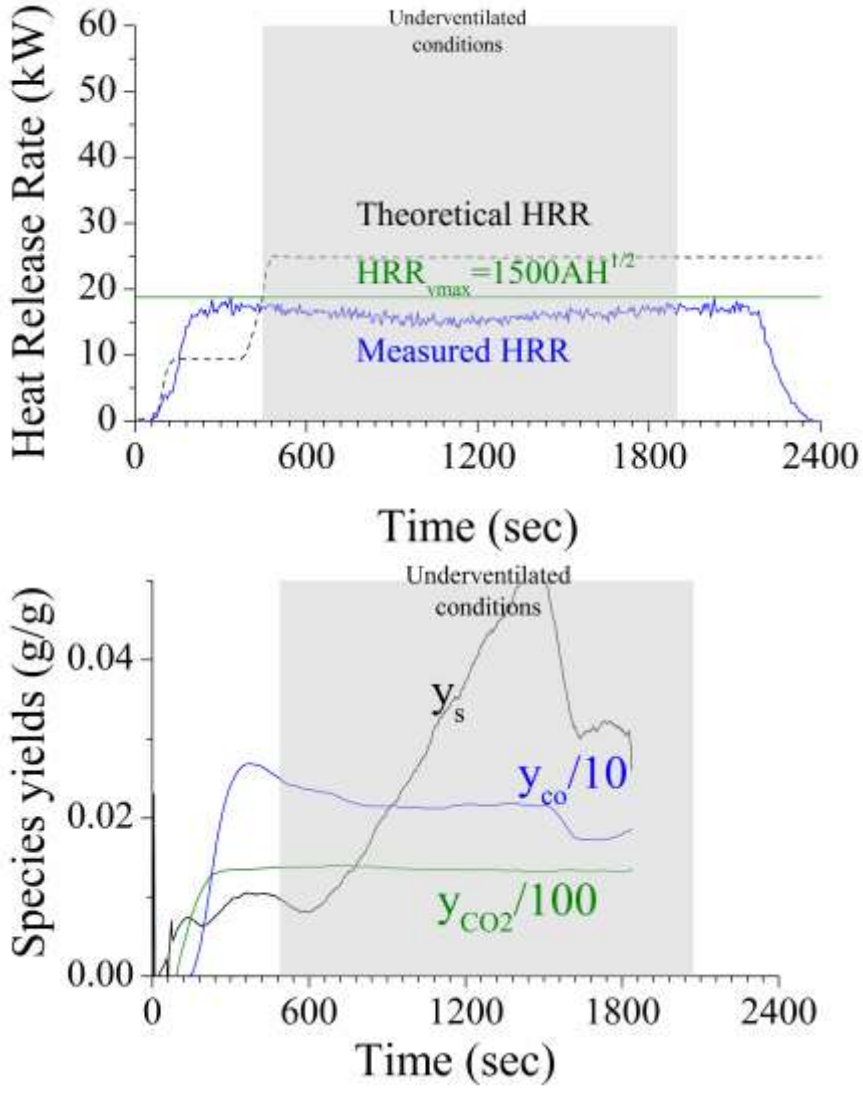

Problems with smoke meters during this test

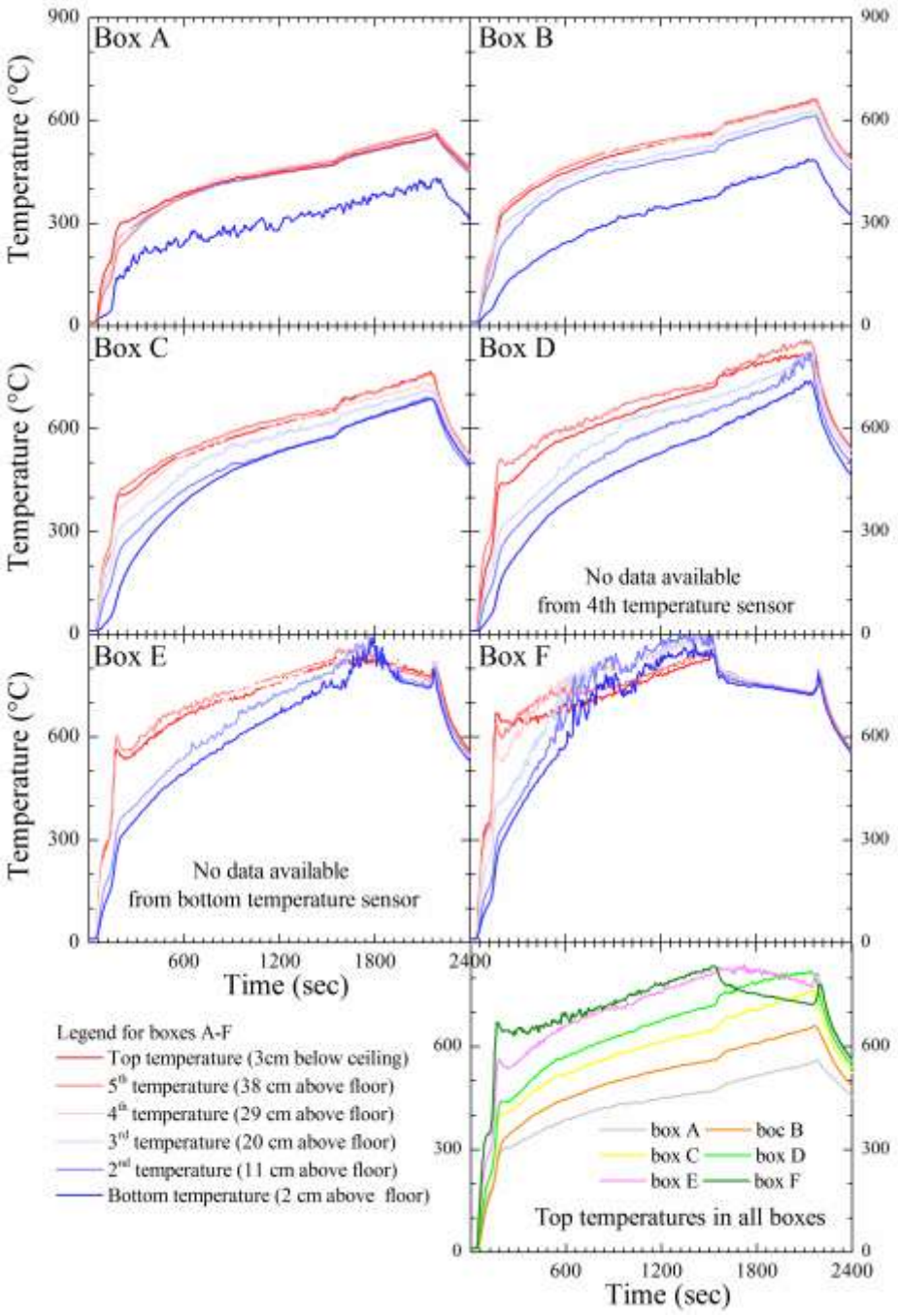

Test no 14 (040110-1)

Test date 4 January 2010
Theoretical HRR = 28kW
Opening size = W10cm x H25cm
Ventilation controlled HRR = 18.8kW
GER = 1.49

Recorded observations:
55sec – ignition
1 min – automatic control of burner started
23 min – shutter doors open outside (possible draughts)
<25 min – flames didn't reach box C yet (by visual observations)
25 min – gas turned off
27 min 07 sec- flame self extinguished

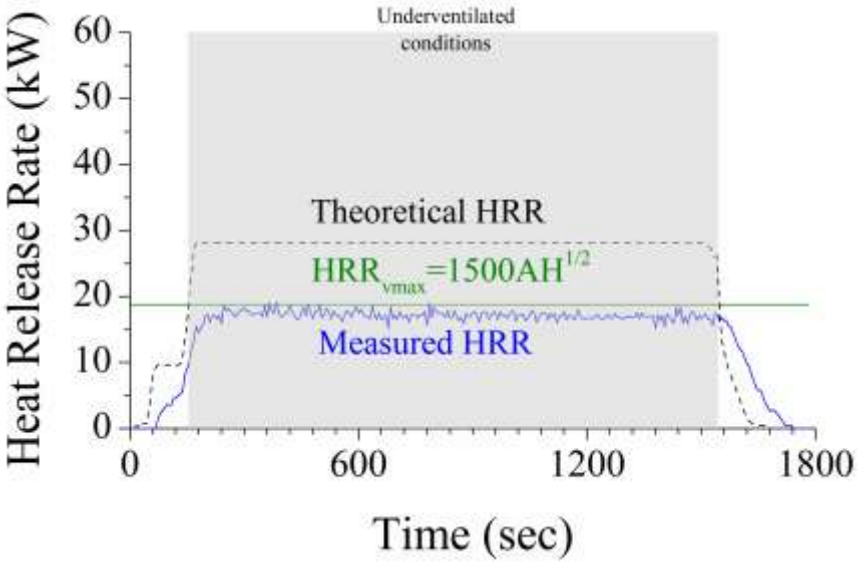

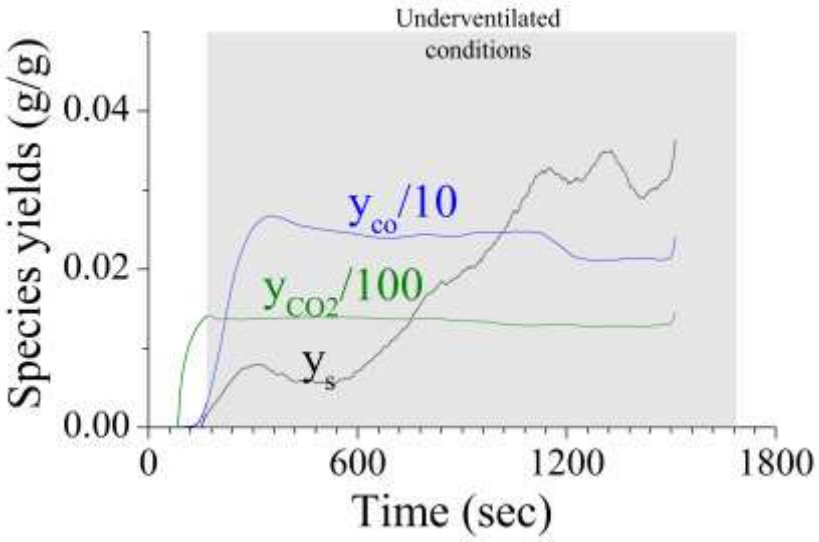

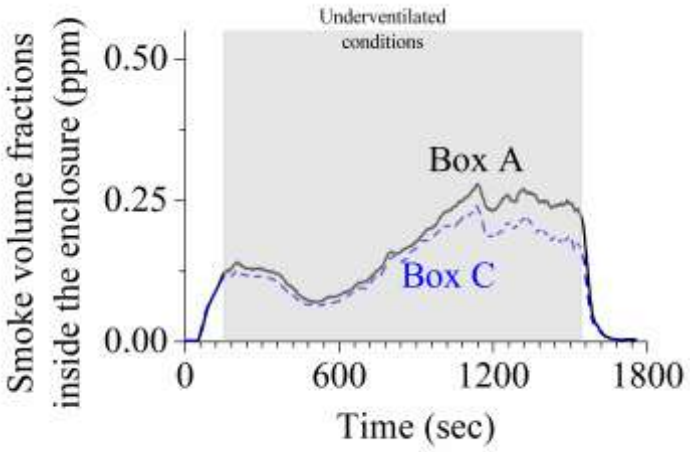
Underventilated
conditions
Smoke volume fractions
inside the enclosure (ppm)
0.50
0.25
0.00
Box A
Box C
0
600
1200
1800
Time (sec)

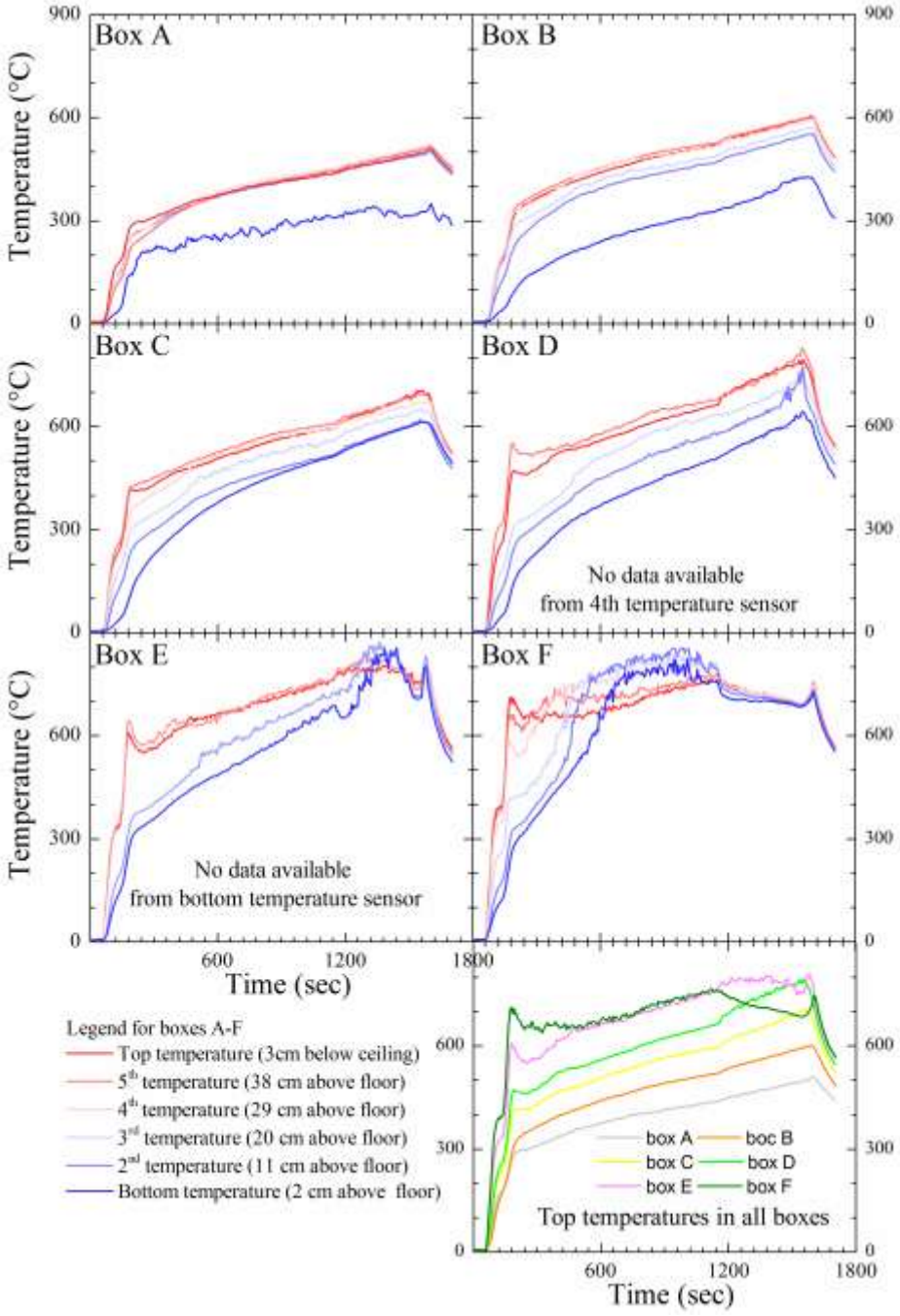
Box A
Box B
Box C
Box D
Box E
Box F
Temperature (°C)
900
600
300
0
No data available
from 4th temperature sensor
No data available
from bottom temperature sensor
600
1200
1800
Time (sec)
Legend for boxes A-F
Top temperature (3cm below ceiling)
5th temperature (38 cm above floor)
4th temperature (29 cm above floor)
3rd temperature (20 cm above floor)
2nd temperature (11 cm above floor)
Bottom temperature (2 cm above floor)
box A
boc B
box C
box D
box E
box F
Top temperatures in all boxes

Test no 15 (050110-2)

Test date 5 January 2010
Theoretical HRR = 35kW
Opening size = W10cm x H25cm
Ventilation controlled HRR = 18.8kW
GER = 1.87

Recorded observations:
55sec – ignition
1 min – automatic control of burner started
23 min – shutter doors open outside (possible draughts)
<25 min – flames didn't reach box C yet (by visual observations)
25 min – gas turned off
27 min 07 sec- flames self extinguished

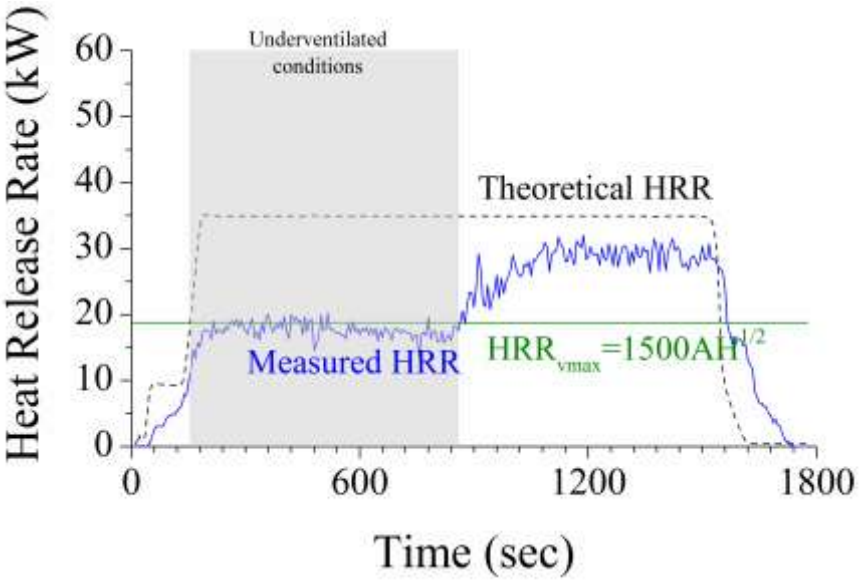

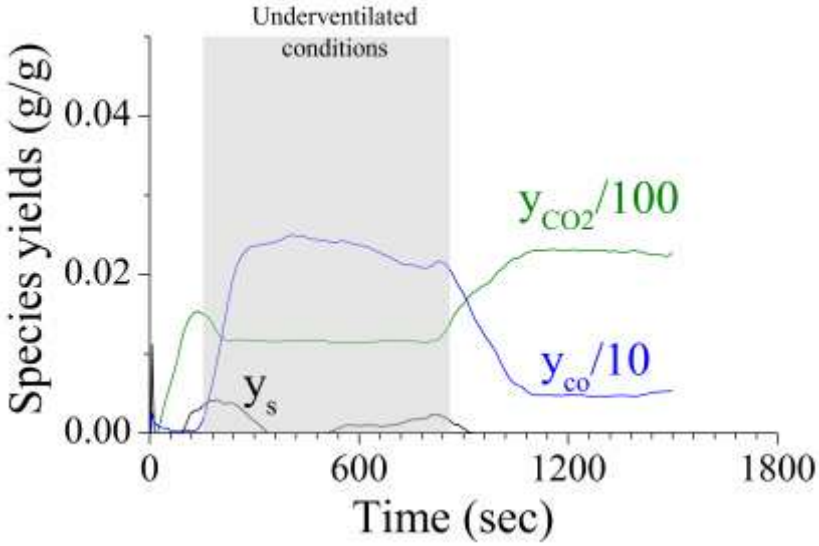

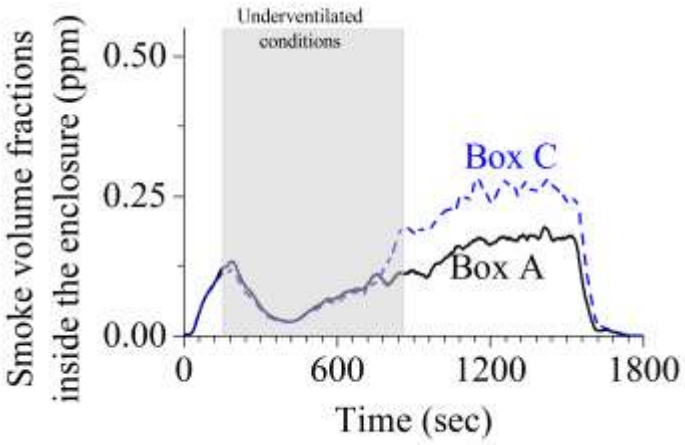
Underventilated conditions
Smoke volume fractions inside the enclosure (ppm)
0.50
0.25
0.00
Box C
Box A
0
600
1200
1800
Time (sec)

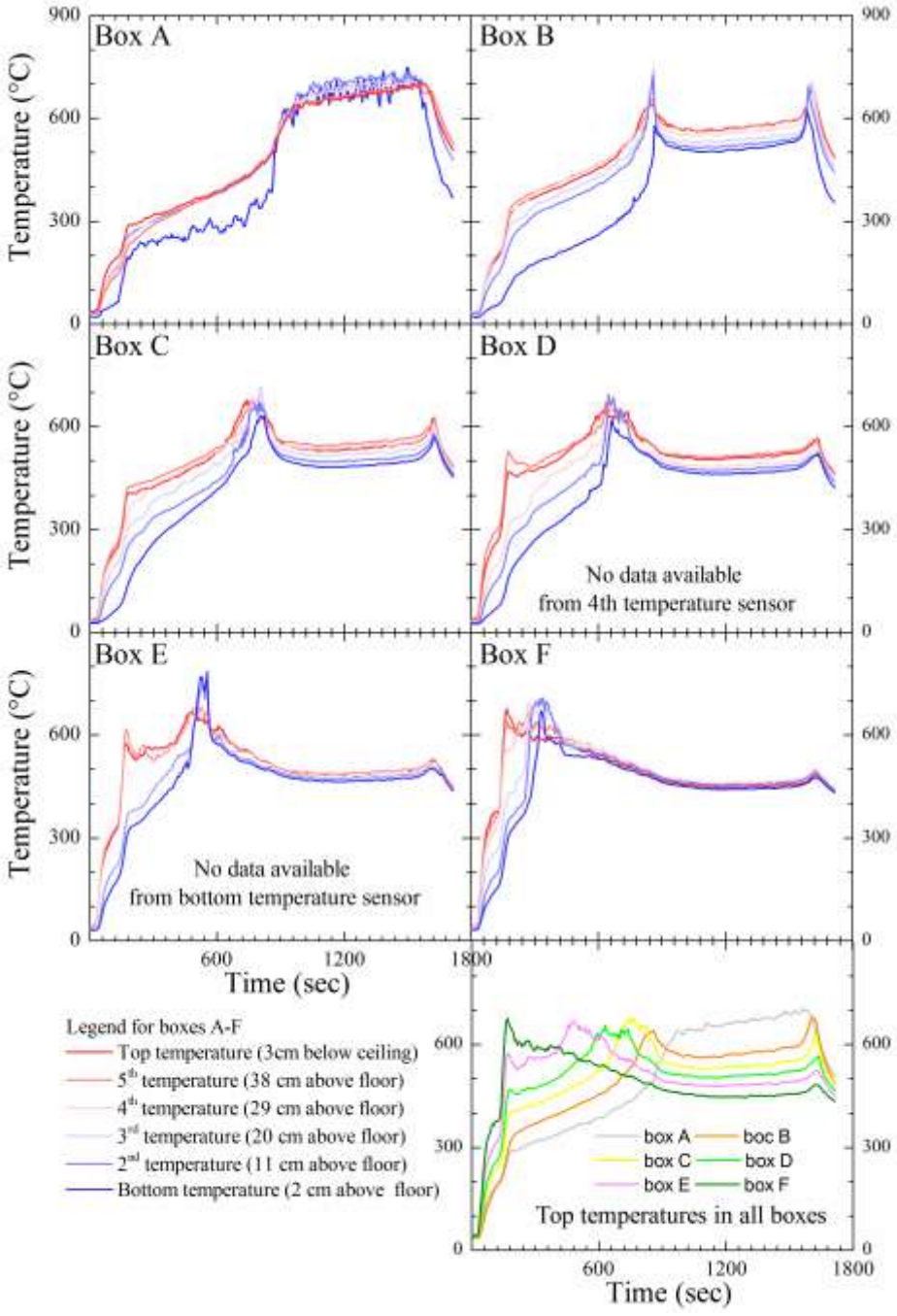
Box A
Box B
Box C
Box D
Box E
Box F
Temperature (°C)
900
600
300
0
No data available from 4th temperature sensor
No data available from bottom temperature sensor
600
1200
1800
Time (sec)
Legend for boxes A-F
Top temperature (3cm below ceiling)
5th temperature (38 cm above floor)
4th temperature (29 cm above floor)
3rd temperature (20 cm above floor)
2nd temperature (11 cm above floor)
Bottom temperature (2 cm above floor)
box A
boc B
box C
box D
box E
box F
Top temperatures in all boxes

Test no 16 (070110-1)

Test date 7 January 2010
Theoretical HRR = 50kW
Opening size = W10cm x H25cm
Ventilation controlled HRR = 18.8kW
GER = 2,67

Recorded observations:
34sec – ignition
1 min – automatic control of burner started
<7 min 09 sec – flames visible outside
25 min – gas turned off
27 min 07 sec – no flames visible outside
28 min 25 sec- flames self extinguished

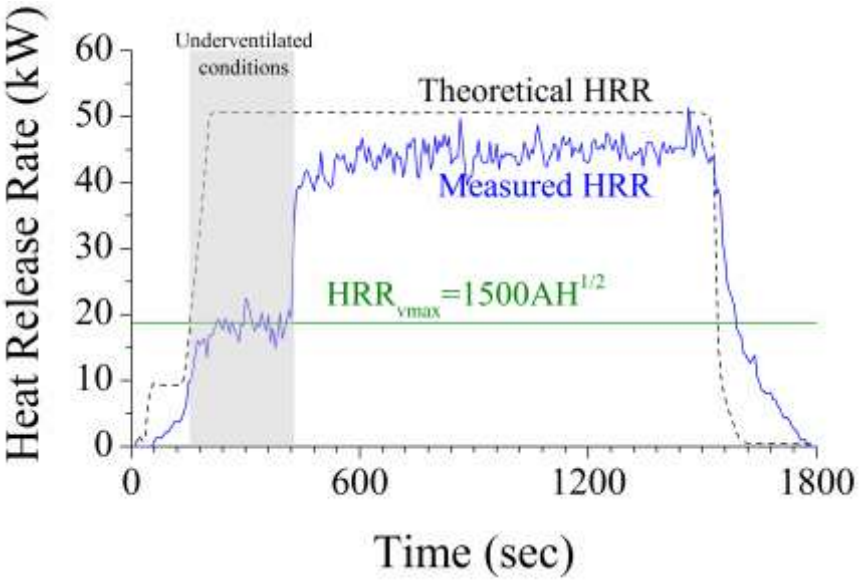

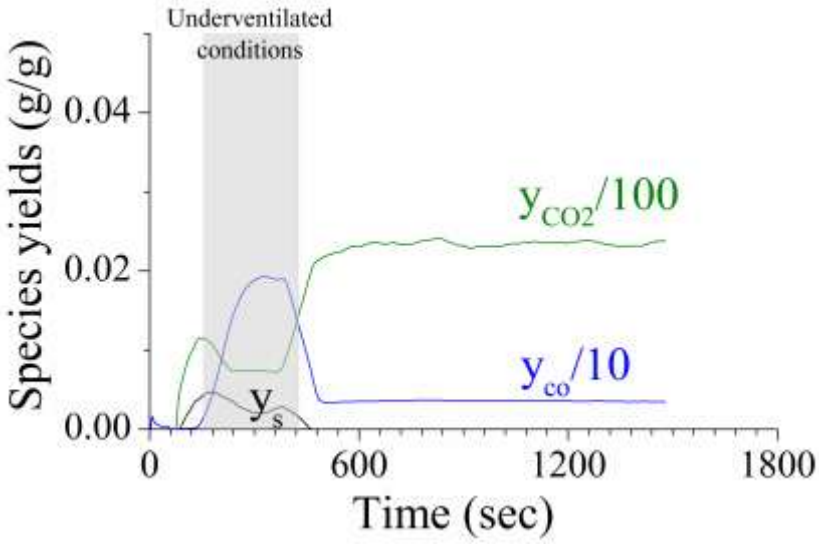

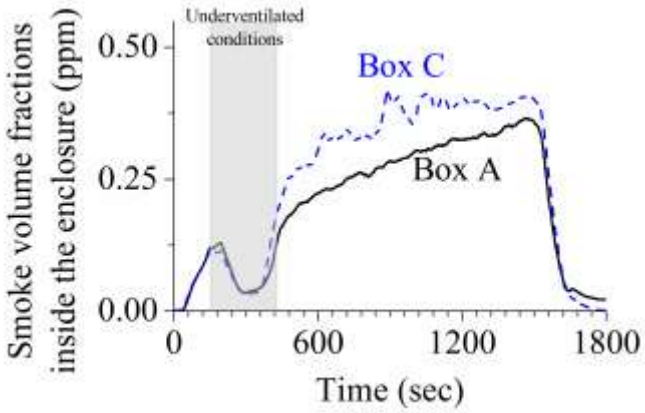
Underventilated conditions
Box C
Box A
Smoke volume fractions inside the enclosure (ppm)
0.50
0.25
0.00
0
600
1200
1800
Time (sec)

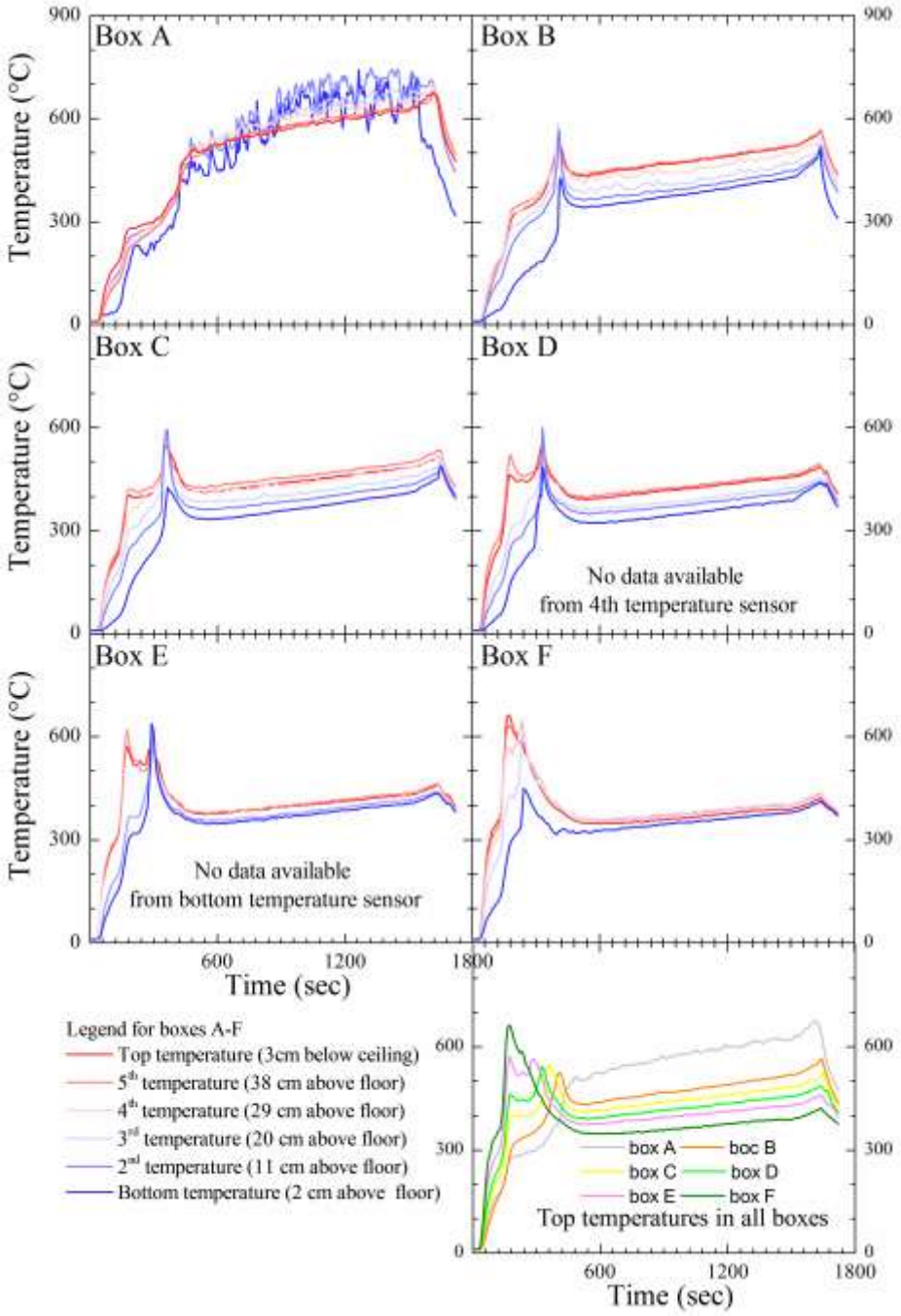
Box A
Box B
Box C
Box D
Box E
Box F
Temperature (°C)
900
600
300
0
No data available from 4th temperature sensor
No data available from bottom temperature sensor
600
1200
1800
Time (sec)
Legend for boxes A-F
Top temperature (3cm below ceiling)
5th temperature (38 cm above floor)
4th temperature (29 cm above floor)
3rd temperature (20 cm above floor)
2nd temperature (11 cm above floor)
Bottom temperature (2 cm above floor)
box A
boc B
box C
box D
box E
box F
Top temperatures in all boxes

Test no 17 (070110-2)

Test date 7 January 2010
Theoretical HRR = 60kW
Opening size = W10cm x H25cm
Ventilation controlled HRR = 18.8kW
GER = 3.2

Recorded observations:
35sec – ignition
1 min – automatic control of burner started
5 min 36 sec – flames visible outside
12 min 20 sec – gas sampling line in box C corrected – previous results could be incorrect
25 min 01 sec– gas turned off
27 min 30 sec – no flames visible outisde
28 min 35 sec- flames self extinguished

Laser in box C – wrong results after the test

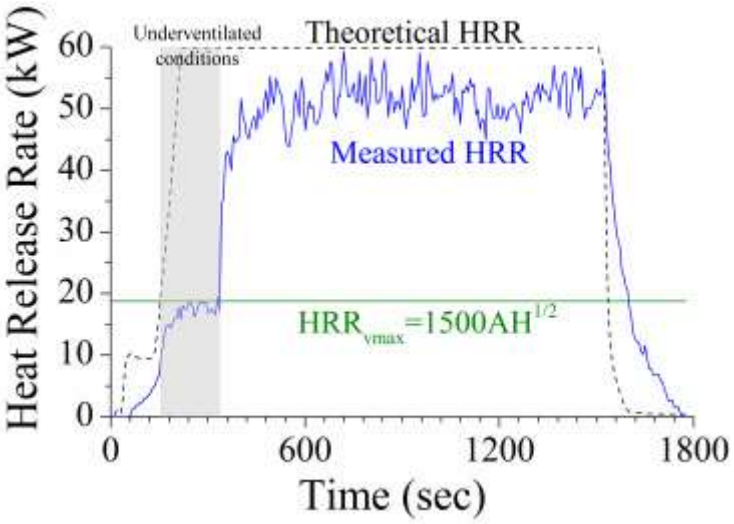

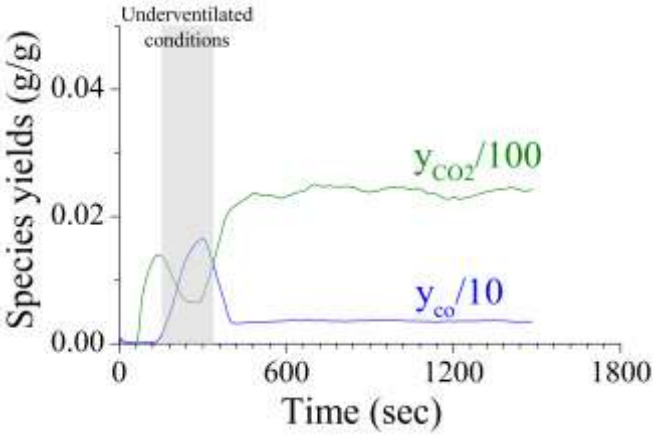

NO SMOKE DATA AVAILABLE for measurements in the duct

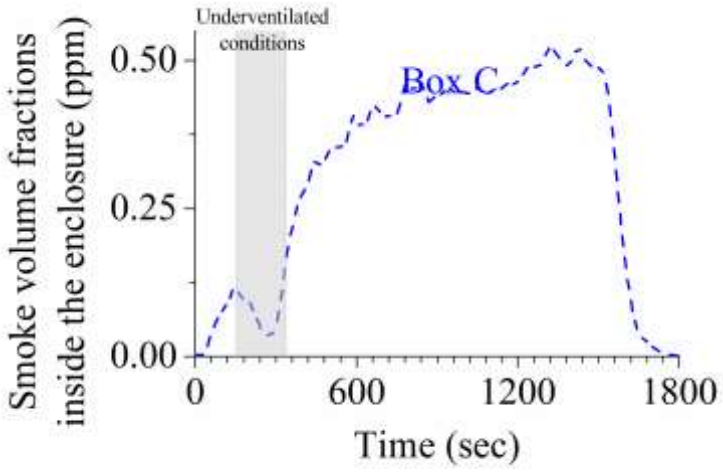
Underventilated conditions
Box C
Smoke volume fractions inside the enclosure (ppm)
0.50
0.25
0.00
0
600
1200
1800
Time (sec)

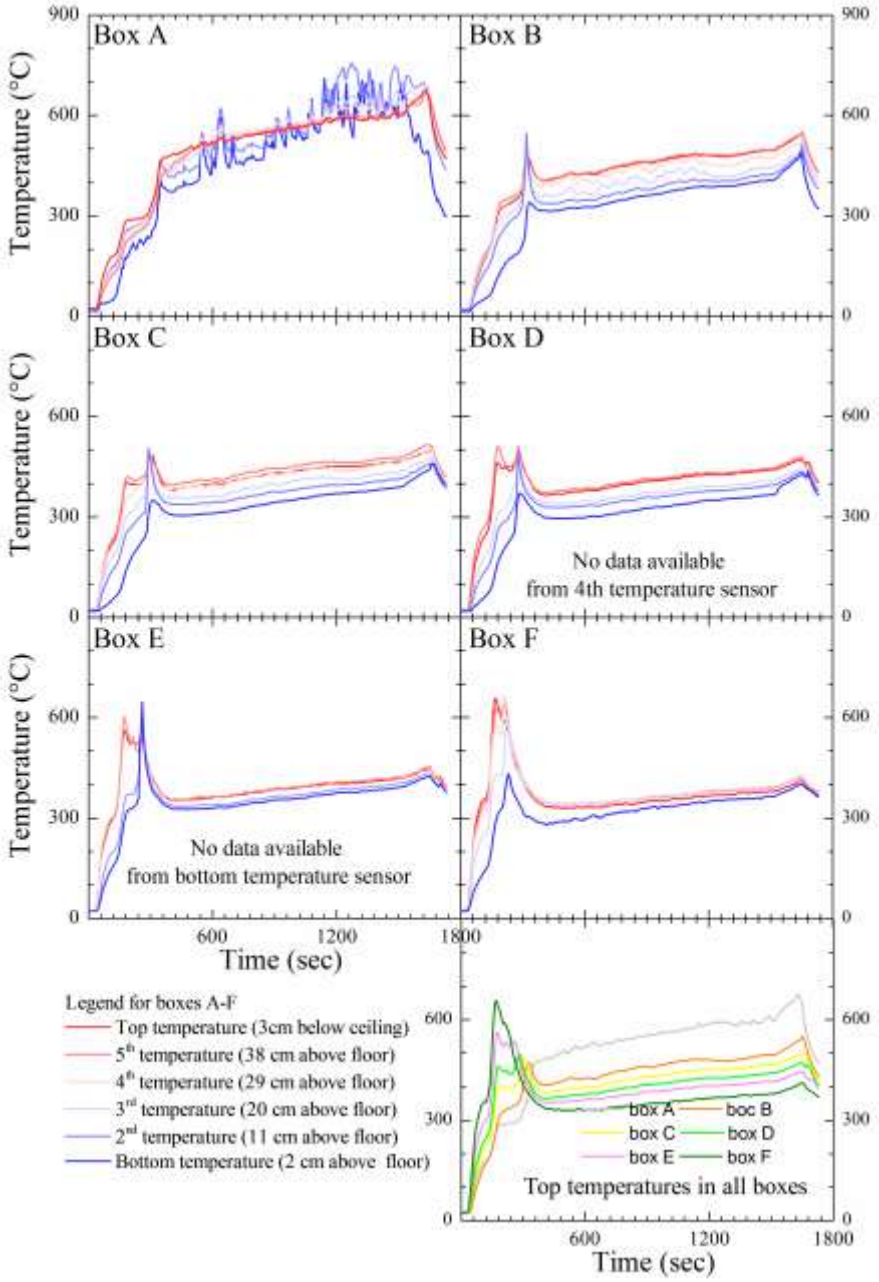
Box A
Box B
Box C
Box D
Box E
Box F
Temperature (°C)
900
600
300
0
No data available from 4th temperature sensor
No data available from bottom temperature sensor
600
1200
1800
Time (sec)
Legend for boxes A-F
Top temperature (3cm below ceiling)
5th temperature (38 cm above floor)
4th temperature (29 cm above floor)
3rd temperature (20 cm above floor)
2nd temperature (11 cm above floor)
Bottom temperature (2 cm above floor)
box A
boc B
box C
box D
box E
box F
Top temperatures in all boxes

Test no 18 (110110-1)

Test date 11 January 2010
Theoretical HRR = 15kW
Opening size = W7.5cm x H20cm
Ventilation controlled HRR = 10.06
GER = 1.49

Recorded observations:
32sec – ignition and fuel supply set at 15kW
3 min 10 sec – gas sampling probe in lower layer corrected
4 min 30 sec – flame on/off - flickering
Oscillations
8 min 38 sec – gas turned off

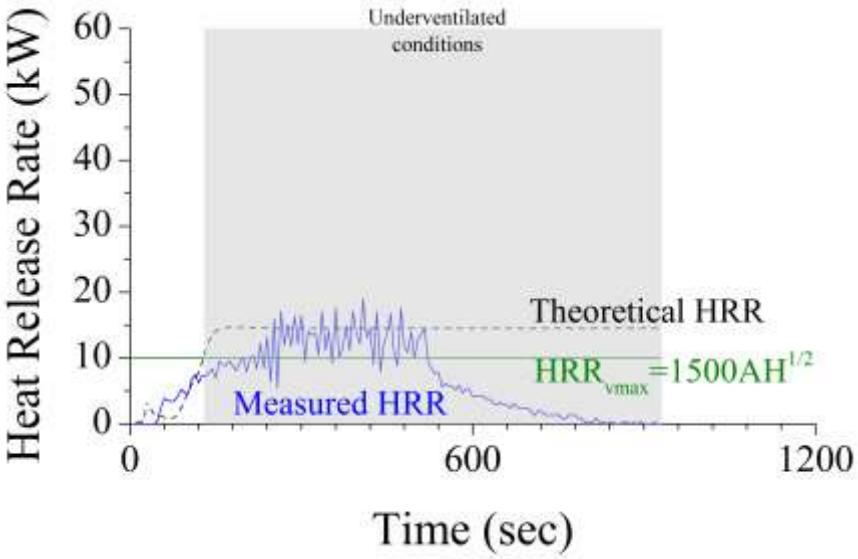

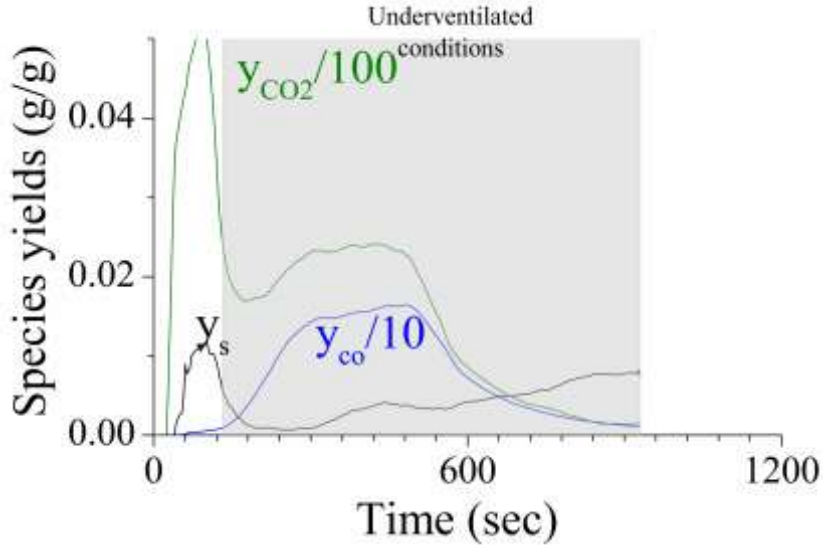

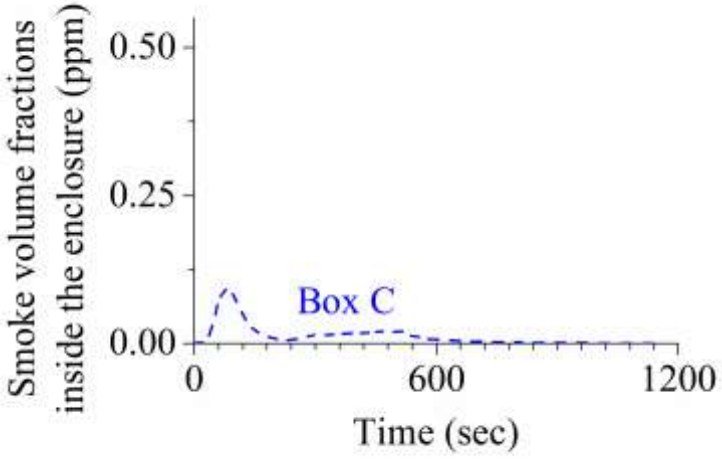
Smoke volume fractions inside the enclosure (ppm)
0.50
0.25
0.00
Box C
0
600
1200
Time (sec)

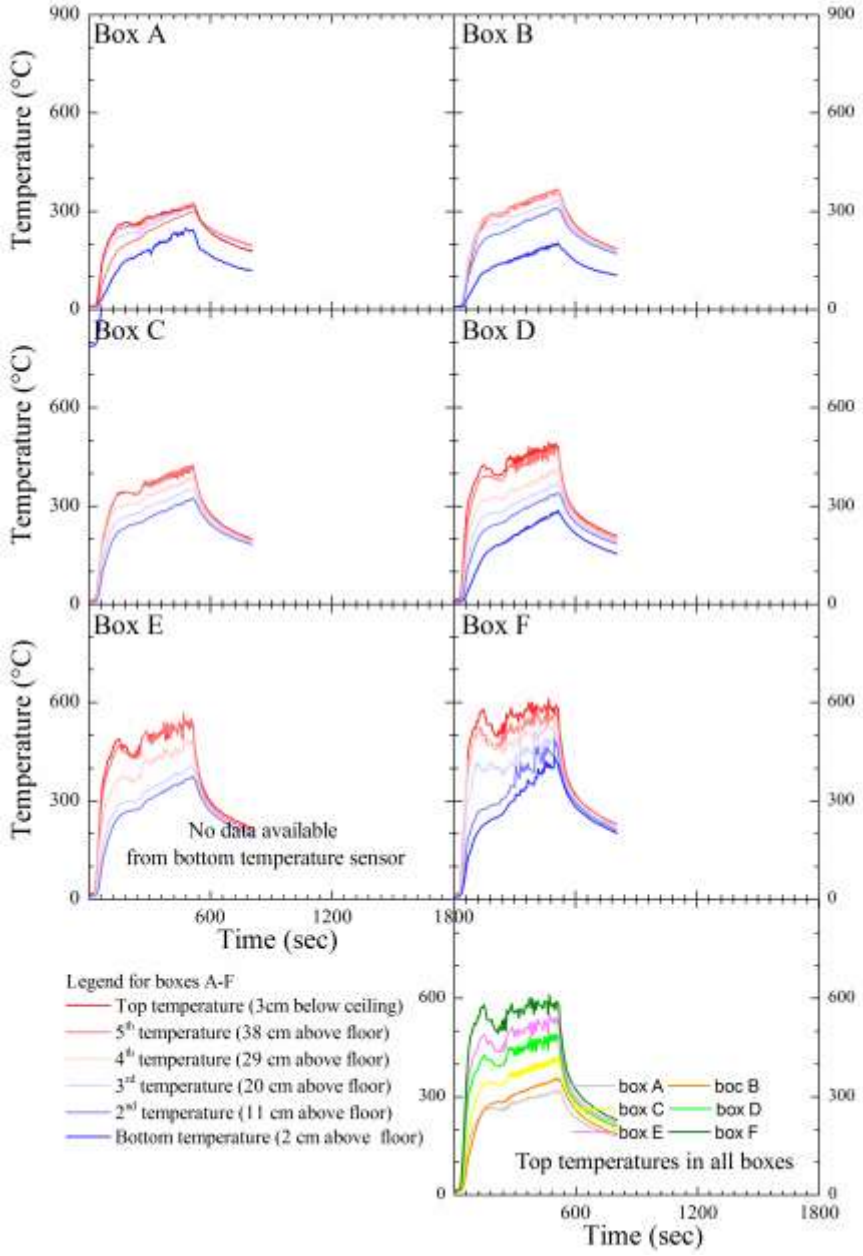
Box A
Box B
Box C
Box D
Box E
Box F
Temperature (°C)
900
600
300
0
No data available
from bottom temperature sensor
600
1200
1800
Time (sec)
Legend for boxes A-F
Top temperature (3cm below ceiling)
5th temperature (38 cm above floor)
4th temperature (29 cm above floor)
3rd temperature (20 cm above floor)
2nd temperature (11 cm above floor)
Bottom temperature (2 cm above floor)
box A
boc B
box C
box D
box E
box F
Top temperatures in all boxes

Test no 19 (120110-1)

Test date 12 January 2010
Theoretical HRR = 24.4 kW
Opening size = W7.5cm x H30cm
Ventilation controlled HRR = 18.49
GER = 1.32

Recorded observations:
37 sec – ignition
1 min – automatic control started
<3 min – water for radiometer in box F turned on
7 min – door in the lab open and louvers open
15 min 30 sec – office divider in place to shield from drafts
24 min 30 sec – really full of smoke inside – free layer lower than usually
Ok 25 min – observed some leak of smoke around radiometer in box F
27min 57 sec – >62000 THC indicating that flame started to move
30 min – gas supply turned off
<32 min 40 sec – flame self extinguished

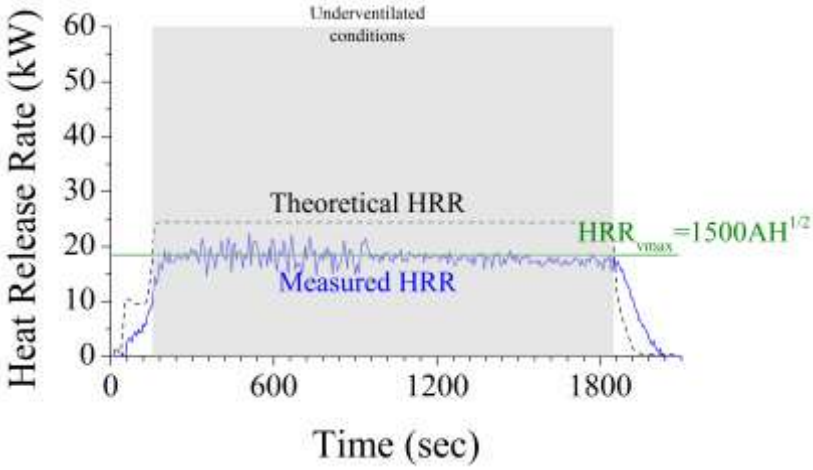

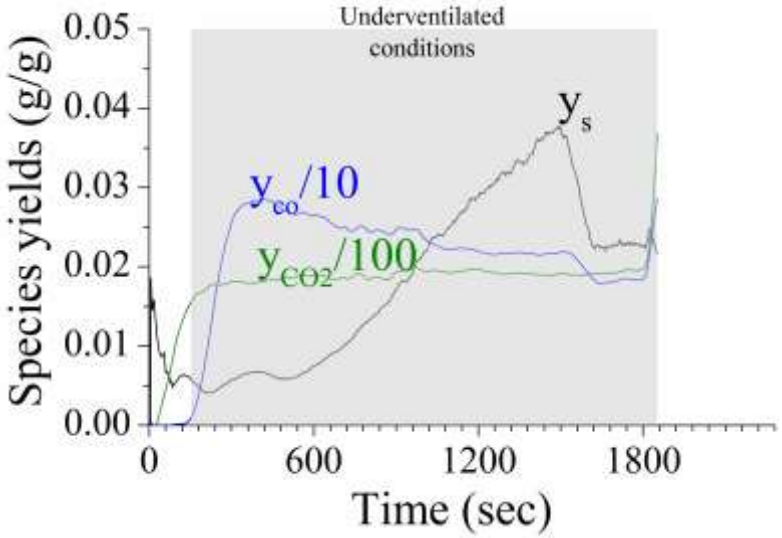

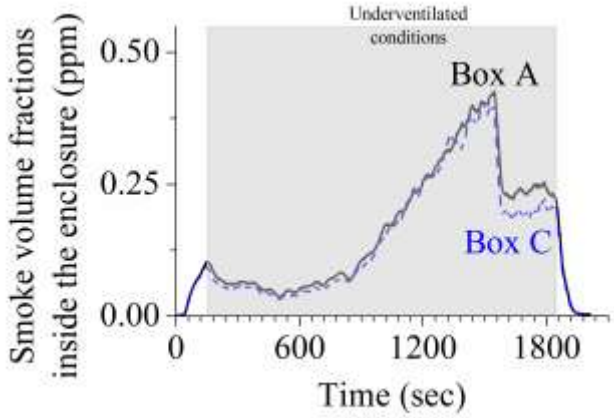
Underventilated
conditions
Box A
Box C
Smoke volume fractions
inside the enclosure (ppm)
0.50
0.25
0.00
0
600
1200
1800
Time (sec)

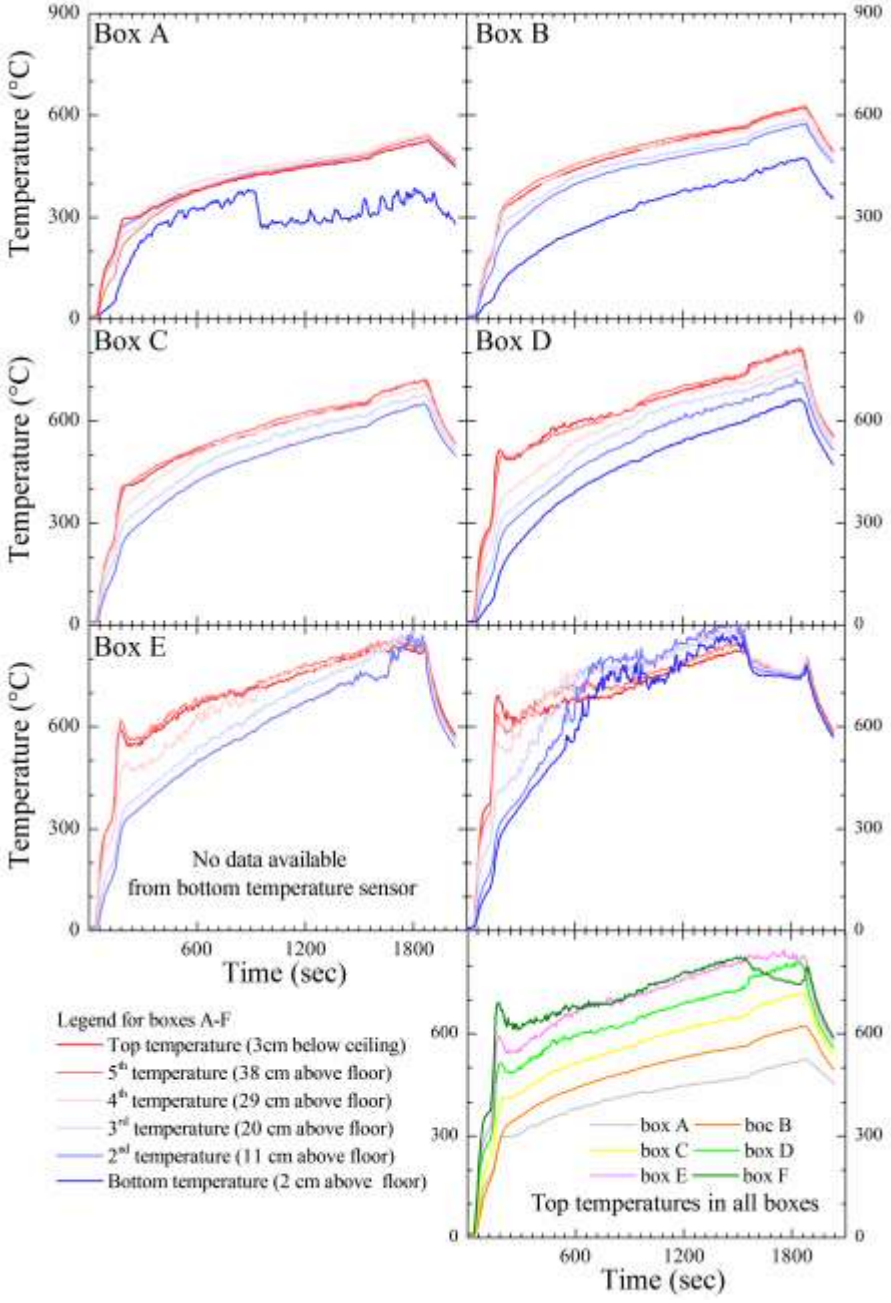
Box A
Box B
Box C
Box D
Box E
Temperature (°C)
900
600
300
0
No data available
from bottom temperature sensor
Time (sec)
Legend for boxes A-F
Top temperature (3cm below ceiling)
5th temperature (38 cm above floor)
4th temperature (29 cm above floor)
3rd temperature (20 cm above floor)
2nd temperature (11 cm above floor)
Bottom temperature (2 cm above floor)
box A
boc B
box C
box D
box E
box F
Top temperatures in all boxes

Test no 20 (120110-2)

Test date 12 January 2010
Theoretical HRR = 30kW
Opening size = W7.5cm x H30cm
Ventilation controlled HRR = 18.49
GER = 1.62

Recorded observations:
39 sec – ignition
40 sec – small fans for smoke meters turned on
1 min – automatic control of the burner started
26 min 35 sec – first flame tip outside, but flame anchored inside
31 min 20 sec– gas turned off
33 min 38 sec – flame self extinguished

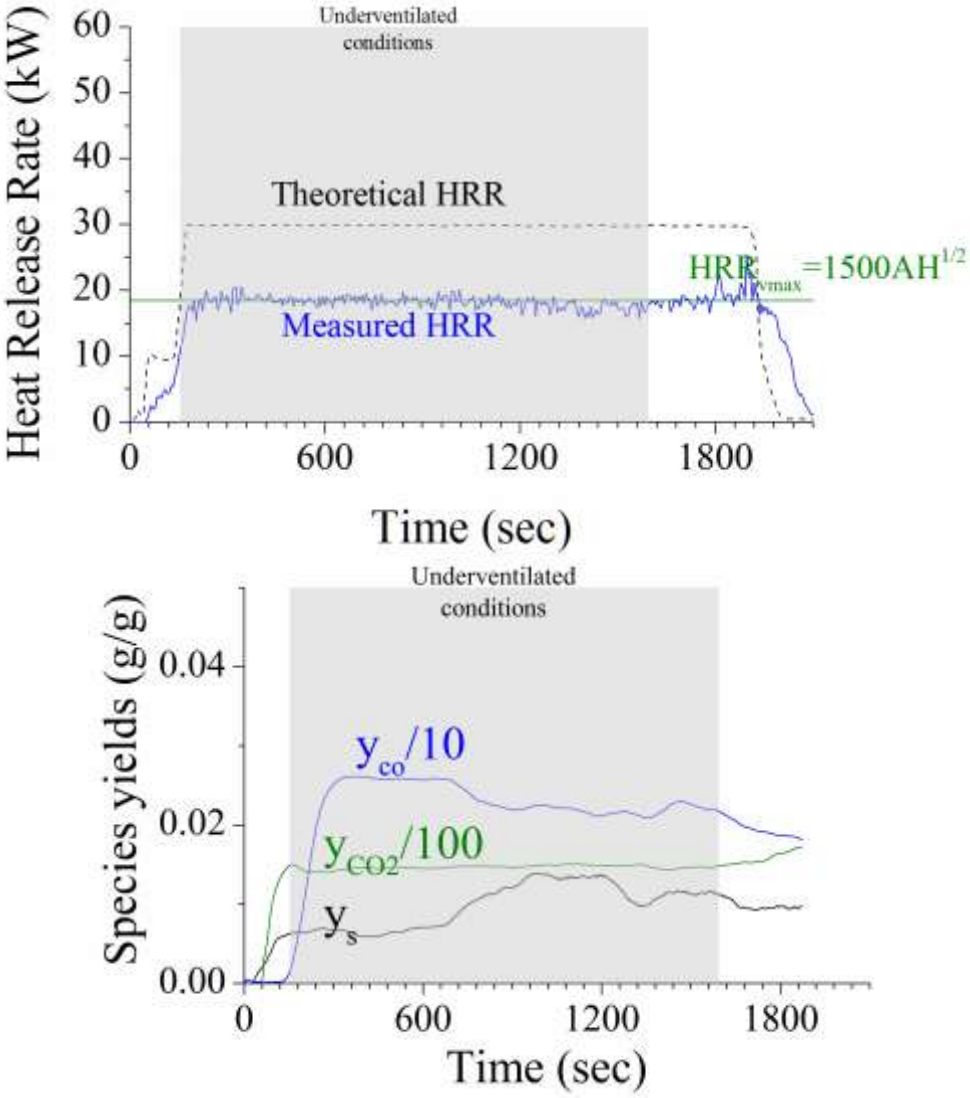

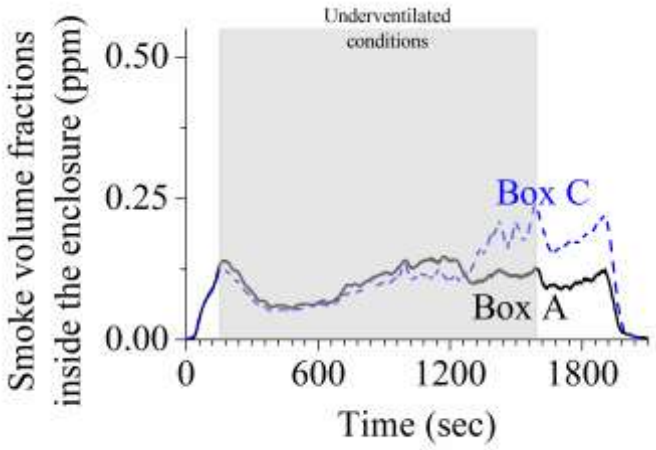
Underventilated
conditions
Smoke volume fractions
inside the enclosure (ppm)
0.50
0.25
0.00
Box C
Box A
0
600
1200
1800
Time (sec)

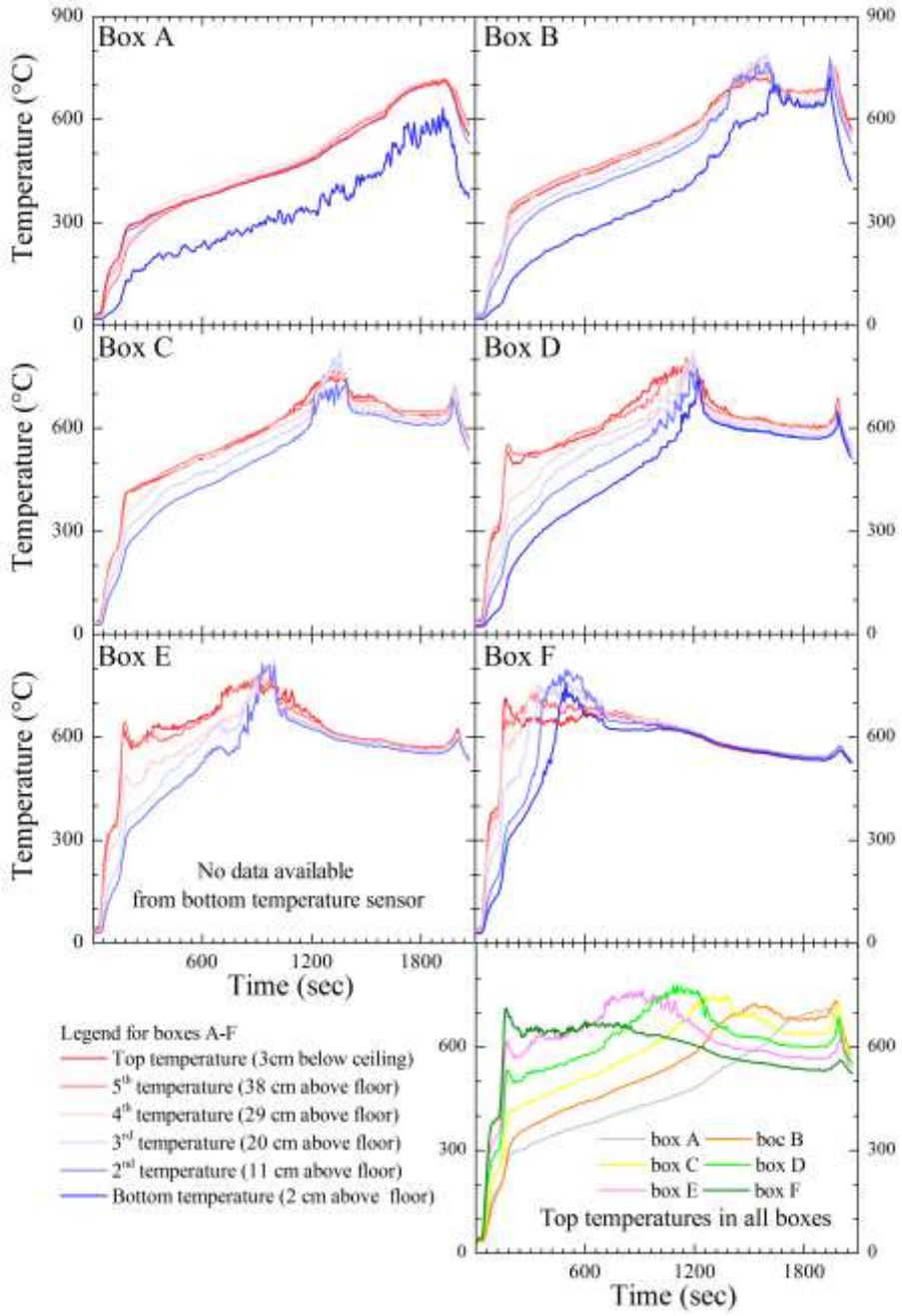
Box A
Box B
Box C
Box D
Box E
Box F
Temperature (°C)
900
600
300
0
No data available
from bottom temperature sensor
600
1200
1800
Time (sec)
Legend for boxes A-F
Top temperature (3cm below ceiling)
5th temperature (38 cm above floor)
4th temperature (29 cm above floor)
3rd temperature (20 cm above floor)
2nd temperature (11 cm above floor)
Bottom temperature (2 cm above floor)
box A
box B
box C
box D
box E
box F
Top temperatures in all boxes

Test no 21 (140110-1)

Test date 14 January 2010
Theoretical HRR = 50kW
Opening size = W7.5cm x H30cm
Ventilation controlled HRR = 18.49
GER = 2.70

Recorded observations:
53 sec – ignition
1 min – automatic control of the burner started
7 min 03 sec - flame tip visible outside
25 min – gas turned off
27 min 20 sec – no flames visible outside
< 27 min 40 sec – flame self extinguished

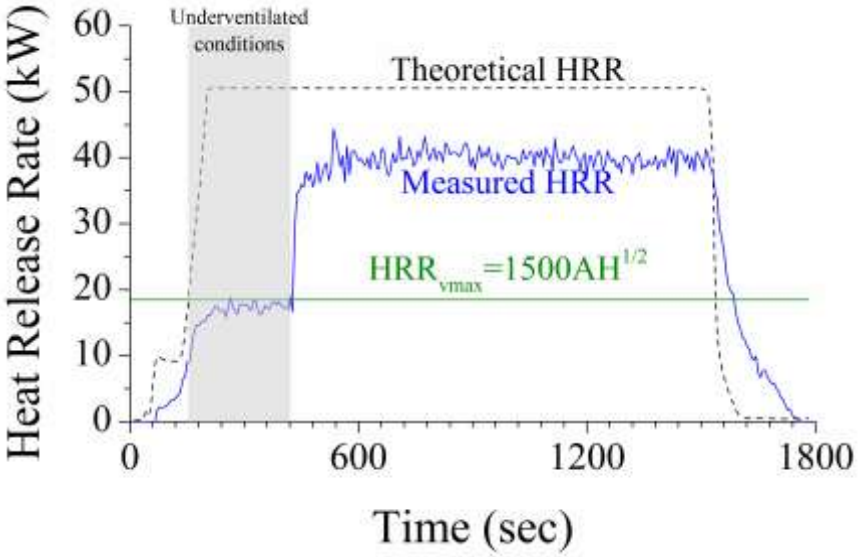

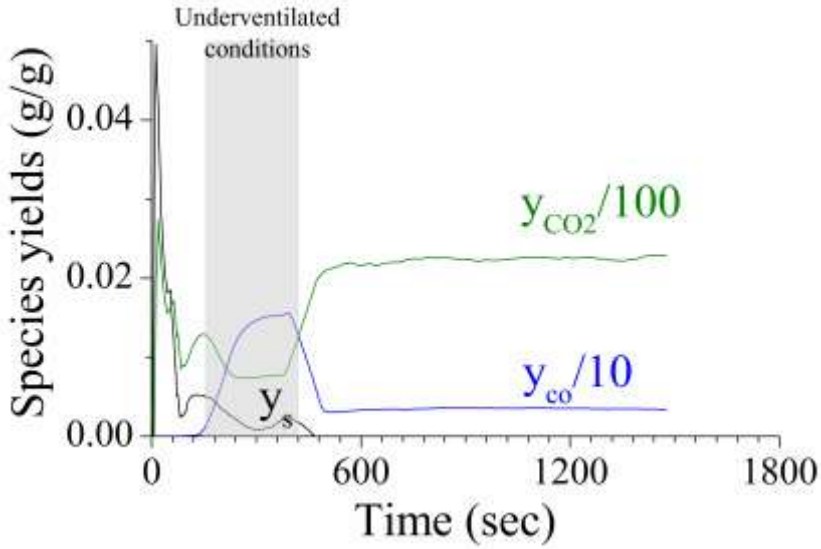

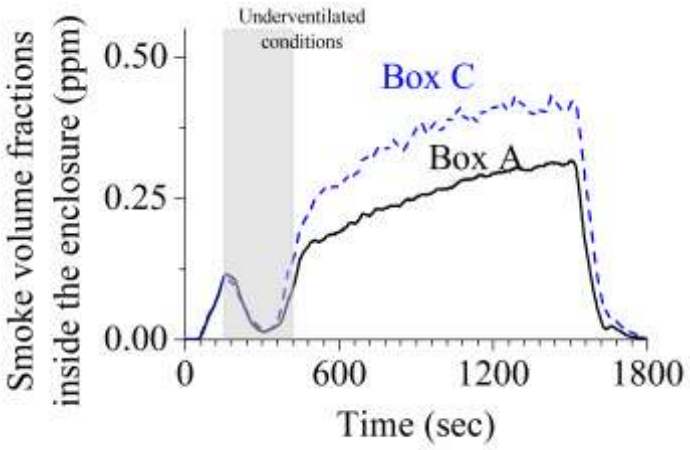
Underventilated conditions
Box C
Box A
Smoke volume fractions inside the enclosure (ppm)
0.50
0.25
0.00
0
600
1200
1800
Time (sec)

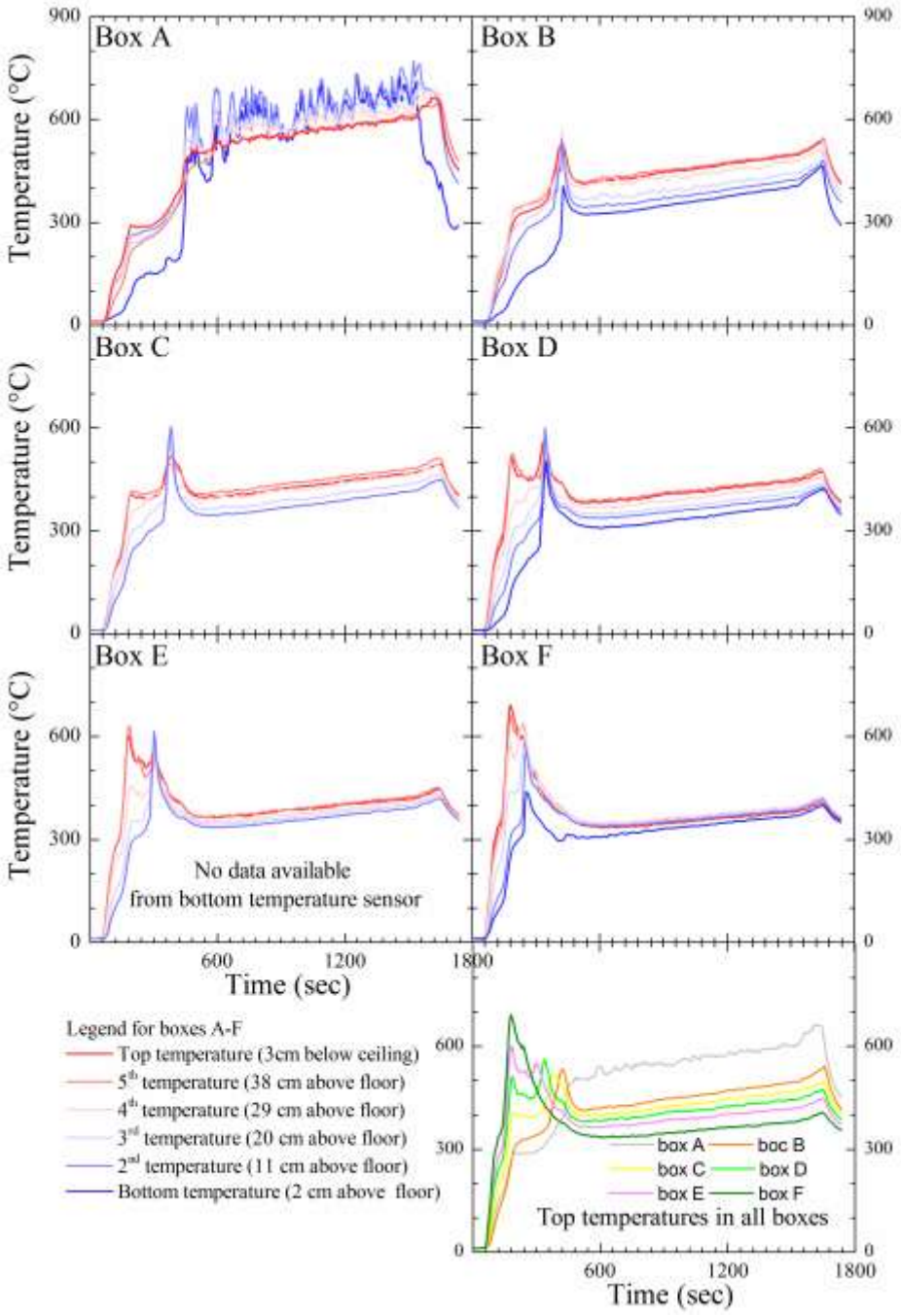
Box A
Box B
Box C
Box D
Box E
Box F
Temperature (°C)
900
600
300
0
No data available
from bottom temperature sensor
600
1200
1800
Time (sec)
Legend for boxes A-F
Top temperature (3cm below ceiling)
5th temperature (38 cm above floor)
4th temperature (29 cm above floor)
3rd temperature (20 cm above floor)
2nd temperature (11 cm above floor)
Bottom temperature (2 cm above floor)
box A
box B
box C
box D
box E
box F
Top temperatures in all boxes
Time (sec)

Test no 22 (140110-2)

TEST ON PRE-WARMED ENCLOSURE
Test date 14 January 2010
Theoretical HRR = 50kW
Opening size = W7.5cm x H30cm
Ventilation controlled HRR = 18.49
GER = 2.70

Recorded observations:
5 min 32 sec – ignition
6 min – automatic control of burner started
9 min 42 sec – flame visible outside
30 min – gas turned off
32 min 0 sec – no flames visible outside
32 min 39 sec – flame self extinguishment

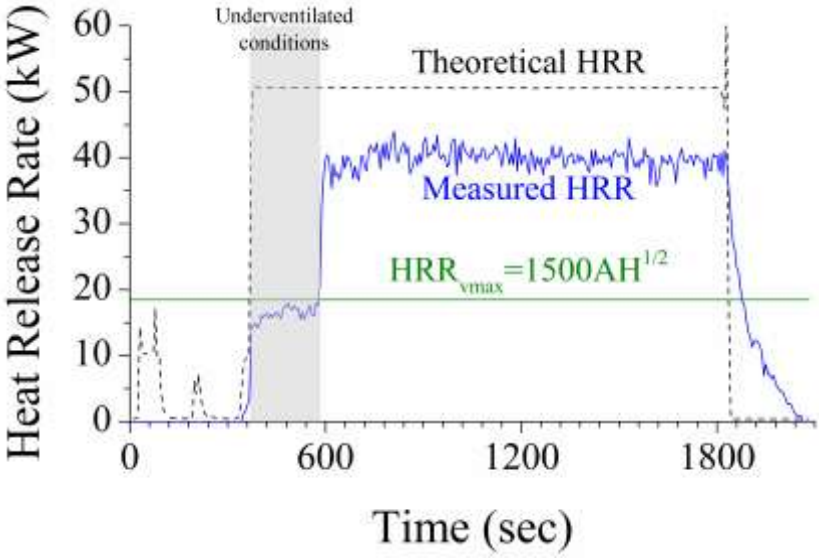

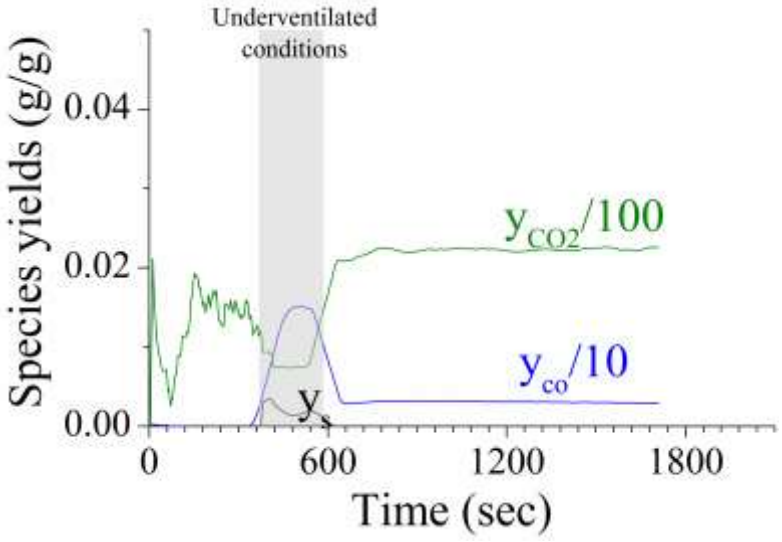

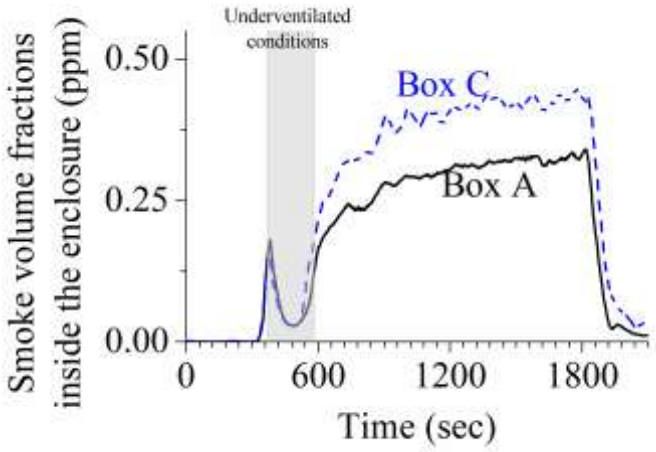
Underventilated conditions
Box C
Box A
Smoke volume fractions inside the enclosure (ppm)
0.50
0.25
0.00
0
600
1200
1800
Time (sec)

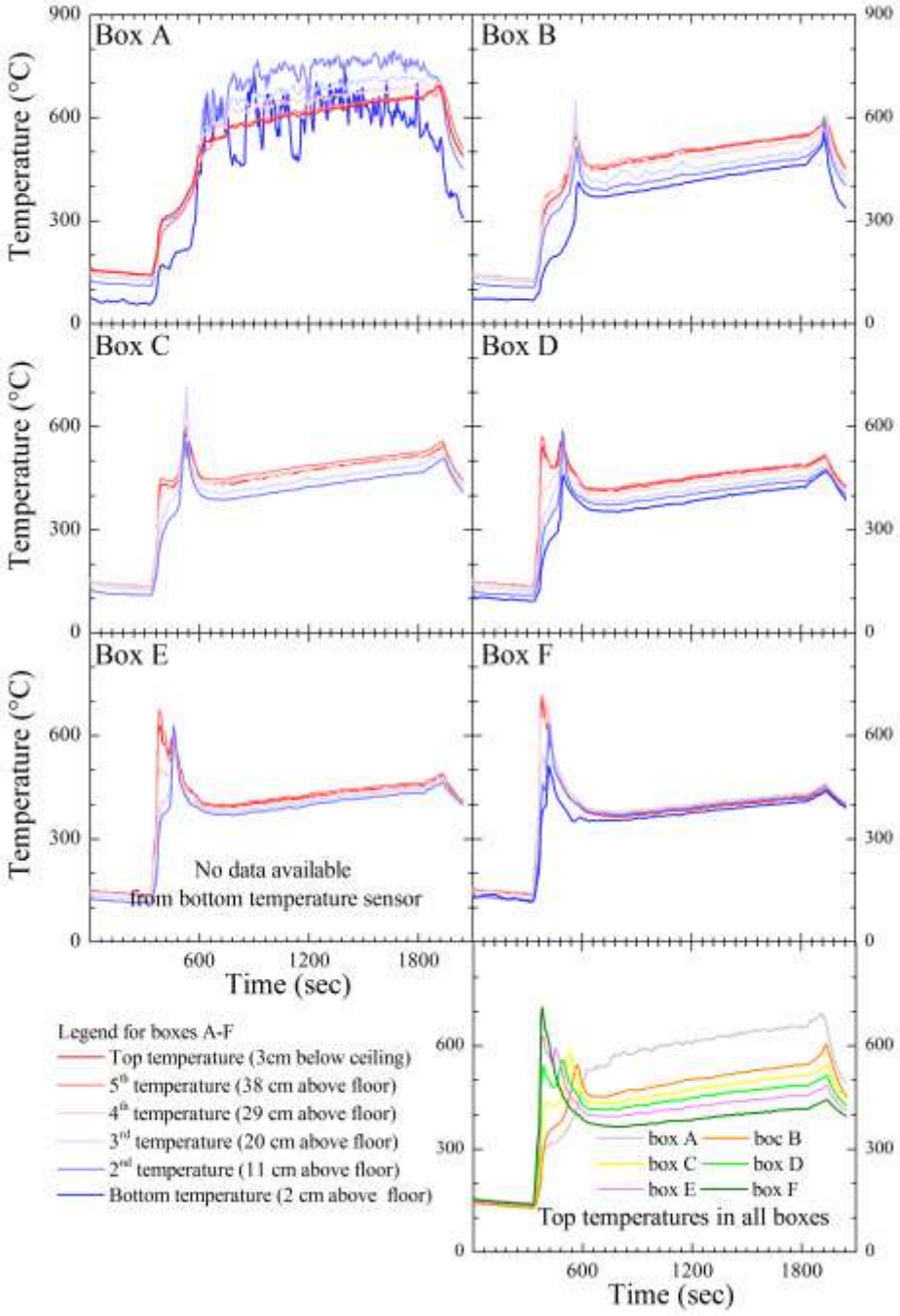
Box A
Box B
Box C
Box D
Box E
Box F
Temperature (°C)
900
600
300
0
No data available
from bottom temperature sensor
600
1200
1800
Time (sec)
Legend for boxes A-F
Top temperature (3cm below ceiling)
5th temperature (38 cm above floor)
4th temperature (29 cm above floor)
3rd temperature (20 cm above floor)
2nd temperature (11 cm above floor)
Bottom temperature (2 cm above floor)
box A
box B
box C
box D
box E
box F
Top temperatures in all boxes

Test no 23 (200110-1)

Test date 20 January 2010
Theoretical HRR = 40kW
Opening size = W7.5cm x H30cm
Ventilation controlled HRR = 18.49
GER = 2.16

Recorded observations:
None available

Not all data saved in the same time scale

Test no 24 (200110-2)

Test date 20 January 2010
Theoretical HRR = 60kW
Opening size = W7.5cm x H30cm
Ventilation controlled HRR = 18.49
GER = 3.25

Recorded observations:
35 sec – ignition
60 sec – automatic control started (deducted from data)
5 min 39 sec – flame visible outside
25 min – gas turned off
27 min 32 sec – no flames visible outside
28 min 35 sec – flame self extinguishment

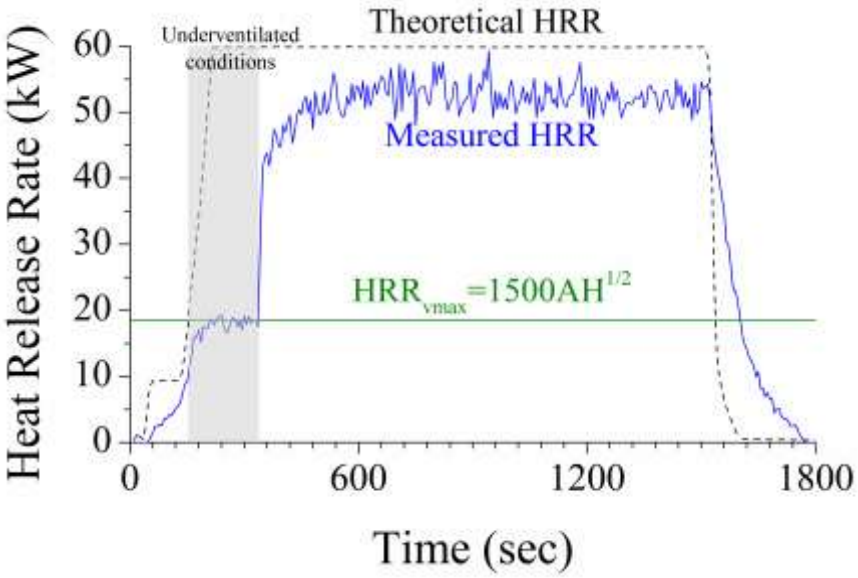

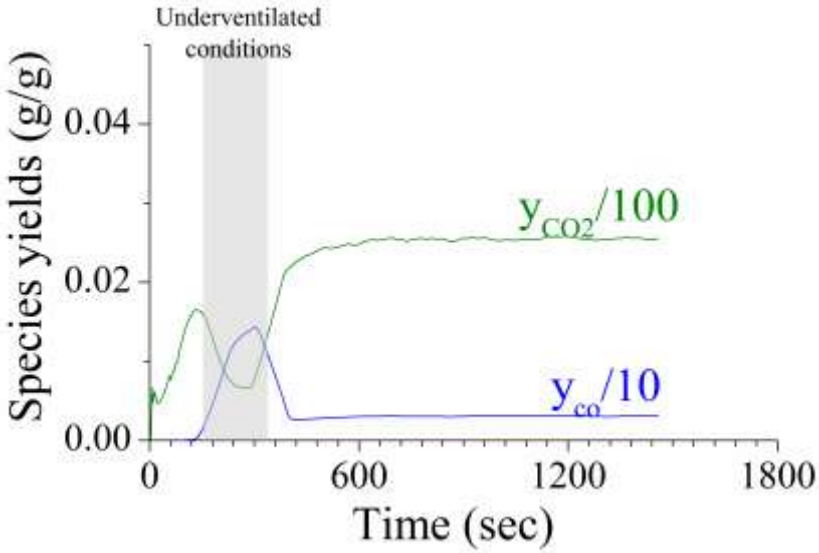

NO SMOKE DATA AVAILABLE for measurements in the duct

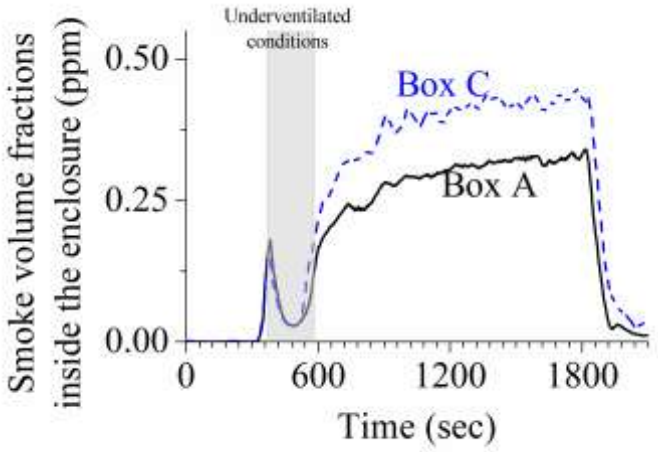
Underventilated conditions
Box C
Box A
Smoke volume fractions inside the enclosure (ppm)
0.50
0.25
0.00
0
600
1200
1800
Time (sec)

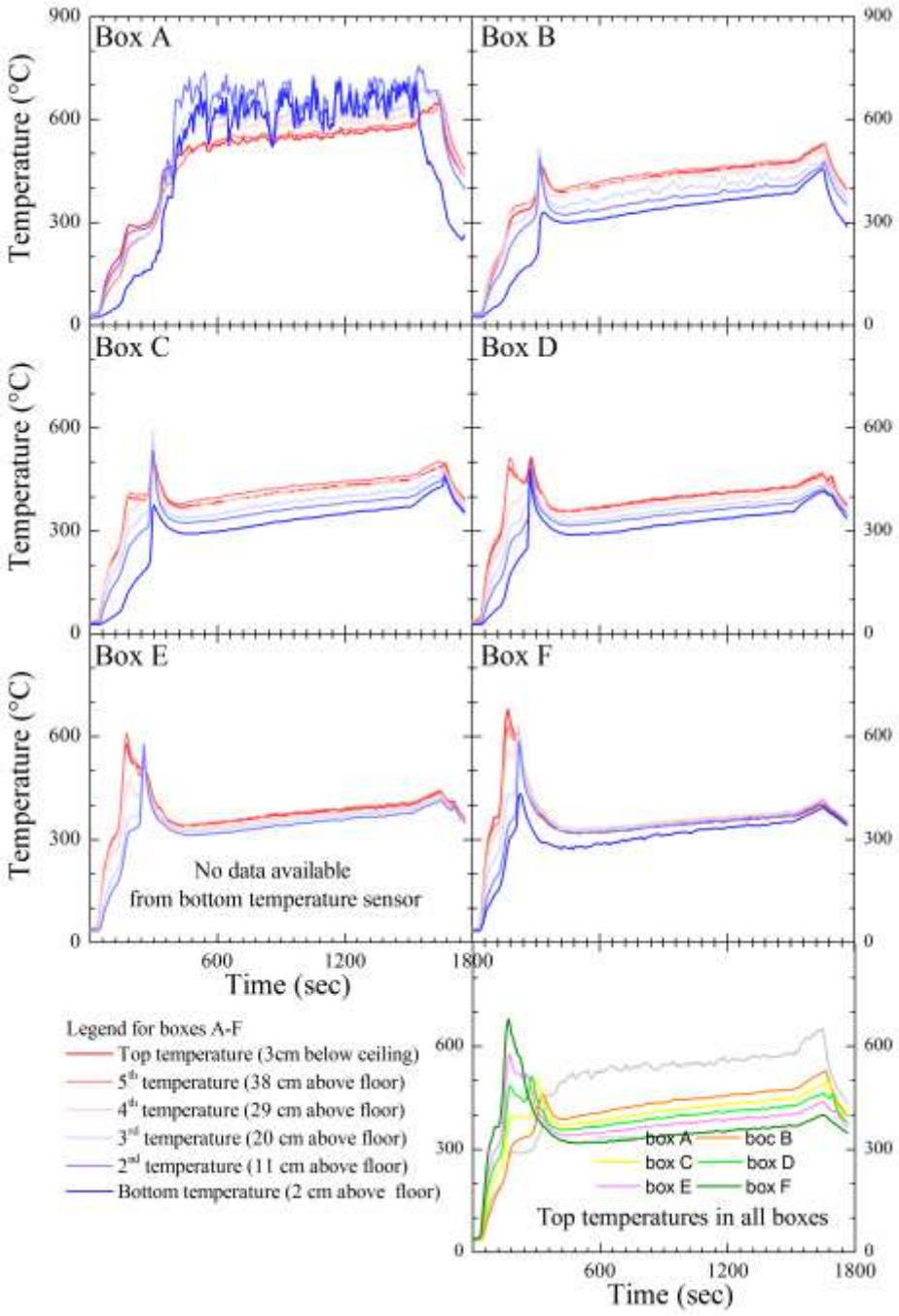
Box A
Box B
Box C
Box D
Box E
Box F
Temperature (°C)
900
600
300
0
No data available
from bottom temperature sensor
600
1200
1800
Time (sec)
Legend for boxes A-F
Top temperature (3cm below ceiling)
5th temperature (38 cm above floor)
4th temperature (29 cm above floor)
3rd temperature (20 cm above floor)
2nd temperature (11 cm above floor)
Bottom temperature (2 cm above floor)
box A
box B
box C
box D
box E
box F
Top temperatures in all boxes
Time (sec)

Test no 25 (110210-1)

Test date 11 February 2010
Theoretical HRR = 15kW
Opening size = W25cm x H10cm
Ventilation controlled HRR = 11.86
GER = 1.26

Recorded observations:
None available

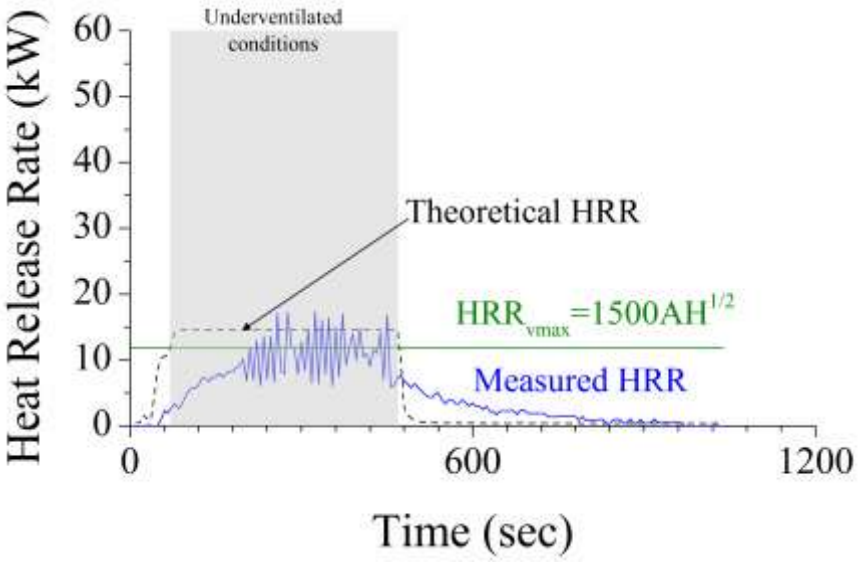

Erratic data on species yields

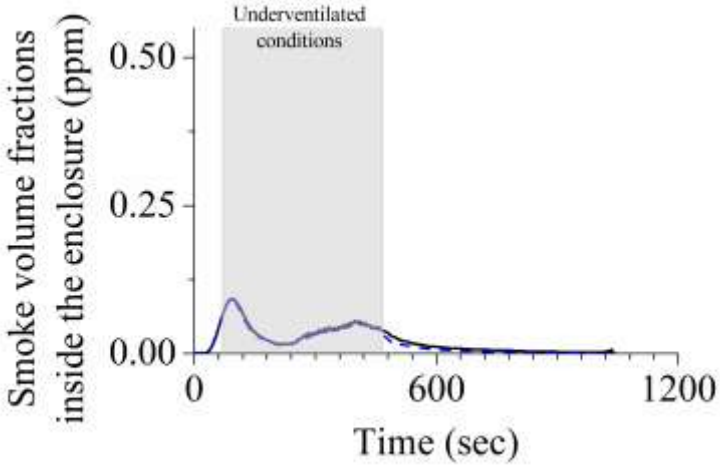

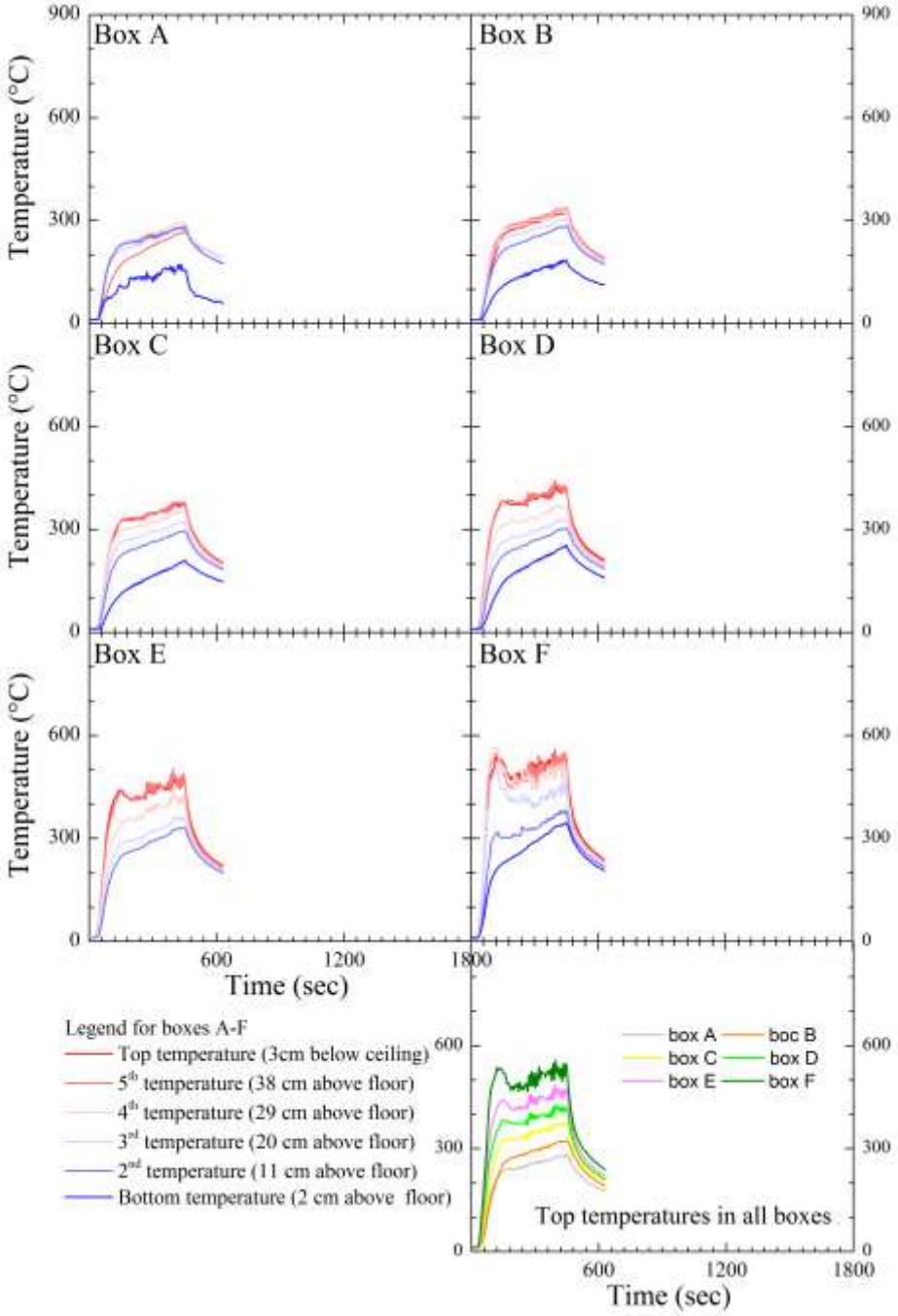
Box A
Box B
Box C
Box D
Box E
Box F
Temperature (°C)
Time (sec)
0
300
600
900
1200
1800
Legend for boxes A-F
Top temperature (3cm below ceiling)
5th temperature (38 cm above floor)
4th temperature (29 cm above floor)
3rd temperature (20 cm above floor)
2nd temperature (11 cm above floor)
Bottom temperature (2 cm above floor)
box A
boc B
box C
box D
box E
box F
Top temperatures in all boxes

Test no 26 (030310-1)

Test date 3 March 2010
Theoretical HRR = 10kW
Opening size = W25cm x H10cm
Ventilation controlled HRR = 11.86
GER = 0.84

Recorded observations:
39 sec – ignition
4 min 30 sec – small oscillations
Lots of bluish flames
25 min gas turned off
28 min 06 sec – flames self extinguished

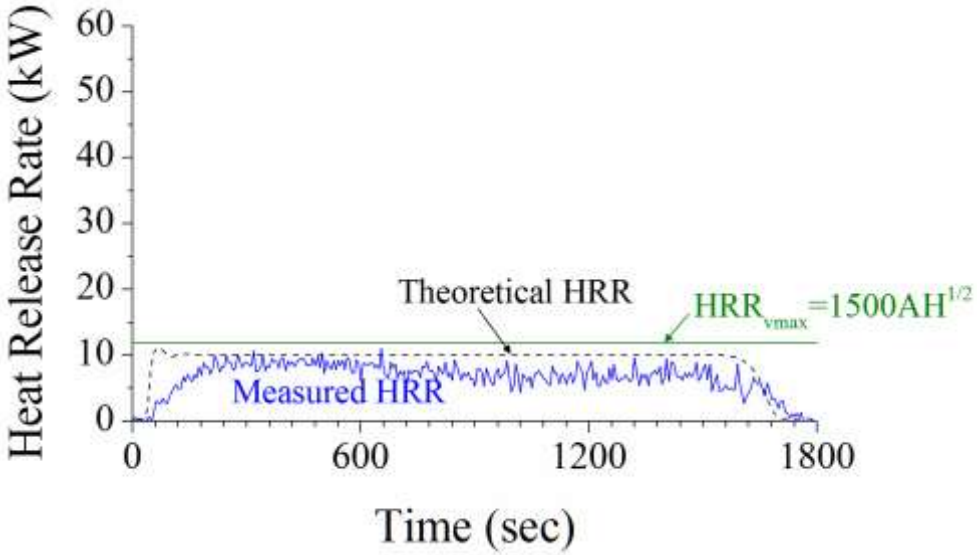

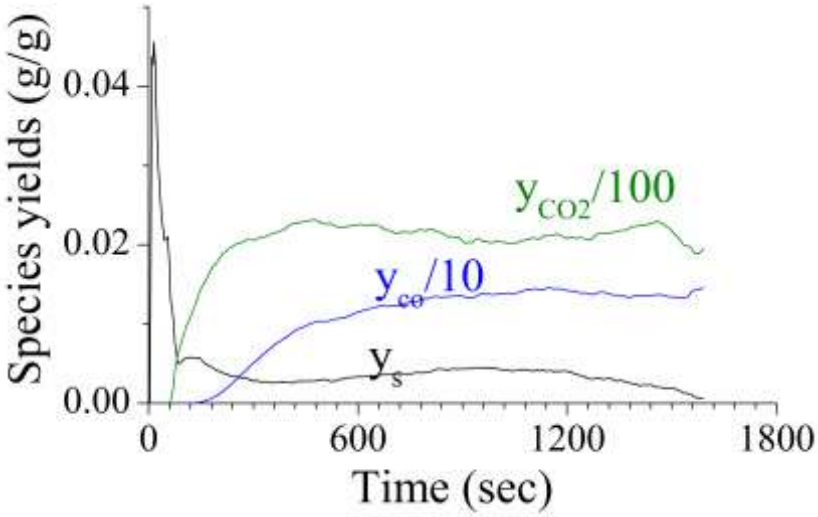

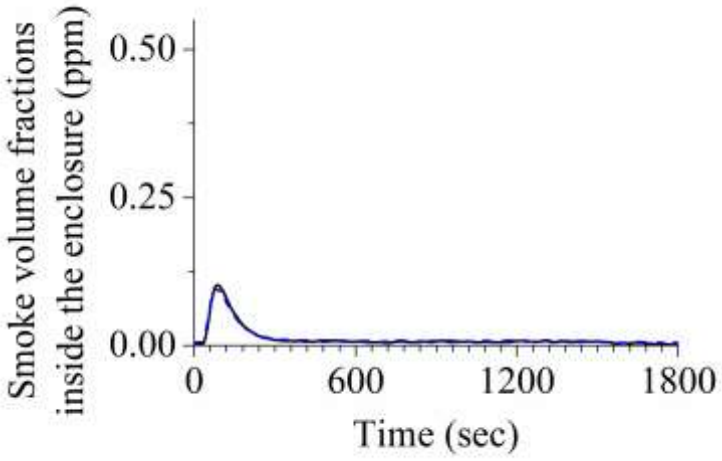
Smoke volume fractions inside the enclosure (ppm)
0.50
0.25
0.00
0
600
1200
1800
Time (sec)

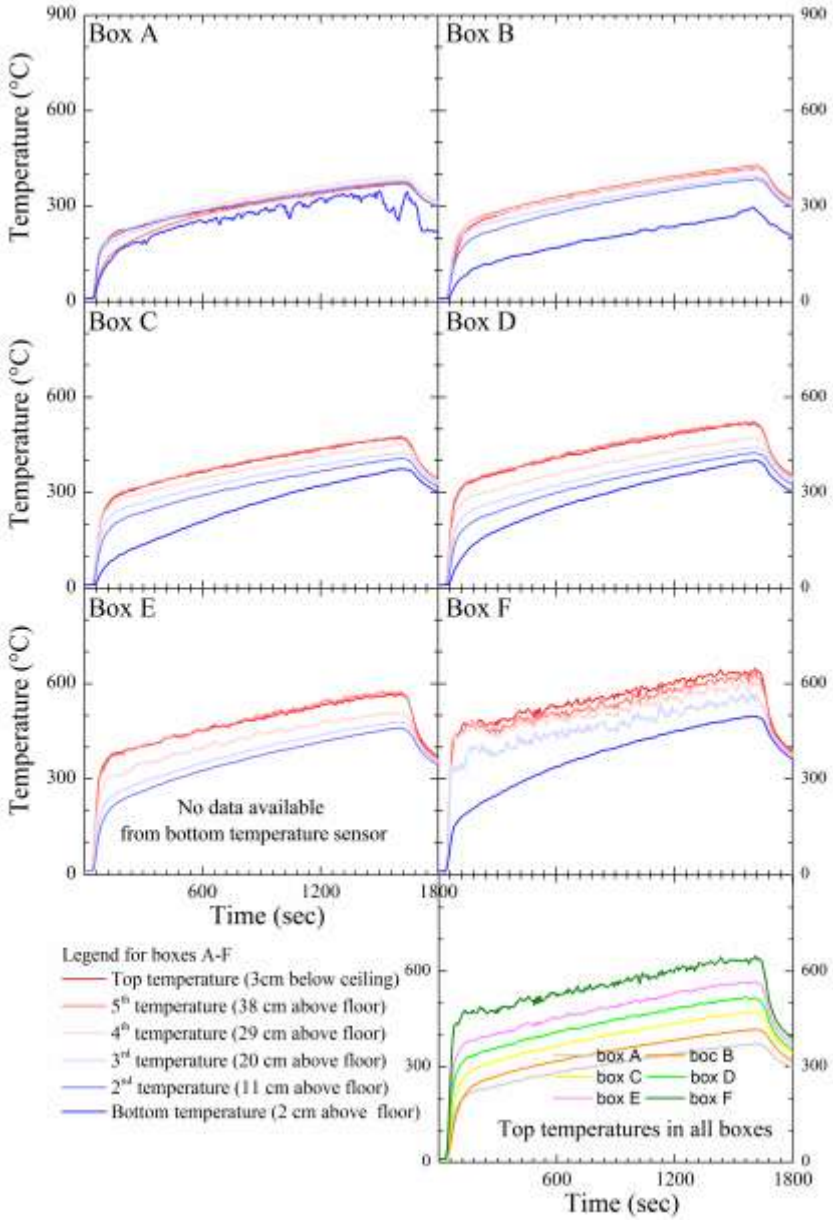
Box A
Box B
Box C
Box D
Box E
Box F
Temperature (°C)
900
600
300
0
No data available
from bottom temperature sensor
600
1200
1800
Time (sec)
Legend for boxes A-F
Top temperature (3cm below ceiling)
5th temperature (38 cm above floor)
4th temperature (29 cm above floor)
3rd temperature (20 cm above floor)
2nd temperature (11 cm above floor)
Bottom temperature (2 cm above floor)
box A
box B
box C
box D
box E
box F
Top temperatures in all boxes

Test no 27 (050310-1)

Test date 5 March 2010
Theoretical HRR = 30kW
Opening size = W25cm x H10cm
Ventilation controlled HRR = 11.86
GER = 2.53

Recorded observations:
29sec – ignition
1 min 00 sec – automatic control started
2 min 10 sec – flame oscilations to the left and right
3 min – flame become small but not bluish
4 min 07 sec – bluish in the lower part – whole lower layer in flames – photos taken
7 min 03 sec – flames around sampling lines in box C
7 min 46 sec – flames visible outside
15 min 10 sec – video started
25 min 20 sec – gas turned off
28 min 37 sec – No flame outside/inside (as if all extinguished at once)

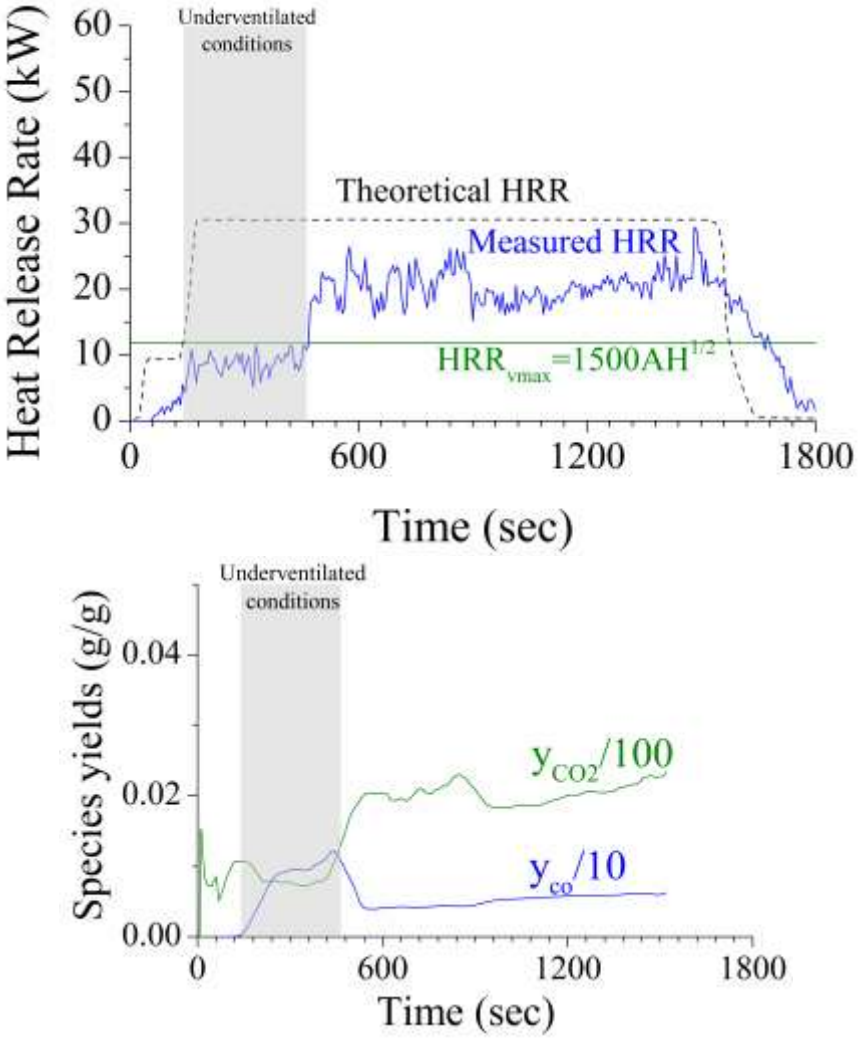

NO SMOKE DATA AVAILABLE for measurements in the duct

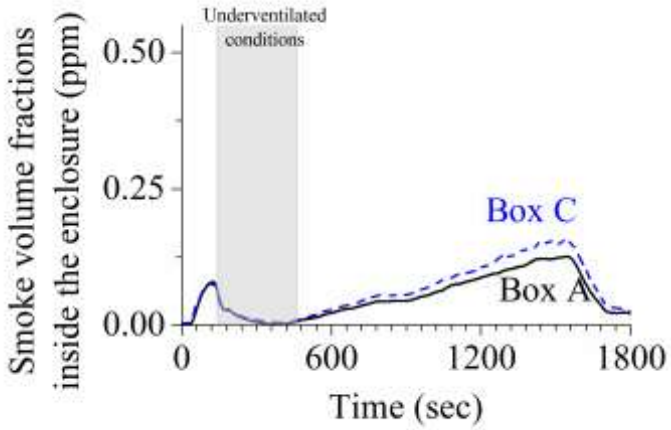
Underventilated conditions
Smoke volume fractions inside the enclosure (ppm)
0.50
0.25
0.00
Box C
Box A
0
600
1200
1800
Time (sec)

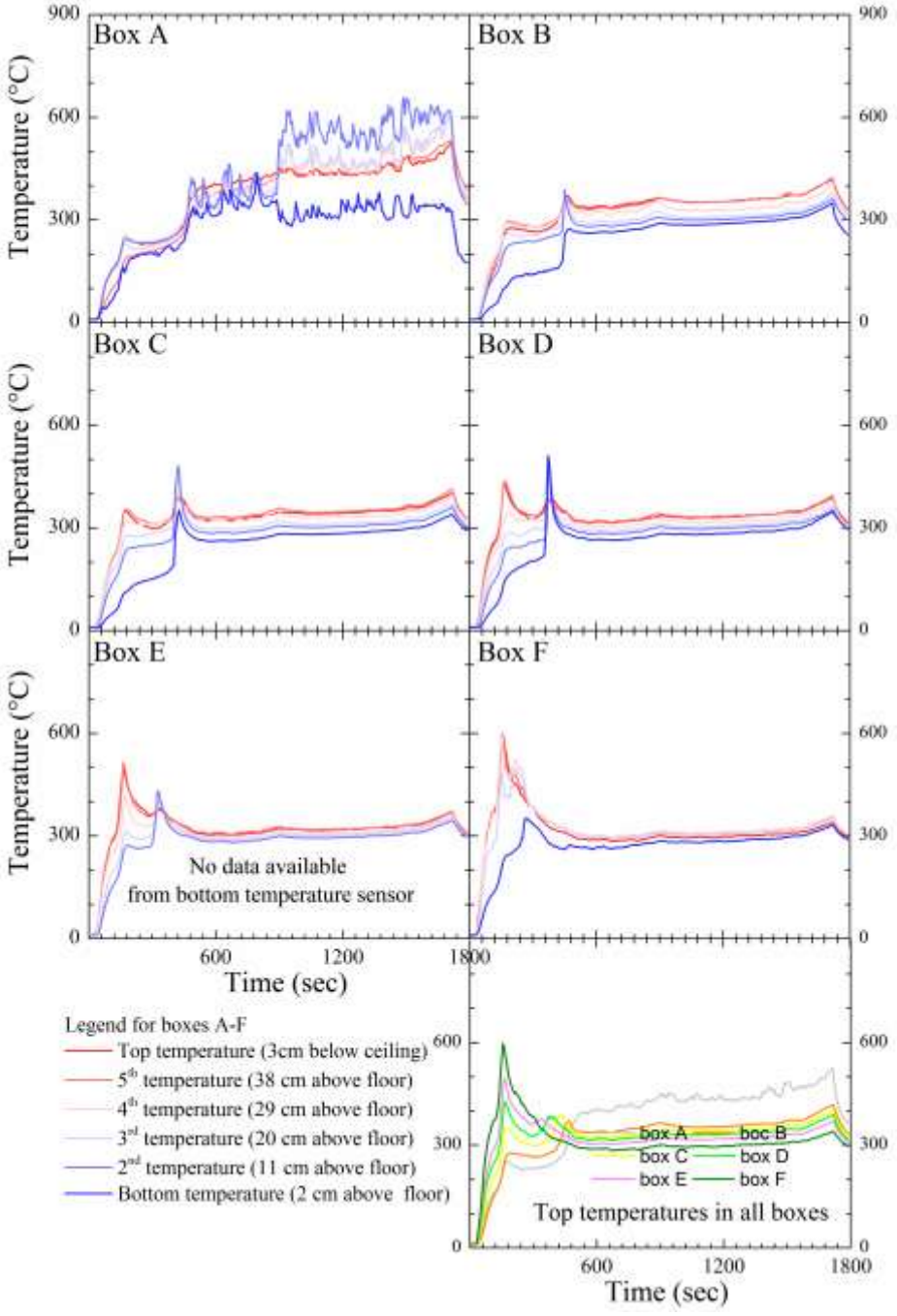
Box A
Box B
Box C
Box D
Box E
Box F
Temperature (°C)
900
600
300
0
No data available
from bottom temperature sensor
Time (sec)
Legend for boxes A-F
Top temperature (3cm below ceiling)
5th temperature (38 cm above floor)
4th temperature (29 cm above floor)
3rd temperature (20 cm above floor)
2nd temperature (11 cm above floor)
Bottom temperature (2 cm above floor)
box A
boc B
box C
box D
box E
box F
Top temperatures in all boxes

Test no 28 (080310-1)

Test date 8 March 2010
Theoretical HRR = 40kW
Opening size = W25cm x H10cm
Ventilation controlled HRR = 11.86
GER = 3.37

Recorded observations:
30 sec – ignition
1 min – automatic control started
5 min 32 sec – flame visible outside (movment of blusih flames was observed inside)
For long time bluish flames visible outside. There were not anchored at the opening but as if there was a niche – see photos.)
22 min – video taken
25 min – gas turned off
32 min 55 sec – no flame visible outside

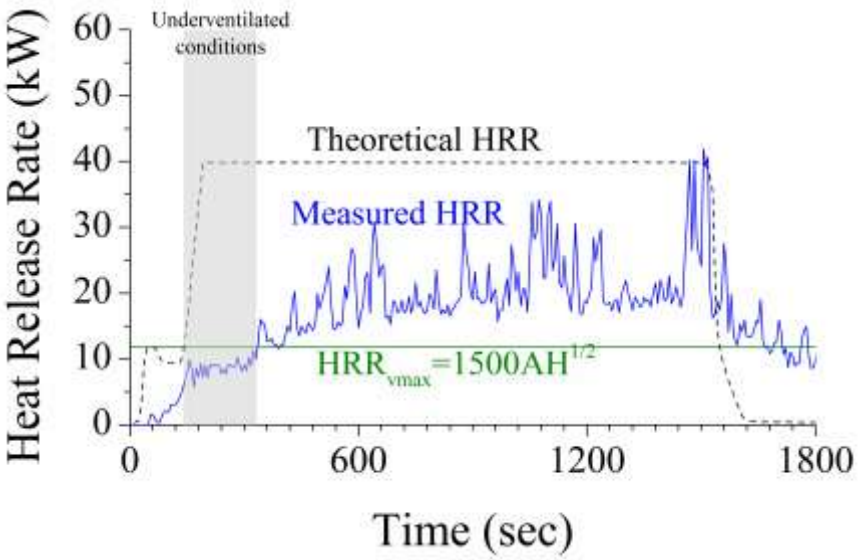

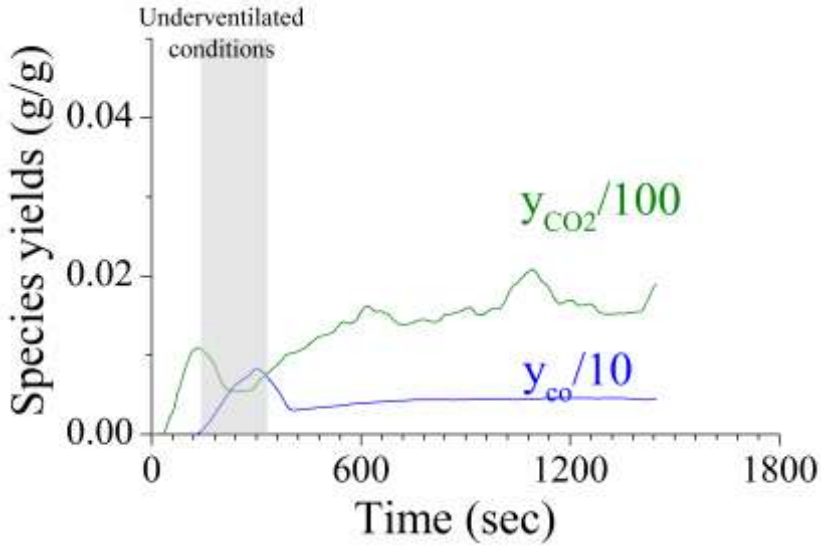

NO SMOKE DATA AVAILABLE for measurements in the duct

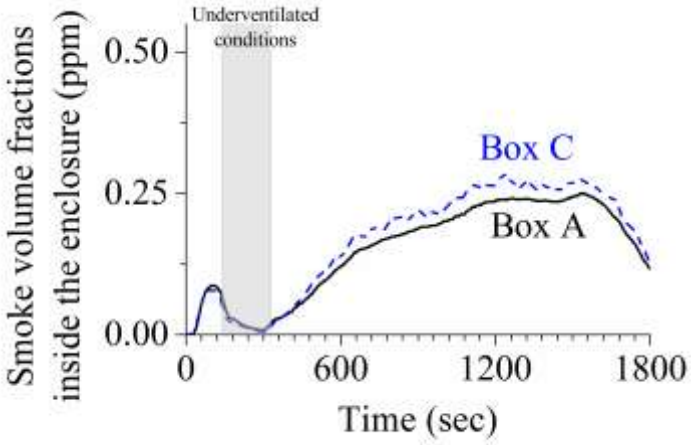
Underventilated conditions
Smoke volume fractions inside the enclosure (ppm)
0.50
0.25
0.00
Box C
Box A
0
600
1200
1800
Time (sec)

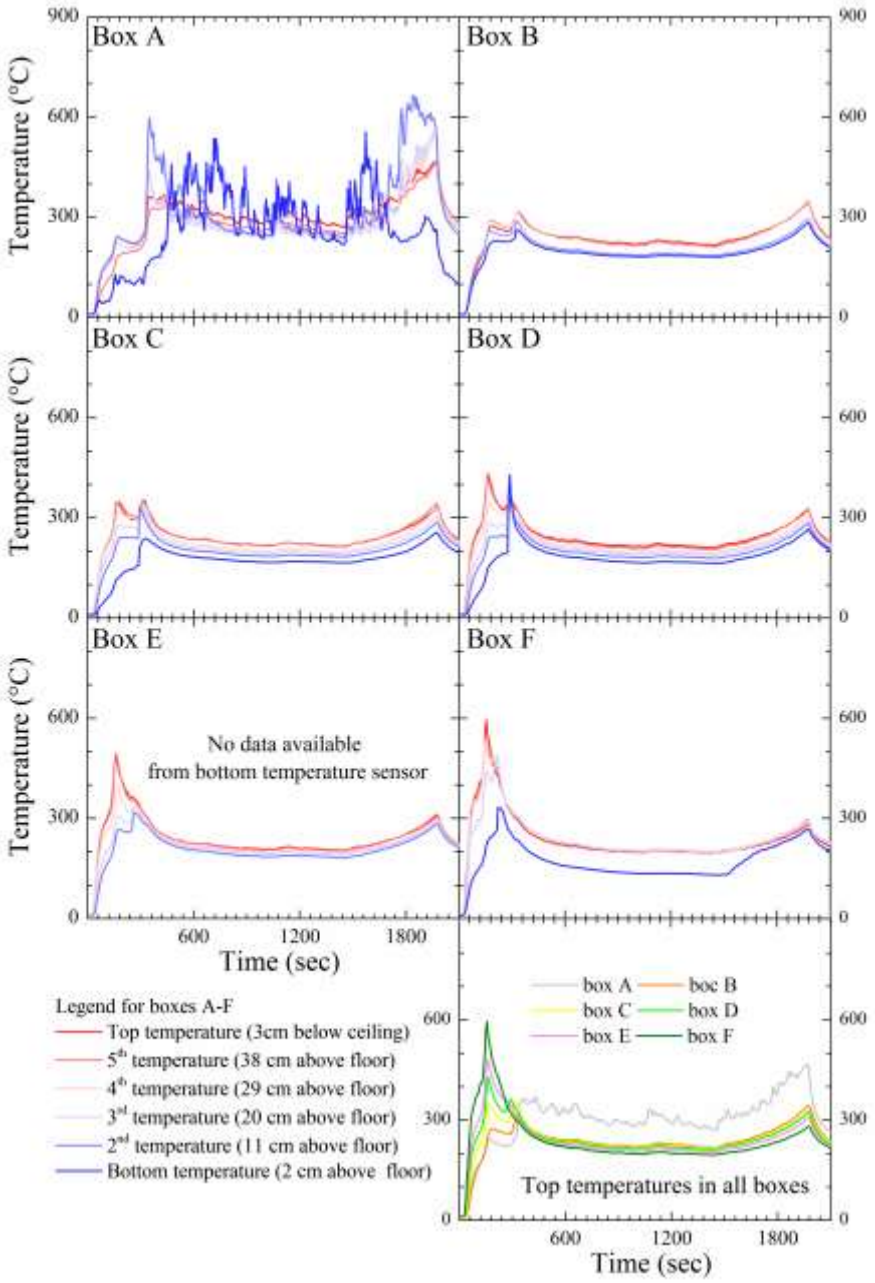
Box A
Box B
Box C
Box D
Box E
Box F
Temperature (°C)
900
600
300
0
No data available
from bottom temperature sensor
600
1200
1800
Time (sec)
Legend for boxes A-F
Top temperature (3cm below ceiling)
5th temperature (38 cm above floor)
4th temperature (29 cm above floor)
3rd temperature (20 cm above floor)
2nd temperature (11 cm above floor)
Bottom temperature (2 cm above floor)
box A
boc B
box C
box D
box E
box F
Top temperatures in all boxes
Time (sec)

Test no 29 (110310-1)

Test date 11 March 2010
Theoretical HRR = 50kW
Opening size = W25cm x H10cm
Ventilation controlled HRR = 11.86
GER = 4.22

Recorded observations:
50 sec – ignition
1 min 01 sec– automatic control started
2 min 50 sec –flames were getting
3 min 10 sec – oscillations
3 min 30 -40 sec – whole bottom layer in flames
4 min 43 sec – flame visible outside
22 min – video started
25 min – gas turned off
32 min 45 sec – no flame visible outside

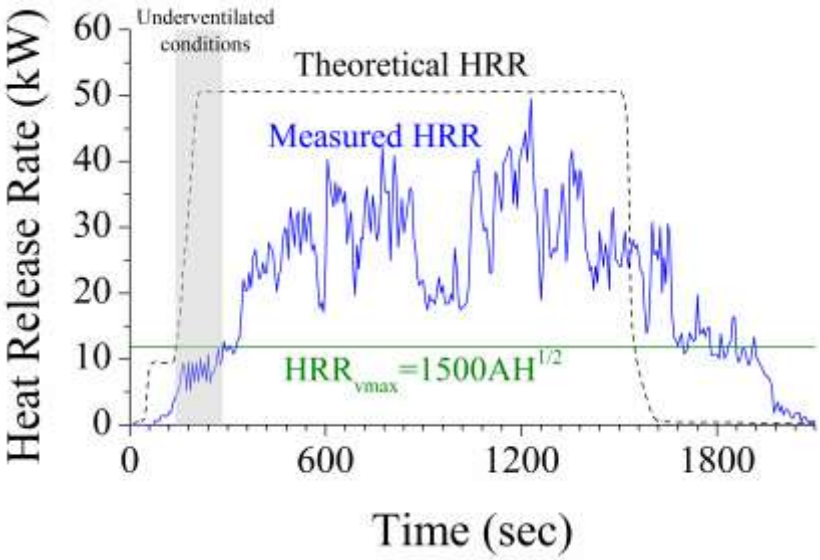

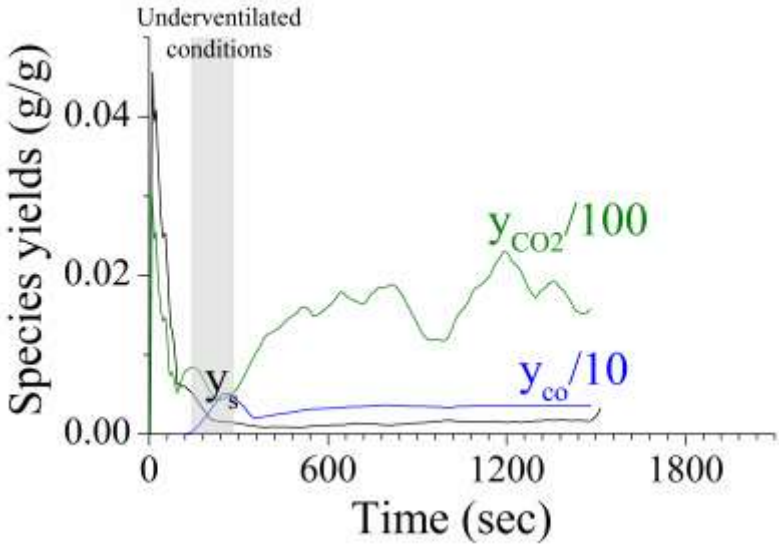

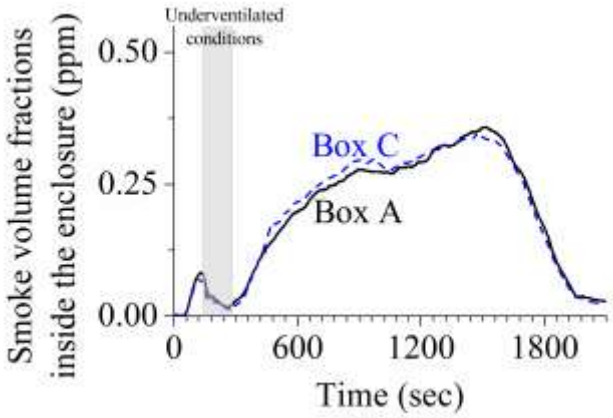
Underventilated conditions
Smoke volume fractions inside the enclosure (ppm)
0.50
0.25
0.00
Box C
Box A
0
600
1200
1800
Time (sec)

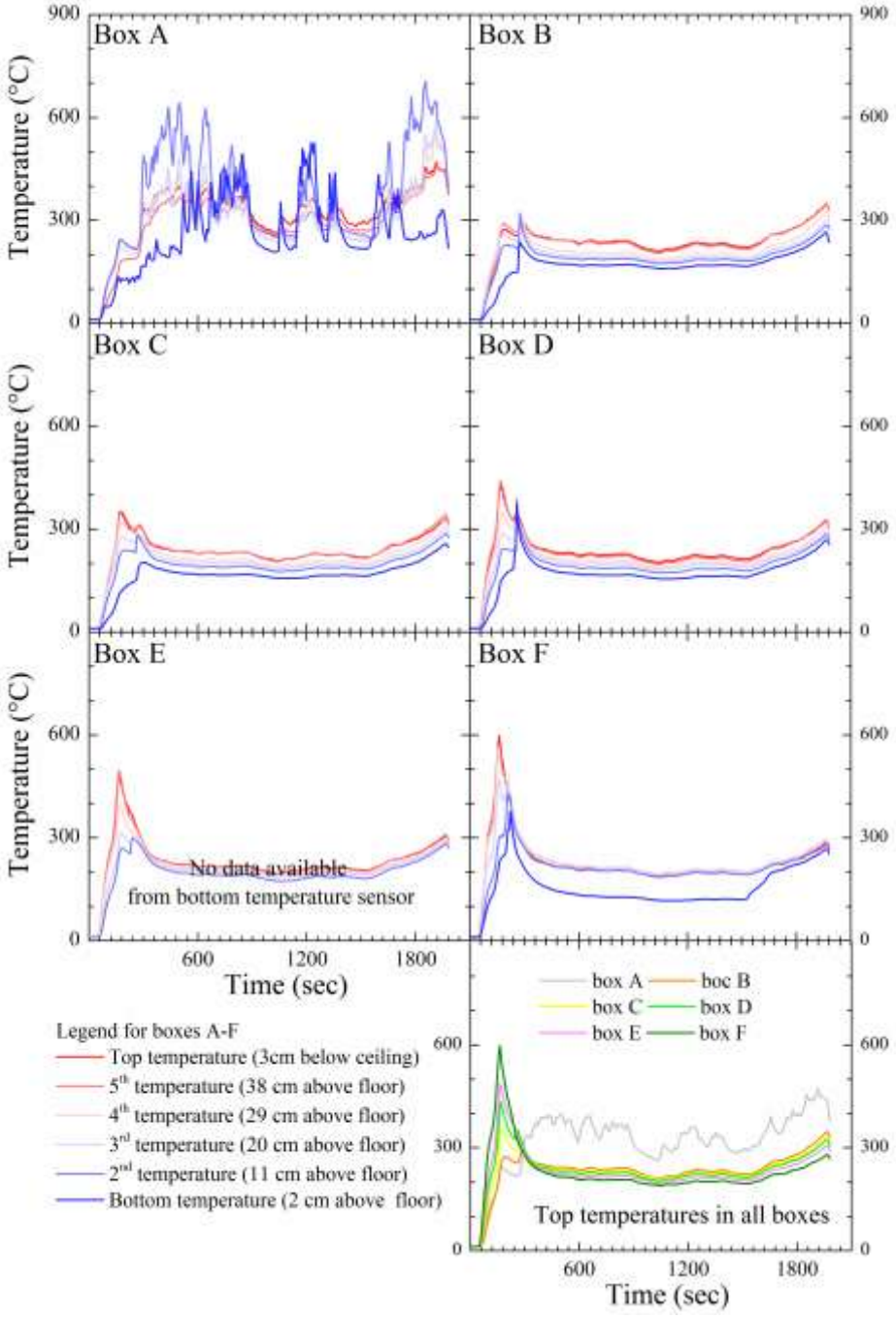
Box A
Box B
Box C
Box D
Box E
Box F
Temperature (°C)
900
600
300
0
No data available
from bottom temperature sensor
Time (sec)
Legend for boxes A-F
Top temperature (3cm below ceiling)
5th temperature (38 cm above floor)
4th temperature (29 cm above floor)
3rd temperature (20 cm above floor)
2nd temperature (11 cm above floor)
Bottom temperature (2 cm above floor)
box A
boc B
box C
box D
box E
box F
Top temperatures in all boxes

Test no 30 (120310-1)

Test date 12 March 2010
Theoretical HRR = 20kW
Opening size = W25cm x H10cm
Ventilation controlled HRR = 11.86
GER = 1.69

Recorded observations:
39 sec – ignition
1 min– automatic control started
2 min 50 sec - oscillations
4 min 20 sec – during oscillations “puffs” of smoke
7 min 48 sec – flames in the whole bottom layer
9 min 20 sec – flames pass sampling line in box C
11 min 30 sec – very small movement, only bluish flames
13 min 30 sec – is it air tight? Is not air coming through sampling holes at walls?
15 min 05 sec – gas stopped due to H&S
17 min 45 sec – flame self extinguished

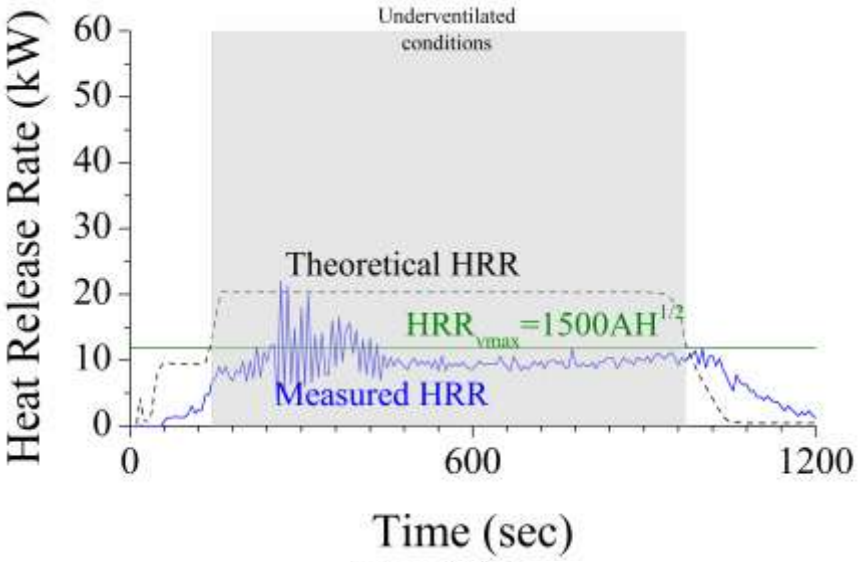

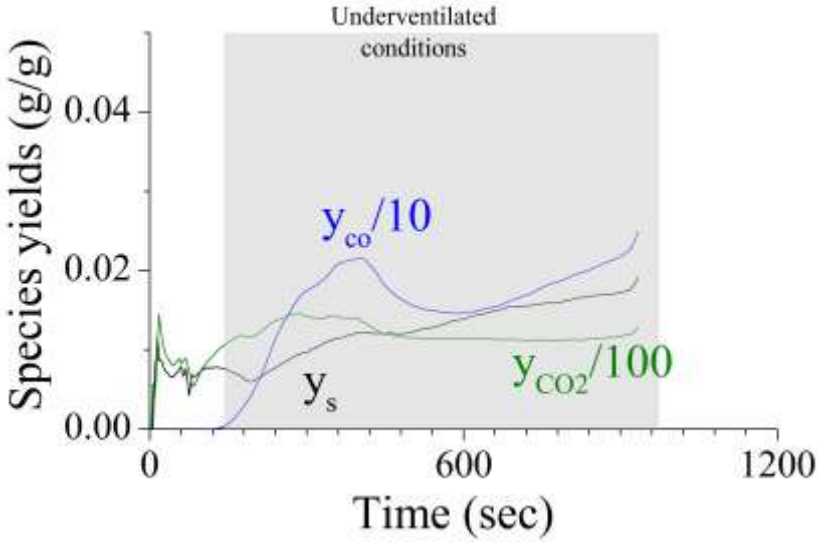

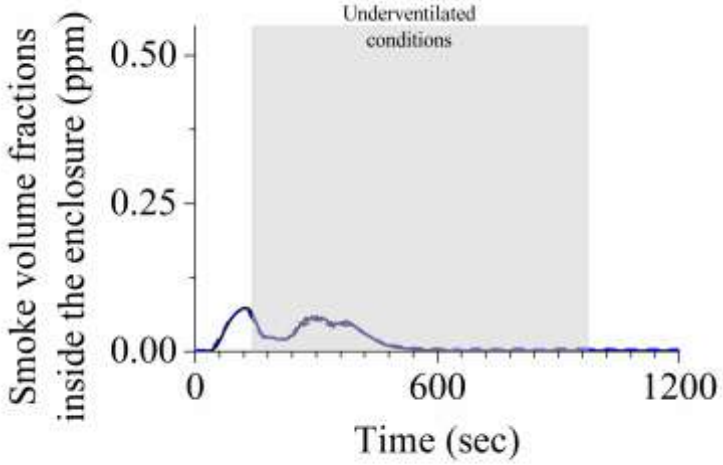
Underventilated
conditions
Smoke volume fractions
inside the enclosure (ppm)
0.50
0.25
0.00
0
600
1200
Time (sec)

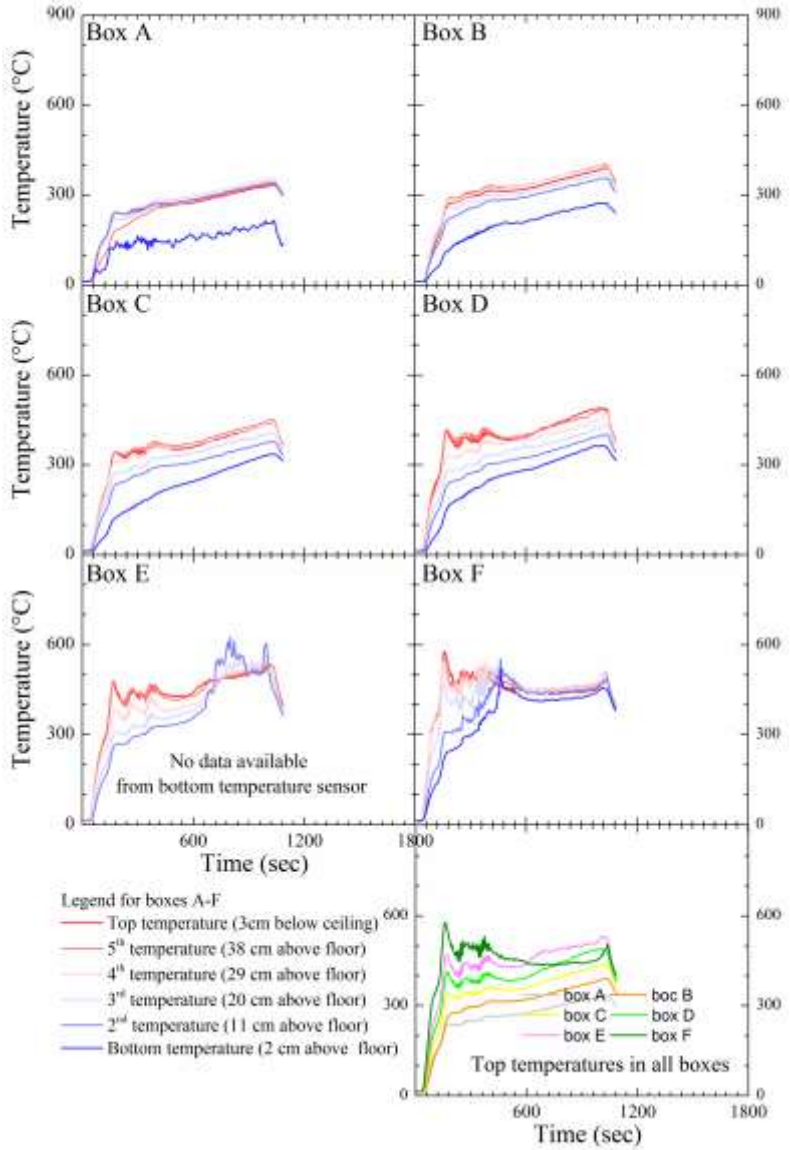
Box A
Box B
Box C
Box D
Box E
Box F
Temperature (°C)
900
600
300
0
No data available
from bottom temperature sensor
600
1200
1800
Time (sec)
Legend for boxes A-F
Top temperature (3cm below ceiling)
5th temperature (38 cm above floor)
4th temperature (29 cm above floor)
3rd temperature (20 cm above floor)
2nd temperature (11 cm above floor)
Bottom temperature (2 cm above floor)
box A
boc B
box C
box D
box E
box F
Top temperatures in all boxes

Test no 31 (300410-1)

Test date 30 April 2010
Theoretical HRR = 50kW
Opening size = W20cm x H20cm
Ventilation controlled HRR = 26.86
GER = 1.86

Bi-directional probes installed

Recorded observations:
62 sec - ignition
1 min 15 sec automatic control started
9 min 03 sec – flames visible outside
25 min – gas turned off
26 min 40 sec – no flames visible outside
27 min 28 sec- flame self extinguishment

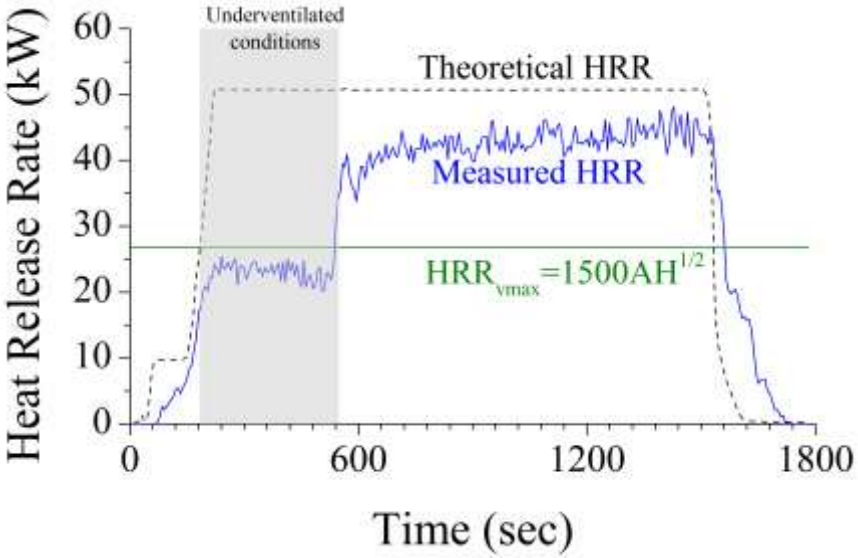

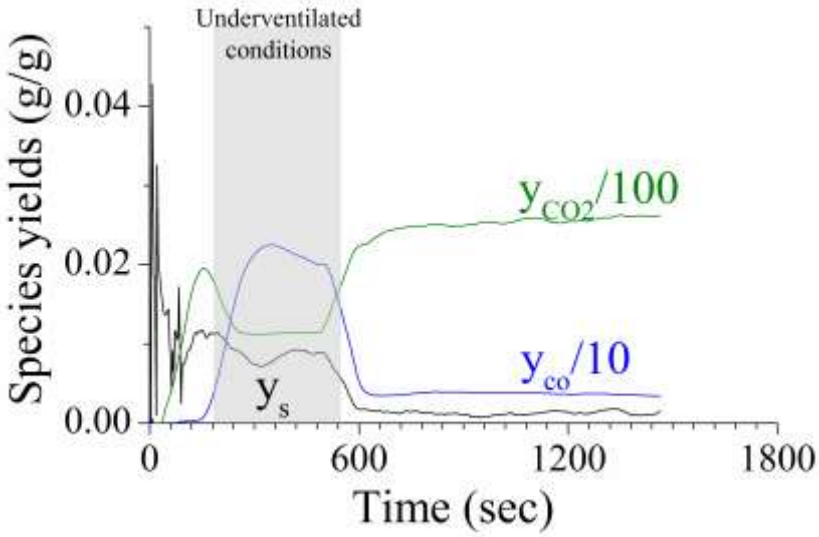

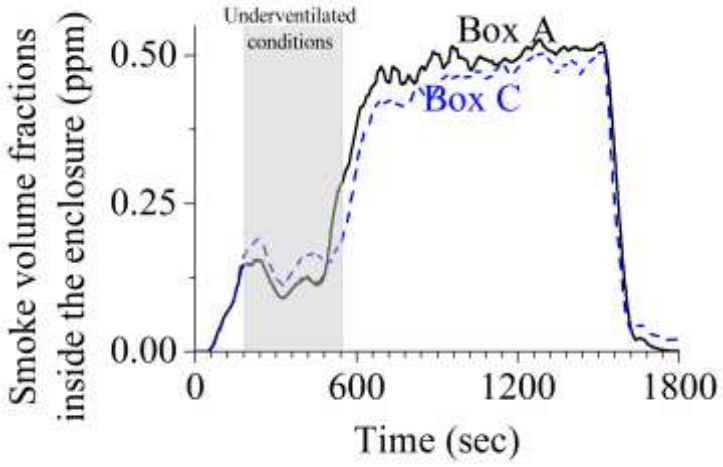
Underventilated conditions
Box A
Box C
Smoke volume fractions inside the enclosure (ppm)
0.50
0.25
0.00
0
600
1200
1800
Time (sec)

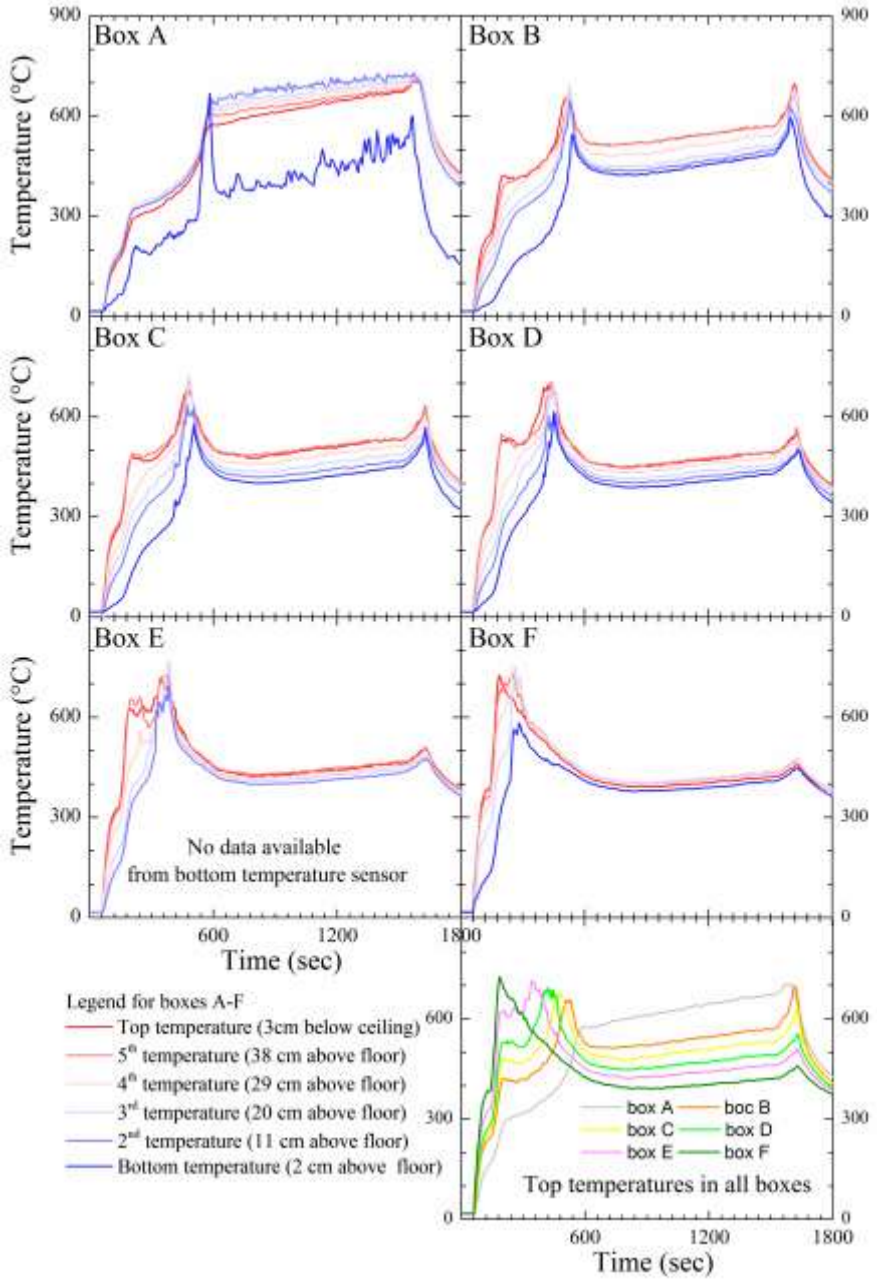
Box A
Box B
Box C
Box D
Box E
Box F
Temperature (°C)
900
600
300
0
No data available
from bottom temperature sensor
600
1200
1800
Time (sec)
Legend for boxes A-F
Top temperature (3cm below ceiling)
5th temperature (38 cm above floor)
4th temperature (29 cm above floor)
3rd temperature (20 cm above floor)
2nd temperature (11 cm above floor)
Bottom temperature (2 cm above floor)
box A
boc B
box C
box D
box E
box F
Top temperatures in all boxes
Time (sec)

Test no 32 (100510-1)

Test date 10 May 2010
Theoretical HRR = 50kW
Opening size = W20cm x H20cm
Ventilation controlled HRR = 26.86
GER = 1.86

Bi-directional probes installed

Recorded observations:
61 sec - ignition
2 min 00 sec automatic control started
5 min – fans for smoke meters started (earlier smoke data may be invalid)
9 min 40 sec – flames visible outside
25 min – gas turned off
27 min 46 sec- flame self extinguishment

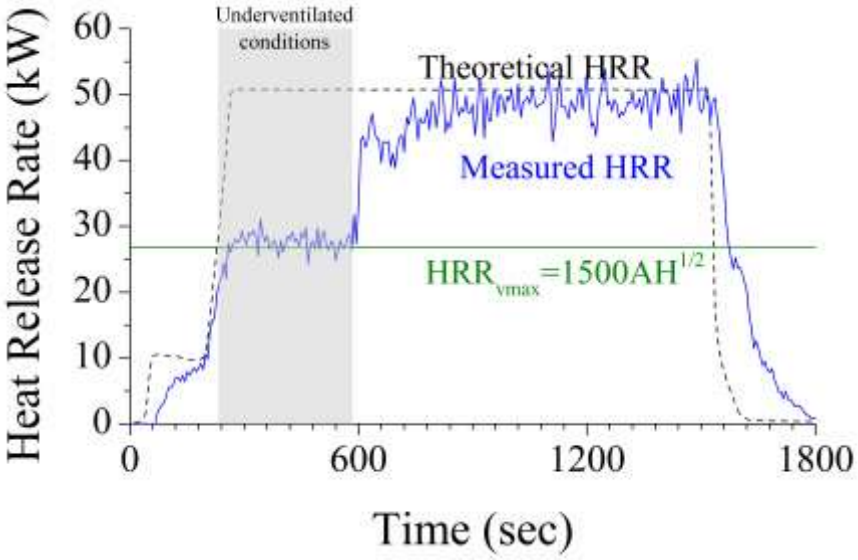

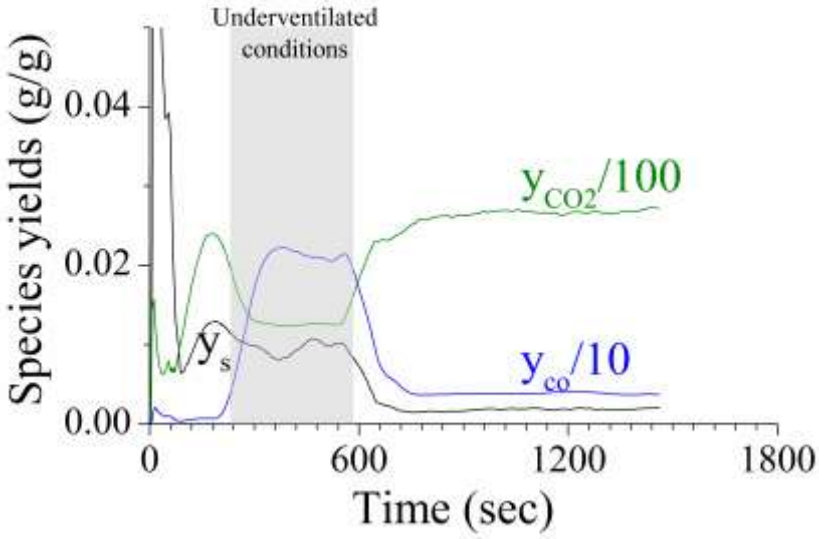

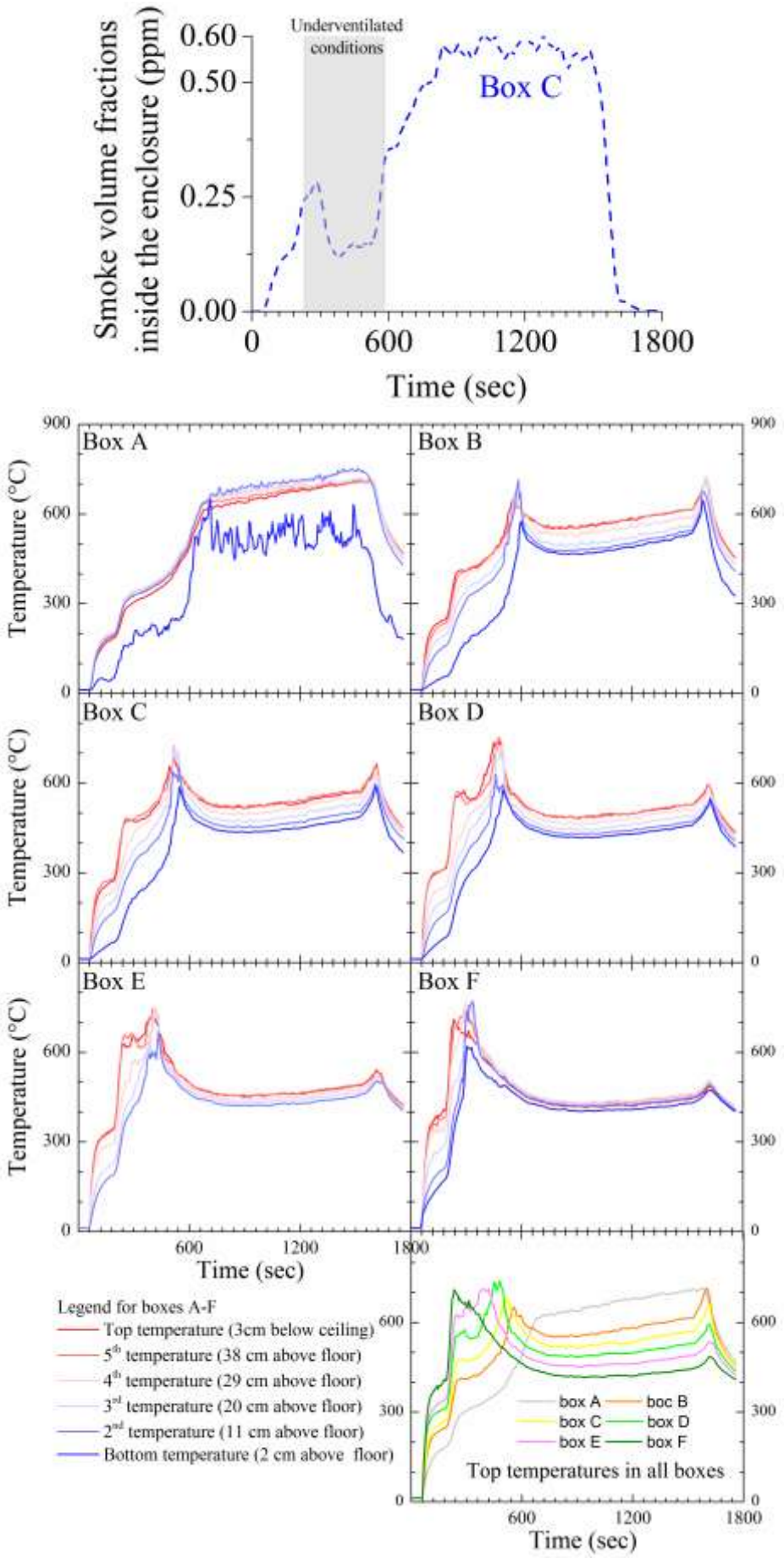
Smoke volume fractions inside the enclosure (ppm)
Underventilated conditions
Box C
0.60
0.50
0.25
0.00
0
600
1200
1800
Time (sec)
Box A
Box B
Box C
Box D
Box E
Box F
Temperature (°C)
900
600
300
0
Time (sec)
Legend for boxes A-F
Top temperature (3cm below ceiling)
5th temperature (38 cm above floor)
4th temperature (29 cm above floor)
3rd temperature (20 cm above floor)
2nd temperature (11 cm above floor)
Bottom temperature (2 cm above floor)
box A
boc B
box C
box D
box E
box F
Top temperatures in all boxes

Test no 33 (240510-1)

Test date 24 May 2010
Theoretical HRR = 50kW
Opening size = W20cm x H20cm
Ventilation controlled HRR = 26.86
GER = 1.86

Bi-directional probes installed

Recorded observations:
55 sec - ignition
1 min 17 sec automatic control started
9 min 34 sec – flames visible outside
25 min – gas turned off
26min 10sec – no flames visible outside
27 min 58 sec- flame self extinguishment

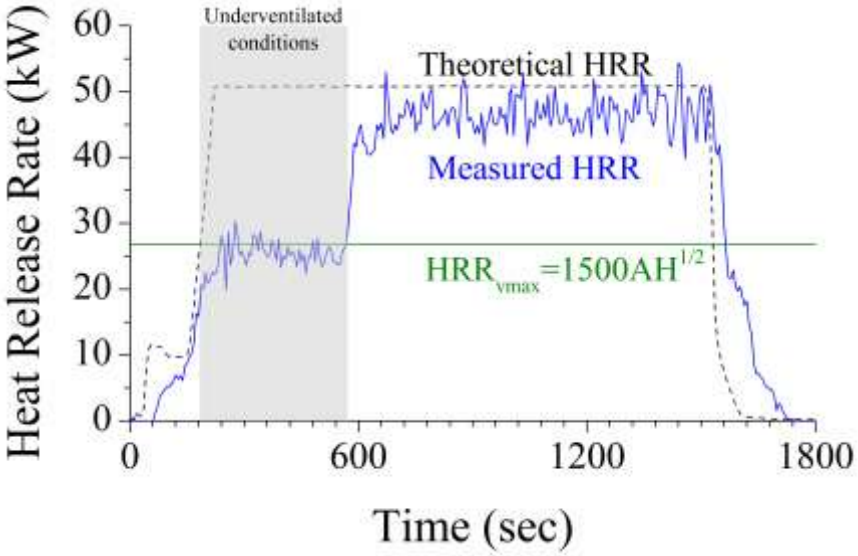

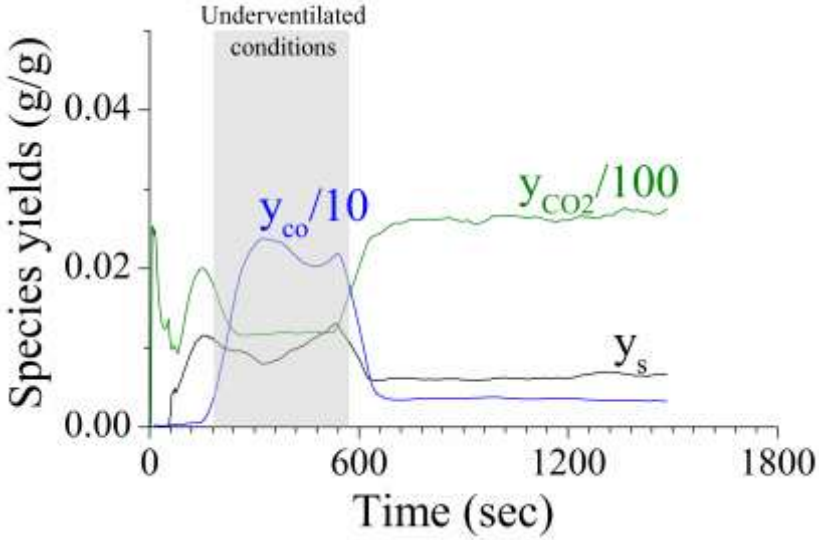

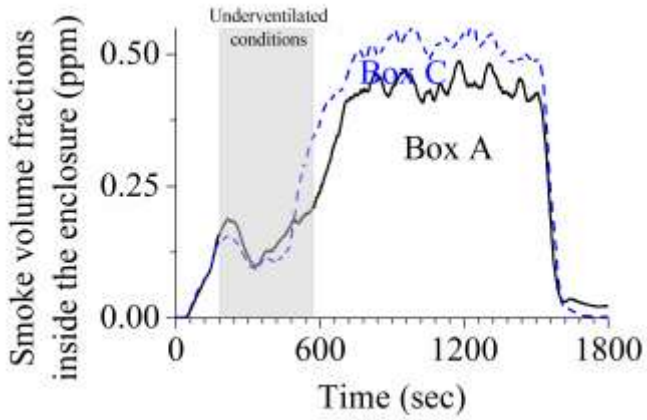
Underventilated conditions
Box C
Box A
Smoke volume fractions inside the enclosure (ppm)
0.50
0.25
0.00
0
600
1200
1800
Time (sec)

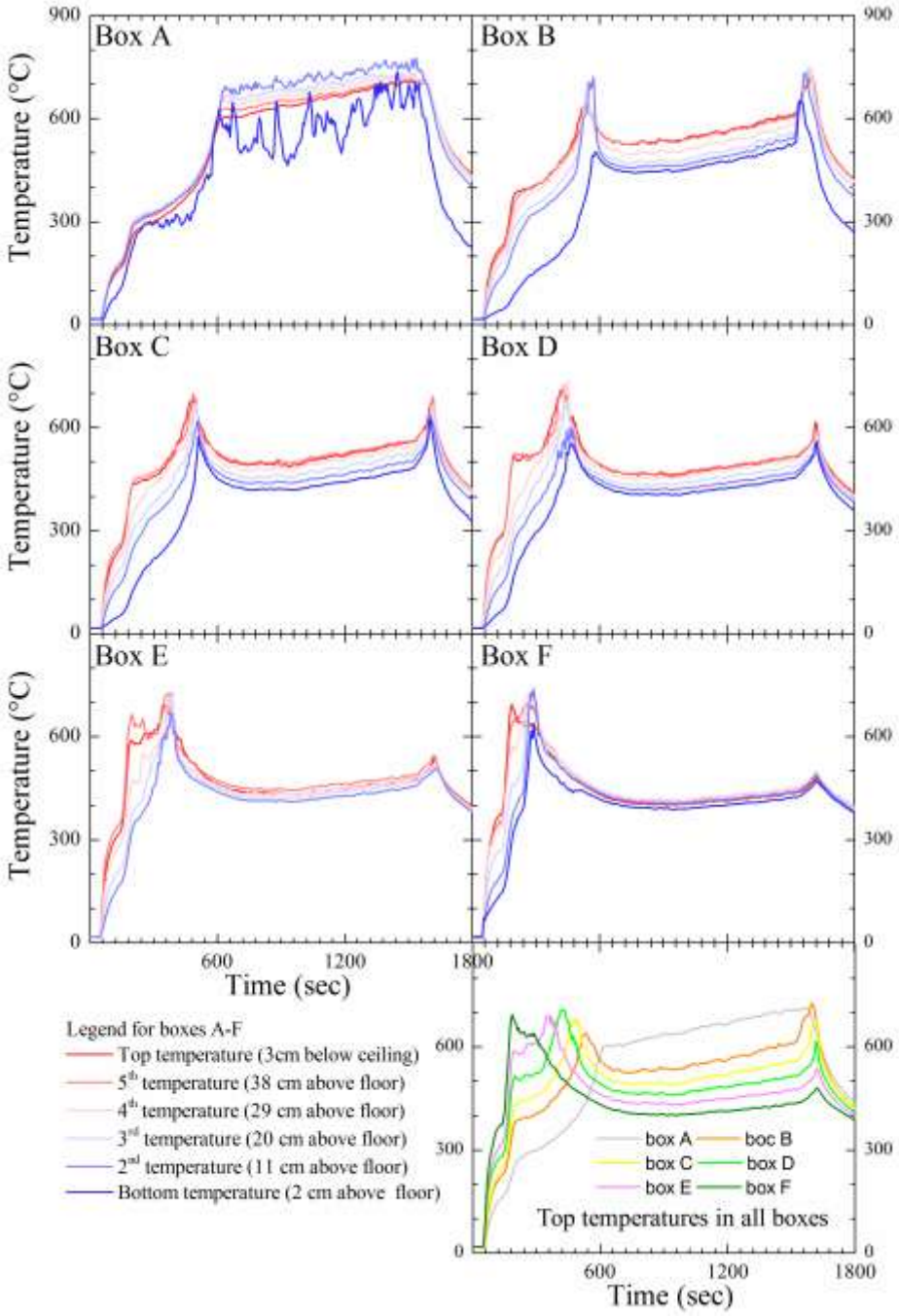
Box A
Box B
Box C
Box D
Box E
Box F
Temperature (°C)
900
600
300
0
600
1200
1800
Time (sec)
Legend for boxes A-F
Top temperature (3cm below ceiling)
5th temperature (38 cm above floor)
4th temperature (29 cm above floor)
3rd temperature (20 cm above floor)
2nd temperature (11 cm above floor)
Bottom temperature (2 cm above floor)
box A
boc B
box C
box D
box E
box F
Top temperatures in all boxes

Test no 34 (070610-1)

Test date 7 June 2010
Theoretical HRR = 50kW
Opening size = W20cm x H20cm
Ventilation controlled HRR = 26.86
GER = 1.86

Bi-directional probes installed

Recorded observations:
57 sec - ignition
1 min 01 sec automatic control started
7 min 26 sec – flames reaching lower bi-directional probe
9 min 18 sec – flames visible outside
25 min – gas turned off
<26min 20sec – no flames visible outside
26 min 50 sec – flames passed through lower bi-probe
27 min 33 sec- flame self extinguished

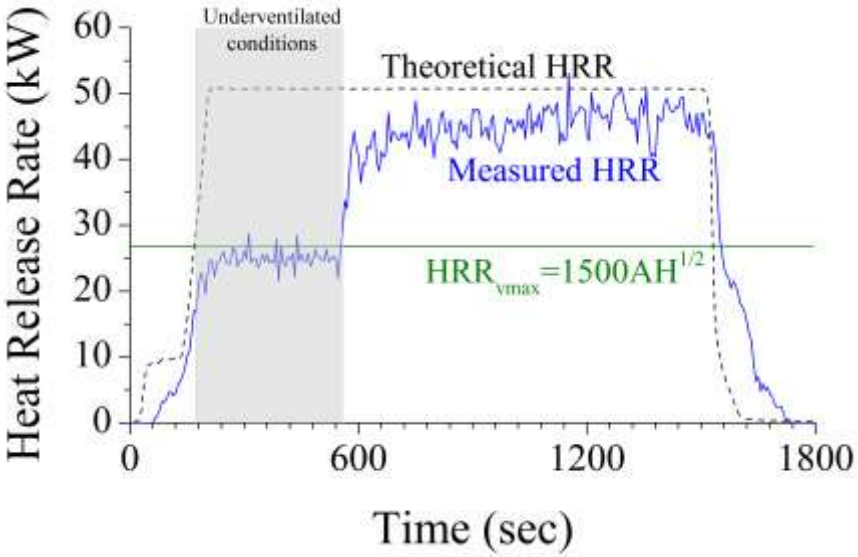

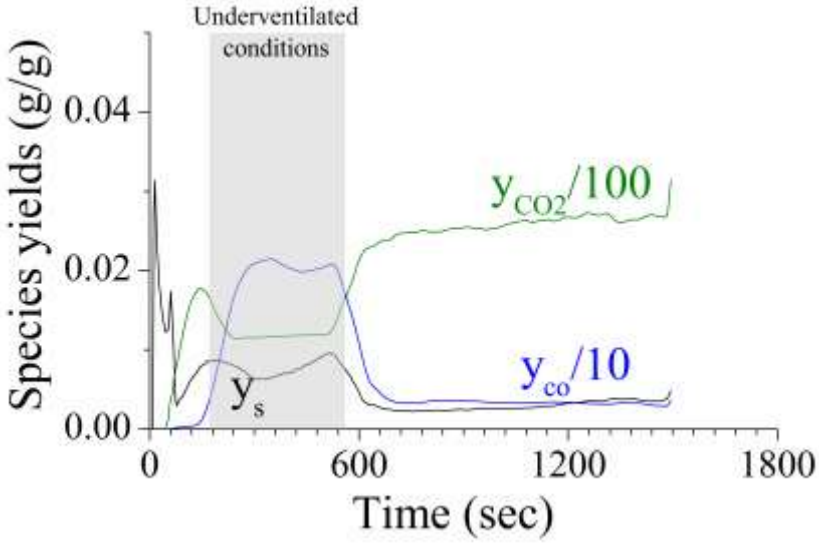

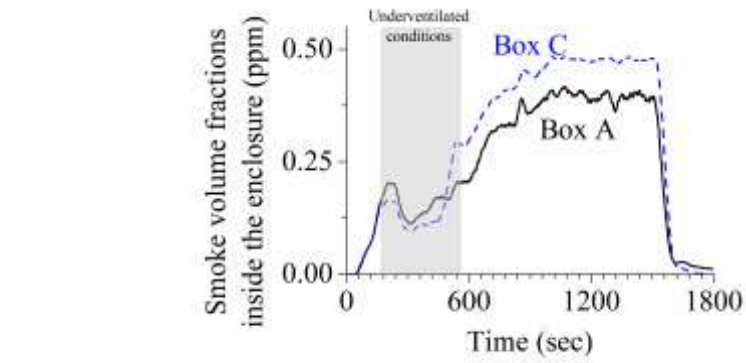
Underventilated conditions
Box C
Box A
Smoke volume fractions inside the enclosure (ppm)
0.50
0.25
0.00
0
600
1200
1800
Time (sec)

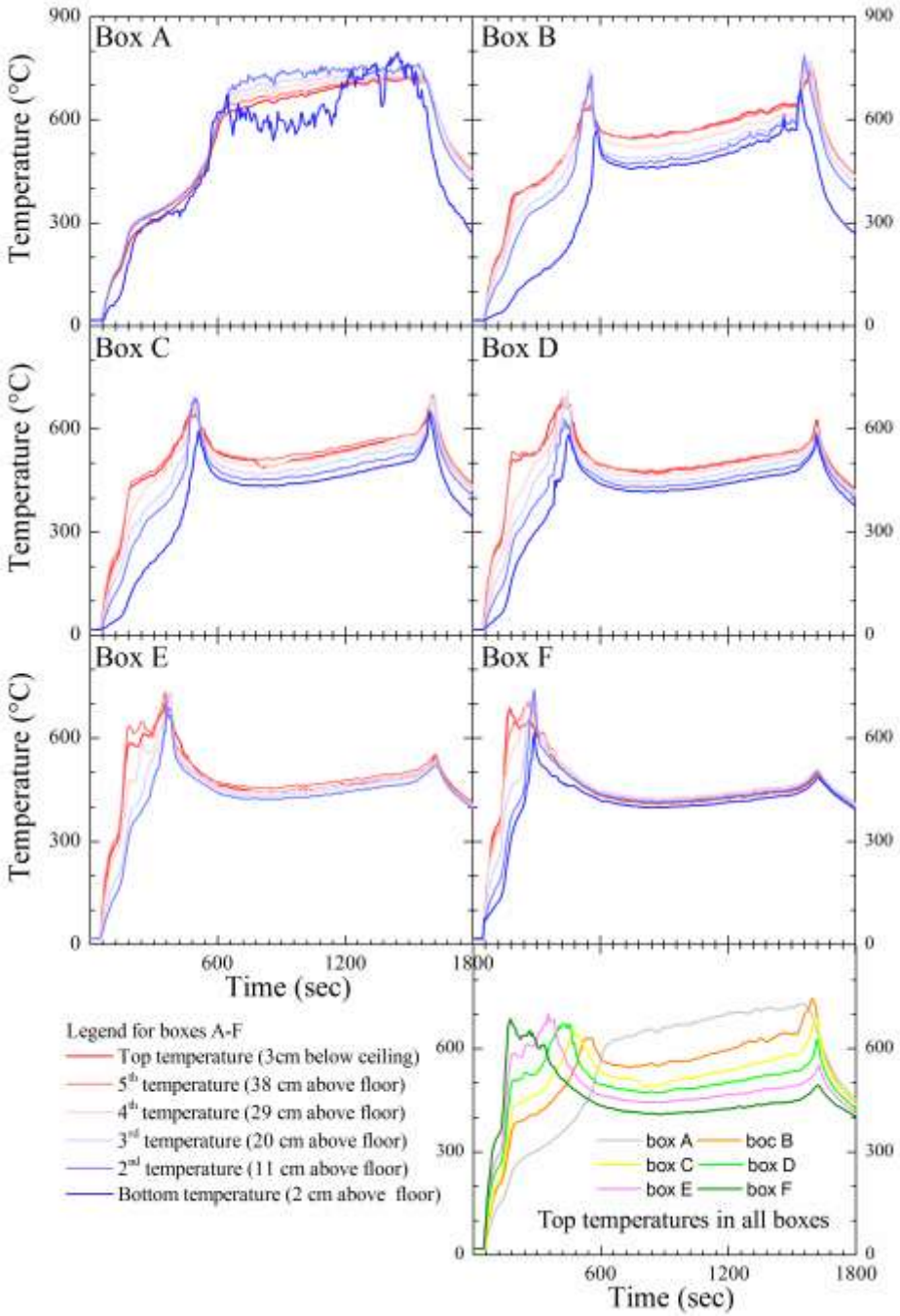
Box A
Box B
Box C
Box D
Box E
Box F
Temperature (°C)
900
600
300
0
600
1200
1800
Time (sec)
Legend for boxes A-F
Top temperature (3cm below ceiling)
5th temperature (38 cm above floor)
4th temperature (29 cm above floor)
3rd temperature (20 cm above floor)
2nd temperature (11 cm above floor)
Bottom temperature (2 cm above floor)
box A
boc B
box C
box D
box E
box F
Top temperatures in all boxes

Test no 35 (250610-1)

Test date 25 June 2010
Theoretical HRR = 50kW
Opening size = W10cm x H25cm
Ventilation controlled HRR = 18.75
GER = 2.67

Bi-directional probes installed

Recorded observations:
2 min 40 sec - ignition
2 min 40 sec automatic control started
8 min 42 sec – flames visible outside
25 min – gas turned off
28 min 23 sec- flame self extinguished

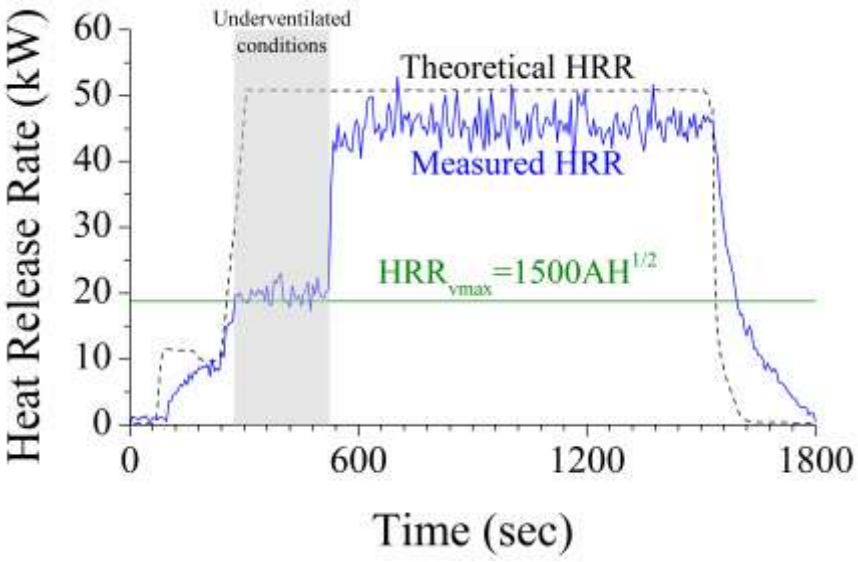

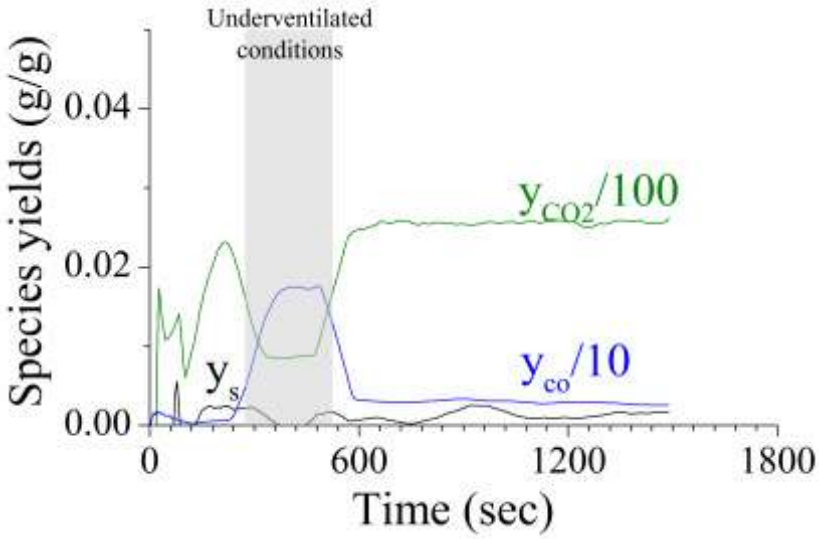

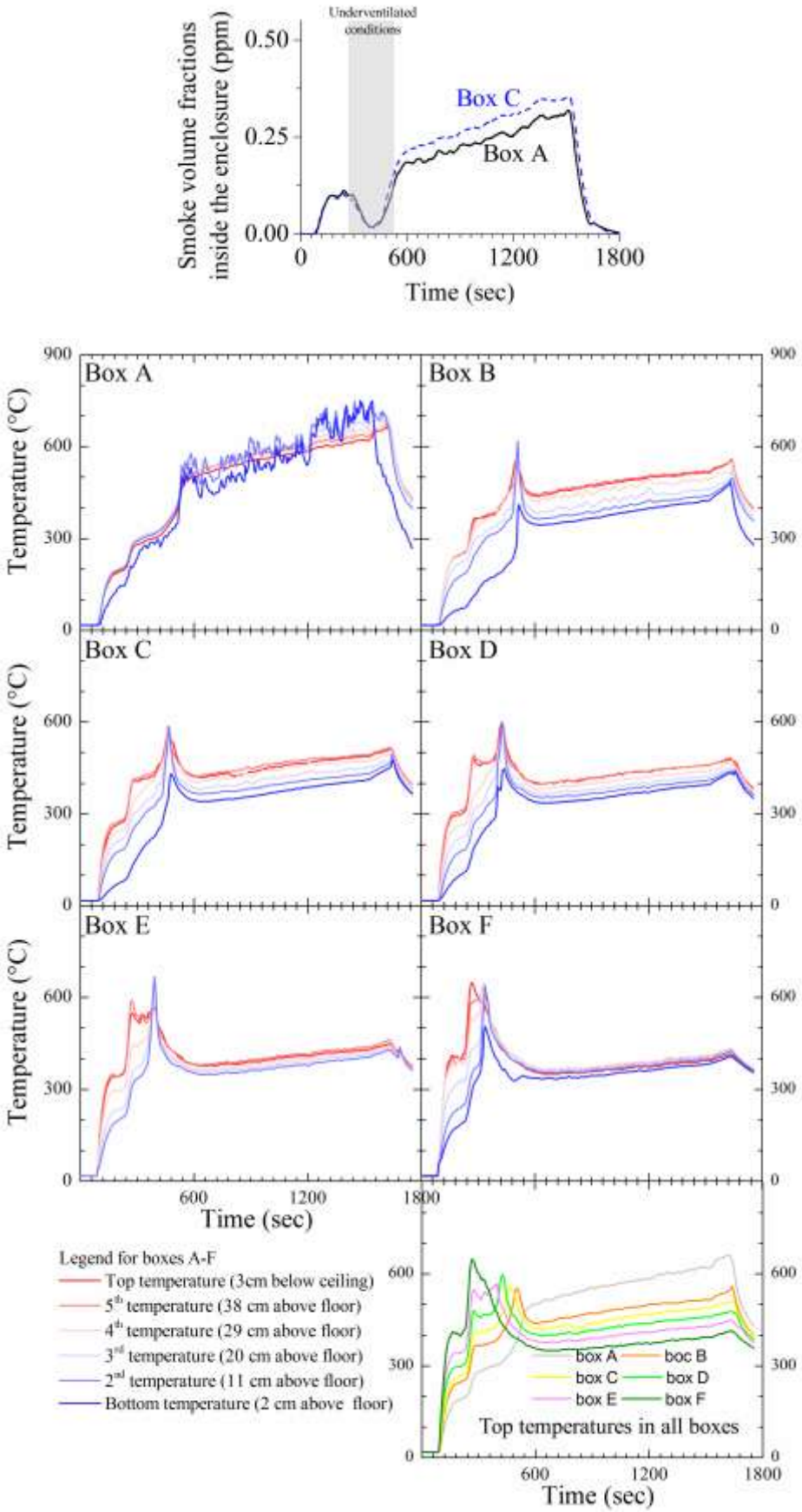
Underventilated conditions
Smoke volume fractions inside the enclosure (ppm)
0.50
0.25
0.00
Box C
Box A
0
600
1200
1800
Time (sec)
Box A
Box B
Box C
Box D
Box E
Box F
Temperature (°C)
900
600
300
0
Time (sec)
Legend for boxes A-F
Top temperature (3cm below ceiling)
5th temperature (38 cm above floor)
4th temperature (29 cm above floor)
3rd temperature (20 cm above floor)
2nd temperature (11 cm above floor)
Bottom temperature (2 cm above floor)
box A
boc B
box C
box D
box E
box F
Top temperatures in all boxes

Test no 36 (060810-1)

Test date 6 August 2010
Theoretical HRR = 50kW
Opening size = W10cm x H25cm
Ventilation controlled HRR = 18.75
GER = 2.67

Bi-directional probes installed

Recorded observations:
1 min 14 sec - ignition
3 min 00 sec automatic control started
3 min 00 sec – laser in box A turned off to see the effect of flames on detector response
8 min 40 sec - flames outside/ detector in box A reads nothing
25 min 15 sec – gas turned off
28 min 44 sec- flame self extinguishment

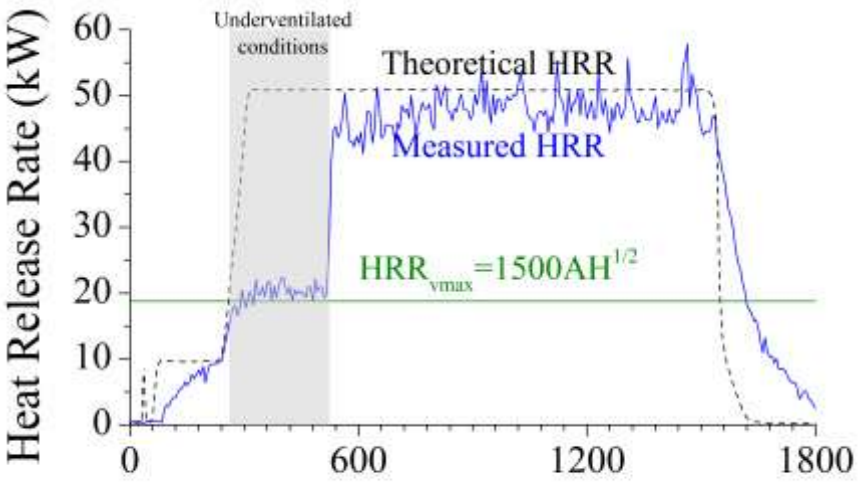

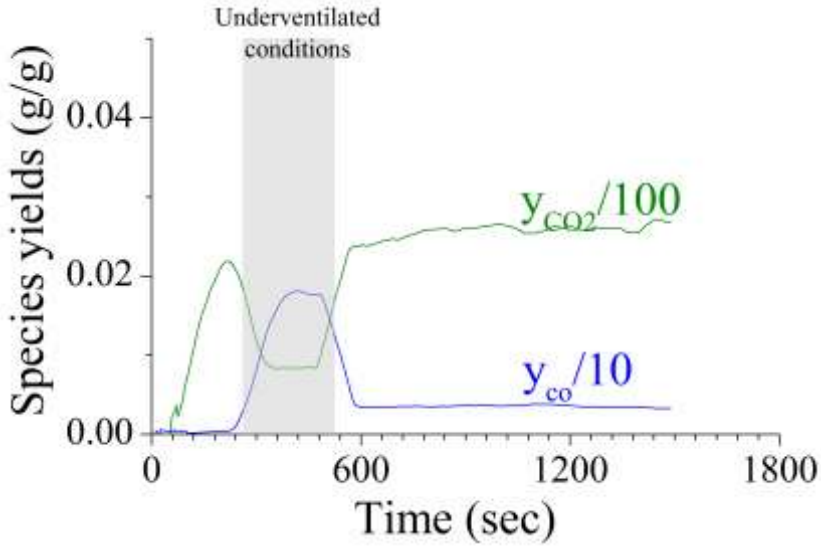

NO SMOKE DATA AVAILABLE for measurements in the duct

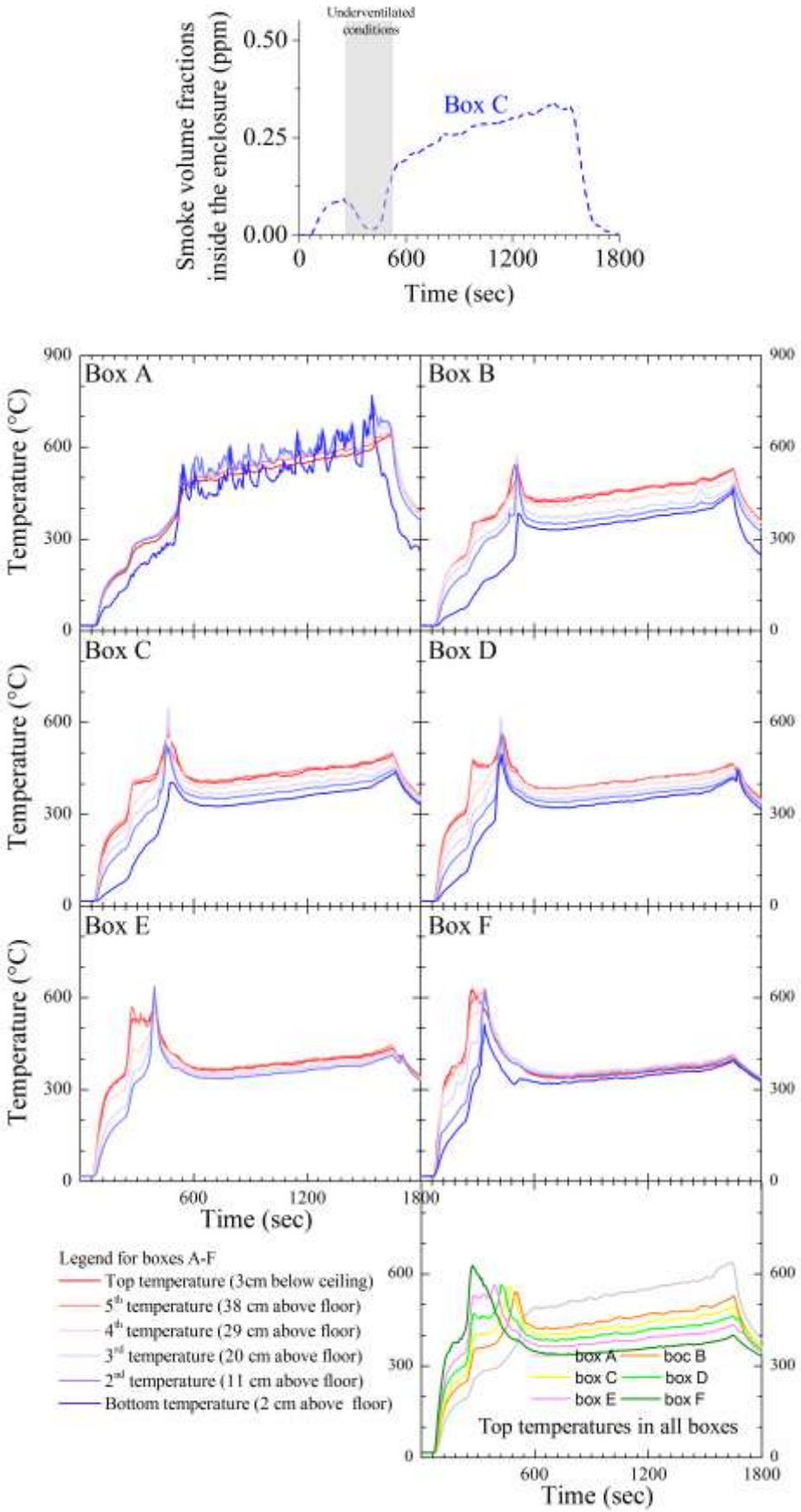
Underventilated conditions
Smoke volume fractions inside the enclosure (ppm)
0.50
0.25
0.00
Box C
0
600
1200
1800
Time (sec)
Box A
Box B
Box C
Box D
Box E
Box F
Temperature (°C)
900
600
300
0
Time (sec)
Legend for boxes A-F
Top temperature (3cm below ceiling)
5th temperature (38 cm above floor)
4th temperature (29 cm above floor)
3rd temperature (20 cm above floor)
2nd temperature (11 cm above floor)
Bottom temperature (2 cm above floor)
box A
boc B
box C
box D
box E
box F
Top temperatures in all boxes

Test no 37 (090810-1)

Test date 9 August 2010
Theoretical HRR = 30kW
Opening size = W10cm x H25cm
Ventilation controlled HRR = 18.75
GER = 1.6

Bi-directional probes installed

Recorded observations:
0min 46 sec - ignition
1 min 30 sec automatic control started
NO FLAMES visible OUTSIDE
20 min 25 sec – gas turned off
23 min 32 sec- flame self extinguishment

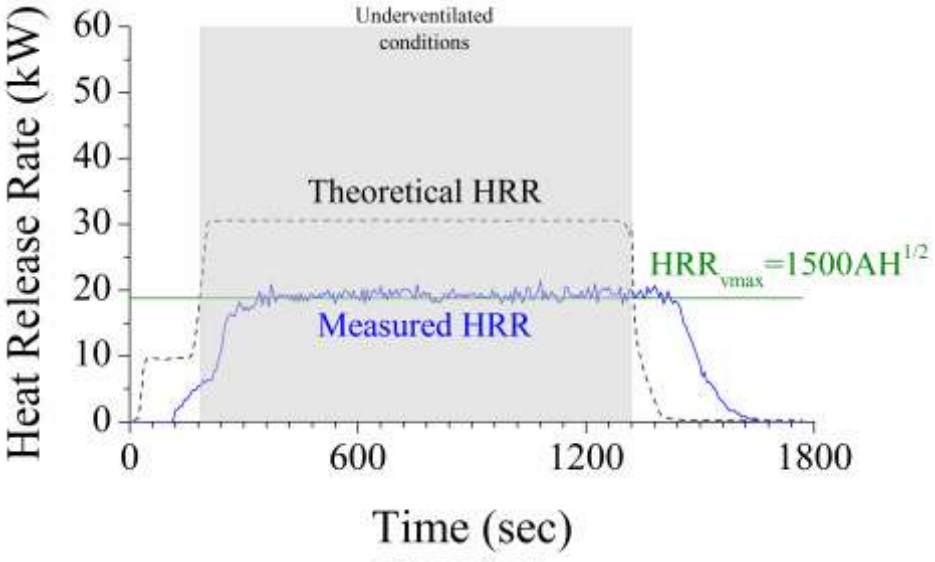

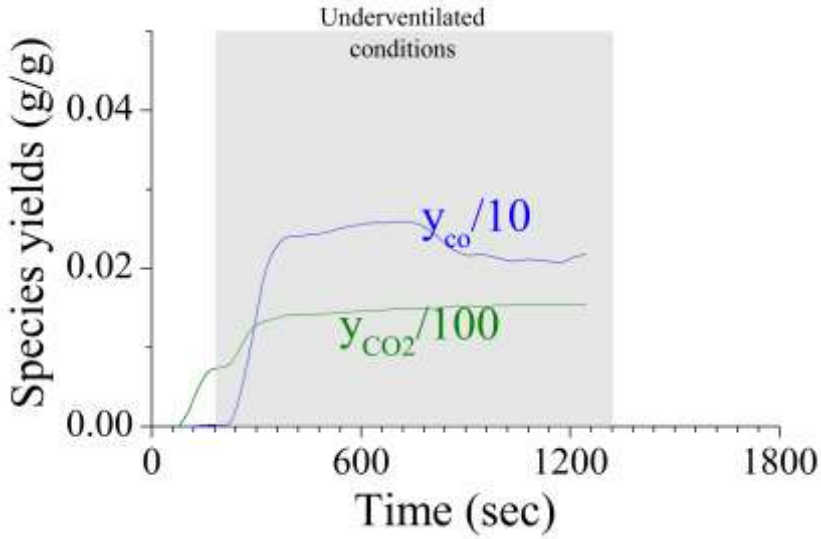

NO SMOKE DATA AVAILABLE for measurements in the duct

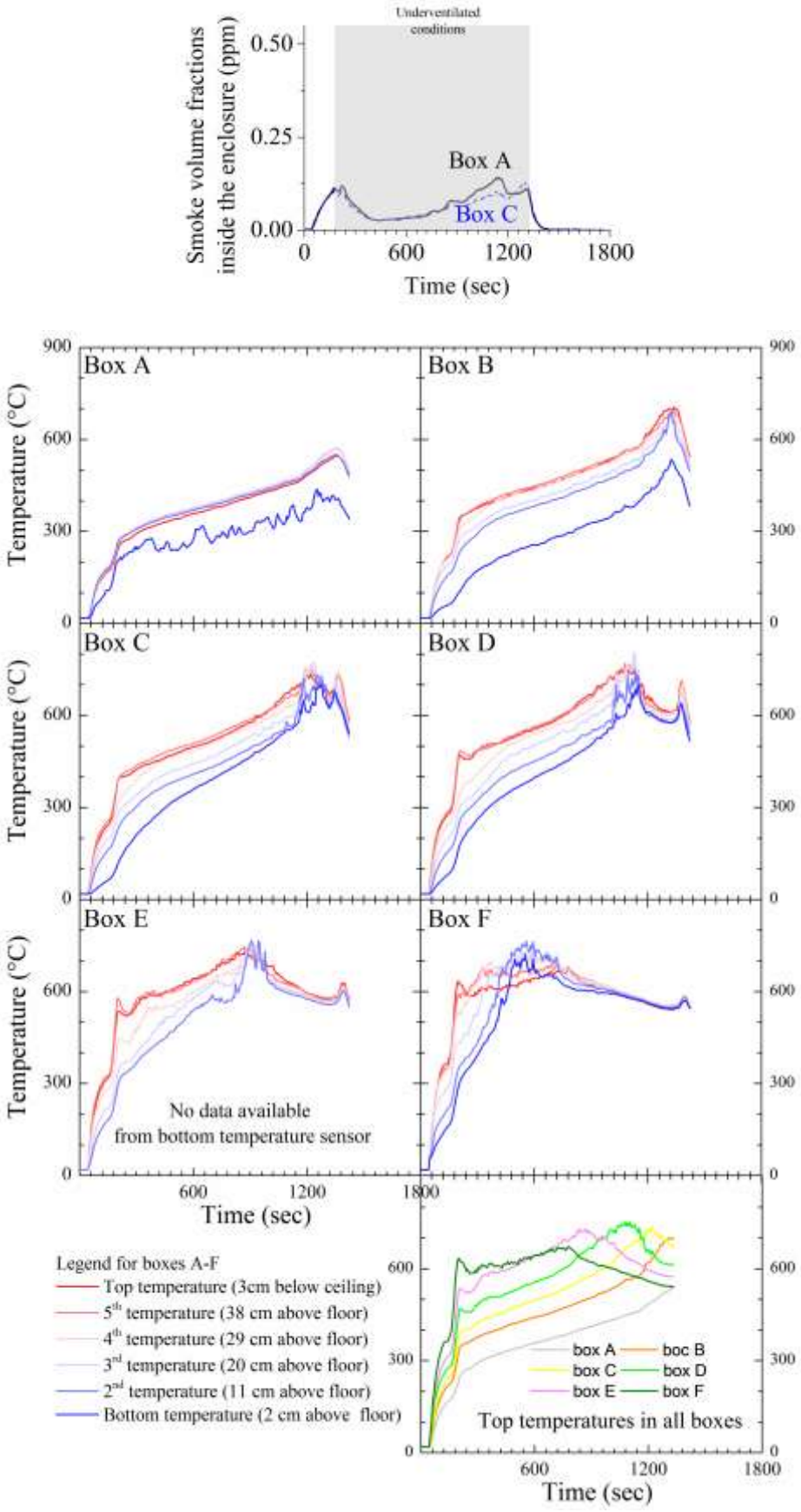
Underventilated conditions
Smoke volume fractions inside the enclosure (ppm)
0.50
0.25
0.00
Box A
Box C
0
600
1200
1800
Time (sec)
Box A
Box B
Box C
Box D
Box E
Box F
Temperature (°C)
900
600
300
0
No data available
from bottom temperature sensor
Time (sec)
Legend for boxes A-F
Top temperature (3cm below ceiling)
5th temperature (38 cm above floor)
4th temperature (29 cm above floor)
3rd temperature (20 cm above floor)
2nd temperature (11 cm above floor)
Bottom temperature (2 cm above floor)
box A
boc B
box C
box D
box E
box F
Top temperatures in all boxes

Test no 38 (130810-1)

Test date 13 August 2010
Theoretical HRR = 40kW
Opening size = W10cm x H25cm
Ventilation controlled HRR = 18.75
GER = 2.13

Bi-directional probes installed

Recorded observations:
0min 46 sec - ignition
1 min 0 sec automatic control started
11 min 07 sec – flames visible outside
25 min – gas turned off
27 min 43 sec – flame self extinguishment

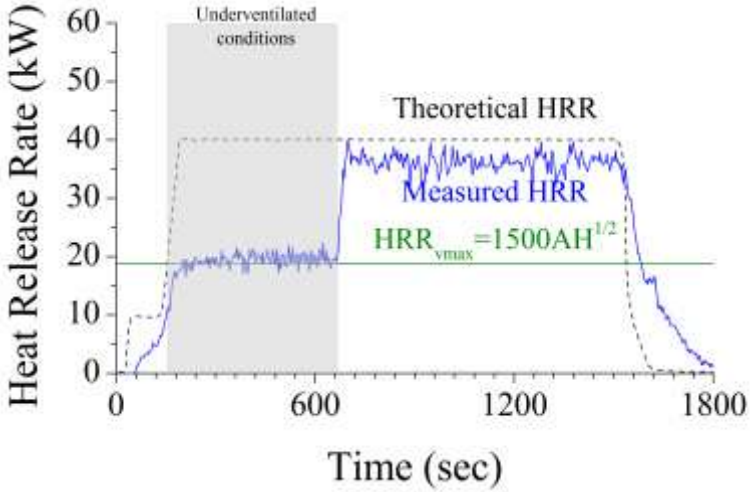

PROBLEMS WITH TIME SYNCHRONISATION SPECIES Yields

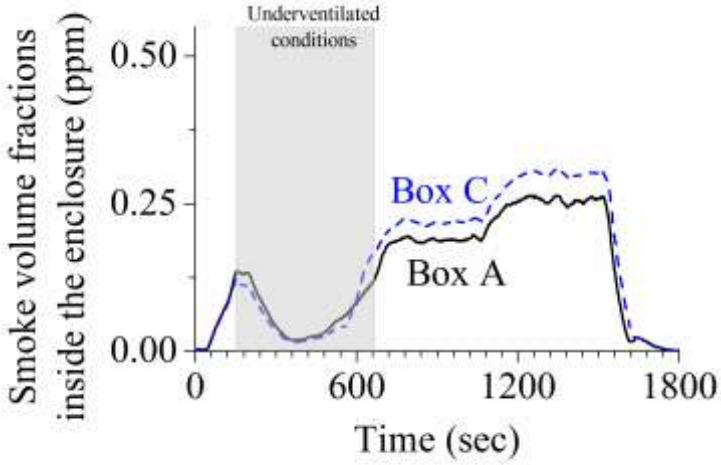

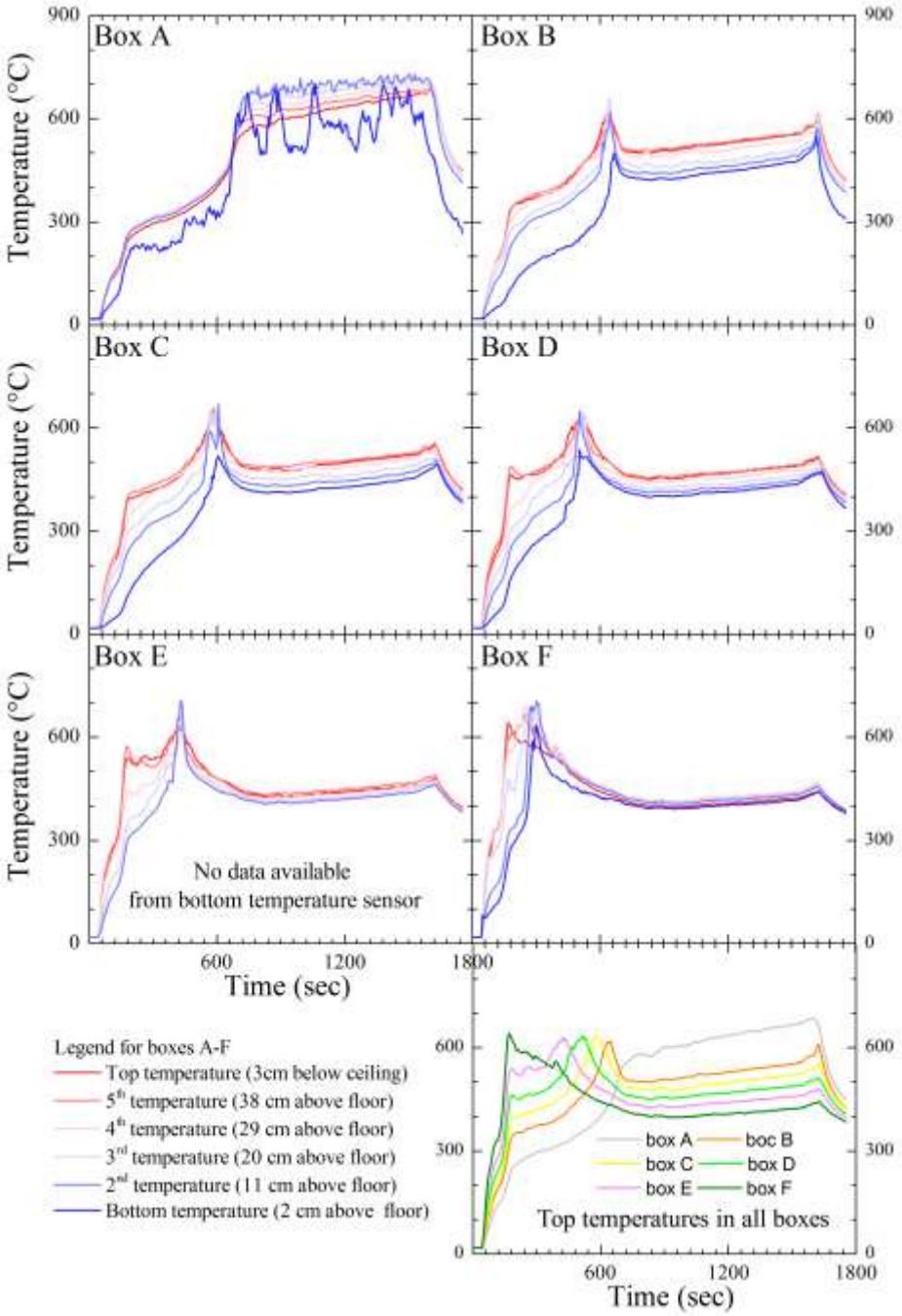
Box A
Box B
Box C
Box D
Box E
Box F
Temperature (°C)
Time (sec)
No data available
from bottom temperature sensor
Legend for boxes A-F
Top temperature (3cm below ceiling)
5th temperature (38 cm above floor)
4th temperature (29 cm above floor)
3rd temperature (20 cm above floor)
2nd temperature (11 cm above floor)
Bottom temperature (2 cm above floor)
box A
boc B
box C
box D
box E
box F
Top temperatures in all boxes

REFERENCES

Abecassis Empis, C., Cowlard, A., Welch, S. and Torero, J.,L., 2007. Test One: The 'Uncontrolled' Fire. In:*The Dalmarnock Fire Tests: Experiments and Modelling* ., eds. G. Rein, C. Abecassis Empis and R.O. Carvel, UK: School of Engineering and Electronics, University of Edinburgh, pp.63-81.

Andersson, B., Markert, F. and Holmstedt, G., 2005. Combustion products generated by hetero-organic fuels on four different fire test scales. *Fire Safety Journal,* 40, (5), pp.439-465.

ASTM, 2003. *Standard Test Methods for Measurement of Synthetic Polymer Material Flammability Using a Fire Propagation Apparatus (FPA). E 2058-03.* USA: ASTM International.

ASTM, 1979. *Standard test method for specific optical density of smoke generated by solid materials, ANSI/ASTM E663-79.* American Society for Testing and Materials.

Audouin, L., Such, J.M., Malet, J.C. and Casselman, C., 1997. A Real Scenario For A Ghosting Flame. *5th International Symposium on Fire Safety Science,* Interscience Communications Ltd, pp. 1261-1272.

Babrauskas, V. 2011, *Online discussion forum communication*, mailing list of the International Association for Fire Safety Science.

Babrauskas, V., 2002. The Cone Calorimeter. In: *SFPE Handbook of Fire Protection Engineering* ., eds. DiNenno,P.,J., and et. al, , Third edn,USA: National Fire Protection Association, pp.3-63-3-81.

Babrauskas, V., 1995. The Generation of CO in Bench-scale Fire Tests and the Prediction for Real-scale Fires. *Fire and Materials,* 19, (5), pp.205-213.

Babrauskas, V., Gann, R.G., Levin, B.C., Paabo, M., Harris, R.H., Peacock, R.D. and Yusa, S., 1998. A methodology for obtaining and using toxic potency data for fire hazard analysis. *Fire Safety Journal,* 31, pp.345-358.

Babrauskas, V. and Mulholland, G.W. , 1987. Smoke and Soot Data Determinations in the Cone Calorimeter. In: *Mathematical Modeling of Fires, ASTM STP 983* .Philadelphia: American Society for Testing and Materials, pp.83-104.

Babrauskas, V. and Williamson, R.B., 1978. Post-flashover compartment fires: Basis of a theoretical model. *Fire and Materials,* 2, (2), pp.39-53.

Beji, T., 2009. *Theoretical and experimental investigation on soot and radiation in fires.* PhD thesis. University of Ulster.

Beji, T., Ukleja, S., Zhang, J. and Delichatsios, M.A., 2011a. Fire behaviour and external flames in corridor and tunnel-like enclosures. Accepted for publication in *Fire and Materials,* doi: 10.1002/fam.1124.

Beji, T., Zhang, J.P., Yao, W. and Delichatsios, M., 2011b. A novel soot model for fires: Validation in a laminar non-premixed flame. *Combustion and Flame,* 158, (2), pp.281-290.

Bertin, G., Most, J. and Coutin, M., 2002. Wall fire behavior in an under-ventilated room. *Fire Safety Journal,* 37, (7), pp.615-630.

Best, R. and Demers, D.P., 1982. *Investigation report on the MGM Grand Hotel fire - Las Vegas, Nevada, November 21, 1980.* National Fire Protection Association.

Beyler, C.L., 1986a. Major species production by diffusion flames in a two-layer compartment fire environment. *Fire Safety Journal,* 10, pp.47-56.

Beyler, C.L., 1986b. Major Species Production by Solid Fuels in a Two Layer Compartment Fire Environment. In: *Fire Safety Science, Proceedings of the First International Symposium.* Hemisphere Publ Corp, Washington, DC, USA, pp.431-440.

Beyler, C.L., 1984. Ignition and burning of a layer of incomplete combustion products. *Combustion Science and Technology,* 39, pp.287-303.

Beyler, C.L., 1983. *Development and burning of a layer of products of incomplete combustion generated by a buoyant diffusion flame.* PhD Thesis. Harvard University.

Bilger, R.W., 1977. Reaction rates in diffusion flames. *Combustion and Flame,* 30, (0) pp.277-284.

Bohren, C.F. and Huffman, D.R., 1983. *Absorption and Scattering of Light by Small Particles.* New York: John Wiley & Sons Inc..

Bond, T.C. and Bergstrom, R.W., 2006. Light Absorption by Carbonaceous Particles: An Investigative Review. *Aerosol Science and Technology,* 40, pp.27-67.

British Standards Institution, 2007. *Fire test — Large-scale room reference test for surface products. British Standard no BS EN 14390:2007.* UK: British Standards Institution.

British Standards Institution, 2003. *Tube furnace method for the determination of toxic product yields in fire effluent. BS 7990:2003.* UK: British Standards Institution.

British Standards Institution, 1998. *Guide to Smoke measurement units - Their basis and use in smoke opacity test methods. British Standard no BS 7904:1998.* UK: British Standards Institution.

Brohez, S., Delvosalle, C. and Marlair, G., 2004. A two-thermocouples probe for radiation corrections of measured temperatures in compartment fires. *Fire Safety Journal,* 39, (5), pp.399-411.

Bryant, R.,A., Ohlemiller, T., J., Johnsson, E., Hamins, A., Grove, B., S., Guthrie, W.,F., Maranghides, A. and Mulholland, G.W., 2004. *The NIST 3 Megawatt Quantitative Heat Release Rate Facility – Description and Procedures.* National Institute of Standards and Technology.

Bryner, N., Johnsson, R.J. and Pitts, W.M., 1994. *Carbon Monoxide Production in Compartment Fires – Reduced-Scale Enclosure Test Facility , NISTIR 5568.* National Institute of Standards and Technology.

Bundy, M., Hamins, A., Johnsson, E., Kim, S., Ch., Ko, G.H. and Lenhert, D.B., 2007. *Measurements of Heat and Combustion Products in Reduced-Scale Ventilation-Limited Compartment Fires . NIST Technical Note 1483.* NIST.

Cetegen, B.M., Zukoski, E.E. and Kubota, T., 1982. *Entrainment and Flame Geometry of Fire Plumes.* National Bureau of Standards.

Choi, M.Y., Mulholland, G.W., Hamins, A. and Kashiwagi, T., 1995. Comparisons of the Soot Volume Fraction Using Gravimetric and Light Extinction Techniques. *Combustion and Flame,* 102, (1/2), pp.161-169.

Christian, S.D. and Shields, T.J., 1998Tests for toxic potency and their relationship with long term sequelae from a single, acute, sub-lethal exposure to carbon monoxide. In: *First International Symposium on Human Behaviour in Fire.* University of Ulster, Northern Ireland: .

Christian, W.J. and Wterman, T.E., 1971. Ability of small- scale tests to predict full- scale smoke production. *Fire technology,* 7, (4), pp.332-344.

Delichatsios, M.A., 1994. A Phenomenological Model for Smoke-Point and Soot Formation in Laminar Flames. *Combustion Science and Technology,* 100, (1-6), pp.283-298.

Delichatsios, M.A., 1993. Smoke yields from turbulent buoyant jet flames. *Fire Safety Journal,* 20, (4), pp.299-311.

Delichatsios, M.A., 1990. The Outflow of Buoyant Releases Including Fire Gases from a Long Corridor Closed at One End. *Journal of Fluids Engineering-Transactions of the Asme,* 112, (1) pp.28-32.

Department for Communities and Local Government, 2011. *Fire Statistics: Great Britain, 2010 - 2011*. London, UK: Department for Communities and Local Government.

Department for Communities and Local Government , 2007. *Fire Statistics, United Kingdom 2005.* Department for Communities and Local Government, UK.

Dobbins, R.A., Mulholland, G.W. and Bryner, N.P., 1994. Comparison of a fractal smoke optics model with light extinction measurements. *Atmospheric Environment,* 28, (5), pp.889-897.

Dod, R.L., Brown, N.J., Mowrer, F.W., Novakov, T. and Williamson, R.B., 1989. Smoke Emission Factors from Medium-Scale Fires: Part 2. *Aerosol Science and Technology,* 10, pp.20-27.

Drysdale, D., 2011. *An Introduction to Fire Dynamics.* 3rd ed. edn, UK: Wiley.

Drysdale, D., 1998. *An Introduction to Fire Dynamics.* 2nd ed. edn, UK: Chichester : Wiley.

Ergut, A. and Levendis, Y., 2005. An Investigation on Thermocouple-Based Temperature Measurements in Sooting Flames. *ASME Conference Proceedings,* 2005, (42215), pp.397-403.

European Committee for Standardisation, 2002. *Reaction to fire tests for building products — Building products excluding floorings exposed to the thermal attack by a single burning item. European Standard No BS EN 13823:2002.* European Committee for Standardisation.

Faraday, M., 2002. *The Chemical History of a Candle. A Course of Six Lectures Delivered before a Juvenile Auditory at the Royal Institution of Great Britain during the Christmas Holidays of 1860-1.* (republication of the text published circa 1885-89) edn, USA: Dover Publications, Inc.

Forell, B., 2007. *A Methodology to assess Species Yields of Compartment Fires by means of an extended Global Equivalence Ratio Concept.* University of Braunschweig – Institute of Technology, Germany.

Forell, B. and Hosser, D., 2007. The relationship between ventilation conditions and carbon monoxide source term in fully-developed compartment fires. In: *Proceedings of the 5th International Seminar on Fire and Explosion Hazards.* Edinburgh: pp. 825-835.

Friedman, R., 1998. *Principles of fire protection chemistry and physics.* 3rd edition edn, USA: Jones and Bartlett Publishers.

Friedman, R., 1986 Some Unresolved Fire Chemistry Problems. In: *Fire Safety Science. Proceedings of the First International Symposium.* International Association for Fire Safety Science, pp. 349-359.

Fujita, K., n.d. *Characteristics of fire inside a non-combustible room and prevention of fire damage. Report No 2(h).* Japanese Ministry of Construction, Building Research Institute.

Gottuk, D., T., 1992. *Generation of Carbon Monoxide in Compartment Fires.* PhD thesis. Virginia Polytechnic Inst. and State University, Blacksburg, VA.

Gottuk, D., T. and Lattimer, B., Y., 2008. Effect of Combustion Conditions on Species Production. In:*SFPE Handbook of Fire Protection Engineering* ., eds. DiNenno,P.,J., D. Drysdale, C.L. Beyler, et al, , Fourth edn,USA: National Fire Protection Association, pp.2-67-2-95.

Gottuk, D., T. and Lattimer, B., Y., 2002. Effect of Combustion Conditions on Species Production. In:*SFPE Handbook of Fire Protection Engineering.* eds. DiNenno,P.,J., D. Drysdale, C.L. Beyler, et al, , Third edn, USA: National Fire Protection Association, pp.2-54-2-82.

Gottuk, D., T. and Roby, R., J., 1995. Effect of Combustion Conditions on Species Production. In: *SFPE Handbook of Fire Protection Engineering* ., eds. P. DiNenno J., C.L. Beyler, R. Custer L., et al, , Second edn,USA: National Fire Protection Association, pp.2-64-2-84.

Gottuk, D., T., Roby, R.J. and Beyler, C.L., 1992. Study of carbon monoxide and smoke yields from compartment fires with external burning. In: *Proceedings of the 24th International Symposium On Combustion.* Publ by Combustion Inst, Pittsburgh, PA, USA, pp. 1729-1735.

Hasemi, Y., Yokobayahi, S., Wakamatsu, T. and Ptchelintsev, A., 1995. Fire safety of Building Components Exposed to a Localized Fire-Scope and Experiments on Ceiling/Beam System Exposed to a Localized Fire. In: *Proceedings of ASIAFlam 1995, 1st International Conference,* pp. 351-361.

Hayes, B.S. ,1991. Soot and hydrocarbons in combustion. In: *Fossil Fuel Combustion.* eds. W. Bartok and A.F. Sarofim, New York: John Wiley & Sons, pp.261-327.

Heskestad, A.W., 1994. *Reaction to Fire Classification of Building Products: Assessment of teh Smoke Production. Hazard Assessment, ISO Fire Test Methods and Development of Empirical Prediction Models.* Norwegian University of Science and Technology.

Heskestad, A.W. and Hovde, P.,J., 1994. Assessment Of Smoke Production From Building Products. *Proceedings from fourth Inernational Symposium on Fire Safety Science.* pp. 527-538.

Heskestad, A.W. and Hovde, P.,J., 1993. Smoke Production from Building Products. Comparision of Test Methods and Correlation of Test Results. In: *Proceedings from the Sixth International Interflam Conference.* Interscience Communications Ltd, London: p. 189.

Heskestad, G., 1995. Fire Plumes. In: *SFPE Handbook of Fire Protection Engineering* ., eds. P. DiNenno J., C.L. Beyler, R. Custer L., et al, 2nd edition edn, USA: Society of Fire Protection Engineers, pp.2-9-2-19.

Hirschler, M., 1993. Comparision of Smoke Release Data from Full Scale Room Tests with Results in the Cone Calorimeter and the NBS Smoke Chamber. In: *Proceedings from the Sixth International Interflam Conference.* Interscience Communications Ltd, London: p. 203.

Hobbs, P.C.D., 1997. Ultrasensitive laser measurements without tears. *Applied Optics,* 36, (4) pp.903-920.

Hwang, C., Lock, A., Bundy, M., Johnsson, E. and Gwon Hyun Ko, 2010. Studies on Fire Characteristics in Over- and Underventilated Full-scale Compartments. *Journal of Fire Sciences,* 28, (5), pp.459-486.

ISO, 2010. *BS EN ISO 13943:2010. Fire safety — Vocabulary (ISO 13943:2008).* Technical Committee ISO/TC 92 “Fire safety” of the International Organization for Standardization (ISO).

ISO, 1993. *ISO 9705:1993, Fire Tests – Full-Scale Room Test for Surface Products.* International Organization for Standardisation;.

Janssens, M.L. and Parker, W.,J. , 1992. Oxygen Consumption Calorimetry. In: *Heat Release in Fires* . eds. V. Babrauskas and S. Grayson J., E & FN Spon, pp.31-59.

Janssens, M.L. and Tran, H.C., 1992. Data Reduction of Room tests for Zone Model Validation. *Journal of Fire Sciences,* 10, (Nov/Dec) pp.528-555.

Jin, T. , 2002. Visibility and Human Behavior in Fire Smoke. In: *SFPE Handbook of Fire Protection Engineering* ., eds. DiNenno,P.,J., and et. al, , Third edn,USA: National Fire Protection Association, pp.2-42-2-53.

Jin, T., 1978. Visibility through fire smoke. *Journal of Fire and Flammability,* 9, pp.135-157.

Jin, T. and Yamada, T., 1990. Experimental Study on Human Emotional Instability in Smoke Filled Corridor: Part 2. *Journal of Fire Sciences,* 8, pp.124-134.

Jin, T. and Yamada, T., 1989. Experimental Study of Human Behaviour in Smoke Filled Corridors. *Procedings of the Second International Symposium of Fire Safety Science.* International Association for Fire Safety Science, Boston: pp. 511-519.

Kawagoe, K., 1958. *Fire Behaviour in Rooms.* Building Research Institute.

Kennedy, I.M., 1997. Models of soot formation and oxidation. *Progress in Energy and Combustion Science,* 23, (2), pp.95-132.

Kent, J.H. and Wagner, H.G., 1984. Why Do Diffusion Flames Emit Smoke? *Combustion Science and Technology,* 41, (5-6), pp.245-269.

Klote, J.,H. and Milke, J.,A., 1992. *Design of Smoke Management Systems.* USA: ASHRAE.

Ko, G.H., Hamins, A., Bundy, M., Johnsson, E.L., Kim, S.C. and Lenhert, D.B., 2009. Mixture fraction analysis of combustion products in the upper layer of reduced-scale compartment fires. *Combustion and Flame,* 156, (2), pp.467-476.

Kondo, A., Saito, Y., Seki, A., Sugiura, C., Maegaki, Y., Nakayama, Y., Yagi, K. and Ohno, K., 2007/4. Delayed neuropsychiatric syndrome in a child following carbon monoxide poisoning. *Brain and Development,* 29, (3), pp.174-177.

Köylü, Ü.Ö. and Faeth, G.M., 1991. Carbon monoxide and soot emissions from liquid-fueled buoyant turbulent diffusion flames. *Combustion and Flame,* 87, (1), pp.61-76.

Krishnan, S.S., Lin, K.C. and Faeth, G.M., 2000. Optical properties in the visible of overfire soot in large buoyant turbulent diffusion flames. *Journal of Heat Transfer-Transactions of the Asme,* 122, (3) pp.517-524.

Lautenberger, C., de Ris, J., Dembsey, N., Barnett, J. and Baum, H., 2005. A simplified model for soot formation and oxidation in CFD simulation of non-premixed hydrocarbon flames. *Fire Safety Journal,* 40, (2) pp.141-176.

Lee, Y., 2006. *Heat fluxes and flame heights on external facades from enclosure fires.* PhD thesis. University of Ulster.

Lee, Y., Delichatsios, M.A. and Silcock, G.W.H., 2007. Heat fluxes and flame heights in facades from fires in enclosures of varying geometry. *Proceedings of the Combustion Institute,* 31, (2) pp.2521-2528.

Lemmon, E.W. and Jacobsen, R.T., 2004. Viscosity and Thermal Conductivity Equations for Nitrogen, Oxygen, Argon, and Air. *International Journal of Thermophysics,* 25, (1), pp.21-69.

Leonard, S., Mulholland, G.W., Puri, R. and Santoro, R.J., 1994. Generation of CO and smoke during underventilated combustion. *Combustion and Flame,* 98, (1), pp.20-34.

Levchik, S., Hirschler, M. and Weil, E., 2011. *Practical Guide to Smoke and Combustion Products from Burning Polymers - Generation, Assessment and Control.* UK: iSmithers.

Lock, A., Bundy, M., Johnsson, E., Hamins, A., Hyun Ko, G., Hwang, C., Fuss, P. and Harris, R. , 2008. *Experimental Study of the Effects of Fuel Type, Fuel Distribution, and Vent Size on Full-Scale Underventilated Compartment Fires in an ISO 9705 Room. NIST Technical Note 1603.* National Institute of Standards and Technology.

Lönnermark, A. and Babrauskas, V., 1996. *TOXFIRE - Fire Characteristics and Smoke Gas Analyses in Under-ventilated Large-scale Combustion Experiments. Theoretical Background and Calculations. SP Report 1996:49.* SP Swedish National Testing and Research Institute. Fire Technology.

Mannaioni, P.F., Vannacci, A. and Masini, E., 2006. Carbon monoxide: the bad and the good side of the coin, from neuronal death to anti-inflammatory activity. *Inflammation Research,* 55, (7), pp.261-273.

McCaffrey, B.J. and Heskestad, G., 1976. A Robust Bidirectional Low-Velocity Probe for Flame and Fire Application. *Combustion and Flame,* 26, (1), pp.125-127.

McGrattan, K., Hostikka, S., Floyd, J., Baum, H. and Rehm, R. , 2007. *Fire Dynamics Simulator (Version 5). Technical Reference Guide. (Draft: April 15, 2007). NIST Special Publication 1018-5.* National Institute of Standards and Technology.

Milke, J.,A. , 2008. Smoke Management by Mechanical Exhaust or Natural Venting. In:*SFPE Handbook of Fire Protection Engineering* ., eds. P.J. DiNenno, D. Drysdale, C.L. Beyler, et al, , Fourth edn,USA: National Fire Protection Association, pp.4-387-4-412.

Morehart, J.H., Zukoski, E.E. and Kubota, T., 1991Characteristics of Large Diffusion Flames Burning in a Vitiated Atmosphere. In: *Fire Safety Science - Proceedings of the Third International Symposium.* IAFFS, London and New York: pp. 575-583.

Most, J.M. and Saulnier, J.B., 2011. Under-ventilated Wall Fire Behaviour during the Post-flashover Period. *Journal of Applied Fluid Mechanics,* 4, (3) pp.129-135.

Mulholland, G.W. , 2008. Smoke Production and Properties. In:*SFPE Handbook of Fire Protection Engineering* ., eds. P.J. DiNenno, D. Drysdale, C.L. Beyler, et al, , Fourth edn,USA: National Fire Protection Association, pp.2-291-2-301.

Mulholland, G.W. , 1990a. Comparison of predicted CO yield with results from fire reconstruction of Sharon, PA fire , Appendix C to FPETOOL, NISTIR 4380. In:*FPETOOL: Fire Protection Engineering Tools for Hazard Estimation* ., ed. H.E. Nelson, Gaithersburg, USA: National Institute of Standards and Technology, pp.101-105.

Mulholland, G.W. , 1990b. Position Paper Regarding CO Yield, Appendix C. In:*FPETOOL: Fire Protection Engineering Tools for Hazard Estimation* ., ed. H.E. Nelson, Gaithersburg, USA: National Institute of Standards and Technology, pp.93-100.

Mulholland, G.W., 1982. How Well are we Measuring Smoke? *Fire and Materials,* 6, (2), pp.65-67.

Mulholland, G.W. and Choi, M.Y., 1998. Measurement Of The Mass Specific Extinction Coefficient for Acetylene And Ethene Smoke Using The Large Agglomerate Optics Facility. *Twenty-seventh symposium (International) on combustion.* The Combustion Institute., pp. 1515-1522.

Mulholland, G.W. and Croarkin, C., 2000. Specific Extinction Coeficient of Flame Generated Smokes. *Fire and Materials,* 24, pp.227-230.

Mulholland, G.W., Henzel, V. and Babrauskas, V., 1989The Effect of Scale on Smoke Emission. *Proc. of the 2nd International Symposium on Fire Safety Science.* pp. 347.

Mulholland, G.W., Janssens, M.L., Yusa, S., Twilley, W.H. and Babrauskas, V., 1991a. Effect of Oxygen Concentration on CO and Smoke Produced by Flames. In: *Fire Safety Science. Proceedings. 3rd International Symposium.* Elsevier Applied Science, New York: pp. 585-594.

Mulholland, G.W., Janssens, M.L., Yusa, S., Twilley, W. and Babrauskas, V., 1991b. The Effect of Oxygen Concentration on CO and Smoke Production by Flames. In: *Fire Safety Science - Proceedings of the Third International Symposium.* IAFFS, London and New York: pp. 585-594.

Mulholland, G.W., Johnsson, E., L., Shear, D., A. and Fernandez, M., G., 2000. Design and Testing of a New Smoke Concentration Meter. *Fire and Materials,* 24, pp.231-243.

Newman, J.S. and Steciak, J., 1987. Characterization of Particulates from Diffusion Flames. *Combustion and Flame,* 67, pp.55-64.

NFPA, 2005. *NFPA 92B: Standard for Smoke Management Systems in Malls, Atria, and Large Spaces.* Quincy, MA, USA: National Fire Protection Association.

Ostman, B.A.L. , 1996. Smoke and soot. In:*Heat Release in Fires* ., eds. V. Babrauskas and S. Grayson J., , 1996th edn,London: E & FN Spon, pp.233-250.

Ostman, B.A.L. , 1992. *Smoke production in the Cone Calorimeter and the Room Fire Test for surface products - Correlation studies. Report 9208053.* Swedish Institute for Wood Technology Research.

Ostman, B.A.L. and Tsantaridis, L.D., 1991. Smoke production in the cone calorimeter and the room fire test. *Fire Safety Journal,* 17, (1) pp.27-43.

Ouf, F., Vendel, J., Coppalle, A., Weill, M. and Yon, J., 2008. Characterization of soot particles in the plumes of over-ventilated diffusion flames. *Combustion Science and Technology,* 180, (4) pp.674-698.

Pchelintsev, A., Hasemi, Y., Wakamatsu, T. and Yokobayahi, S., 1997Experimental and Numerical Study on the Behaviour of a Steel Beam under Ceiling Exposed to a Localized Fire. In: *Fire Safety Science – Proceedings of the Fifth International Symposium.* pp. 1153-1164.

Pearson, A., Most, J. and Drysdale, D., 2007. Behaviour of a confined fire located in an unventilated zone. *Proceedings of the Combustion Institute,* 31, pp.2529-2536.

Pitts, W.M. , 2007. Personal Communication. In: *A Methodology to assess Species Yields of Compartment Fires by means of an extended Global Equivalence Ratio Concept.*, B. Forell, PhD thesis. University of Braunschweig – Institute of Technology.

Pitts, W.M., 2001. Toxic Yield. *Technical Basis for Performance Based Fire Regulations. A Discussion of Capabilities, Needs and Benefits of Fire Safety Engineering. United Engineering Foundation Conference Proceedings.* United Engineering Foundation, Inc, New York, USA: pp. 76-88.

Pitts, W.M., 1997. An Algorithm for Estimation Carbon Monoxide Formation in Enclosure Fires. *Fire Safety Science - Proceedings pf the 5th International Symposium.* International Association for Fire Safety Science, pp. 535-546.

Pitts, W.M., 1995. Global equivalence ratio concept and the formation mechanisms of carbon monoxide in enclosure fires. *Progress in Energy and Combustion Science,* 21, (3), pp.197-237.

Pitts, W.M., 1994a. *Global Equivalence Ratio Concept and the Prediction of Carbon Monoxide Formation in Enclosure Fires NIST Monograph 179.* USA, National Institute of Standards and Technology.

Pitts, W.M., 1994b. Application of thermodynamic and detailed chemical kinetic modeling to understanding combustion product generation in enclosure fires. *Fire Safety Journal,* 23, (3) pp.271-303.

Pitts, W.M., 1992. Limitations of the Global Equivalence Ratio Concept for Predicting CO Formation in Room Fires. *U.S./Japan Government Cooperative Program on Natural Resources (UJNR). Fire*

Research and Safety. 12th Joint Panel Meeting. Japan Fire Research Institute, Tokyo, Japan: pp. 152-159.

Pitts, W.M., 1990. Carbon Monoxide Production and Prediction. NISTIR 4449. *U.S./Japan Government Cooperative Program on Natural Resources (UJNR). Fire Research and Safety. 11th Joint Panel Meeting.* Berkeley, CA, USA: pp. 33-39.

Purser, D.A., 2002. Toxicity Assessment of Combustion Products. In:*SFPE Handbook of Fire Protection Engineering* ., eds. DiNenno,P.,J., and et. al, , Third edn,USA: National Fire Protection Association, pp.2-83-2-171.

Putorti, A.D.J., 1999. *Design Parameters for Stack-Mounted Light Extinction Measurement Devices. NIST Technical report NISTIR 6215.* National Institute of Standards and Technology.

Quintiere, J.G., 1998. *Principles of Fire Behavior.* USA: Delmar Publishers an International Thomson Publishing Company.

Rasbash, D.J. and Drysdale, D.D., 1982. Fundamentals of smoke production. *Fire Safety Journal,* 5, (1), pp.77-86.

Rasbash, D.J. and Pratt, B.T., 1980. Estimation of the smoke produced in fires. *Fire Safety Journal,* 2, (1), pp.23-37.

Rasbash, D.J. and Stark, G.W.V., 1966. *The Generation of Carbon Monoxide by Fires in Compartments. Fire Research Note No 614.* Fire Research Station. BRE Trust.

Richter, H. and Howard, J.B., 2000. Formation of polycyclic aromatic hydrocarbons and their growth to soot - a review of chemical reaction pathways. *Progress in Energy and Combustion Science,* 26, pp.565-608.

Robinson, A., 1999. Scandinavian Star incident: A case study. *Fire Engineers Journal,* 59, (198) p. 36.

Rozenberg, G.V., 1966. *Twilight.* New York: Plenum Press.

Santo, G. and Delichatsios, M.A., 1984. Effects of vitiated air on radiation and completeness of combustion in propane pool fires. *Fire Safety Journal,* 7, (2), pp.159-164.

Seader, J.D. and Chien, W.P., 1974. Physical Aspects of Smoke Development in the NBS smoke density chamber. *Journal of Fire and Flammability,* 6, pp.294-310.

Shaddix, C.R. and Williams, T.C., 2007. Soot: Giver and Taker of Light. *American Scientist,* 95, (3) pp.232-239.

Siegmann, K., Sattler, K. and Siegmann, H.C., 2002. Clustering at high temperatures: carbon formation in combustion. *Journal of Electron Spectroscopy and Related Phenomena,* 126, (1-3) pp.191-202.

Stark, G.W.V., 1972. Smoke and Toxic Gases from Burning Plastics. *Joint Symposium on Prevention and Control of Fires in Ships.* The Institute of Marine Engineers and the Royal Institution of Naval Architects, UK: p. 25.

Stec, A.A., Hull, T.R., Purser, J.A. and Purser, D.A., 2009. Comparison of toxic product yields from bench-scale to ISO room. *Fire Safety Journal,* 44, (1), pp.62-70.

Sugawa, O., Kawagoe, K., Oka, Y. and Ogahara, I., 1989. Burning Behavior in a Poorly-Ventilated Compartment Fire-Ghosting Fire-. *Fire Science and Technology,* 9, (2), pp.2_5-2_14.

Taylor, B.,N. and Kuyatt, C.,E., 1994. *Guidelines for Evaluating and Expressing the Uncertainty of NIST Measurement Results. NIST Technical Note 1297.* National Institute of Standards and Technology.

Tewarson, A., 2008. Generation of Heat and Chemical Compounds in Fires. In:*The SFPE Handbook of Fire Protection Engineering* ., eds. DiNenno,P.,J., D. Drysdale, C.L. Beyler, et al, 4th Edition edn,USA: National Fire Protection Association.

Tewarson, A., 2007. Carbon monoxide and smoke emissions in fires. *INTERFLAM 2007. Proceedings of the eleventh international conference.* Interscience Communications Limited, London: p. 1059.

Tewarson, A., 2002. Generation of Heat and Chemical Compounds in Fires. In:*The SFPE Handbook of Fire Protection Engineering* ., eds. DiNenno,P.,J., D. Drysdale, C.L. Beyler, et al. 3rd Edition ,USA: National Fire Protection Association, pp.3-82-3-161.

Tewarson, A., 1995. Generation of Heat and Chemical Compounds in Fires. In:*The SFPE Handbook of Fire Protection Engineering* ., eds. J. Linville L. and et al, 2nd Edition edn,USA: National Fire Protection Association, pp.3-53-3-124.

Tewarson, A., 1984. Fully Developed Enclosure Fires of Wood Cribs. *Twentieth Symposium (International) on Combustion.* The Combustion Institute, pp. 1555-1566.

Tewarson, A., Jiang, F.H. and Morikawa, T., 1993. Ventilation-controlled combustion of polymers. pp. 151-169.

Tewarson, A. and Steciak, J., 1983. Fire ventilation. *Combustion and Flame,* 53, (1-3), pp.123-134.

Thiry, A., 2011, *Personal communication on possible conversion of CO to CO2.*

Thomas, P., 2004. SFPE Classic Paper Review: Fire Behavior in Rooms by Kunio Kawagoe. *Journal of Fire Protection Engineering,* 14, (1) pp.5-8.

Thomas, P., H. and Nilsson, L., 1973. *Fully Developed Compartment Fires: New Correlations of Burning Rates. Fire Research Note 979.* Fire Research Station.

Thomas, P.H., Heselden, A.J.M. and Law, M., 1967. *Fully-developed compartment fires - two kinds of behaviour.* UK Ministry of Technology and Fire Offices' Commitee.

Tolocka, M.P., Richardson, P.B. and Houston Miller, J., 1999. The effect of global equivalence ratio and postflame temperature on the composition of emissions from laminar ethylene/air diffusion flames. *Combustion and Flame,* 118, (4), pp.521-536.

Ukleja, S., Delichatsios, M.A., Delichatsios, M.M. and Lee, Y.P., 2009. Carbon monoxide and smoke production downstream of a compartment for underventilated fires. In: *Fire Safety Science. Proceedings of the Ninth International Symposium.* The International Association of Fire Safety Science, pp. 849-860.

Watson, A.Y. and Valberg, P.A., 2001. Carbon Black and Soot: Two Different Substances. *American Industrial Hygiene Association Journal,* 62, (2) pp.218-228.

Whiteley, R., H., 2008. Smoke Production, Properties and Measurement. *Proceedings of Hazards of Combustion Products: Toxicity, Opacity, Corrosivity and Heat Release Conference.* Interscience Communications Limited, London, UK. p. 185.

Widmann, J.F., 2003. Evaluation of the planck mean absorption coefficients for radiation transport through smoke. *Combustion Science and Technology,* 175, (12), pp.2299-2308.

Widmann, J.F., Duchez, J., Yang, J.C., Conny, J.M. and Mulholland, G.W., 2005. Measurement of the optical extinction coefficient of combustion-generated aerosol. *Journal of Aerosol Science,* 36, (2), pp.283-289.

Widmann, J.F., Yang, J.C., Smith, S.L., Manzello, G.W. and Mulholland, G.W., 2003. Measurement of the optical extinction coefficients of postflame soot in the infrared. *Combustion and Flame,* 134, pp.119-129.

Wieczorek, C.J., 2003. *Carbon Monoxide Generation and Transport From Compartment Fires.* PhD thesis. Virginia Polytechnic Institute and State University.

Wieczorek, C.J., Vandsburger, U. and Floyd, J., 2004a. Evaluating the Global Equivalence Ratio Concept for Compartment Fires: Part II–Limitations for Correlating Species Yields. *Journal of Fire Protection Engineering,* 14, (3), pp.175-197.

Wieczorek, C.J., Vandsburger, U. and Floyd, J., 2004b. An Evaluation of the Global Equivalence Ratio Concept for Compartment Fires: Data Analysis Methods. *Journal of Fire Protection Engineering,* 14, (1), pp.9-31.

Wu, J.S., Krishnan, S.S. and Faeth, G.M., 1997. Refractive Indices at Visible Wavelengths of Soot Emitted From Buoyant Turbulent Diffusion Flames. *Journal of Heat Transfer,* 119, pp.230-237.

Yij, E.H., Fleischmann, C.M. and Buchanan, A.H., 2007. Vent Flows in Fire Compartments with Large Openings. *Journal of Fire Protection Engineering,* 17, (3), pp.211-237.

Zuev, V.E., 1974. *Propagation of Visible and Infrared Radiation in the Atmosphere.* New York: John Wiley and Sons.

Zuev, V.E., Kabanov, M.V. and Savelev, B.A., 1969. Propagation of Laser Beams in Scattering Media. *Applied Optics,* 8, pp.137-141.

Zukoski, E.E., Kubota, T. and Lim, C.S., 1985. *Experimental Study of Environment and Heat Transfer in a Room Fire. Mixing in Doorway Flows and Entrainment in Fire Plumes* . National Bureau of Standards.

Zukoski, E.E., Toner, S.J., Morehart, J.H. and Kubota, T., 1989. Combustion Processes in 2-Layered Configurations. In: *Fire Safety Science, Proceedings of the Second International Symposium,* The International Association of Fire Safety Science, pp. 295-304.